

CONTENTS

100	Environmental and experimental studies of aluminium toxicity on the liver of <i>Oreochromis niloticus</i> (Linnaeus, 1758) fish Mohammad M.N. Authman	764-776
101	The Mushroom Extract Schizophyllan Reduces Cellular Proliferation and Induces G2/M Arrest in MCF-7 Human Breast Cancer Cells Eiman Aleem	777-784
102	Glutathione S-Transferase Gene Polymorphisms (GSTM1 and GSTT1) in Vitiligo Patients Fatma A. Abd Rabou, Hesham A. Elserogy, Shereen F. Gheida and Amal A. EL-Ashmawy1	785-792
103	Pneumonia and Impaired T Cell Function in Children with Down's Syndrome: Double Strike Amany Abuelazm, Zeinab Galal and Samia El Sahn	793-799
104	Double Paraproximity Spaces A. Kandi I, O. Tantawy, K. Barakat, and N. Abdelnaby	800-804
105	Combined Effects of Temperature and Algal Concentration on Filtration and Ingestion Rates of <i>Crassostrea gigas</i>: Bivalvia Mona, M. H., Elkhodary, G.M. and Khalil, A.M	805-813
106	Leadership behavior as perceived by clinical teacher and nursing students Olfat A. Salem; Fatma M. Baddar and Gusrina Komara Putri	814-820
107	Pneumonia and Impaired T Cell Function in Children with Down's Syndrome: Double Strike Amany Abuelazm, Zeinab Galal and Samia El Sahn	821-827
108	Bayesian censored data viewpoint in Weibull distribution Abd-Elfattah A.M. And Marwa O. Mohamed	828-837
109	Histopathological and Immunohistochemical Studies on the Prognostic Significance of Angiogenesis in Renal Cell Carcinoma Samia, M. Sanad, Mahmoud, A. El-Baz and Mohamed, A. Erfan	838-851
110	Construction of a HSV-1 strain HF Based Replication Defective Vector with LR-Recombination Sites Qingzhi Wang, Bo Song, Xinjing Liu, Zhiqiang Han, Jiameng Lu, Ting Yang, Chenyang Jiang, Xiaolu Zhang, Chandra Avinash, Shilei Sun, Yuming Xu	852-857
111	Evaluation of Different Immunological Techniques for Diagnosis of Schistosomiasis haematobium in Egypt Mahfouz, A., Mahana, N., Rabee, I., El Amir, A.	858-867
112	Effect of Intratympanic Dexamethasone Administration on Cisplatin-Induced Ototoxicity in Adult Guinea Pigs, Is It Time-Dependent? Audiological and Histological Study	868-882

Mirahan T. Thabet, Rasha Elkabarity, NevineBahaa E. Soliman, NagwaKostandy Kalleney and Amr Gouda

- 113 Extracellular Metabolites Produced by a Novel Strain, *Bacillus alvei* NRC-14: 3. Synthesis of a Bioflocculant that has Chitosan-Like Structure** **883-890**
Shadia M. Abdel-Aziz, Hoda A. Hamed, Foukia E. Mouafi and Nayera A. M. Abdelwahed
- 114 Resveratrol Mediated Protection of Dacarbazine-Induced Mutagenicity in Mice** **891-899**
Ramadan, A.M. Ali
- 115 Nervi Terminalis, Vomeronasalis and Olfactorius of *Uromastyxaegyptius* (Squamata – Lacertilia - Agamidae)** **900-907**
Dakrory, A.I.; Issa, A.Z. and Ali, R.S
- 116 Role of IL28B Gene Polymorphisms in Response to the Standard of Care Treatment in Egyptian Patients with Chronic HCV Genotype Four** **908-915**
Olfat M Hendy, ElhamyAbd El Moneam, Mona A Al shafie, Maha El-Sabawy, Mohammed A Rady and Sherif A El Baz

Environmental and experimental studies of aluminium toxicity on the liver of *Oreochromis niloticus* (Linnaeus, 1758) fish

Mohammad M.N. Authman

Hydrobiology Department, National Research Centre, Dokki 12622, Giza, Egypt
mmauthman@yahoo.com

Abstract: Specimens of water and the freshwater fish (*Oreochromis niloticus*) were sampled from Al-Atf drainage canal, Al-Minufiya Province, Egypt, for one year to determine aluminium (Al) concentrations in water and its accumulation in livers of such fish. It was found that Al accumulated in livers of *O. niloticus* in levels higher than that of the canal water. The concentrations of Al in water were higher than the world permissible limits. Experimentally, *O. niloticus* fishes were exposed to three doses of Aluminium sulphate and Al effects were evaluated with regard to hepatosomatic index and liver histopathological alterations. The hepatosomatic indices of fish treated with the three doses of Aluminium sulphate were higher compared to the control group. Fish exposed to the highest dose had significantly higher ($P < 0.05$) hepatosomatic indices than the control fish. Liver tissues of treated fish revealed various histopathological lesions. From this investigation, it was suggested that, the liver of *O. niloticus* is convenient for testing the toxicity of metals such as aluminium.

[Mohammad M.N. Authman. **Environmental and experimental studies of aluminium toxicity on the liver of *Oreochromis niloticus* (Linnaeus, 1758) fish.** Life Science Journal. 2011;8(4):764-776] (ISSN:1097-8135).
<http://www.lifesciencesite.com>

Keywords: *Oreochromis niloticus*, liver, bioaccumulation, aluminium sulphate, hepatosomatic index, histopathology, Egypt.

1. Introduction:

Environmental pollution represents a major problem in both developed and undeveloped countries (Kazi *et al.*, 2009; Ozden, 2010). There has been an increasing awareness that the aquatic pollution and other anthropogenic impacts on water resources may have the potential to damage natural fish stocks (Abdelmeguid *et al.*, 1999). The agricultural and industrial wastes partially treated or without treatment are being discharged into surface water (Zaki *et al.*, 2009).

Any change in the natural conditions of aquatic medium causes several adjustments in fish and metals are the main culprit for these undesirable changes in water quality (Garg *et al.*, 2009). Due to their toxicity, long persistence, bioaccumulative and nonbiodegradable properties in the food chain, metals constitute a core group of aquatic pollutants. In spite of their natural occurrence in the aquatic ecosystem, metals represent a major environmental problem of increasing concern, and their monitoring has received significant attention in the field (Pandey *et al.*, 2003; Barnhoorn and van Vuren, 2004) and under laboratory conditions (Long *et al.*, 2003; Osman *et al.*, 2007).

In Egypt; tilapias are the main species of freshwater fishes that inhabit River Nile, irrigation network and drainage canals connected to it. The Nile tilapia, *Oreochromis niloticus* (Pisces: Cichlidae), is an important fish in the ecology of tropical and sub-

tropical region including Egypt and the most popular species of the bony fish in Africa (Abdel Tawwab *et al.*, 2007; Offem *et al.*, 2007; Shalloof and Salama, 2008).

In the last years the problems of the drainage canals in Egypt have extremely increased. These problems include the presence of high concentrations of different metals and pesticides in both water and various fish organs (Khallaf *et al.*, 1994, 1995, 1998, 2003; Ane-na-ei, 1998, 2000, 2003; Authman, 2008; Authman *et al.*, 2008). As a result, fish are exposed to water that contains high concentrations of metals including aluminium.

Aluminium (Al) is the third most common and abundant metal on earth after oxygen and silicon (Sargazi *et al.*, 2001; Ščančar *et al.*, 2004; Camargo *et al.*, 2009). Aluminium is similar to many other metals in that it is generally considered most toxic in its soluble ionic form (Walton *et al.*, 2009). Al is a harmful metal to the aquatic ecosystem, being responsible for events of toxicity with serious ecological consequences (Correia *et al.*, 2010). It is also found in the atmospheric air of the big cities and industrialized areas (Casarini *et al.*, 2001), and is used as a flocculation agent in water treatment (Silva *et al.*, 2007; Camargo *et al.*, 2009).

Different physiological alterations frequently observed in different fish species exposed to Al were cardiovascular, hematologic, respiratory, ionoregulatory, reproductive, metabolic, endocrine

and gill damage (Brodeur *et al.*, 2001; Vuorinen *et al.*, 2003; Barcarolli and Martinez, 2004).

The liver is the main and important detoxifying organ in fish and is essential for both the metabolism and the excretion of toxic substances in the body (van Dyk *et al.*, 2007); and several categories of hepatocellular pathology are now regarded as reliable biomarkers of toxic injury and representative of biological endpoints of contaminant exposure (Stentiford *et al.*, 2003; Feist *et al.*, 2004; ICES, 2006). Exposure to metals such as Al may therefore cause histological changes in the liver and a histological investigation of exposed specimens may therefore produce meaningful results (van Dyk *et al.*, 2007).

The present study was concerned with aluminium because its detection in some drainage canals water in Al-Minufiya Province, Egypt was high, reach to 26.77 mg/l (Authman, 2008; Authman *et al.*, 2008).

So, the specific aims of this study were to determine Al concentrations in an drainage canal water to evaluate its occurrence, investigate the tissue accumulation of Al in the liver of Nile tilapia *O. niloticus* inhabiting this canal in order to establish the accumulation factor between metal in water and tissues, and document the effect of Al on the liver of *O. niloticus* in the laboratory to identify histological changes and effects on hepatosomatic index after exposing the fish to Al.

2. Materials and Methods

(1) Field investigations

A- Study area

Al-Atf drainage canal (Fig. 1) is one of the important drainage canals present in Al-Minufiya Province, which extends more than 40 km throughout two governorates (Al-Minufiya and Al-Gharbiya), into the Egyptian delta. Its length is surrounded by more than 17 villages that begin by Meat Al-Beadah. It is shallow and narrow canal where the average depth and width are about 1.5 and 6 m respectively. Wastes from more than 25,250 feddan of the cultivable land is directly discharged into this canal but the indirect discharges come from cultivable land (about to 93,000 feddan,) and also illegal sewage find its way to it from various villages. The fish fauna, in this canal, includes *Oreochromis niloticus*, *Tilapia zillii*, *Oreochromis aureus* and *Clarias gariepinus* (El-Sehamy, 2001). This canal drains in Al-Rayah Al-Abbasy in Al-Gharbiya Province that finally drains into Damietta Branch of the River Nile near Zefra city.

B- Water sampling and analysis

Samples were collected monthly from Al-Atf drainage canal for a complete year. Water samples were obtained from six sites covered the whole length of the canal by a water sampler. Samples were preserved and Al was extracted according to APHA (1998), where 500 ml of water sample were acidified with 5 ml of 6N HNO₃ and heated until the color was discharged. Other 2 ml of conc. HNO₃ were added and the sample warmed slightly to dissolve the residue. The sample was then cooled, filtered and stored for Al detection.

C- Fish sampling and Al residual analysis of liver tissue

Random samples of *O. niloticus* of different sizes were collected monthly from the studied area during the same period of waters sampling. Fishes (9.0–18.0 cm in total length and 12–125 g in total weight) were collected by the fishermen using bottom nets. Fish specimens were kept in an ice box, and transported to the laboratory, where they were killed by blows on the head and then the abdominal cavity was incised from the anus to the isthmus. The liver was dissected out using a sharp safety razor.

Parts of the liver were stored in a deep freezer until processing for aluminium detection. Wet liver samples were digested using HNO₃ (4 ml per gram liver tissue) at 70°C on a hot plate until NO₂ evaporation ceased (Chernoff, 1975). A volume of reagent grade 10% H₂O₂ equal to the initial HNO₃ was added to the digested samples until the sample become clear and then allowed to cool. After cooling, the solution was filtered and the filtrate made up to a known volume (100 ml) with de-ionized water. The samples were stored cool till analyzed.

Different samples of water and fish liver were analyzed using flame atomic absorption spectrophotometer (G.B.C. 908 Avanta Σ), GBC Scientific Equipment PTY LTD, Australia, at the Atomic Absorption Laboratory, Egyptian Mineral Resources Authority, Ministry of Petroleum, Dokki, Giza, Egypt, to detect the concentrations of aluminium.

D- Accumulation factor (AF)

The accumulation factor (AF) was calculated (Authman and Abbas, 2007) using the following equation:

$$AF = \frac{\text{aluminium concentration in fish liver (mg kg}^{-1} \text{ wet wt)}}{\text{aluminium concentration in water (mg l}^{-1}\text{)}}$$

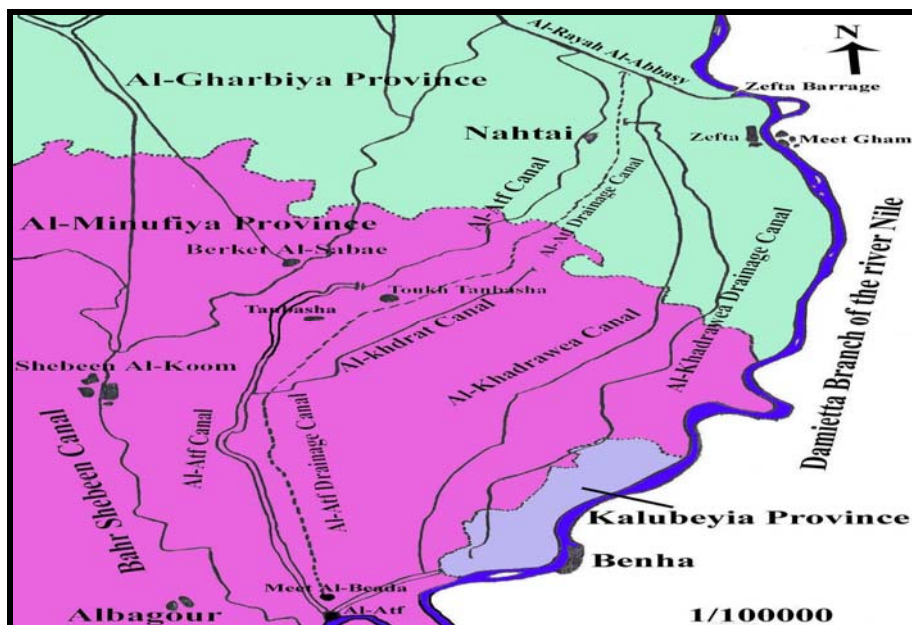


Figure (1): Map showing the area of study (Al-Atf drainage canal, dotted line).

(2) Experimental investigations

A- Sample collection for experimental test

Specimens of *O. niloticus* were obtained from Bahr Shebeen Canal, Al-Minufiya Province, Egypt, throughout commercial fishing using trammel nets. The average total length and body weight were 14.8 ± 2.7 cm and 68.1 ± 5.2 g, respectively. The fish were transported alive to the laboratory in special small water tanks provided by oxygen pumps working with battery; then kept in the laboratory in equipped glass aquaria (40x50x60 cm) containing dechlorinated tap water, and were continuously aerated by air pumps. The fish with external abnormalities such as damaged fins, fallen scales, swelling body and unnatural pigmentation were avoided. Fish were allowed to acclimate to laboratory conditions for two weeks, and were provided with suitable food composed of fishmeal (25% protein of total mass) once per day at a level of 5% of body weight.

B- Experiment design

The experiment was conducted to evaluate the aluminium toxicity in the laboratory. For the experiment, control and exposure tanks were set up in duplicate. A total number of 240 apparently healthy *O. niloticus* were used in this experiment.

Glass tanks (120-liter capacity) were used for the experiment and labeled for control, dose I, dose II and dose III treatments and the number of tanks was duplicated (total number = eight). Thirty fish were introduced in control and each treatment,

and all tanks were moderately aerated during the experiment. Three concentrations of aluminium sulphate [$Al_2(SO_4)_3$] were used as 0.05, 0.30 and 1.00 mg/l which represent 1/2, 3 and 10 times the dose used by **Peuranen et al. (2003)**. Also, the lowest used concentration was nearly equal to the highest concentration detected in the canal water samples in the present study. The stock solution of toxicant was prepared by dissolving in dechlorinated tap water. Renewal design experiment was conducted by replacing 90% of the solution in each exposure tank with fresh solution every 2 days to maintain the concentrations as needed. The control tank was treated similarly without addition of toxicant solution.

The water physico-chemical characteristics which were maintained during the study were presented in table (1). Temperature, salinity, conductivity, dissolved oxygen, and pH were measured using electronic portable meters (Yellow Springs Instrument Co., Ohio, USA, YSI S-C-T meter Model 33 and YSI oxygen meter Model 54 ARC) and digital pH meter, Model 206, Lutron, Taiwan). Total hardness, total alkalinity, total dissolved solids, ammonia, nitrate and nitrite were determined according to the methods of **APHA (1998)**.

C- Hepatosomatic (HSI) index

Twenty fish from control and each treatment (duplication) were sampled after 1, 3 and 7 days of exposure and the weight was recorded for each fish to

the nearest 0.1 mg. Every fish was killed by blows on the head, then the abdominal cavity was incised from the anus to the isthmus and the liver was dissected out using a sharp safety razor. This was weighed to the nearest 0.1 mg, and hepatosomatic index (HSI) was calculated (Khallaf and Authman, 1991) as follows:

$$\text{HSI} = \text{liver weight (g)} / \text{body weight (g)} \times 100$$

Table (1): Physico-chemical characteristics of the water used in the experiment.

Parameter	Value
PH	7.20±0.39
Dissolved Oxygen (DO)	7.71±0.07 mg/l
Temperature	24.3±0.1°C
Total hardness	40.0±2.1 mg/l as CaCO ₃
Total alkalinity	96.0±3.48 mg/l as CaCO ₃
Electric conductivity	68.017±0.114 µmohs/cm
Salinity	0.001±0.00 mg/l
NH ₃ (Ammonia)	0.041±0.004 mg/l
NO ₂ (Nitrite)	0.013±0.002 mg/l
NO ₃ (Nitrate)	0.220±0.066 mg/l
Total dissolved solids	74.92±4.52 mg/l

D- Histopathological examination

After 1, 3 and 7 days, parts of livers from control and each treatment were preserved in 10 % phosphate buffered formalin for 24 hours, then dehydrated by a series of upgraded ethanol solution, embedded in paraffin, and sectioned at 5 µm thick. Tissue sections were routinely processed and stained with Hematoxylin and Eosin (H & E) and examined by light microscopy according to Roberts (2001).

(3) Statistical analyses

Statistical analyses were performed using a computer program SPSS, version 17 for Windows. The comparison between means and standard deviations was tested for significance using ANOVA analysis. The differences between exposed and control fishes were considered significant if $P < 0.05$.

3. Results

(1) Field observations

A) Al concentrations in water and liver

Table (2) and figure (2) illustrated the monthly variations of Al concentrations levels in canal water and liver of *O. niloticus*. The results indicated that, the average Al concentrations in water showed irregular distribution pattern. In water, it was ranged between 0.0018 and 0.0540 mg/l in September and April, respectively. The irregularities were also apparent in the changes of the Al concentrations in liver. Al concentrations in liver were higher than in water all over the year. These concentrations ranged between 0.92 mg/Kg wet wt in July and 6.49 mg/Kg wet wt in February.

B) Accumulation Factor (AF):

It was found that Al concentrations in liver of the studied fish species were several times higher than its concentrations in water. In addition, it is obvious from the data given in table (2) and figure (2) that, these factors in liver were ranged between 21.86 and 1475.14 times in April and September, respectively.

Table (2): Monthly variations of aluminum concentrations in water and liver of *O. niloticus* collected from Al-Atf drainage canal and the accumulation factor.

Months	No. of Fishes	Al Concentrations		Accumulation Factor (AF)
		Water (mg/l)	Liver (mg/Kg wet wt)	
January	33	0.0026	2.29	877.39
February	37	0.0129	6.49	502.71
March	31	0.0069	1.23	179.56
April	33	0.0540	1.18	21.86
May	34	0.0054	1.06	198.13
June	32	0.0043	1.20	277.14
July	33	0.0187	0.92	49.17
August	32	0.0056	4.00	720.72
September	35	0.0018	2.67	1475.14
October	34	0.0021	1.54	751.22
November	36	0.0046	2.87	622.56
December	31	0.0103	3.11	301.06

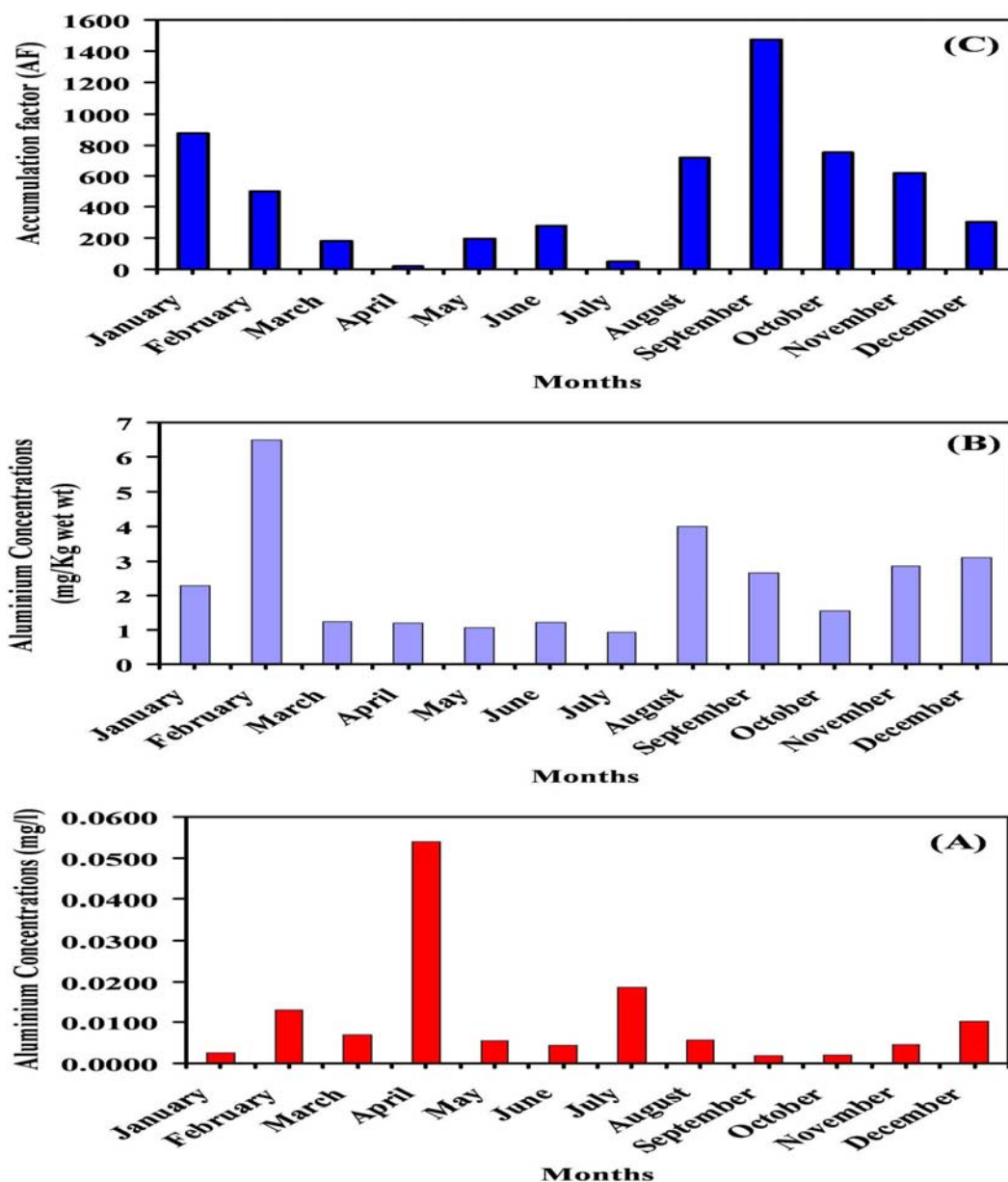


Figure (2): Monthly variations of aluminium concentrations in water (A) and liver of *O. niloticus* (B) and the accumulation factor (C).

(2) Experimental observations

Over the course of the study, the values of physico-chemical characteristics of water did not varied among control and Al groups (Table 1). Also, it was noticed that mortality did not occur and the fish demonstrated no visual signs of distress during the experiment, where an external investigation of each specimen was executed after the exposure and it was found that all fish seem to be of good health with regard to the macroscopic condition of

their fins, eyes, mouth, and scales and their general external appearance.

A) Hepatosomatic index (HSI)

The HSI values of fish treated with all doses of Al were higher compared to the control group (Table 3; Figure 3). However, on the basis of the statistical analysis, HSI values of the fish of group III exposed to the 1.00 mg/l dose of Al were significantly higher ($P < 0.05$) than the control fish.

Table (3): The effect of aluminum sulphate on the hepatosomatic index (HSI) of *O. niloticus* at different used concentrations.

Duration time (Day)	Hepatosomatic index (HSI)							
	C		I		II		III	
1	1.987	± 0.822	2.075	± 0.496	2.238	± 0.613	2.415*	± 0.496
3	2.054	± 0.363	2.174	± 0.465	2.395	± 0.673	2.498*	± 0.059
7	2.063	± 0.588	2.192	± 0.119	2.399	± 0.673	2.698*	± 0.799

C = Control.

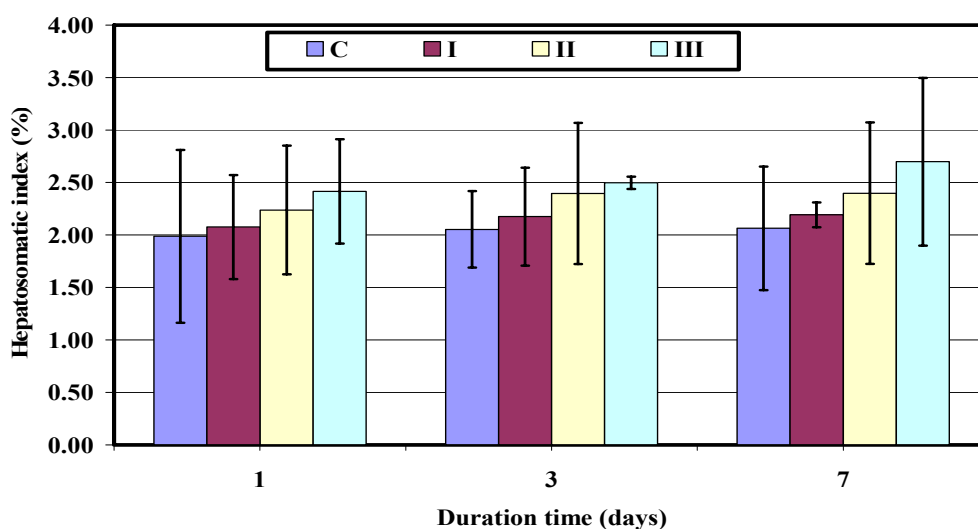
I = 0.05 mg/l of aluminum sulphate.

II = 0.30 mg/l of aluminum sulphate.

III = 1.00 mg/l of aluminum sulphate.

The values are expressed as means ± standard deviation (95% confidence limits).

Number of fish samples in each treatment = 20.

* Values significantly different ($P < 0.05$) compared with control group.**Figure (3): The effect of aluminum sulphate on the hepatosomatic index (HSI) of *O. niloticus* at different used concentrations. (Mean ± standard deviation; C = Control, I = 0.05 mg/l, II = 0.30 mg/l and III = 1.00 mg/l of aluminum sulphate).****B) Histopathologic lesions of liver**

The histology of normal hepatopancreas of *O. niloticus* consisted of hepatocytes arranged in cords, central vein, and pancreatic acini in the portal area, with numerous vacuoles indicates glycogen deposition which can be considered normal (Fig. 4a).

After 24 hrs of Al exposure, the microscopical examination of liver cells revealed loss of their regular morphology with mild congestion of blood vessels at all doses. Massive numbers of mononuclear inflammatory cells infiltration in the hepatic tissue were detected (Fig. 4b) associated with melanin carrying cells (melano-macrophages) surrounding the dilated central veins (Fig. 4c). Extravasated red blood cells and few melanin (melano-macrophages) cells were demonstrated in

the portal area in between and surrounding the pancreatic acini (Fig. 4d).

On the third day of Al exposure, focal necrosis in the hepatic parenchyma (Fig. 4e) was detected. Degenerated hepatocytes in diffuse manner (Fig. 4f) were noticed. Hyperactivation of melano-macrophage centers in the portal area in focal manner (Fig. 5a) were detected.

On day 7 of Al exposure, the severe congestion in the portal veins and sinusoids (Fig. 5b) were obvious. Necroses with inflammatory cells infiltration in the hepatocytes adjacent as well as surrounding the dilated central vein (Fig. 5c) were detected. Atrophy in the pancreatic acini (Fig. 5d) was demonstrated. Vacuolated hepatocytes in diffuse manner due to glycogen infiltration (Fig. 5e) were noticed. Hepatocytes had intra-cytoplasmic round

vacuoles (vacuolation) supposed to indicate fatty changes in diffuse manner (Fig. 5f) were visible in all specimens.

All these changes were more severe in the 2nd and 3rd groups of Al exposure and the frequencies

and the severity of these changes were directly correlated to the increase in the Al sulphate concentrations.

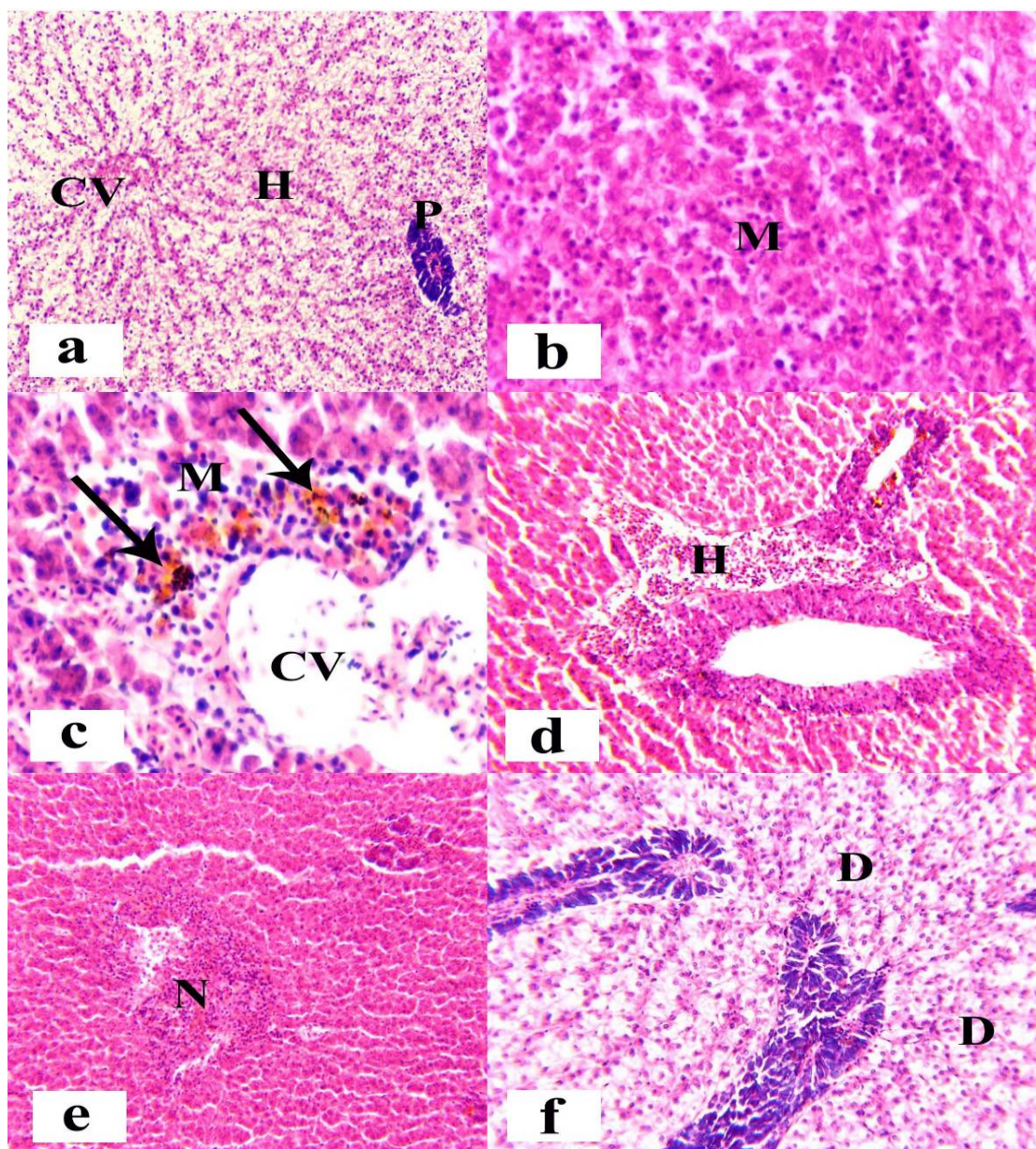


Figure (4): Transverse sections of *O. niloticus* liver. (a) Normal histology of liver showing the hepatocytes (H) in cords, central vein (CV), and pancreatic acini in the portal area (P), with diffuse glycogen deposition which can be considered normal (H&E, X40). (b) Liver after 24 hrs of Al exposure showing mononuclear inflammatory cells infiltration (M) in the hepatic tissue (H&E, X160). (c) Liver after 24 hrs of Al exposure showing the inflammatory cells infiltration (M) and melano-macrophage cells (arrows) surrounding dilated central vein (CV) (H&E, X160). (d) Liver after 24 hrs of Al exposure showing the extravasated red blood cells (H) and few melano-macrophage cells in the portal area in between and surrounding the pancreatic acini (H&E, X64). (e) Liver after 3 days of Al exposure showing the focal necrosis (N) in the hepatic parenchyma (H&E, X64). (f) Liver after 3 days of Al exposure showing the degenerated hepatocytes (D) in diffuse manner (H&E, X64).

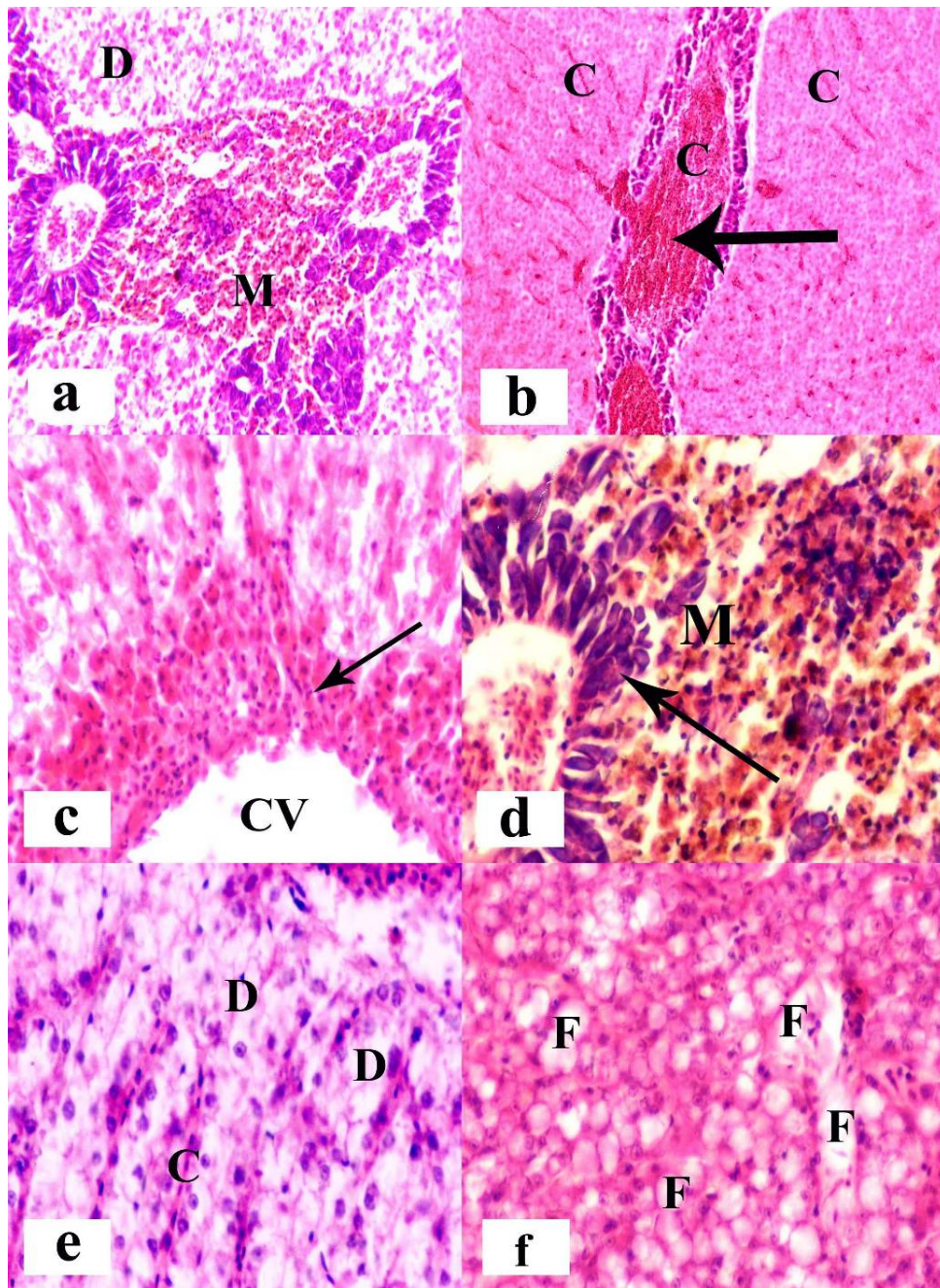


Figure (5): Transverse sections of *O. niloticus* liver. (a) Liver after 3 days of Al exposure showing activation of melano-macrophage centers (M) were allocated in the portal area in focal manner and degenerated hepatocytes (D) (H&E, X64). (b) Liver after 7 days of Al exposure showing severe congestion (C) in the portal vein (arrow) and sinusoids (H&E, X40). (c) Liver after 7 days of Al exposure showing hepatocytic necrosis adjacent as well as surrounding the dilated central vein (CV) with inflammatory cells infiltration (arrow) (H&E, X160). (d) Liver after 7 days of Al exposure showing atrophy (arrow) in the pancreatic acinar cells and activation of melano-macrophage centers (M) adjacent to the pancreatic acinar area (H&E, X160). (e) Liver after 7 days of Al exposure showing vacuolated hepatocytes (D) in diffuse manner (Glycogen infiltration) and congestion (C) (H&E, X160). (f) Liver after 7 days of Al exposure showing hepatocytes had intra-cytoplasmic round vacuoles supposed to indicate fatty change (F) in diffuse manner (H&E, X160).

4. Discussion

The pollution of the aquatic environment with metals has become a serious health concern because of their toxicity and accumulation by organisms (Mendil *et al.*, 2010; Shah *et al.*, 2010). Fish, in comparison with invertebrates, are more sensitive to many toxicants and are a convenient test subject for indication of ecosystem health (Moiseenko *et al.*, 2008).

Domestic sewage, agricultural drainage water and other wastes heavily contaminate the drainage canals in the Egyptian Delta (Alne-na-ei, 1998). Polluted drainage water heavily loaded with different contaminants such as pesticides and metals (Alne-na-ei, 1998; Khallaf *et al.*, 1998, 2003). In the present study, it was determined that, the Al concentrations in the canal water tended to vary among months, and displayed particularly high levels (Table 2). The increase of metals in drainage water attributed to the large amount of sewage and other pollutants discharged at Al-Atf drain and the decomposition of the organic matter and/or the use of fertilizers and other chemicals in agriculture (Abdel-Satar, 2005; Ibrahim and Tayel, 2005). The mean Al concentrations in Al-Atf drainage canal water are lower than the mean Al concentrations recorded previously by Authman (2008) and Authman *et al.* (2008) in the Sabal drainage canal. This variation may be due to the differences in the sources of Al pollution and physical-chemical conditions of the water. It was noticed that Al concentrations detected in Al-Atf drainage canal water have exceeded the world permissible limits [i.e. $1 \mu\text{g l}^{-1}$ at $\text{pH} < 6.5$ and $55 \mu\text{g l}^{-1}$ at $\text{pH} > 6.5$, ANZECC and ARMCANZ (2000)] for the protection of freshwater ecosystems. The present results indicated that, Al-Atf drainage canal water in Al-Minufiya Province is contaminated by elevated quantities of Al. From an ecological standpoint, this is a matter of concern as this metal represent a threaten for the fish resources in River Nile, where this canal drains in Al-Rayah Al-Abbasy which finally drains in Damietta branch of the River Nile. This will be causing changes in water quality and considerable amount of pollution in Nile aquatic environment, and fish health may suffer and mortality rates increase.

Many studies showed that metals accumulate mainly in metabolic organs such as liver that stores metals to detoxificate, thus, the liver in fish is more often recommended as environmental indicator organ of water pollution than any other fish organs (Karadede *et al.*, 2004; Yilmaz *et al.*, 2007). In the present study, it was found that, the levels of Al concentrations in *O. niloticus* livers are higher than in the canal water. This is in agreement with that obtained previously by Authman *et al.*

(2008) who found that, metals concentrations in livers of *O. niloticus* caught from Sabal drainage canal were higher than their concentrations in canal water. The values of Al in *O. niloticus* livers obtained in the present study were lower than those recorded by Authman *et al.* (2008) in livers of the same species in the Sabal drainage canal. The accumulation factor (AF) or the relative index of the concentration (Khallaf *et al.*, 1998) of Al in the fish liver to that in canal water, in the present study, showed dreadful results when compared to the real concentrations of this pollutant in water (Table 2). Moon *et al.* (1985) and Triebkorn *et al.* (1997) mentioned that, the liver has a key role in basic metabolism and is the major site of accumulation, biotransformation, and excretion of contaminants in fish.

Consistent with the present observations, Authman (2008) and Authman *et al.* (2008) have detected highest levels of Al in the Sabal drainage canal in Al-Minufiya Province. Also, Authman (2008) found that, the Al concentrations in the muscles of *O. niloticus* were above the tolerance levels for human consumption. Accordingly, the long-term and frequent intake of fishes with high Al levels constitutes a human health risk, where Al is not considered to be an essential element in humans, but its toxicity is known, particularly in patients with chronic renal failure (D'Haese and De Broe, 1994). Also, the accumulation of aluminium has been related to the neurodegenerative process in Alzheimer's disease (Sarzaghi *et al.*, 2001; Ščančar *et al.*, 2004).

Hepatosomatic index (HSI) is general measurement of the overall condition of fish or the growth status of liver (West, 1990) and can be an excellent predictor of adverse health in fish (Adams and McLean, 1985). In the present study, there was insignificant difference in the values of hepatosomatic indices (HSI) between control and treated fish with either I or II doses of aluminium sulphate. On the other hand, *O. niloticus* fishes treated with dose III of aluminium sulphate showed significantly high values of HSI. This may be attributed to the accumulation of lipid in liver tissue of fish exposed to highly dose of aluminium sulphate. The fatty changes that were detected in histological sections may confirm this suggestion. Similarly, Abdelmeguid *et al.* (1999) reported that, hepatosomatic index of *Oreochromis niloticus* exposed to lead acetate was increased as a result of change in quantity of fat in liver. Munshi and Dutta (1996) stated that the HSI of *Osteichthyes* is normally between 1% and 2%. The HSI values of the treated specimens exposed to the three doses of Al exceeded this range. Although hepatosomatic indices can vary

with nutrition, season, fish condition and disease, a relationship between hepatosomatic index and levels of contamination was reported by **Sloof et al. (1983)**. The possible interpretation of the variation of hepatosomatic index may coincide with that suggested by **Fabacher and Baumann (1985)**, that the enlarged livers could result in increased activity of hepatic mixed-function oxidase enzymes and thus develops an increased ability to metabolize xenobiotics.

The teleost liver is one of the most sensitive organs with regard to showing alterations in histoarchitecture, biochemistry, and physiology following exposure to various types of environmental pollutants (**Roy and Bhattacharya, 2006**). **Brulé and González I Anadon (1996)** stated that, fish liver histology could serve as a model for studying the interactions between environmental factors and hepatic structures and functions. The harmful effect of metal pollution on fish liver histology may, however, depend on the duration of the exposure and the concentration level of the specific metal (**van Dyk et al., 2007**).

The present study documents pathologic changes in fish treated with three different doses of Al for 7 days. The degree of pathology gradually increased during the entire days of experiment which exhibited dose-and time-dependent changes.

During the present investigation intense degenerative changes in the livers of *O. niloticus* were found to occur within the period of exposure to Al. The degenerative changes were characterized by vacuolation of the hepatocytes, necrotic cells, atrophy of the pancreatic tissue, and congestion of blood veins. The widespread vacuolation might be likely due to accumulation of glycogen in hepatocytes (**Wester and Canton, 1986**). Also, the widespread vacuolation of the liver might be a common response in fish hepatocyte to various chemical stressors, which indicates a higher hepatocellular lipid, water and/or glycogen content (**Liao et al., 2006**). Vacuolation of the hepatocyte, pycnosis in many of the necrotic cells, necrosis of the pancreatic tissue, and disintegration of blood sinusoids (**Roy and Bhattacharya, 2006**) characterized the degenerative changes. The vacuolizations is commonly found following toxic injury of the fish liver (**Abdelmeguid et al., 1999**). Hepatocellular lipid vacuolation commonly occurs in fish as a histopathological reaction to aquatic pollutants (**Alne-na-ei, 1998**). Degeneration and necrosis of hepatocytes may be attributed to the cumulative effect of the metal such as Al and to the increase of its concentration in the hepatic tissue during experimental period (**Zaki et al., 2009**). These results agreed with **Förlin et al. (1986)**, who stated that, liver has an important

detoxical role of exogenous waste products as well as externally derived toxins such as metals.

Among the observed histopathological lesions of liver, the melano-macrophage aggregates have been shown to be involved in a number of fish diseases, and as phagocytic cells (**Agius and Robert, 2003**). It was noticed by **Stentiford et al. (2003)** that, the prevalence of melano-macrophage centers was highest in flounder captured from the sites with the highest PAH contamination. The prevalent of this pathologic condition in the present study may be because, with the expenditure of energy in the detoxification process, more melano-macrophage aggregates appeared from increases in metabolic byproducts (**Authman et al., 2008**). These histopathological findings are similar to those mentioned by **Liao et al. (2006)** when exposed medaka (*Oryzias latipes*) to sublethal exposure of methylmercury chloride, **Roy and Bhattacharya (2006)** when exposed *Channa punctatus* to arsenic, and **van Dyk et al. (2007)** when exposed *Oreochromis mossambicus* to cadmium and zinc.

5. Conclusion

In conclusion, the present study points out the contamination of Al-Atf drainage canal by aluminium. Also, it could be concluded that Al induced deleterious effect in *O. niloticus* such as damage of the liver. It induced cumulative effect; therefore equivalent lesions of fish may occur in humans. In addition, the experimental results demonstrated that *O. niloticus* liver could be used as a useful tool in the research on Al toxicologies.

*Corresponding Author:

Dr. Mohammad M.N. Authman
Hydrobiology Department, National Research
Centre, Dokki 12622, Giza, Egypt
E-mail: mmauthman@yahoo.com

References:

- Abdel Tawwab, M.; Mousa, A.A.M.; Ahmed, M.H and Sakr, S.F.M. (2007): The use of calcium pre-exposure as a protective agent against environmental copper toxicity for juvenile Nile tilapia, *Oreochromis niloticus* (L.). Aquaculture, 264:236-246.
- Abdelmeguid, N.E.; Khallaf, E.A.; Alne-na-ei, A. A. and Yossif, G.A. (1999): Electron microscopic study on the effect of lead acetate on the liver of cichlid fish *Oreochromis niloticus* (Linnaeus). J. Egypt. Ger. Soc. Zool., 29(C):49-69.
- Abdel-Satar, A. M. (2005): Water quality assessment of River Nile from Idfo to Cairo, Egypt. Egypt. J. Aquat. Res., 31(2):200-223.

- Adams, S.M. and McLean, R.B. (1985): Estimation of largemouth bass, *Micropterus salmoides* Lacepede, growth using the liver somatic index and physiological variables. *J. Fish Biol.*, 26:111-126.
- Agius, C. and Robert, R.J. (2003): Melanomacrophage centres and their role in fish pathology. *J. Fish Diseases*, 26:499-509.
- Alne-na-ei, A. A. (1998): The illegal fish farms in the Egyptian Delta: External lesions frequency, liver histopathology and heavy metals concentrations in the muscle tissue. *Egypt. J. Aquat. Biol. & Fish.*, 2(4):119-144.
- Alne-na-ei, A.A. (2000): Levels of organochlorine pesticides (OCPS) and polychlorinated biphenyls (PCBS) in a common fish from illegal fish farms in Almenofiya province, Egypt. *Egypt. J. Aquat. Biol. & Fish.*, 4(4):17-36.
- Alne-na-ei, A.A. (2003): Contamination of irrigation and drainage canals and ponds in the Nile delta by heavy metals and its association with human health risks. *Egypt. J. Zool.*, 41:47-60.
- ANZECC and ARMCANZ, (2000): Australian and New Zealand guidelines for fresh and marine water quality. Australian and New Zealand Environment and Conservation Council and Agriculture and Resource Management Council of Australia and New Zealand, Canberra, Australia.
- APHA-American Public Health Association (1998): Standard methods for the examination of water and wastewater. 20th Ed., Greenberg, A.E.; Clesceri, L.S. and Eaton, A.D. (editors). APHA, WEF and AWWA, Washington D.C., USA, 1193 p.
- Authman, M.M.N. (2008): *Oreochromis niloticus* as a biomonitor of heavy metal pollution with emphasis on potential risk and relation to some biological aspects. *Global Veterenaria*, 2(3):104-109.
- Authman, M.M.N. and Abbas, H.H.H. (2007): Accumulation and distribution of copper and zinc in both water and some vital tissues of two fish species (*Tilapia zillii* and *Mugil cephalus*) of Lake Qarun, Fayoum Province, Egypt. *Pakistan J. Biol. Sci.*, 10(13):2106-2122.
- Authman, M.M.N.; Bayoumy, E.M. and Kenawy, A. M. (2008): Heavy metal concentrations and liver histopathology of *Oreochromis niloticus* in relation to aquatic pollution. *Global Veterenaria*, 2(3): 110-116.
- Barcarolli, I.F. and Martinez, C.B.R. (2004): Effects of aluminum in acidic water on hematological and physiological parameters of the neotropical fish *Leporinus macrocephalus* (Anostomidae). *Bull. Environ. Contam. Toxicol.*, 72:639-646.
- Barnhoorn, I.E.J. and van Vuren, J.H.J. (2004): The use of different enzymes in feral freshwater fish as a tool for the assessment of water pollution in South Africa. *Ecotox. Environ. Saf.*, 59:180-185.
- Brodeur, J.C.; Økland, F.; Finstad, B.; Dixon, D.G. and Mckinley, R.S. (2001): Effects of subchronic exposure to aluminium in acidic water on bioenergetics of Atlantic salmon (*Salmo salar*). *Ecotox. Environ. Saf.*, 49:226-234.
- Bruslé, J. and González I Anadon, G. (1996): The structure and function of fish liver. In: Munshi, J.S.D. and Dutta, H.M. (Eds.), *Fish Morphology*. Science Publishers Inc., USA, pp.: 77-93.
- Camargo, M.M.P.; Fernandes, M.N. and Martinez, C.B.R. (2009): How aluminium exposure promotes osmoregulatory disturbances in the neotropical freshwater fish *Prochilus lineatus*. *Aquat. Toxicol.*, 94: 40-46.
- Casarini, D.C.P.; Dias, C.L. and Alonso, C.D. (2001): Relatório de estabelecimento de valores orientadores para solos e águas subterrâneas no Estado de São Paulo. Série Relatórios. CETESB, São Paulo.
- Chernoff, B. (1975): A method for wet digestion of fish tissue for heavy metal analyses. *Trans. Am. Fish. Soc.*, 104:803-804.
- Correia, T.G.; Narcizo, A.M.; Bianchini, A. and Moreira, R.G. (2010): Aluminum as an endocrine disruptor in female Nile tilapia (*Oreochromis niloticus*). *Comp. Biochem. Physiol., Part C* 151:461-466.
- D'Haese, P. C. and De Broe, M. E. (1994): Recent insights in the monitoring, diagnosis and treatment of aluminum-overload in dialysis patients. pp. 215-224. In: Nicolini, M.; Zatta, P. F. and Corain, B. (Eds.), *Aluminium in chemistry, biology and medicine*. Vol. 2, Life Chemistry Reports 11, Switzerland: Harwood Academic Publishers GmbH.
- El Sehamy, M.I.I. (2001): Ecological studies on various categories of the zooplankton in Bahr Shebeen Canal and Al-Atf drainage, Al-Minufiya Province. Ph. D. Thesis, Zoology Department, Faculty of Science, Minufiya University, 331p.
- Fabacher, D.L. and Baumann, P.C. (1985): Enlarged livers and hepatic microsomal mixed-function oxidase components in tumor-bearing brown bullheads from a chemically contaminated river. *Environ. Toxicol. Chem.*, 4:703-710.
- Feist, S. W.; Lang, T.; Stentiford, G. D. and Köhler, A. (2004): The use of liver pathology of the European flatfish, dab (*Limanda limanda* L.)

- and flounder (*Platichthys flesus* L.) for monitoring biological effects of contaminants. ICES Techniques in Marine Environmental Science, 28:47p.
- Förlin, L.; Haux, C.; Karkson-Norgren, L.; Runn, P. and Larsson, A. (1986): Biotransformation enzyme activities and histopathology in rainbow trout, *Salmo gairdneri*, treated with cadmium. *Aquat. Toxicol.*, 8(1):51-64.
- Garg, S.; Gupta, R.K. and Jain, K.L. (2009): Sublethal effects of heavy metals on biochemical composition and their recovery in Indian major carps. *J. Hazard. Mater.*, 163:1369-1384.
- Ibrahim, S.A. and Tayel, S.I. (2005): Effect of heavy metals on gills of *Tilapia zillii* inhabiting the River Nile water (Damietta branch) and El-Rahawy drain. *Egypt. J. Aquat. Biol. & Fish.*, 9(2):111-128.
- ICES (2006): Report of the ICES/BSRP Sea-going Workshop on Fish Disease Monitoring in the Baltic Sea (WKFDM), 5–12 December 2005. ICES CM 2006/BCC:02, 89pp.
- Karadede, H.; Oymak, S. A. and Ünlü, E. (2004): Heavy metals in mullet, *Liza abu* and Catfish, *Silurus triostegus*, from the Atatürk Dam Lake (Euphrates), Turkey. *Environ. Int.*, 30(2):183-188.
- Kazi, T.G.; Jalbani, N.; Baig, J.A.; Kandhro, G.A.; Afridi, H.I.; Arain, B.M.; Jamali, M.K. and Shah, A.Q. (2009): Assessment of toxic metals in raw and processed milk samples using electrothermal atomic absorption spectrophotometer. *Food Chem. Toxicol.*, 47: 2163-2169.
- Khallaf, E.A. and Authman, M. (1991): A study of some reproduction characters of *Bagrus bayad*, Forskal, in Bahr Shebeen Canal. *J. Egypt. Ger. Soc. Zool.*, 4:123-138.
- Khallaf, E.A.; Galal, M. and Authman, M. (1994): A study of pesticides residues in *Oreochromis niloticus* (L.) muscles from a Nile drainage canal. *J. Egypt. Ger. Soc. Zool.*, 15(A):491-508.
- Khallaf, E.A.; Galal, M. and Authman, M. (1995): A study of the seasonal variation of pesticides contamination in a Nile Drainage Canal water, and their subsequent occurrence in some *Oreochromis niloticus* organs. pp. 89-120. In: Proceedings of the Fifth International Conference, Environmental Protection is A Must, 25-27 April 1995, National Institute of Oceanography and Fisheries, Alexandria, Egypt.
- Khallaf, E.A.; Galal, M. and Authman, M. (1998): Assessment of heavy metals pollution and their effects on *Oreochromis niloticus* in aquatic drainage water. *J. Egypt. Ger. Soc. Zool.*, 26(B):39-74.
- Khallaf, E.A.; Galal, M. and Authman, M. (2003): The biology of *Oreochromis niloticus* in a polluted canal. *Ecotoxicology*, 12:405-416.
- Liao, Chun-Yang; Fu, Jian-Jie; Shi, Jian-Bo; Zhou, Qun-Fang; Yuan, Chun-Gang and Jiang, Gui-Bin (2006): Methylmercury accumulation, histopathology effects, and cholinesterase activity alterations in medaka (*Oryzias latipes*) following sublethal exposure to methylmercury chloride. *Environ. Toxicol. & Pharmacol.*, 22:225-233.
- Long, S.M.; Ryder, K.J. and Holdway, D.A. (2003): The use of respiratory enzymes as biomarkers of petroleum hydrocarbon exposure in *Mytilus edulis planulatus*. *Ecotox. Environ. Saf.*, 55:261-270.
- Mendil, D.; Demirci, Z.; Tuzen, M. and Soylak, M. (2010): Seasonal investigation of trace element contents in commercially valuable fish species from the Black sea, Turkey. *Food Chem. Toxicol.*, 48:865-870.
- Moiseenko, T.I.; Gashkina, N.A.; Sharova, Yu.N. and Kudriavtseva, L.P. (2008): Ecotoxicological assessment of water quality and ecosystem health: A case study of the Volga River. *Ecotox. Environ. Saf.*, 71:837- 850.
- Moon, T.W.; Walsh, P.J. and Mommsen, T.P. (1985): Fish hepatocytes: a model metabolic system. *Can. J. Fish & Aquat. Sci.*, 42:1772-1782.
- Munshi, J.S.D. and Dutta, H.M. (Eds.) (1996): *Fish Morphology: Horizon of New Research*. Science Publishers, Inc., USA.
- Offem, B.O.; Akegbejo-Samsons, Y. and Omoniyi, I.T. (2007): Biological assessment of *Oreochromis niloticus* (Pisces: Cichlidae; Linne, 1958) in a tropical floodplain river. *African J. Biotechnol.*, 6(16):1966-1971.
- Osman, A.G.M.; Mekkawy, I.A.; Verreth, J. and Kirschbaum, F. (2007): Effects of lead nitrate on the activity of metabolic enzymes during early developmental stages of the African catfish, *Clarias gariepinus* (Burchell, 1822). *Fish Physiol. Biochem.*, 33:1-13.
- Ozden, O. (2010): Micro, macro mineral and proximate composition of Atlantic bonito and horse mackerel: a monthly differentiation. *Int. J. Food Sci. Technol.*, 45:578-586.
- Pandey S.; Parvez S.; Sayeed I.; Haque R.; Bin-Hafeez B. and Raisuddin S. (2003): Biomarkers of oxidative stress: a comparative study of river Yamuna fish *Wallago attu* (Bl. & Schn.). *Sci. Total. Environ.*, 309:105-115.
- Peuranen, S.; Keinänen, M.; Tigerstedt, C. and Vuorinen, P.J. (2003): Effects of temperature on

- the recovery of juvenile grayling (*Thymallus thymallus*) from exposure to Al+Fe. *Aquat. Toxicol.*, 65: 73-84.
- Roberts, R. J. (2001): *Fish Pathology*. 3rd ed., W.B. Saunders, Philadelphia, PA, 462p.
- Roy, S. and Bhattacharya, S. (2006): Arsenic-induced histopathology and synthesis of stress proteins in liver and kidney of *Channa punctatus*. *Ecotox. Environ. Saf.*, 65:218-229.
- Sargazi, M.; Roberts, N.B. and Shenkin, A. (2001): In-vitro studies of aluminium-induced toxicity on kidney proximal tubular cells. *J. Inorg. Biochem.*, 87:37-43.
- Ščančar, J.; Stibilj, V. and Milačič, R. (2004): Determination of aluminium in Slovenian foodstuffs and its leachability from aluminium-cookware. *Food Chem.*, 85:151-157.
- Shah, A.Q.; Kazi, T.G.; Baig, J.A.; Arain, M.B.; Afridi, H.I.; Kandhro, G.A.; Wadhwa, S.K. and Kolachi, N.F. (2010): Determination of inorganic arsenic species (As³⁺ and As⁵⁺) in muscle tissues of fish species by electrothermal atomic absorption spectrometry (ETAAS). *Food Chem.*, 119:840-844.
- Shalloof, K.A.Sh. and Salama, H.M.M. (2008): Investigations on Some Aspects of Reproductive Biology in *Oreochromis niloticus* (Linnaeus, 1757) Inhabited Abu-Zabal Lake, Egypt. *Global Veterinaria*, 2(6):351-359.
- Silva, V.S.; Nunes, M.A.; Cordeiro, J.M.; Calejo, A.I.; Santos, S.; Neves, P.; Sykes, A.; Morgado, F.; Dunant, Y. and Gonçalves, P.P. (2007): Comparative effects of aluminum and ouabain on synaptosomal choline uptake, acetylcholine release and (Na⁺/K⁺)ATPase. *Toxicology*, 236:158-177.
- Sloof, W.; van Kreul, C.F. and Baars, A.J. (1983): Relative liver weights and xenobiotic-metabolizing enzymes of fish from polluted surface waters in The Netherlands. *Aquat. Toxicol.*, 4:1-14.
- Stentiford G.D.; Longshaw, M.; Lyons, B.P.; Jones, G.J.; Green, M. and Feist, S.W. (2003): Histopathological biomarkers in estuarine fish species for the assessment of biological effects of contaminants. *Mar. Environ. Res.*, 55(2):137-159.
- Triebkorn, R.; Köhler, H.R.; Honnen, W.; Schramm, M. and Adams, S.M. (1997): Induction of heat shock proteins, changes in liver ultra-structure, and alterations of fish behaviour: are these biomarkers related and are they useful to reflect the state of pollution in the field? *J. Aquat. Ecosyst. Stress Recov.*, 6:57-73.
- van Dyk, J.C.; Pieterse, G.M. and van Vuren, J.H.J. (2007): Histological changes in the liver of *Oreochromis mossambicus* (Cichlidae) after exposure to cadmium and zinc. *Ecotox. Environ. Saf.*, 66:432-440.
- Vuorinen, P.J.; Keinänen, M.; Peuranen, S. and Tigerstedt, C. (2003): Reproduction, blood and plasma parameters and gill histology of vendace (*Coregonus albula* L.) in long-term exposure to acidity and aluminium. *Ecotox. Environ. Saf.*, 54:255-276.
- Walton, R.C.; McCrohan, C.R.; Livens, F.R. and White, K.N. (2009): Tissue accumulation of aluminium is not a predictor of toxicity in the freshwater snail, *Lymnaea stagnalis*. *Environ. Pollut.*, 157:2142-2146.
- West, G. (1990): Methods of assessing ovarian development in fishes – a review. *Australian Journal of Marine and Freshwater Research*, 41: 199-222.
- Wester, P.W. and Canton, J.H. (1986): Histopathological study of *Oryzias latipes* (medaka) after long-term β -hexachlorocyclohexane exposure. *Aquat. Toxicol.*, 9:21-45.
- Yilmaz, F.; Özdemir, N.; Demirak, A. and Levent Tuna, A. (2007): Heavy metal levels in two fish species *Leuciscus cephalus* and *Lepomis gibbosus*. *Food Chem.*, 100: 830-835.
- Zaki, M.S.; Mostafa, S.O.; Fawzi, O.M.; Khafagy M. and Bayumi, F.S. (2009): Clinicopathological, Biochemical and Microbiological Change on Grey Mullet Exposed to Cadmium Chloride. *American-Eurasian J. Agric. & Environ. Sci.*, 5(1): 20-23.

11/25/2011

The Mushroom Extract Schizophyllan Reduces Cellular Proliferation and Induces G2/M Arrest in MCF-7 Human Breast Cancer Cells

Eiman Aleem

Alexandria University, Faculty of Science, Department of Zoology, Division of Molecular Biology, Moharram Bey 21511, Alexandria, Egypt.

eiman.aleem@gmail.com

Abstract: Breast cancer is the most common cancer in women worldwide. It is also the principle cause of death from cancer among women globally. Several lines of evidence suggest that dietary mushrooms may decrease breast cancer incidence. Schizophyllan (SCH) is a polysaccharide isolated from the medicinal mushroom *S. commune* and has potential anticancer effects. In a recent study we have demonstrated that SCH alone or in combination with tamoxifen (TAM) reduced the incidence of 7, 12 Dimethylbenz(α)anthracene (DMBA)-induced mammary carcinomas in mice through inhibition of cellular proliferation. The goal of the present work was to study the molecular mechanism through which SCH inhibits cell proliferation using the estrogen receptor positive human breast cancer cells (MCF-7) in vitro. MCF-7 cells were treated with different concentrations of SCH, and the following parameters were studied: cell growth, apoptosis, cell cycle kinetics using flow cytometry and expression of cell cycle regulatory proteins by Western blot. It was found that 1500 μ g/ml of SCH reduced cell viability and this was not due to cell death by apoptosis but due to G2/M cell cycle phase arrest. Furthermore, the molecular mechanism underlying the G2/M phase arrest involved an increased phosphorylation at the inhibitory tyrosine 15 site of CDK1 associated with accumulation of p53. Taken together, this is the first study to show direct anticancer effects of SCH on human breast cancer cells in culture. The therapeutic implications of SCH in human breast cancer warrant further investigation.

[Eiman Aleem **The Mushroom Extract Schizophyllan Reduces Cellular Proliferation and Induces G2/M Arrest in MCF-7 Human Breast Cancer Cells**] Life Science Journal, 2011; 8(4):777-784] (ISSN: 1097-8135). <http://www.lifesciencesite.com>.

Keywords: schizophyllan, mushroom, MCF-7 cells, *Schizophyllum commune*, apoptosis, cell cycle, CDK1, p53

1. Introduction

Breast cancer is the most common cancer in women worldwide. It is also the principle cause of death from cancer among women globally (Parkin, 2008). Treatment options for breast cancer patients include surgery, radiation therapy, chemotherapy, and targeting therapies. However, most drugs for chemoprevention have deleterious side effects. It has been reported that long-term administration of tamoxifen (TAM), a widely used antiestrogenic drug for chemotherapy and for the chemoprevention of breast cancer (Jordan, 2003), results in serious adverse effects including endometrial cancer (Killackey *et al.*, 1985; Bernstein *et al.*, 1999). Mushroom species or their constituent bioactive agents have been tested against several major forms of human cancer including stomach, colon, lung and liver and have been shown to be protective in numerous experimental models (Kidd, 2000). Several lines of evidence suggest that dietary mushrooms may decrease breast cancer incidence. In a case-control study of Chinese women with breast cancer, dietary intake of 10 g of fresh mushrooms or 4 g of dried mushroom powder significantly decreased breast cancer in pre- and postmenopausal women (Zhang *et al.*, 2009). Furthermore, (Kodama *et al.*, 2002)

reported that 69% of breast cancer patients consuming whole maitake mushroom powder showed significant cancer regression and marked symptom improvement. In cancer patients the maitake D-fraction, an antitumor polysaccharide fraction, hindered metastatic progression, reduced the expression of tumor markers and increased natural killer cell activity in all patients (Kodama *et al.*, 2003). Schizophyllan (SCH) is a polysaccharide isolated from the inedible mushroom *S. commune* (Mwt ~ 450 kD). It inhibits solid Sarcoma 180 tumor when injected by intraperitoneal or intravenous route (Komatsu *et al.*, 1969). In cervical cancer, SCH prolonged survival and time to recurrence for stage II but not stage III cases (Okamura *et al.*, 1989; Miyazaki *et al.*, 1995) and showed added effectiveness when injected directly into the tumor mass (Nakano *et al.*, 1996). In a randomized trial SCH, also known as SPG, combined with conventional chemotherapy improved the long term survival rate of patients with ovarian cancer (Inoue *et al.*, 1993). In a recent study (Aleem *et al.*, 2011) have demonstrated that SCH alone or in combination with TAM reduced the incidence of 7, 12 Dimethylbenz(α)anthracene (DMBA)-induced mammary carcinomas in mice. The DMBA-induced mammary carcinomas were estrogen receptor-positive

(ER+ve). SCH and TAM equally decreased the proliferating cell nuclear antigen (PCNA) labeling index, a marker for proliferating cells, relative to DMBA in mammary tumors. These mice developed hepatocellular carcinoma (HCC) as well and SCH but not TAM reduced the development of HCC, decreased PCNA labeling index in HCC as well as increased the levels of caspase-3 expression. It is noteworthy to mention that SCH did not have any adverse side effects on normal mammary gland or liver (Aleem et al., 2011). The results of the in vivo study prompted the further investigation of the molecular mechanisms of anticancer effects of SCH in vitro in an ER+ve breast cancer cell line (MCF-7). In the present study SCH reduced cell proliferation, and induced cell cycle arrest at the G2/M phase, however it did not induce apoptosis. The G2/M arrest in the present work was caused by an increased tyrosine 15 phosphorylation of CDK1 and gradual accumulation of p53.

2 Materials and Methods

Cell culture

The human breast cancer cell line MCF-7 (ATCC, USA) was maintained in culture in DMEM containing glucose, sodium pyruvate and glutamine (Gibco, UK) supplemented with 10% Fetal Bovine Serum (FBS), penicillin (100 units/ml), and streptomycin (50 µg/ml) (Gibco, UK). Cells were maintained at 37 °C in a humidified atmosphere containing 5% CO₂ and treated with different concentrations of SCH (CPN spol. s.r.o, Czech Republic) dissolved in sterile water.

Viability assay

Cell viability was measured using alamar blue® viability assay (Ahmed *et al.*, 1994) according to manufacturer's protocol. Briefly, cells were seeded at a density of 5000 cells per one well of 96-well plates in triplicates and allowed to grow for 24 hrs. Different concentrations of SCH were added and cells incubated for four days. Four hours before analysis 10% of alamar blue® solution diluted in culture medium was added and cells were incubated at 37 °C. Fluorescence was measured at 550/590 nm using a microplate reader.

Cell Cycle and flow cytometry

Cells were seeded in 10 cm dishes, allowed to grow until subconfluency then treated with different concentrations of SCH for 24 hrs. Cells were then trypsinized, collected by centrifugation and washed twice with PBS then incubated for 10 min at 37°C in (0.34 mM Trisodium citrate.2 H₂O, 0.1% NP-40, 1.5 mM spermine tetrahydrochloride and 0.5 mM Tris (hydroxymethyl)-aminomethane containing trypsin)

followed by another 10 min incubation at 37°C in an equal volume of the same buffer, however, trypsin was substituted with a trypsin inhibitor. An equal volume of propidium iodide (PI) was added and cells were incubated for at least 15 min on ice in the dark. The samples were then finally analysed with a FACS Calibur (Becton Dickinson), and the data were processed with the Cell Quest software (Becton Dickinson).

Apoptosis assay

Cells were seeded in 96-well plates, treated with different concentrations of SCH for 48 h then processed for apoptosis analysis using the M30 Apoptosense® Elisa kit (Peviva Ab, Sweden) according to manufacturer's protocol.

Preparation of lysates and Western blot

Cells were lysed in modified RIPA buffer (50 mM Tris pH 7.4, 150 mM NaCl, 1% NP-40, 1 mM EDTA, 0.25% sodium deoxycholate). Proteases inhibitor cocktail (Roche, Germany) and phosphatase inhibitors (Sigma-aldrich, Germany) were freshly added. Lysates were centrifuged for 30 min at 16,100 xg at 4 °C, and supernatants were frozen at -80 °C until use. Protein concentrations were determined using the BCA protein assay (Pierce Biotechnology, Rockford, USA) according to manufacturer's protocol and concentrations measured in a microplate reader. Lysates (20 µg total protein per lane) were resolved on 12 % Bis-Tris SDS-PAGE gels. Proteins were transferred onto nitrocellulose membranes (Hybond, Amersham, UK), blocked with 5% milk in a Tris-Buffered Saline and Tween 20 (TBST) [19.97 mM Tris base, 135 mM NaCl, 0.1% Tween 20] or 5% Bovine Serum Albumin in TBST, and blotted with the following primary antibodies: mouse anti-p53 (Becton Dickenson, USA), rabbit anti-Cdk1 (Calbiochem), rabbit anti-phospho-Y15 Cdk1 (Cell Signaling Technology, USA), rabbit anti-cyclin D (Cell Signaling Technology, USA) and anti-tubulin (Sigma-aldrich, Germany). Membranes were routinely washed using TBST and incubated with anti-rabbit- or anti-mouse-IgG horseshoe peroxidase (HRP)-conjugated secondary antibody (Amersham, UK) and protein bands detected with the ECL chemiluminescence system (Amersham, UK). The bands were scanned and analysed by densitometry using ImageJ 1.44p software (Wayne Rasband, NIH, USA).

Statistics

Data were analysed for mean and standard deviation and significance was determined using student's t test. A *p* value ≤ 0.05 was considered significant.

3. Results

SCH reduces viability of MCF-7 cells

In the present study MCF-7 cells were treated with different concentrations of SCH (250, 500, 1000, and 1500 $\mu\text{g/ml}$) and cell viability was measured. The 250 and 500 $\mu\text{g/ml}$ SCH concentrations did not have an effect on viability of MCF-7 cells (Fig.1). After 48 hrs of treatment the surviving fraction of cells treated with 1000 and 1500 was 75% and 50%, respectively (Fig. 1). There were no surviving cells after treatment with 2000 $\mu\text{g/ml}$ (data not shown).

SCH does not induce apoptosis

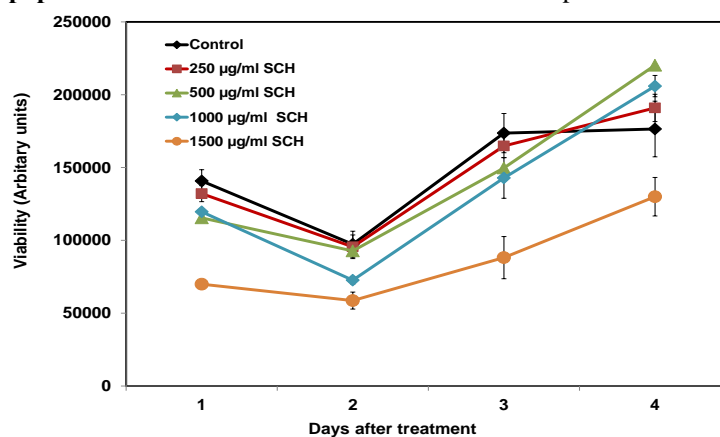


Figure 1. Schizophyllan reduces viability of MCF-7 cells in a dose-dependent manner. Cells were seeded in 96-well plates, treated with different concentrations of schizophyllan and their viability was monitored daily for 4 days. Viability was measured using alamar blue® viability assay.

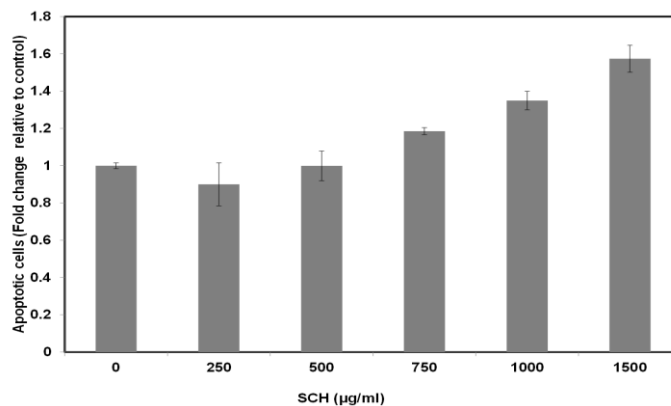


Figure 2. Schizophyllan does not induce apoptosis in MCF-7 cells. Cells were seeded in 96-well plates, treated with different concentrations of schizophyllan and apoptosis was scored after 48 hrs using M30 Apoptosense® Elisa assay.

SCH induces G2/M arrest

Analysis of the cell cycle profile by flow cytometry in control and SCH-treated MCF-7 cells revealed that SCH induced a gradual dose-dependent accumulation of cells at the G2/M phase, which was accompanied with a concomitant decrease in

In order to investigate why SCH reduced viability of breast cancer cells MCF-7 cells were treated with different concentrations of SCH for 48 hrs and measured apoptosis using M30 Apoptosense® Elisa assay (Fig. 2). Although SCH did induce some apoptotic death at high concentrations, however, the values were not statistically significant. This result was also confirmed by flow cytometry (Fig. 3E, the sub-G1 fraction). The values in Fig. 2 are expressed as fold change relative to untreated cells. The highest SCH concentration (1500 $\mu\text{g/ml}$) induced only a 1.6 fold increase in apoptotic cell death in comparison to untreated cells (Fig. 2).

the population of cells in G1 phase (Fig. 3). While the 500 $\mu\text{g/ml}$ concentration of SCH caused a 2.4 fold increase in the percentage of cells at G2/M phase, the 1000 and 1500 $\mu\text{g/ml}$ concentrations induced a 3.6 and 3.7 fold increase in comparison to untreated cells, respectively (Fig. 3 A, B, C, D, E).

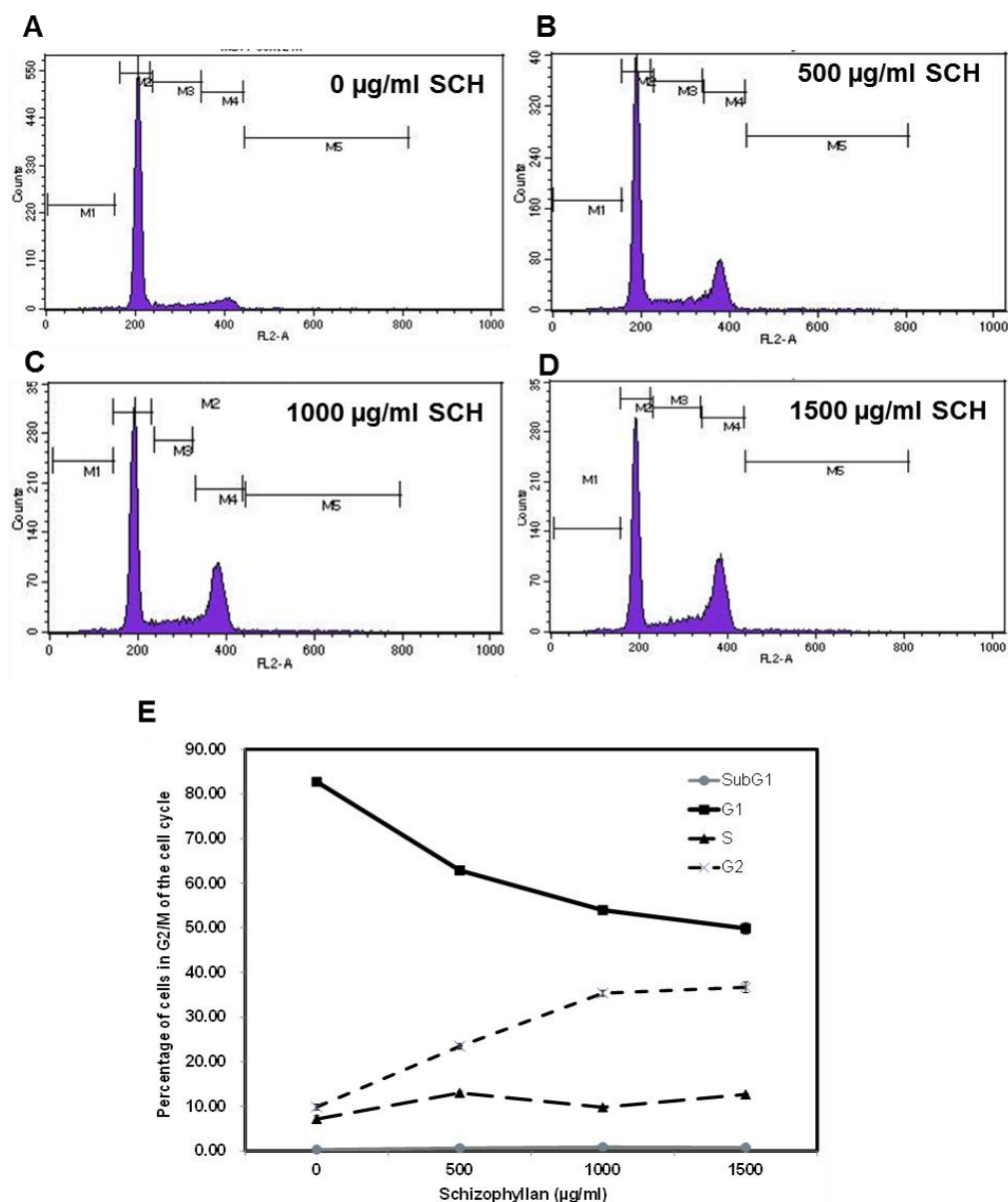


Figure 3. Schizophyllan induces G2/M arrest in MCF-7 cells. Cells were seeded in 10 cm dishes, treated with 0 µg/ml (A), 500 µg/ml (B), 1000 µg/ml (C) and 1500 µg/ml schizophyllan (D) for 24 hrs and the cell cycle profiles were then measured using propidium iodide staining and flow cytometry. Data were analysed using Cell Quest software.

SCH increases tyrosine 15 phosphorylation of CDK1 and induces p53 accumulation

To investigate the mechanisms underlying the G2/M cell cycle arrest the protein levels of CDK1, the kinase regulating G2/M phase transition, and its phosphorylation status, as well as p53, which is one of the major proteins regulating G2 arrest were studied. SCH did not affect the levels of CDK1 protein but it significantly increased the tyrosine15 (Y15) phosphorylation (Fig. 4A). Densitometric analysis revealed a 4.5 fold increase in the Y15

phosphorylation by 1500 µg/ml SCH compared to control cells (Fig. 4B). Furthermore, SCH induced p53 accumulation in a dose-dependent dose. The highest concentration (1500 µg/ml) of SCH induced a 2.3 fold increase in p53 levels relative to control (Fig. 4C). In addition, SCH did not alter the levels of Cyclin D1, a major regulatory protein during G1 phase progression. The membrane was stripped and incubated with α -tubulin as loading control (Fig. 4A).

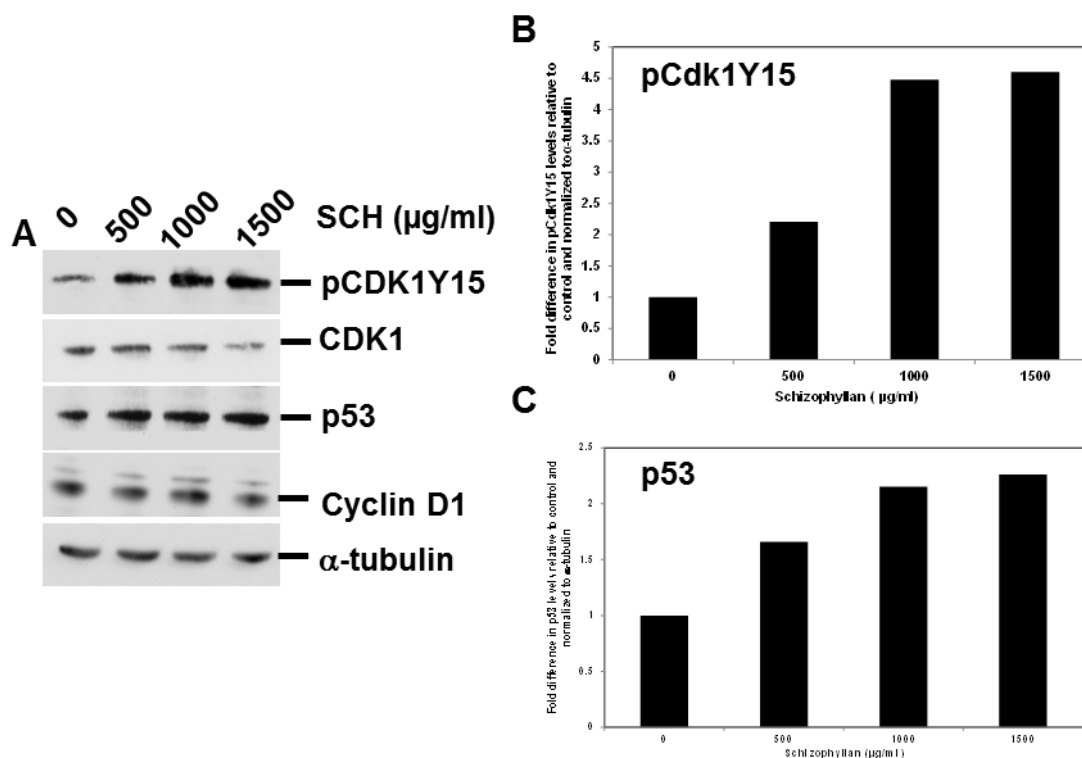


Figure 4. Schizophyllan increased the tyrosine 15 phosphorylation of CDK1 and induced accumulation of p53 in MCF-7 cells. Lysates were prepared from MCF-7 cells treated with 0 µg/ml, 500 µg/ml, 1000 µg/ml and 1500 µg/ml schizophyllan for 24 hrs, run on 12% SDS-PAGE, and analysed by Western blot (A). The intensities of the pCDK1Y15 and p53 protein bands normalized to α -tubulin were studied by densitometry, and the values plotted in (B) and (C), respectively.

4. Discussion

Medicinal mushrooms have been shown to have promising antitumor, immune modulating, antiviral and antiparasitic effects (Wasser and Weis, 1999). In a recent study (Aleem et al., 2011) demonstrated for the first time that schizophyllan (SCH), a β -D-glucan isolated from *S. commune* inhibited mammary and hepatic carcinomas induced in mice by DMBA through reduction of cell proliferation in both mammary and liver tumors and induction of apoptosis in liver but not in mammary tumors. The goal of the present study was to investigate the molecular mechanisms underlying the inhibition of cell proliferation using human breast cancer cells in vitro.

In the present work, treatment of the human breast cancer cell line MCF-7 with different concentrations of SCH resulted in significant reduction of cell growth at the 1500 µg/ml concentration. It has been previously reported that

mushroom polysaccharides primarily exert their antitumor activity via activation of the immune response of the host organism (Kim *et al.*, 2006), which may imply that they do not have a direct effect on tumor cells. However, the present study and previous reports have demonstrated direct effects of mushroom extracts on cell growth, cell cycle and apoptosis of several human cancer cell lines in vitro.

This is the first study to report a direct effect of the inedible mushroom schizophyllan on breast cancer cells in vitro, and is consistent with a previous study showing that extracts from five different edible mushrooms significantly suppressed cellular proliferation in MCF-7 cells (Martin and Brophy, 2010). Furthermore, extracts from PORT, shiitake and OYS mushrooms suppressed proliferation of both the ER-positive MCF-7 and the ER-negative MDA-MB-231 human breast cancer cells, without affecting proliferation of normal cells

(Jedinak and Sliva, 2008). In agreement with these results, extracts from *Inonotus obliquus* showed also antiproliferative effect on HT-29 cancer cells (Lee *et al.*, 2009), as well as on melanoma B16-F10 and HepG2 liver cancer cells (Youn *et al.*, 2008; Youn *et al.*, 2009). In the present study, it was found that the reduction in cell proliferation of MCF-7 cells was not due to cell death by apoptosis but due to G2/M cell cycle phase arrest. This result supports our recent *in vivo* study in which we demonstrated that SCH markedly reduced cell proliferation in DMBA-induced mammary carcinomas in mice without affecting the levels of caspase-3 expression, a central protein in the execution of apoptosis (Aleem *et al.*, 2011). Similarly, (Martin and Brophy, 2010) found only one mushroom species out of five (Maitake) that induced apoptosis in addition to inhibition of cell growth in MCF-7 cells. The results from the present study are also consistent with previous studies that demonstrated that extracts from the mushroom *Agaricus blazei* induced an arrest at the G2/M phase of the cell cycle in human gastric epithelial AGS cells (Jin *et al.*, 2006). Furthermore, the current study demonstrated that the molecular mechanism underlying the G2/M phase arrest by SCH is due to increased phosphorylation at the tyrosine 15 inhibitory site of CDK1 coupled with an accumulation of p53. It is known that CDK1 is the central regulator of mitosis and it has to bind to cyclin B in mitosis to be activated (Desai *et al.*, 1992). CDK1 bound to cyclin B is phosphorylated on residue T161 by CDK-activating kinase (CAK) to stabilize the cyclin B-CDK1 interaction and to induce the conformational rearrangements needed for kinase activity (Russo *et al.*, 1996; Larochelle *et al.*, 2007). However, the WEE1 and MYT1 kinases rapidly inactivate CDK1 by phosphorylating residues T14 and Y15, thereby blocking ATP binding and hydrolysis. Consequently, at low levels of cyclin B, CDK1 is inactive (Solomon *et al.*, 1990). Once cyclin B concentrations exceed a threshold, CDK1 is activated. Cyclin B-CDK1 phosphorylates and activates the CDC25 phosphatase, allowing CDC25 to remove the inhibitory T14 and Y15 phosphorylations on CDK1. Cyclin B-CDK1 is also a negative regulator of both MYT1 and WEE1, as these two kinases are inactivated upon cyclin B-CDK1 phosphorylation (Watanabe *et al.*, 1995; Okamoto and Sagata, 2007). Therefore, in the present study the increased Y15 phosphorylation induced by SCH deactivated CDK1 and this may be a potential mechanism leading to an accumulation of cells in the G2/M cell cycle phase. Furthermore, SCH induced the accumulation of p53. p53 protects mammals from neoplasia by inducing apoptosis, DNA

repair and cell cycle arrest in response to a variety of stresses (Taylor and Stark, 2001). P53 regulates the G2/M transition through several mechanisms. Part of the mechanism by which p53 blocks cells at the G2 checkpoint involves inhibition of CDK1. CDK1 is inhibited simultaneously by three transcriptional targets of p53, Gadd45, p21, and 14-3-3a (Taylor and Stark, 2001). Repression of the cyclin B1 gene by p53 also contributes to blocking entry into mitosis. p53 also represses the *cdk1* gene, to help ensure that cells do not escape the initial block. Repression of the topoisomerase II gene by p53 helps to block entry into mitosis and strengthens the G2 arrest (Taylor and Stark, 2001). Consistent with the present results (Zhou *et al.*, 2011) reported a G2/M phase arrest induced by *Ganoderma lucidum* (mushroom) and this arrest was associated with an accumulation of p53 in ovarian cancer cells.

Taken together, results from the present study coupled with recent results *in vivo* (Aleem *et al.*, 2011) provide a strong line of evidence that schizophyllan exerts multiple antitumor effects on human and mouse breast cancer cells. It inhibits cell proliferation and induces cell cycle phase arrest associated with the induction of p53, and therefore, its therapeutic implications in breast cancer warrant further investigation.

Acknowledgements

E.A. is currently funded by grants from the Science and Technology Development Fund, Egypt, and FP7 program from the European Union.

Corresponding author

Eiman Aleem

Alexandria University, Faculty of Science, Department of Zoology, Division of Molecular Biology, Moharram Bey 21511, Alexandria, Egypt.
eiman.aleem@gmail.com

References

- Aleem A, Daba A, Baddour N, El-Saadani M and Mansour A. (2011). Schizophyllan decreases the incidence of DMBA-induced mammary tumors in mice through reduction in cell proliferation without inducing apoptosis. *Proceedings of the American Association for Cancer Research's special conference on Advances in Breast Cancer Research: Genetics, Biology and Clinical Applications* p.138.
- Ahmed, S. A., Gogal, R. M., Jr., and Walsh, J. E. (1994). A new rapid and simple non-radioactive assay to monitor and determine the proliferation of lymphocytes: an alternative to [3H]thymidine

- incorporation assay. *Journal of immunological methods* **170**, 211-224.
- Bernstein, L., Deapen, D., Cerhan, J. R., Schwartz, S. M., Liff, J., McGann-Maloney, E., Perlman, J. A., and Ford, L. (1999). Tamoxifen therapy for breast cancer and endometrial cancer risk. *J Natl Cancer Inst* **91**, 1654-1662.
- Desai, D., Gu, Y., and Morgan, D. O. (1992). Activation of human cyclin-dependent kinases in vitro. *Molecular biology of the cell* **3**, 571-582.
- Inoue, M., Tanaka, Y., Sugita, N., Yamasaki, M., Yamanaka, T., Minagawa, J., Nakamuro, K., Tani, T., Okudaira, Y., Karita, T., and et al. (1993). Improvement of long-term prognosis in patients with ovarian cancers by adjuvant sizofiran immunotherapy: a prospective randomized controlled study. *Biotherapy* **6**, 13-18.
- Jedinak, A., and Sliva, D. (2008). Pleurotus ostreatus inhibits proliferation of human breast and colon cancer cells through p53-dependent as well as p53-independent pathway. *International journal of oncology* **33**, 1307-1313.
- Jin, C. Y., Choi, Y. H., Moon, D. O., Park, C., Park, Y. M., Jeong, S. C., Heo, M. S., Lee, T. H., Lee, J. D., and Kim, G. Y. (2006). Induction of G2/M arrest and apoptosis in human gastric epithelial AGS cells by aqueous extract of Agaricus blazei. *Oncology reports* **16**, 1349-1355.
- Jordan, V. C. (2003). Tamoxifen: a most unlikely pioneering medicine. *Nature reviews. Drug discovery* **2**, 205-213.
- Kidd, P. M. (2000). The use of mushroom glucans and proteoglycans in cancer treatment. *Alternative medicine review* **5**, 4-27.
- Killackey, M. A., Hakes, T. B., and Pierce, V. K. (1985). Endometrial adenocarcinoma in breast cancer patients receiving antiestrogens. *Cancer Treat Rep* **69**, 237-238.
- Kim, Y. O., Park, H. W., Kim, J. H., Lee, J. Y., Moon, S. H., and Shin, C. S. (2006). Anti-cancer effect and structural characterization of endopolysaccharide from cultivated mycelia of Inonotus obliquus. *Life sciences* **79**, 72-80.
- Kodama, N., Komuta, K., and Nanba, H. (2002). Can maitake MD-fraction aid cancer patients? *Alternative medicine review* **7**, 236-239.
- Kodama, N., Komuta, K., and Nanba, H. (2003). Effect of Maitake (Grifola frondosa) D-Fraction on the activation of NK cells in cancer patients. *Journal of medicinal food* **6**, 371-377.
- Komatsu, N., Okubo, S., Kikumoto, S., Kimura, K., and Saito, G. (1969). Host-mediated antitumor action of schizophyllan, a glucan produced by Schizophyllum commune. *Gann* **60**, 137-144.
- Larochelle, S., Merrick, K. A., Terret, M. E., Wohlbold, L., Barboza, N. M., Zhang, C., Shokat, K. M., Jallepalli, P. V., and Fisher, R. P. (2007). Requirements for Cdk7 in the assembly of Cdk1/cyclin B and activation of Cdk2 revealed by chemical genetics in human cells. *Molecular cell* **25**, 839-850.
- Lee, S. H., Hwang, H. S., and Yun, J. W. (2009). Antitumor activity of water extract of a mushroom, Inonotus obliquus, against HT-29 human colon cancer cells. *Phytotherapy research : PTR* **23**, 1784-1789.
- Martin, K. R., and Brophy, S. K. (2010). Commonly consumed and specialty dietary mushrooms reduce cellular proliferation in MCF-7 human breast cancer cells. *Exp Biol Med (Maywood)* **235**, 1306-1314.
- Miyazaki, K., Mizutani, H., Katabuchi, H., Fukuma, K., Fujisaki, S., and Okamura, H. (1995). Activated (HLA-DR+) T-lymphocyte subsets in cervical carcinoma and effects of radiotherapy and immunotherapy with sizofiran on cell-mediated immunity and survival. *Gynecologic oncology* **56**, 412-420.
- Nakano, T., Oka, K., Hanba, K., and Morita, S. (1996). Intratumoral administration of sizofiran activates Langerhans cell and T-cell infiltration in cervical cancer. *Clinical immunology and immunopathology* **79**, 79-86.
- Okamoto, K., and Sagata, N. (2007). Mechanism for inactivation of the mitotic inhibitory kinase Wee1 at M phase. *Proceedings of the National Academy of Sciences of the United States of America* **104**, 3753-3758.
- Okamura, K., Suzuki, M., Chihara, T., Fujiwara, A., Fukuda, T., Goto, S., Ichinohe, K., Jimi, S., Kasamatsu, T., Kawai, N., and et al. (1989). Clinical evaluation of sizofiran combined with irradiation in patients with cervical cancer. A randomized controlled study; a five-year survival rate. *Biotherapy* **1**, 103-107.
- Parkin, D. M. (2008). The role of cancer registries in cancer control. *International journal of clinical oncology* **13**, 102-111.
- Russo, A. A., Jeffrey, P. D., and Pavletich, N. P. (1996). Structural basis of cyclin-dependent kinase activation by phosphorylation. *Nature structural biology* **3**, 696-700.
- Solomon, M. J., Glotzer, M., Lee, T. H., Philippe, M., and Kirschner, M. W. (1990). Cyclin activation of p34cdc2. *Cell* **63**, 1013-1024.
- Taylor, W. R., and Stark, G. R. (2001). Regulation of the G2/M transition by p53. *Oncogene* **20**, 1803-1815.
- Wasser, S. P., and Weis, A. L. (1999). Therapeutic effects of substances occurring in higher Basidiomycetes mushrooms: a modern perspective. *Critical reviews in immunology* **19**, 65-96.

- Watanabe, N., Broome, M., and Hunter, T. (1995). Regulation of the human WEE1Hu CDK tyrosine 15-kinase during the cell cycle. *The EMBO journal* **14**, 1878-1891.
- Youn, M. J., Kim, J. K., Park, S. Y., Kim, Y., Kim, S. J., Lee, J. S., Chai, K. Y., Kim, H. J., Cui, M. X., So, H. S., Kim, K. Y., and Park, R. (2008). Chaga mushroom (*Inonotus obliquus*) induces G0/G1 arrest and apoptosis in human hepatoma HepG2 cells. *World journal of gastroenterology : WJG* **14**, 511-517.
- Youn, M. J., Kim, J. K., Park, S. Y., Kim, Y., Park, C., Kim, E. S., Park, K. I., So, H. S., and Park, R. (2009). Potential anticancer properties of the water extract of *Inonotus* [corrected] *obliquus* by induction of apoptosis in melanoma B16-F10 cells. *Journal of ethnopharmacology* **121**, 221-228.
- Zhang, M., Huang, J., Xie, X., and Holman, C. D. (2009). Dietary intakes of mushrooms and green tea combine to reduce the risk of breast cancer in Chinese women. *International journal of cancer* **124**, 1404-1408.
- Zhou, H., Roy, S., Cochran, E., Zouaoui, R., Chu, C. L., Duffner, J., Zhao, G., Smith, S., Galcheva-Gargova, Z., Karlgren, J., Dussault, N., Kwan, R. Y., Moy, E., Barnes, M., Long, A., Honan, C., Qi, Y. W., Shriver, Z., Ganguly, T., Schultes, B., Venkataraman, G., and Kishimoto, T. K. (2011). M402, a novel heparan sulfate mimetic, targets multiple pathways implicated in tumor progression and metastasis. *PloS one* **6**, e21106.

11/25/2011

Glutathione S-Transferase Gene Polymorphisms (GSTM1 and GSTT1) in Vitiligo Patients

Fatma A. Abd Rabou¹, Hesham A.Elserogy², Shereen F. Gheida^{*1} and Amal A. EL-Ashmawy¹

Departments of Dermatology and Venereology¹ and Clinical Pathology², Faculty of Medicine, Tanta University, Egypt
gheidas@yahoo.com

Abstract: Background: Vitiligo is an acquired pigmentary disorder of the skin characterized by white areas on the skin and pigment-producing cells (melanocytes) are absent from vitiligo lesions. Oxidative stress is a major pathogenesis hypothesis of vitiligo. The glutathione S-transferases (GSTs) are group of polymorphic enzymes that are important in protection against oxidative stress and chemical toxicity. *Objectives:* The aim of this work was to study the relation between glutathione S-transferase gene polymorphisms (GSTM1 and GSTT1) and pathogenesis of vitiligo. *Subjects and Methods:* This study included 40 patients with vitiligo and 10 healthy subjects served as controls, attending the Outpatient Clinic of Dermatology and Venereology Department of Tanta University Hospitals. Blood samples were collected from all patients for detection of GSTM1 and GSTT1 polymorphisms using the multiplex polymerase chain reaction (PCR) and blood samples were collected from control subjects for comparison. *Results:* In this study, there was non significant association with null type of both GSTM1& GSTT1 genotype and vitiligo susceptibility. There was significant association of vitiligo risk with GSTM1 null/ GSTT1 null type as well as GSTM1 present/GSTT1 null and GSTM1 null/ GSTT1 present when compared to the GSTT1 present/ GSTM1 present. There was non significant association with GSTM1 null type of vitiligo in focal, segmental and generalized subtypes. There was significant association with GSTT1 null type of vitiligo in generalized subtypes but GSTT1 null type of vitiligo in focal and segmental types showed non significant association with vitiligo susceptibility. Non significant association was shown in GSTM1 null/GSTT1 null type of vitiligo in focal and generalized types while it was significant in segmental type. Significant association with GSTM1 present/GSTT1 null type of vitiligo in focal and generalized types but non significant in segmental type. The GSTM1 null/GSTT1 present types of vitiligo subtypes showed a significant association with focal and generalized types but non significant association in segmental type. Significant association with GSTM1 present/ GSTT1 present type in segmental and generalized types but non significant in focal type. *Conclusion:* Collectively, the mechanistic study revealed new pieces in the vitiligo "puzzle", such as GST and 4-Hydroxy-2-nonenal (HNE)-protein which, together with the known one, namely hydrogen peroxide (H₂O₂), may well be included in the hypothetic redox-regulated mechanism of melanocyte loss, and might represent good candidates as therapeutic targets for this skin disease.

[Fatma A. Abd Rabou, Hesham A.Elserogy, Shereen F. Gheida and Amal A. EL-Ashmawy **Glutathione S-Transferase Gene Polymorphisms (GSTM1 and GSTT1) in Vitiligo Patients**] Life Science Journal, 2011;8(4):785-792] (ISSN:1097-8135). <http://www.lifesciencesite.com>

Key words: Vitiligo, Glutathione S-transferase, Oxidative stress

1. Introduction

Vitiligo is an acquired skin disorder characterized by white depigmented patches due to disappearance of functioning melanocytes and loss of melanin in the epidermis. It is the most common pigmentary disorder affecting 0.1-2% of the world's population, irrespective of race and gender⁽¹⁾. The pathogenesis of vitiligo is proposed to be associated with many factors as genetic, mechanical, biochemical, neurological and immunological factors. The genetic background underlying vitiligo susceptibility had been proposed in various studies⁽²⁾. Oxidative stress and accumulation of free radicals in the epidermal layer of affected skin have been suspected to be involved in the pathophysiology of vitiligo. There is an impairment of antioxidative system in vitiligo melanocytes with resultant free radical mediated damage in melanocyte⁽³⁾.

The GST genes represent major group of

detoxification enzymes, and are main defense against oxidative stress⁽⁴⁾. They comprise several isoenzymes, including alpha, mu, pi, theta, and zeta gene families and are known to be induced under conditions of oxidative stress⁽⁵⁾. The GST contribute in the protection against a broad range of compounds including carcinogens, pesticides, antitumor agents, and environmental pollutants⁽⁶⁾. The GST gene polymorphisms (GSTM1 and GSTT1) were thought that they play a role in the susceptibility of several diseases e.g. asthma and rheumatoid arthritis⁽⁷⁾. It was suggested to have a role in susceptibility to vitiligo⁽⁸⁾.

Aim of the Work

The aim of the work was to study the relation between the glutathione S- transferase gene polymorphism (GSTM1 and GSTT1) and pathogenesis of vitiligo.

2. Subjects and Methods

This study included 40 patients with vitiligo and 10 healthy subjects served as controls, attending the Outpatient Clinic of Dermatology and Venereology Department of Tanta University Hospitals during the period from February 2010 to April 2011.

(I) Control group:

They included 10 normal healthy subjects; 6 males and 4 females. Their ages ranged from 24-36 years.

(II) Vitiligo patients:

They included 40 vitiligo patients; 23 males and 17 females. Their ages ranged from 7-67 years.

Vitiligo patients group was subdivided into:

Focal type, segmental type and generalized type

All the studied persons were subjected to:

1-Full history taking: including personal (age and gender), past, present (onset and duration), family history.

2-Informed consent signing.

3-Full clinical examination : to exclude any other skin or systemic diseases as vitiligo, alopecia areata, systemic lupus erythromatosus and other autoimmune diseases as thyroid disease , rheumatoid arthritis, bronchial asthma and alcoholic liver disease

4-Laboratory investigations:

A-Routine laboratory investigations

B-Specific laboratory investigations which included:

Identification of the distribution of GSTT1 and GSTM1 genotypes

Blood samples:

About 2 ml venous blood samples were collected in the morning into an EDTA vacutainer tubes used for genomic DNA extraction.

Extraction of genomic DNA from whole blood:

By utilizing silica-based membrane technology in the form of a convenient spin column provided by Gene JET genomic DNA Purification Kit cat. no. K0722.

Blood samples were digested with proteinase K. RNA was removed by treating the samples with RNAase. The lysate was then mixed with ethanol and loaded on the purification column where the DNA binds to the silica membrane. Genomic DNA was then eluted under low ionic strength conditions with the Elution Buffer.

Amplification of samples DNA:

DNA amplification by multiplex PCR was used

to detect the presence or absence of the GSTM1, GSTT1 and CYP1A1 genes in the genomic DNA samples, simultaneously in the same tube. The CYP1A1 genes were co-amplified and used as an internal control. The primers of GSTM1 gene were as follow: 5'-GAG GAA CTC CCT GAA AAG CTA AAG-3/ (forward) and 5'- CTC AAA TAT ACG GTG GAG GTC AAG-3/ (reverse). The GSTT1 gene was amplified with the following primers: 5'-TTC CCT ACT GGT CCT CAC ATC TC-3\ (forward) and 5'-TCA CCG GAT CAT GGC CAG CA-3/ (reverse). The primers of CYP1 gene are as follows: 5'-CTC CCT CTG GTT ACA GGA AGC TAT-3/ (forward) and 5'-CAA CCA GAC CAG GTA GAC AGA GTC-3/ (reverse).

The DNA of each sample was introduced in a reagent mixture containing an excess of deoxynucleoside 5'-triphosphates (dNTPs), biotinylated primers, and thermostable DNA polymerase (Taq) supplied by Dream Taq Green PCR Master Mix. Cat. no. K1089. (Fermentas)

The PCR was carried out using a GeneAmp PCR system 2700. The conditions were as follows; 35 cycles, each consisting of denaturation at 94°C for 30 s, annealing at 61°C for 30 s. and extension at 72°C for 30 s. The reaction cycles were preceded by 5 min denaturation at 94°C and were followed by 7 min extension at 72°C.

Detection of PCR products:

The PCR products were confirmed by electrophoresis on 2% agarose gel and visualized by ethidium bromide staining. DNA from samples positive for GSTM1 and GSTT1 genotypes yielded bands of 216bp and 459bp, respectively while the internal positive control (CYP1A1) PCR product corresponded to 349bp [Fig. 1].

Statistical analysis

Statistical presentation and analysis of the present study was conducted, using the mean, standard deviation, and chi-square test by SPSS V.11. Statistical significance was determined at a level of $p < 0.05^*$. $P < 0.001^*$ was considered highly significant.

3. Results

I- Clinical results were demonstrated in table-1

II-Laboratory results:-

In this study, there was non significant association with null type of GSTM1 ($P=0.790$) and null type of GSTT1 genotypes ($P=0.119$) and vitiligo susceptibility ($P > 0.05$) [Table 2].

In this study, further analysis of the combined effect of GSTM1 and GSTT1, both present type of GSTM1 and GSTT1 genes were compared to both

null, GSTM1 null, and GSTT1 null types. The results suggested a significant association of vitiligo risk with GSTM1 null/ GSTT1 null type ($P=0.048^*$) as well as GSTM1 present/ GSTT1 null ($P=0.011^*$) and GSTM1 null/GSTT1 present ($P=0.050^*$) when compared to the GSTM1 present/ GSTT1 present [Table 3].

Further analysis of GSTM1 and GSTT1 polymorphism in the vitiligo subtypes, three clinical types of vitiligo, such as focal, segmental, and generalized types were analyzed. As shown in [Table 4], there was non significant association with GSTM1 null type of vitiligo in focal, segmental and generalized subtypes (Focal $P=0.342$; Segmental $P=0.793$ and Generalized $P=0.752$). There was significant association with GSTT1 null type of vitiligo in generalized subtypes (Generalized $P=0.014^*$) but GSTT1 null type of vitiligo in focal and segmental types (Focal $P=0.813$; Segmental $P=0.583$) showed non significant association with vitiligo susceptibility [Table 4].

To analyze combined effect of GSTM1 and

GSTT1 in vitiligo subtypes, both present type of GSTM1 and GSTT1 genes were compared to both null, GSTM1 null, and GSTT1 null types with each subtypes. Non significant association was found in GSTM1 null/GSTT1 null type of vitiligo in focal and generalized types (Focal $P=0.058$; Generalized $P=0.099$) while it was significant in segmental type (Segmental $P=0.028^*$). Significant association with GSTM1 present/GSTT1 null type of vitiligo in focal and generalized types (Focal $P=0.028^*$ and generalized $P=0.009^*$) but non significant in segmental type (Segmental $P=0.357$). The GSTM1 null/GSTT1 present types of vitiligo subtypes showed a significant association with focal and generalized types (Focal $P=0.028^*$ and generalized $P=0.041^*$) but non significant association in segmental type (Segmental $P=0.179$). Significant association with GSTM1 present/ GSTT1 present type in segmental and generalized types (Segmental $P=0.028^*$ and generalized $P=0.050^*$) but non significant in focal type (Focal $P=0.059$) [Table 4].

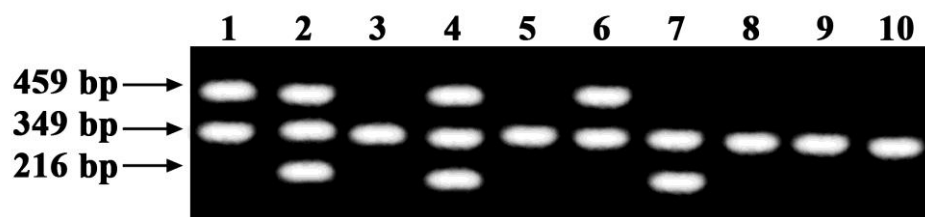


Fig. (1): Polymerase chain reaction products were analyzed on 2% ethidium bromide stained agarose gel.

Lanes 1, 6: GSTT1 positive (459, 349 bp).

Lanes 2, 4: GSTT1 and GSTM1 positive (459, 349 and 216 bp).

Lanes 3, 5, 8, 9, 10: GSTT1 and GSTM1 null alleles (349 bp)

Lanes 7: GSTM1 positive (349, 216 bp).

Table (1): Clinical characteristics of 40 Egyptian vitiligo patients and 10 healthy controls

	Vitiligo patient (NO=40)	Healthy controls (NO=10)	p. value	
Average age (year, mean \pm SD)	27.90 \pm 19.8	29.60 \pm 3.89	0.790	>0.05
Male/Female	23/17	6/4	0.886	>0.05
Duration (year, mean \pm SD)	5.12 \pm 5.84	-	-	-
Onset age (year, mean \pm SD)	22.77 \pm 17.91	-	-	-
Clinical types (Focal/ segmental/ generalized)	8/2/30	-	-	-
With/without family history +ve/ -ve	1/39	-	-	-

P.value <0.05 significant*

Table (2): Genotype and allele frequencies of the GSTs polymorphism among the patients and controls and the associations with risk of vitiligo

Genotypes	Patients (NO=40)		Controls (NO=10) ¹		X ²	p. value	
	NO	%	NO	%			
GSTM1	—	—	—	—	0.504	0.790	>0.05
Present (+)	19	47.5	6	60			
Null (-)	21	52.5	4	40			
GSTT1	—	—	—	—	2.42	0.119	>0.05
Present (+)	17	42.5	7	70			
Null (-)	23	57.5	3	30			

Table (3): Frequencies of the combined genotypes of GSTM1 and GSTT1 among the patients and controls and the associations with risk of vitiligo

Combined genotypes	Patients (NO=40)		Controls (NO=10)		X ²	p. value	
	n	%	n	%			
<i>GSTM1/GSTT1</i>	—	—	—	—			
<i>Null/null(-/-)</i>	12	30	2	20	3.256	0.048	<0.05*
<i>Present /Null(+/-)</i>	11	27.5	1	10	4.523	0.011	<0.05*
<i>Null/present(-/+)</i>	9	22.5	2	20	2.996	0.050	<0.05*
<i>Present/present(+/+)</i>	8	20	5	50	1.582	0.052	>0.05

P. value <0.05 significant*

Table (4): Comparison of GSTM1/GSTT1 frequencies between controls and clinical subtypes of vitiligo patients

Genotypes	Control (n=10)	Focal (n=8)			Segmental (n=2)			Generalized (n=30)		
	n (%)	n(%)	X ²	P	n (%)	X ²	P	n (%)	X ²	P
GSTM1										
Null (-)	4 (40)	5 (12.5)	0.900	0.342	1 (2.5)	0.075	0.793	15(37.5)	0.63	0.752
Present(+)	6 (60)	3 (7.5)			1 (2.5)			15(37.5)		
GSTT1										
Null (-)	3 (30)	2 (5)	0.063	0.813	1 (2.5)	0.305	0.583	20(50)	2.636	0.014
Present(+)	7 (70)	6 (15)			1 (2.5)			10(25)		
GSTM1/GSTT1										
-/-	2 (20)	2 (5)	1.325	0.058	1 (2.5)	1.865	0.028*	9(22.5)	2.72	0.099
+/-	1 (10)	-	2.63	0.028*	-	0.85	0.357	11(27.5)	3.25	0.009*
-/+	2(20)	3 (7.5)	1.963	0.028*	-	1.80	0.179	6(15)	2.93	0.041*
+/+	5 (50)	3 (7.5)	0.28	0.059	1 (2.5)	1.865	0.028*	4(10)	2.14	0.050*

3. Discussion

The results of the present study showed that, the genotype distribution of the GSTM1 and GSTT1 polymorphism between the patients and controls were detected as; there was a non-significant association with null type of GSTM1 and null type of GSTT1 genotypes and vitiligo susceptibility. These results agreed with *Guarneri et al.*⁽⁹⁾ as their study showed a non-significant association of GSTM1-null genotype and also GSTT1-null genotype with vitiligo patients. Also the current study agreed with *Uhm et al.*,⁽¹⁰⁾ as they showed a non-significant association between the disease and GSTT1-null genotype. But our results were different from *Uhm et al.*,⁽¹⁰⁾ as they showed significant associations between the disease and GSTM1-null genotype. On the other hand *Liu et al.*,⁽¹¹⁾ showed significant associations between the disease and GSTT1-null genotype, whereas the GSTM1-null genotype showed a trend toward association with vitiligo patients, in contrast to the current study, which showed neither associations.

In the present study, further analysis of the combined effect of GSTM1 and GSTT1, both present type of GSTM1 and GSTT1 genes were compared to both null, GSTM1 and GSTT1 types. The present results found a significant association of vitiligo risk with GSTM1 null/ GSTT1 null types as well as GSTM1 present/ GSTT1 null and GSTM1 null/GSTT1 present when compared to the GSTM1 present/ GSTT1 present and these results agreed with the study by *Liu et al.*,⁽¹¹⁾ as they showed the same significant association. Also the present results agreed with the study by *Uhm et al.*,⁽¹⁰⁾ that showed a significant association of the disease with GSTM1 null/GSTT1 null type as well as GSTM1 null/GSTT1 present type but not go with them as they found a non-significant association of the disease with GSTM1 present/ GSTT1 null type. This study goes with that done by *Guarneri et al.*,⁽⁹⁾ as it showed a significant association of GSTM1 null/GSTT1 null genotype and different from the present study as it showed a non-significant association of the disease with GSTM1 present/ GSTT1 null genotype and GSTM1 null/GSTT1 present genotype when compared to the GSTM1 present/ GSTT1 present and *Guarneri et al.*,⁽⁹⁾ who explained it on the basis that; increased vitiligo in GSTM1/GSTT1 double null subject can be expected because of the significant reduction in the basal antioxidant potential of melanocytes and inability to upregulate GSTM1/GSTT1 expression in response to oxidative stress caused by simultaneous lack of GSTM1 and GSTT1.

Further analysis of GSTM1 and GSTT1 polymorphism on the vitiligo subtypes, such as,

focal, segmental, and generalized were analyzed. In the present study there was non-significant association of GSTM1 null type of vitiligo patient in focal, segmental and generalized subtypes and these results were agreed with the studies by *Uhm et al.*,⁽¹⁰⁾ and *Liu et al.*,⁽¹¹⁾ as they showed that GSTM1 null type of vitiligo in segmental subtype showed non-significant association with the disease but these studies showed a significant association of the GSTM1 null type of vitiligo patients in focal and generalized subtypes and this explained by *Uhm et al.*,⁽¹⁰⁾ as different pathogenic mechanisms have been proposed according to the clinical subtypes of vitiligo, it is accepted that the pathogenic mechanism of segmental type vitiligo differs from focal and generalized types. Segmental type vitiligo is distinct in that distributed in dermatomal pattern and neurohumoral mechanism is considered to be involved.

In the present study, there was significant association with GSTT1 null type of vitiligo in generalized subtypes but GSTT1 null type of vitiligo in focal and segmental showed non-significant association with vitiligo susceptibility and these results agreed with *Liu et al.*,⁽¹¹⁾ as regard generalized and segmental subtypes and disagreed the present study; as it showed a significant association of the GSTT1 null type with vitiligo susceptibility in focal vitiligo. *Uhm et al.*,⁽¹⁰⁾ agreed with the current study about the association between GSTT1 null type and focal, segmental vitiligo subtypes and disagreed the current study as they showed a non-significant association of the GSTT1-null type of vitiligo in generalized subtypes.

In the current study, further analysis of the combined effect of GSTM1 and GSTT1 in vitiligo subtypes, both present type of GSTM1 and GSTT1 genes were compared to both null, GSTM1, and GSTT1 types in each vitiligo subtype. The present study showed a non-significant association of the GSTM1 null/GSTT1 null types of vitiligo in focal and generalized, but both were significant association with segmental type and these results disagreed with *Uhm et al.*,⁽¹⁰⁾ and *Liu et al.*,⁽¹¹⁾ as they showed a significant association in GSTM1 null/GSTT1 null types of vitiligo in focal and generalized subtypes, but non-significant in segmental subtype.

In the present study, there was a significant association of the GSTM1 present/GSTT1 null type of vitiligo in focal and generalized types but non-significant in segmental type and these results agreed with study by *Liu et al.*,⁽¹¹⁾ as it showed that the GSTM1-present/GSTT1-null type were significantly associated with focal and generalized vitiligo but

non-significant association in segmental type. The present study results agreed with *Uhm et al.*,⁽¹⁰⁾ as it showed a non-significant association with GSTM1 present/ GSTT1 null type in segmental subtypes of vitiligo and disagreed with *Uhm et al.*,⁽¹⁰⁾ as it showed a non-significant association with GSTM1 present/ GSTT1 null type in focal and generalized subtypes of vitiligo.

In the current study, the GSTM1 null/GSTT1 present types of vitiligo subtypes show a significant associations with focal and generalized types but non-significantly associated in segmental type of vitiligo and these results agreed with a study by *Liu et al.*,⁽¹¹⁾. Also the present study agreed with *Uhm et al.*,⁽¹⁰⁾ who showed that GSTM1 null/GSTT1 present types of vitiligo subtypes showed a significant association with focal and generalized types and the present study different from *Uhm et al.*,⁽¹⁰⁾ as they showed a significant association of the GSTM1 null/ GSTT1 present type with segmental subtype of vitiligo.

Discrepancies between the studies done in these fields suggest that the role and the relative importance of each GST isoform in the pathogenesis of vitiligo are variable and probably correlated with several factors. Indeed, GSTs are only a part of the system of enzymatic and non-enzymatic component that maintain the redox homeostasis of the organism. The functional equilibrium among these components is the results of evolutionary selection and adaptation to environmental conditions; consequently, multiple configurations of the system exist in different populations, reflecting the wide variability of genetic, geographical, environmental, and lifestyle factors. This view is also supported by literature data on the frequency of GSTM1 null and GSTT1 null in healthy subjects, 36-54.67% and 8-52.6, respectively.⁽⁹⁾

As for GST activity, its inhibition could also be due to polymorphic changes in two GST isoforms (GSTM1 and GSTT1), that are characteristic for vitiligo patients,⁽¹⁰⁾ and cause partial loss of the total enzyme activity and impaired HNE detoxification.⁽¹²⁾ The GSTs, and in particular the isoform GSTM1, exert several nonenzymatic functions relevant to programmed cell death to the control of intracellular nitric oxide (NO) levels, acting as a NO carrier, to the direct regulation of kinase pathways, to inducible NO synthase upregulation through nuclear transcription factor kappa β translocation and other cellular functions.⁽¹³⁾

As oxidative stress is due to increased epidermal levels of H₂O₂ is a leading cytotoxic mechanism of melanocyte loss in vitiligo. Therefore, abnormal levels of H₂O₂ due to HNE-induced formation and to decreased neutralization by

defective catalase(CAT)⁽³⁾ may shift its regulatory action towards the expression of various cytokines and growth factors controlled through redox signaling, among which are vascular endothelial growth factor, platelet-derived growth factor, monocyte chemotactic protein-1⁽¹⁴⁾, IL-6, IL-8, and TNF- α ⁽¹⁵⁾.

The HNE- protein is a stable product of lipid peroxidation, easily reacting with proteins and DNA, thus possessing important regulatory properties towards cell growth and differentiation,⁽¹⁶⁾ as well as towards cellular death and survival⁽¹⁷⁾. HNE homeostasis in the organism is controlled by GSTs gene which is a family of conjugating enzymes playing a key role in the phase II biotransformation of organic xenobiotics, in the metabolism of endogenous electrophils, including HNE, and in the deactivation of reactive oxygen species, that are involved in cellular processes of inflammation and degenerative diseases.⁽¹³⁾ Of note, HNE can be a substrate for GST, either inhibiting enzyme activity, or regulating its expression, depending on concentration⁽¹²⁾. Impaired HNE metabolism consequently increases the probability of HNE protein adduct formation, followed by the inactivation of HNE-sensitive enzymes such as CAT and GST⁽¹⁸⁾. Of interest, it has been shown that HNE-CAT complexes possess neoauto-antigen properties, inducing the consequent autoimmune reaction frequently observed in the patients affected by vitiligo.⁽¹⁹⁾

Notably, HNE has been recognized as an endogenous ligand for epidermal growth factor receptor,⁽¹¹⁾ which may result in NADPH oxidase induction and increased H₂O₂ formation.⁽¹⁵⁾ The defects of GST expression and activity towards HNE in vitiligo keratinocytes result in dysregulated levels of this electrophile. Normally, HNE at low concentrations regulates stress gene response and apoptosis via the activator protein-1 dependent pathways inhibiting the pro-survival extracellular regulation kinase (ERK1/2) and protein kinase B-regulated pathways⁽²⁰⁾

Accordingly, *Townsend et al.*,⁽²¹⁾ found an early time-dependent inhibition of ERK1/2 and protein kinase B- phosphorylation in normal human keratinocytes exposed to HNE. They also observed inhibited UV-induced protein kinase B, and enhanced spontaneous +UV-induced p53 phosphorylation in vitiligo keratinocytes, probably caused by endogenous HNE. Impaired GSTM1 expression/induction may also negatively affect cellular functions, by acting in a nonenzymatic mode, for example, inducing apoptosis signal regulating kinase-1 controlled apoptosis normally inhibited by GSTM1,⁽¹⁷⁾ or dysregulating the protein

kinase cascade⁽²¹⁾.

In cultures of keratinocytes from patients with vitiligo, *Kostyuk et al.*,⁽²²⁾ observed: (i) reduced expression of GSTM1 mRNA and protein, (ii) increase level of HNE- protein, and (iii) dysregulated production of major cytokines, chemokines and growth factors (and alteration of the corresponding plasma level). Addition of exogenous HNE to normal keratinocytes also induces a vitiligo like cytokine pattern and H₂O₂ overproduction but, in this case, adaptive upregulation of CAT and GSTM1 genes occurs, compensating the excess of oxidative stress. The experiment did not consider GSTT1 expression, but a GSTM1-like behavior can be reasonably hypothesized, based on the close functional similarity of the two enzymes.⁽²²⁾ Depending on how much of the individual redox homeostasis relies on the activity of a given GST isoform, possession of the corresponding null allele may or may not significantly increase such a risk because of the severe decrease in the deficiency of the antioxidant system caused by the simultaneous lack of GSTM1 and GSTT1 can not be easily compensated by other components⁽⁹⁾.

Cruciferous vegetables, such as broccoli, and members of the allium family, such as garlic and onion, have been shown to be potent inducers of these enzymes, which would be expected to increase clearance of potential toxins from the body.⁽²³⁾

Collectively, the mechanistic study revealed new pieces in the vitiligo "puzzle",⁽²⁴⁾ such as GST and HNE which, together with the known ones, namely H₂O₂ and CAT, may well be included in the hypothetic redox-regulated mechanism of melanocyte loss, and might represent good candidates as therapeutic targets for this skin disease⁽²²⁾.

Conclusion

The GSTM1 and GSTT1 polymorphisms play an important role in the pathogenesis of vitiligo. Null genotype of both genes either significant or not significant; increase a risk of the disease depending on how much of the individual redox homeostasis relies on the activity of a given GST isoform, because of the severe deficiency of the antioxidant system caused by the simultaneous lack of GSTM1 and GSTT1 can not be easily compensated.

Recommendation

The current study advise the patients and susceptible people to avoid the oxidant agents and to increase the antioxidant agents; as the oxidative stresses may affect GST gene polymorphism (GSTM1 and GSTT1) which have a role in pathogenesis of vitiligo. Further research (using a

larger number of patients) is advisable to achieve a better understanding of the pathophysiological role of GST polymorphism. Depending on the genes involved, their normal functions, and the genetic changes as it might be possible to design new treatments based on understanding those gene

Corresponding author

Shereen F. Gheida

Departments of Dermatology and Venereology,
Faculty of Medicine, Tanta University, Egypt
gheidas@yahoo.com

References

- 1- Ogg GS, Dunbar PR, Romero P, et al. (1998) . High frequency of skin-homing melanocyte-specific cytotoxic T lymphocytes in autoimmune vitiligo. *J Exp Med.*; 6:1203-8.
- 2- Spritz RA (2006) . The genetics of generalized vitiligo and associated autoimmune diseases. *J Dermatol Sci.*; 41:3-10.
- 3- Hazneci E, Karabulut AB, Ozturk C, et al. (2005) . A comparative study of superoxide dismutase, catalase, and glutathione peroxidase activities and nitrate level in vitiligo patients. *Int J Dermatol.*; 44:636-40.
- 4-Maresca V, Roccella M, Camera E, et al. (1997) . Increased sensitivity to peroxidative agents as a possible pathogenic factors of melanocyte damage in vitiligo. *J Invest Dermatol.*; 109:310-13.
- 5- Brind AM, Hurlstone A, Edrington D, et al. (2004) . The role of polymorphisms of glutathione S-transferases GSTM1, M3, P1, T1 and A1 in susceptibility to alcoholic liver disease. *Alcohol and Alcoholism*; 39:478-83.
- 6-Hayes JD and Pulford DJ (1995) . The glutathione S-transferase supergene family: regulation of GST and the contribution of the isoenzymes to cancer chemoprotection and drug resistance. *Crit Rev Biochem Mol Biol.* ; 30:445-600.
- 7- Yun BR, El-sohemy A, Cornelis MC, et al. (2005) . Glutathione S-transferase M1, T1, and P1 genotypes and rheumatoid arthritis. *J Rheumatol.*; 32:992-7.
- 8- Yoon KU, Seo HY, Joo HC, et al. (2007) . Association of glutathione S-transferase gene polymorphisms (GSTM1 and GSTT1) of vitiligo. *J Dermatol Sci.*; 81:233-7.
- 9- Guarneri F, Asmundo A, Sapienza D, et al. (2011) Glutathione S-transferase M1/T1 gene polymorphisms and vitiligo in a Mediterranean population. *Pigment Cell Res.*; 24:731-3.
- 10- Uhm YK, Yoon SH, Kang IJ, et al. (2007) . Association of glutathione S-transferase gene polymorphisms (GSTM1 and GSTT1) of vitiligo

- in Korean population. *Life Sci J.*; 81:223-7.
- 11- Liu L, Li c, Gao J, et al. (2009) . Genetic polymorphisms of glutathione S-transferase and risk of vitiligo in the Chinase population. *J Invest Dermatol.*; 129:2646-52.
 - 12- Mosher DB, Pathak MA , Fitzpatrick TB, et al. (1987) . Vitiligo, Etiology, Pathogenesis and Treatment. In: *Dermatology in General Medicine*. Fitzpatrick DB, Eisen AZ, Wolff W(eds). Mc Graw Hill Inter-national Book Co. 3rd ed : New York; 1:810-21.
 - 13- Yang Y, Yang Y, Xu Y, et al. (2008) . Endothelial glutathione-S-transferase A4-4 protects against oxidative stress and modulates inducible NO synthase expression through nuclear transcription factor kappa-B translocation. *Toxicol Appl Pharmacol.*; 230:187-96.
 - 14- Roy S, Khanna S, Nallu K, et al. (2006) . Dermal wound healing is subject to redox control. *Mol Ther.*; 13:211-20.
 - 15- Korkina L and Pastore S (2009) . The role of redox regulation in the normal physiology and inflammatory diseases of the skin. *Front Biosci.*; 1:123-41.
 - 16- Pizzimenti S, Ferracin M, Sabbioni S, et al (2009) . Micro RNA expression changes during human leukemic HL-60 cell differentiation induced by 4-hydroxynonenal, a product of lipid peroxidation. *Free Rad Biol Med.*; 46:282-8.
 - 17- Hiratsuka A, Saito H, Hirose K, et al. (1999) . Marked expression of glutathione S-transferase A4-4 detoxifying 4-hydroxy-2(E)-nonenal in the skin of rats irradiated by ultraviolet B-band light (UVB). *Biochem Biophys Res Commun.*; 260:740-6.
 - 18- Codreanu SG, Zhang B, Sobel SM, et al. (2009) . Global analysis of protein damage by the lipid electrophile 4-hydroxy-2-nonenal. *Mol Cell Proteomics.*; 8:670-80.
 - 19- Kurien BT, Hensley K, Bachmann M, et al.(2006). Oxidatively modified autoantigens in autoimmune diseases. *Free Rad Biol Med.*; 15:549-56.
 - 20- Sampey BP, Carbone DL, Doorn JA, et al. (2007). 4-hydroxy-2-nonenal adduction of extracellular signal-regulated kinase (Erk) and the inhibition of hepatocyte Erk-Est-like protein-1-activating protein-1 signal transduction. *Mol Pharm.* ; 71:871-83.
 - 21- Townsend DM, Findlay VL, and Tew KD (2005) . Glutathione S-transferases as regulators of kinase pathways and anticancer drug targets. *Methods Enzymol.* ; 401:287-307.
 - 22- Kostyuk VA, Potapovich AI, Cesareo E, et al. (2010) . Dysfunction of glutathione s-transferase leads to excess 4-hydroxy-2-nonenal and H2O2 and impaired cytokine pattern in cultured keratinocytes and blood of vitiligo patients. *Antioxid Redox Signal. Tissue Engineering and Cutaneous Pathophysiology Laboratory, Dermatology Research Institute* ; 13:607-20.
 - 23- Cotton SC, Sharp L, Little J, et al. (2000). Glutathione S-transferase polymorphisms and colorectal cancer: a huge review. *Am J Epidemiol.*; 15:7-32.
 - 24- Westerhof W and D Ischia M (2007). Vitiligo puzzle: The pieces fall in place. *Pigment Cell Res.* ;20:345-59.

11/21/2011

Pneumonia and Impaired T Cell Function in Children with Down's Syndrome: Double StrikeAmany Abuelazm¹, Zeinab Galal*² and Samia El Sahn³Pediatric Department, Ahmed Maher Teaching Hospital¹, Clinical Pathology² and Pediatric Departments, Faculty of medicine, Ain Shams University³*dr_zgalal@hotmail.com

Abstract: Down's syndrome (DS) is the most common chromosomal abnormality in humans and is the most common known genetic cause of intellectual disability. DS is known for increased incidence of respiratory infections and autoimmune diseases, indicating impaired immunity. Subjects and methods: This study included sixty seven children; 49 preschool children with DS, with ages ranging from 2 to 6.5 years and 18 healthy, age- and gender-matched controls. Free T4, TSH, and thyroid autoantibodies (antithyroglobulin and anti-TSH receptor antibodies) were measured. Evaluation of total leucocytic count, lymphocytes, CD3+, CD4+, CD8+ and CD56+ cells was performed for each subject. Sputum specimens were collected from all DS subjects and controls for microscopic examination and culture. Results: Among 49 DS child 23 (46.9%) had signs and symptoms of respiratory tract infection, 11 of DS children (22.4%) were suffering from pneumonia. The culture results of sputum samples revealed that staphylococcus aureus was the most common organism; it represents 37.9% of the total bacterial pathogen isolates and 45.4% of the pneumonic patient's isolates. Nineteen DS subjects (38.78%) were hypothyroid according to the thyroid profile tests. Thyroid autoantibodies were detected in 5 (10.2%) of DS children, 1 euthyroid and 4 hypothyroid children. The values of total leucocytic count, lymphocyte, CD3+ and CD4+ cells ($5772.2 \pm 1861.1/\text{mm}^3$, 2234.2 ± 597.8 , 1774.2 ± 396.5 and 760.9 ± 298.4 respectively), were lower in DS children than healthy controls ($7908.0 \pm 1464.8/\text{mm}^3$, 3158.9 ± 722.5 , 2252.0 ± 636.8 and 1389.3 ± 379.4 respectively) and the differences were statistically significant. CD8+ and CD56+ cells were higher in DS children (979.4 ± 285.2 and 393.2 ± 102.9 respectively) than healthy controls (741.8 ± 170.6 and 175.5 ± 52.8 respectively) with significant statistical differences. CD4/CD8 ratio was reversed in DS children (0.78 ± 0.27). In conclusion, respiratory tract infection is very common in DS children and can easily complicate to pneumonia because of the complex impairment of T-lymphocytes which is one of the reasons of the defective immune responses among DS children. Staphylococcus aureus was the most common organism causing pneumonia in children with DS. Annual screening for thyroid function and thyroid autoantibodies in preschool DS children is very important to prevent further intellectual deterioration and improve overall development.

[Amany Abuelazm, Zeinab Galal and Samia El Sahn **Pneumonia and Impaired T Cell Function in Children with Down's Syndrome: Double Strike**] Life Science Journal, 2011; 8(4):793-799] (ISSN: 1097-8135).

<http://www.lifesciencesite.com>.

Keywords: Pneumonia, T cell, children, Down's syndrome

Introduction

Down syndrome (DS) is the most common chromosomal abnormality among live-born infants and is the most frequent cause of mental retardation in man ^(3,16). Respiratory tract infections are the most important cause of mortality in individuals with DS at all ages ⁽⁴⁾. Acute respiratory tract infections especially pneumonia is a common reason for hospitalization and morbidity in children with DS ^(4,10,13).

In DS, non-immunological factors including structural abnormalities of the airways and lungs, glue ears, obstructive sleep apnoea and gastro-oesophageal reflux, may play a role in the increased frequency of respiratory tract infections ⁽²⁰⁾. Oropharyngeal aspiration (OPA) of food and fluids is known to be associated with pneumonia in dysphagic children with neurological disease and direct causality is often assumed ^(17,29). Secondary immunodeficiency due to

metabolic or nutritional factors in DS, particularly zinc deficiency, has been postulated ^(7,20).

Autoimmune phenomena such as acquired hypothyroidism, coeliac disease and diabetes mellitus occur at higher frequency compared with non-DS subjects. Leukemia is estimated to be 15–20 times more frequent in DS ^(11,16,24). The most common autoimmune disease in DS is related to the thyroid gland. Thyroid autoantibodies were found in 13–34% of subjects with DS ^(14,15,23,28). It is remarkable that the prevalence of thyroid autoantibody increases with age, being common after the age of 8 years ^(14,15). However, **Shalitin and Phillip (2002)** described two infants in whom chronic autoimmune thyroiditis was diagnosed at the age of 5 and 8 months with DS (23)

The increased susceptibility to infection, malignancies, and autoimmune diseases, suggests that immunodeficiency is an integral part of DS ^(1,10). In recent decades several studies have been performed to

elucidate abnormalities of the immune system in DS⁽⁴⁾. The abnormalities of the immune system associated with DS include: mild to moderate T and B cell lymphopenia, with marked decrease of naive lymphocytes, impaired mitogen-induced T cell proliferation, reduced specific antibody responses to immunizations and defects of neutrophil chemotaxis^(16,20). The molecular mechanisms leading to the immune defects observed in DS individuals and the contribution of these immunological abnormalities to the increased risk of infections require further investigation⁽²⁰⁾.

In the current study we aimed to investigate some indicators of T cell immune response, such as white blood cells, total lymphocytes and some indicators of T helper and suppressor cells, to study thyroid function and the presence of thyroid autoantibodies; and above all the life threatening pneumonia infection in preschool DS children.

2. Subject and Methods

This study was conducted on sixty seven pediatric children divided into two groups: Group I comprised 49 children with Down's syndrome, 32 males and 17 females their ages ranged from 2 to 6.5 years (3.8±1.6). DS children were present at the time of the researchers' visit to Early Detection & Intervention Unit of Ahmed Maher Teaching hospital and pediatric out-patient clinics of Ain Shams university Hospitals. They were participated in the study after getting written informed consent from parents of each child. The research was conducted between January 2009 and Desember 2010.

The diagnosis of DS children depends on clinical features and was confirmed by chromosomal analysis of Trisomy 21. Group II comprised 18 healthy children; 10 males and 8 females their ages ranged from 3 to 7.3 years (3.5±1.7). Control subjects were from out-patient clinic coming for trivial symptoms, they were in good general conditions, and had no acute or chronic diseases affecting the immune system. The two groups were matching in age and sex, and they were all subjected to the following:

Complete medical history and clinical examination

were done for DS children and control subjects with a special consideration for symptoms and signs of pneumonia like fever, chills, rigor, myalgia, malaise, diarrhoea, cough and dyspnoea. In addition to lake of air space (consolidation) on chest X-ray⁽⁴⁾. And symptoms and signs of hypothyroidism, mainly constipation, dry skin, prolonged sleep and increased body weight; as identified by using Down's syndrome growth chart⁽¹⁸⁾ and WHO child growth standards, height and weight for age⁽³⁰⁾.

Specimen collection:

I-Blood specimens:

A convenience sample, not less than five ml of venous blood, was collected aseptically from each child. Blood samples were delivered to the laboratory in three aliquots. One ml of blood was anti-coagulated with disodium EDTA for processing in automated hematology cell coulter for blood count. Two ml were anti-coagulated with tripotassium EDTA to be analyzed by flowcytometry for the levels of CD3+, CD4+, CD8+ and CD56+ cells in a FACS Count Flow-cytometer (Becton & Dickinson, USA). And two ml of clotted blood for assay of TSH, free T4 and thyroid auto-antibodies (thyroid peroxidase antibodies and anti TSH receptor antibodies).

Total leucocytic and lymphocytic counts: were carried on Sysmex hematology coulter, Sysmex Corporation, Cobe, Japan.

Flowcytometric analysis of peripheral blood leucocytes:

Monoclonal bodies (MoAbs) directly conjugated with fluorescein isothiocyanate (FITC), phycoerythrin (PE), or phycoerythrin cyanin-5 (PC-5) were used to analyze the surface antigens of peripheral blood lymphocytes (PBL). The following monoclonal antibodies were used; anti-CD3 (anti-Leu4) recognizing all T cells, anti-CD8 (anti-Leu2a) recognizing cytotoxic T-cell subset, anti-CD4 (anti-Leu3) reactive with helper inducer T-cell subset, anti-CD56 (anti-Leu9) recognizing the N-CAM molecule reactive with resting and activated CD16+ cells, and with a small percentage of CD3+ lymphocytes, which are considered a subset of cytotoxic T lymphocytes that mediate non-major histocompatibility complex (MHC) restricted cytotoxicity. Four cytometry tubes were used for each subject in the study. About 100 µL of EDTA treated blood was added to each of the previous tubes. (Becton Dickinson, San Jose, CA, USA).

TSH and free T4 assays: were carried by chemiluminescence Kit (Roch Diagnostics, US). The chemiluminescence's immunoassay test utilizes a unique monoclonal antibody directed against a specific antigenic determinant on the hormone molecule. Hypothyroidism was diagnosed on the basis of a combination of a raised serum concentration of thyroid stimulating hormone (TSH) (reference values range from 0.2-4.2 IU/L) and or a marginally low concentration of free T4 (reference values range from 12-22 pmol/ml) combined with the presence of symptoms and signs associated with hypothyroidism.

Thyroid auto-antibodies detection: Thyroid peroxidase auto-antibodies and anti TSH receptor autoantibodies were detected using a sensitive solid-phase immunosorbent radioassay kit (Biomedical diagnostic division, Solon, Ohio, US) based on binding the human ^{125}I -labeled antigens to the autoantibody. If antibodies were present in a titer of ≥ 5 , the sample was considered positive.

II-Sputum specimens:

Spontaneously expectorated sputum specimens were collected from the subjects in a sterile screw capped containers and transported as soon as possible within 2 hours of collection for culture. Sputum samples were processed by adding an equal volume of sputolysin (sputosol, Unipath, Hampshire, UK) and incubated for 30 minutes at 37°C during which they were vortexed for 5-10 seconds.

Microbiological examination of sputum specimens:(Cheesbrough 2000)⁽⁶⁾

(I) Microscopical examination :

Wet preparation of the sputum examined microscopically by the low power to assess appropriateness of the sample. Only good quality samples were cultured. If large numbers of squamous epithelial cells were detected, the specimen was unsuitable for culturing as it was mostly saliva.

Gram smear was done for pus cells and bacteria. Potassium hydroxide (KOH) preparation when fungal infections were suspected.

Giemsa smears when pneumonic plaque or histoplasmosis was suspected

Eosin preparation: to examine sputum for eosinophils. Ziehl-Neelsen smears to exclude acid fast bacilli.

(II) Culture on different media:

Blood agar with optochin disc, incubated at 37°C aerobically.

Chocolate agar incubated in 5-10% CO_2 for *H. influenzae*.

MacConkey agar for Gram negative bacilli.

Lowenstein Jensen media (Oxoid) was used to exclude *Mycobacterium tuberculosis (M.TB)*. The decontaminated specimens with N-acetyl-L-cysteine-sodium hydroxide (NALC-NaOH) were inoculated on the medium and incubated for 6-8 weeks before being discarded as negative. Media were incubated in a slant position with the screw cap loose for at least a week until the sediment has been adsorbed (*Springer et al 1996*).⁽²⁵⁾

Statistical analysis:

Statistical analysis of the data was performed with SPSS, version 11.0 software, and continuous variables were presented as means and SD. Comparison of qualitative variables of DS group and the control group were carried out using the Fisher's exact test. Student's t-test was used to compare quantitative variables. P value of ≤ 0.05 was considered significant.

3. Results

The present study was conducted on 67 children divided into 2 groups; Group 1 comprised 49 children with Down's syndrome, 32 males and 17 females their ages ranged from 2 to 6.5 years (3.8 ± 1.6). Group II comprised 18 healthy children; 10 males and 8 females their ages ranged from 3 to 7.3 years (3.5 ± 1.7). The two groups are matching in age and sex. Their anthropometric data are represented in table 1. Weight of DS children was on 90th centile and 75th centile for males and females respectively on plotting on Down's chart in comparison with controls who lied on 50th centile for males and females. As regards to height, DS children were on 25th centile and 50th centile for males and females respectively while that of controls were on 50th centile for both males and females. (Table 1)

Among the 49 DS children, 23 (46.9%) had signs and symptoms of acute respiratory tract infection, 11 of the DS children suffering from pneumonia (22.4%). All of the pneumonic patients were admitted to the pediatric department of the university hospital. Regarding the culture results of sputum samples, 29 bacterial pathogens had been isolated from sputum samples of the 23 DS patients but none of the controls. *Staphylococcus aureus* was the most common organism; it represents 37.9% (11/29) of the total culture isolates and 45.4% (5/11) of the pneumonic patient's isolates. *Klebsiella pneumoniae* 24.1% (7/29) and 8.1% (2/11), *Candida albicans* represents 17.2% (5/29) and 18.1% (2/11), *Haemophilus influenzae* 10.3% (3/29) and 9.1% (1/11). While *Streptococcus pyogenes*, *Streptococcus pneumoniae* and *Pseudomonas aeruginosa* represent 3.4% (1/29) of the total isolates. The pathogenic organisms were isolated from sputum of 20 of the DS patients with acute respiratory tract infection; 10 of the pneumonic patients were included.

Atypical pneumonia was diagnosed in one child; he was suffering from severe signs and symptoms of pneumonia with abdominal pain, diarrhea and confusion, his sputum culture showed no growth on the used media and he did not respond to empirical antibiotic treatment. He was admitted to the intensive care unit (ICU) in the university hospital but he passed away. (Table 2)

Total leucocytic count/mm³ was lower in DS children (5772.2 ±1861.1 /mm³) than in normal controls (7908.0±1464.8/mm³) with significant statistical difference (P<0.005). Lymphocyte count/mm³ was lower in DS children (2234.2±597.8 /mm³) than in healthy controls (3158.9±722.5 /mm³) with significant statistical difference (P< 0.005). CD3+ lymphocytes absolute values were lower in DS children (1774.2±396.5) than in healthy controls (2252.0±636.8/mm³) with a significant statistical difference (P<0.05).

Absolute values and percents of CD4+ lymphocytes were found lower in DS children (760.9±298.4 and 33.9 % ±12.5) than in healthy controls (1389.1±379.4 and 45.8% ±4.6) and statistical difference were significant (P<0.005 for both absolute count and percents). CD8+ lymphocytes absolute values and percents were higher in DS children (979.4±285.2 and 45.6% ±15.6)

than in healthy controls (741.8±170.6 and 23.5% ±2.6) with statistical significant difference (P<0.05 and 0.0001 respectively). CD4/CD8 ratio was lower in DS children (0.78± 0.27) than healthy controls (1.8± 0.19) with significant statistical difference (P<0.0001). CD56+ cells count and percents were higher in DS subjects (393.2±102.9 and 18.8% ±6.8) than healthy controls (175.5±52.8 and 5.2% ±1.7) with significant statistical difference (P<0.0001) for both absolute count and percents). (Table 3, Figure 1)

On studying thyroid function, 19/49 (38.78%) of children with DS were hypothyroid, but none of the control group revealed any abnormality in thyroid function. antithyroglobulin (Thyroid peroxidase) auto-antibodies were detected in five (10.2%) DS children; one euthyroid and four hypothyroid and in none of the control group and anti-TSH receptor auto-antibodies were not detected in any of DS children or the normal control group. (Table 4)

Table (1): Anthropometric Data of Down's syndrome children

Group	Down's syndrome children.		control children	
	Males (no.20)	Female (no.10)	Males (no.14)	Female (no.8)
Age	34± 18.6	26± 7.6	35.1± 15.7	27.7± 9
Weight	13.9± 4.6 (90 th *)	10.9± 1 (75 th *)	14.7± 1.7(50 th *)	13±1.4 (50 th *)
Hight	83.2± 8 (25 th *)	80.1±5 (50 th *)	91.7± 10.1(50 th *)	88.3± 6.1(50 th *)

*centile

Table (2): Culture results of DS respiratory tract infection and pneumonia infection.

	Respiratory tract infection (no. and %)	Pneumonia infection (no. and %)
Staphylococcus aureus	11(37.9%)	5 (45.4%)
Klebsiella pneumonia	7 (24.1%)	2 (18.1 %)
Candida albicans	5 (17.2%)	2 (18.1%)
Haemophilus influenza	3 (10.3%)	(9.1%)
Streptococcus pyogenes	1 (3.4%)	0 (0%)
Streptococcus pneumoniae	1 (3.4%)	0 (0%)
Pseudomonas aeruginosa	1 (3.4%)	0 (0%)

Table (3): Immunological profile of the studied subjects

	Down's syndrome No.49, (mm ³)	Healthy controls No.18, (mm ³)	t	P
TLC	5772.2± 1861.1	7908.0± 1464.8	3.150	<0.005**
Lymphocytes	2234.2± 597.8	3158.9± 722.5	3.563	<0.005**
CD3+ count	1774.2± 396.5	2252.0± 636.8	2.353	<0.05*
CD4+count	760.9± 298.4	1389.3± 379.4	4.716	<0.005**
CD4 %	33.9±12.5	45.8± 4.6	2.969	<0.005**
CD8+ count	979.4± 285.2	741.8± 170.6	2.442	<0.05*
CD8 %	45.6± 15.6	23.5± 2.6	4.590	<0.0001**
CD4/ CD8	0.78± 0.27	1.8± 0.19	11.860	<0.0001**
CD 56 count	393.2± 102.9	175.5± 52.8	6.320	<0.0001**
CD56%	18.8± 6.8	5.2± 1.7	6.252	<0.0001**

Total leucocytic count: TLC. * = Significant. ** = Highly Significant. † Insignificant (P>0.05).

Table (4): Thyroid function in Down's syndrome children and healthy controls

	DS children (no.49)	Controls (no.18)
Hypothyroid	19 (38.78%)	0 (0%)
Antithyroglobulin	5 (10.2%)	0 (0%)
anti-TSH receptor	0 (0%)	0 (0%)

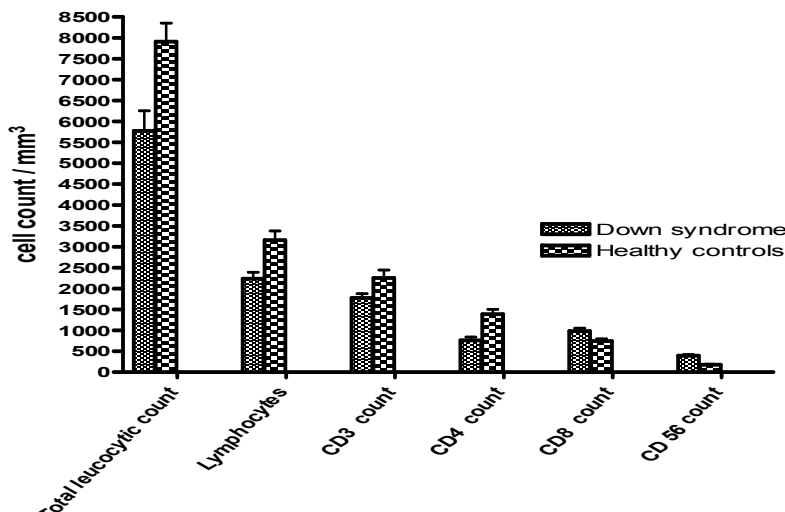


Figure (1): Total leucocytic count, lymphocytes, CD3+, CD4+, CD8+ and CD56+ cells in Down's syndrome children and healthy controls.

DISCUSSION

Down syndrome (DS) is the most common genetic disease and is presented with cognitive impairment, cardiac and gastrointestinal abnormalities, in addition to other miscellaneous clinical conditions ⁽²⁰⁾. DS individuals may have a high frequency of infections, usually of the upper respiratory tract, characterized by increased severity and prolonged course of disease, which are partially attributed to defects of the immune system ^(20,22).

The present study revealed the high incidence of respiratory tract infection among DS preschool children, 23/49 (46.9%), 11/49 (22.4%) of them were suffering from pneumonia. One child, with severe pneumonic condition, was admitted to the ICU, then passed away. It is widely accepted that children with multisystem involvement demonstrated a higher association with pneumonia than normals ⁽²⁹⁾. In agreement with our results, *Hilton et al. (1999)* ⁽¹³⁾ comprehensively reviewed 232 hospital admissions among DS children over 6 year period, and found that lower respiratory tract pathology was the most common cause for acute hospital admission. Based on age groups, the highest percentage of admissions their studies were among 1–5-year-old children (45%). The predominant diagnosis of admission to the ICU was pneumonia (18%). It was found that *Staphylococcus aureus* was the most common organism; it represents 37.9% of our total culture isolates and 45.4% of the pneumonic patient's

specimens. However, *Alonso et al.(2005)* ⁽²⁾ had reported bacterial pathogens isolates from tracheal secretion culture in 58 % of their DS studied group and the most common pathogen was *Staphylococcus aureus* (42 %). Three children (25 %) developed lobar pneumonia.

The increased frequency of haematological malignancies, autoimmune diseases and infections in DS, and the observed high frequency of hepatitis B surface antigen carriers, had already led to the hypothesis that DS is associated with abnormalities of the immune system ^(16,20). The basis of the immune defects is still unclear ⁽⁴⁾. The current study detected a significant decrease of the total leucocytic count in DS children. Some studies noted that in DS children, the immune cellular status is similar to the normal population ^(7,21). Peripheral blood mononuclear cells from DS subjects are characterized by several alterations leading to a decreased response to infection, and a decreased killing ability of microorganisms. This may be one reason for the decreased immunity seen in children with DS ^(1,21).

In accordance with some earlier studies, we detected a significant decrease of the absolute number of circulating lymphocytes. In agreement with *Cossarizza et al.(1990)* ⁽⁹⁾, we confirmed the presence of a significant reduction of CD3+ lymphocyte absolute number in DS children. It has been noted that there is an inefficient release of mature T cells by

the DS thymus, associated with selective failure of tyrosine phosphorylation^(21,26).

We found that DS children had less T helper cells than the control group^(6,21). Some studies documented a normal proportion of CD4+ T cells, whereas the percentage of suppressor-cytotoxic CD8+ lymphocytes is markedly increased and CD4/CD8 ratio of patients with DS and normal controls were similar^(5,19). On the contrary, *Corsi et al. (2003)*⁽⁸⁾ showed that peripheral CD4+ T cells were lower in children with DS, whereas mean values of cytotoxic CD8+ T cells were comparable with those from healthy children. *Cocchi et al. (2007)*⁽⁷⁾ noted that the immune cellular status in DS children is similar to the normal population as far as white blood cell, lymphocyte, CD4 (+), CD8 (+), natural killer and immunoglobulins. *Guazzarotti et al. (2009)*⁽¹²⁾ documented significant increase of both CD4+ and CD8. In our study, absolute values and percents of CD4+ lymphocytes were lower and CD8+ cells were higher in DS children than control group. This was concomitant with *Corsi et al. (2003)*⁽⁸⁾, who reported a decrease in CD4+ and an increase in CD8+ cells with inverted CD4/CD8 ratio.

CD56+ cells are considered the cells capable of non MHC-restricted cytotoxicity, and appear to play an important role as tumor infiltrating lymphocytes⁽⁵⁾. The current study showed that CD56+ cells percents and absolute values are higher in DS children than the control group. It was noted that the expansion of this small subset could be the consequence of an effort of DS immune system to compensate for the functional and numerical reduction of other cytotoxic subsets^(5,9).

Many of immunological alterations in DS subjects are similar to those characteristic of chromosomally normal subjects of advanced age, DS subjects are aging fast^(3,16). Reduced thymic endocrine activity⁽²⁰⁾ and the zinc deficiency characteristic of DS⁽⁷⁾ and molecular abnormalities due to gene over expression of loci located on chromosome 21 might be responsible for the derangement of T and NK subsets^(10,12). It was suggested that zinc sulfate supplementation improves thyroid function in hypozincemic DS children^(7,20).

Thyroid dysfunction, particularly hypothyroidism, is very common in DS. Interestingly, *Unachak et al. (2008)*⁽²⁸⁾ claimed that **sub-clinical** hypothyroidism is very common in children with DS. *Tüysüz and Beker (2001)*⁽²⁷⁾ reported prevalence of congenital hypothyroidism as 1.8% in children with DS, 25.3% of them had compensated hypothyroidism. The prevalence of hypothyroidism varies among different investigators from 3–54% in subjects with DS of all ages^(14,15,23,28). In our work, we detected hypothyroidism in 38.8% of DS group and none of the controls. The variation in prevalence

between different studies might be related to the age variation among the studied subjects and/or to differences in diagnostic criteria.

In the present work, thyroid autoantibodies were detected in 10.2% of DS children, four hypothyroid and one euthyroid. In contrast to our results, *Karlsson et al. (1998)*⁽¹⁵⁾, reported hypothyroidism in 30 DS subjects, half of them acquired the condition before the age of 8 years, but only one of them displayed thyroid autoantibodies at diagnosis. They claimed that, autoimmune thyroid disease is uncommon in young children with DS but is common after 8 years of age

Conclusion:

Respiratory tract infection is very common in DS children and can easily complicate to pneumonia because of the complex impairment of T-lymphocytes subsets, which is one of the reasons of defective immune responses among DS children. *Staphylococcus aureus* was the most common organism causing pneumonia in children with DS. Annual screening for thyroid function and thyroid autoantibodies in DS **preschool** children is very important to prevent further intellectual deterioration and improve overall development. The awareness of the breadth of respiratory problems and a plan to monitor subjects with DS for their development have the potential to improve outcomes, as some of these conditions are readily identifiable and able to be treated.

A major re-appraisal in attitudes towards DS is required to ensure that the medical and social needs of people with the disorder are adequately met across their entire lifespan, accompanied by the provision of appropriate levels of care and management.

Corresponding author

References

1. **Abu Faddan N, Sayed D and Ghaleb F (2011).** T lymphocytes apoptosis and mitochondrial membrane potential in Down's syndrome. *Fetal Pediatr Pathol.*; 30(1):45-52.
2. **Alnos M S, Menchon M N, Nunez RA, et al. (2005).** Bacterial tracheitis: an infectious cause of upper airway obstruction to be considered in children. *An Pediatr (Barc.)*; 63(2):164-8.
3. **Bittles AH, Bower C, Hussain R, et al. (2007).** The four ages of Down syndrome. *Eur J Public Health.*; 17(2):221-5.
4. **Bloemers BL, Broers CJ, Bont L, et al. (2010).** Increased risk of respiratory tract infections in children with Down syndrome: the consequence of an altered immune system. *Microbes Infect.* 12(11):799-808.

5. **Cetiner S, Demirhan O, Inal TC, et al. (2010).** Analysis of peripheral blood T-cell subsets, natural killer cells and serum levels of cytokines in children with Down syndrome. *Int J Immunogenet.*; 37(4):233-7.
6. **Cheesbrough, M (2000).** District laboratory practice in tropical countries, Cambridge University press, part 2, page 75.
7. **Cocchi G, Mastrocola M, Capelli M, et al. (2007).** Immunological patterns in young children with Down syndrome: is there a temporal trend? *Acta Paediatr.*; 96(10):1479-82.
8. **Corsi MM, Ponti W, Venditti A, et al. (2003).** Proapoptotic activated T-cells in the blood of children with Down's syndrome: relationship with dietary antigens and intestinal alterations. *Int J Tissue React*; 25: 117-121.
9. **Cossarizza A, Monti D, Montagnani G, et al. (1990).** Precocious aging of the immune system in Down syndrome: alteration of B lymphocytes, T-lymphocyte subsets, and cells with natural killer markers. *Am J Med Genet Suppl.*;7:213-8.
10. **De Hingh YCM, Van der Vossen PW, et al. (2005).** Intrinsic Abnormalities of Lymphocyte Counts in Children with Down Syndrome. *J Pediatr.*; 147:744–747
11. **Goldacre M, Wotton C, Seagroatt V, et al. (2004).** Cancers and immune related diseases associated with Down syndrome: a record linkage study. *Arch Dis Child.* ; 89:1014–17.
12. **Guazzarotti L, Trabattoni D, Castelletti E, et al. (2009).** T lymphocyte maturation is impaired in healthy young individuals carrying trisomy 21 (Down syndrome). *Am J Intellect Dev Disabil.*; 114(2):100-9.
13. **Hilton JM, Fitzgerald DA and Cooper DM (1999).** Respiratory morbidity of hospitalized children with Trisomy 21. *J Paediatr Child Health.*; 35(4):383-6.
14. **Ivarsson SA, Ericsson UB, orslund M, et al. (1997);** The impact of thyroid autoimmunity in children and adolescents with Down syndrome. *Acta Paediatrica*; (86)10: 1065-67.
15. **Karlsson B, Gustafsson J, Hedov G, et al. (1998).** Thyroid dysfunction in Down's syndrome: relation to age and thyroid autoimmunity. *Arch Dis Child.*;79:242–5
16. **Kusters MA, Verstegen RH, Gemen EF, et al. (2009).** Intrinsic defect of the immune system in children with Down syndrome: a review. *Clin Exp Immunol.*; 156(2):189-93.
17. **Lazenby T. (2006).** The impact of aging on eating, drinking, and swallowing function in people with Down's syndrome. *Dysphagia.*; 23(1):88-97.
18. **Myrelid A, Gustafsson J, Ollars B, et al. (2002).** Growth charts for Down's syndrome from birth to 18 years of age. *Arch. Dis. Child.*; 87: 97-103.
19. **Nespoli L, Burgio GR, Ugazio AG, et al. (1993):** Immunological features of Down's syndrome: a review. *J Intellect Disabil Res*; 37(6): 543-47.
20. **Ram G and Chinen J (2011).** Infections and immunodeficiency in Down syndrome. *Clin Exp Immunol.*; 164(1):9-16.
21. **Roat E, Prada N, Ferraresi R, et al. (2007).** Mitochondrial alterations and tendency to apoptosis in peripheral blood cells from children with Down syndrome. *FEBS Lett.* 6; 581(3):521-5.
22. **Sherman SL, Allen EG, Bean LH, et al. (2007).** Epidemiology of Down syndrome. *Ment Retard Dev Disabil Res Rev.*;13(3):221-7.
23. **Shalitin S and Phillip M (2002):** Autoimmune thyroiditis in infants with Down's syndrome. *J Pediatr Endocrinol Metab.*;15(5):649-52
24. **Söderbergh A, Gustafsson J, Ekwall O, et al. (2006):** Autoantibodies linked to autoimmune polyendocrine syndrome type I are prevalent in Down syndrome. *Acta Paediatr.*; 95(12):1657-60
25. **Springer B, Stockman L, Teschner K, et al. (1996).** Two-laboratory collaborative study on identification of mycobacteria: molecular versus phenotypic methods. *J Clin Microbiol.*; 34(2):296-303.
26. **Tamiolakis D, Venizelos I, Kotini A, et al. (2003).** Prevalence of CD8/CD4 ratio in the fetal thymic parenchyme in Down's syndrome. *Acta Medica (Hradec Kralove).*;46(4):179-82.
27. **Tüysüz B and Beker DB (2001).** Thyroid dysfunction in children with Down's syndrome. *Acta Paediatr.* ; 90(12):1389-93.
28. **Unachak K, Tanpaiboon P, Pongprot Y, et al. (2008).** Thyroid functions in children with Down's syndrome. *J Med Assoc Thai.* ; 91(1):56-61.
29. **Weir K, McMahon S, Barry L, et al. (2007).** Oropharyngeal aspiration and pneumonia in children. *Pediatr Pulmonol.*; 42(11):1024-31.
30. **WHO Child Growth Standards, height and weight for age (2006)** at the WHO website www.who.int/childgrowth

11/25/2011

DOUBLE PARAPROXIMITY SPACES

A. Kandil¹, O. Tantawy², K. Barakat³, AND N. Abdanabi⁴

^{1,3,4}Mathematics Department, Faculty of Science, Helwan University, P.O. Box 11795, Cairo Egypt.

²Mathematics Department, Faculty of Science, Zagazig University
nagahlibya@yahoo.com

Abstract: We introduce the concept of a double completely normal topological space or DT_5 – space and double Paraproximity space showing that every double space induces a double completely normal topological space and vice versa.

[A. Kandil, O. Tantawy, K. Barakat, and N. Abdelnaby **Double Paraproximity Spaces**] Life Science Journal, 2011; 8(4):800-804] (ISSN: 1097-8135). <http://www.lifesciencesite.com>.

Keywords: topological space; double Paraproximity space; mathematics.

1. Introduction

The mathematical idea of double sets was firstly introduced by Kere [9] and studied in many articles by A. Kandil and others “[1], [4], [6], [7], [8]”. They introduced and studied many topics in the double topology. The Paraproximity structure subject has been introduced by E. Hayashi in 1964 [3]. Recently, Kandil and others introduced the fuzzy Paraproximity structure [5].

In this paper we shall introduce the separation axiom DT_5 (double completely normal) on double topological spaces and study some of its properties. Also, we shall introduce the notion of DP-proximity in the case of double topological space showing that every DP-Proximity on X generates a double completely normal (DT_5) topology.

2. Preliminaries

Throughout this section we mention the concepts and notations which we shall use in this paper.

2-1 Double set

Definition 2.1.1. [8] Let X be a non empty set.

1. A double set \underline{A} is an ordered pair $\underline{A} = (A_1, A_2) \in P(X) \times P(X)$ such that $A_1 \subseteq A_2$.
2. $D(X) = \{(A_1, A_2) \in P(X) \times P(X) : A_1 \subseteq A_2\}$ is the family of all double sets on X.
3. Let $x \in X$, then the double sets $x_{\frac{1}{2}} = (\phi, \{x\})$ and $x_1 = (\{x\}, \{x\})$ are said to be double points of X.

$D(X)_p = \{x_t : x \in X, t = \{\frac{1}{2}, 1\}\}$ is the set of all double points on X.

4. Let $\eta_1, \eta_2 \subseteq P(X)$. Then the double product of η_1 and η_2 is denoted by $\eta_1 \times \eta_2$ and is defined by: $\eta_1 \times \eta_2 = \{(A_1, A_2) \in \eta_1 \times \eta_2 : A_1 \subseteq A_2\}$.
5. The double set $\underline{X} = (X, X)$ is called the universal double set.
6. The double set $\underline{\phi} = (\phi, \phi)$ is called the empty double set.

Definition 2.1.2. [8] Let $\underline{A} = (A_1, A_2), \underline{B} = (B_1, B_2) \in D(X)$. Then:

- i- $\underline{A} = \underline{B} \Leftrightarrow A_i = B_i, i = 1, 2$.
- ii- $\underline{A} \subseteq \underline{B} \Leftrightarrow A_i \subseteq B_i, i = 1, 2$.
- iii- If $\{\underline{A}_s : s \in S\} \subseteq D(X)$, then $\bigcup_{s \in S} \underline{A}_s = (\bigcup_{s \in S} A_{1s}, \bigcup_{s \in S} A_{2s})$ and $\bigcap_{s \in S} \underline{A}_s = (\bigcap_{s \in S} A_{1s}, \bigcap_{s \in S} A_{2s})$
- iv- The complement of a double set \underline{A} is $\underline{A}^c = (A_2^c, A_1^c)$
- v- $\underline{A} - \underline{B} = \underline{A} \cap \underline{B}^c$.

Proposition 2.1.3. [8] $(D(X), \cup, \cap, ^c)$ is a Morgan Algebra.

Definition 2.1.4. [8] For any two double sets \underline{A} and \underline{B} , \underline{A} is called quasi-coincident to \underline{B} , denoted by $\underline{A} Q \underline{B}$, if $A_1 \cap B_2 \neq \phi$ or $A_2 \cap B_1 \neq \phi$.

\underline{A} is not quasi – coincident to \underline{B} , denoted by $\underline{A} \overline{Q} \underline{B}$, if $A_1 \cap B_2 = \phi$ and $A_2 \cap B_1 = \phi$.

Theorem 2.1.5. [8] Let $\underline{A}, \underline{B}, \underline{C} \in D(X)$ and $x_t \in D(X)_p$. Then :

- 1- $\underline{A} Q \underline{B} \Rightarrow \underline{A} \cap \underline{B} \neq \phi$

- 2- $AQB \Leftrightarrow \exists x_t \in A$ such that $x_t QB$
- 3- $A \overline{QB} \Leftrightarrow A \subseteq B^c$, and $x_t \overline{QA} \Leftrightarrow x_t \in A^c$.
- 4- $A \overline{QA} \Leftrightarrow A^c$.
- 5- $A \subseteq B \Leftrightarrow x_t QA \Rightarrow x_t QB$.
- 6- $A \overline{QB}, B \subseteq C \Rightarrow A \overline{QC}$.
- 7- $x_t \overline{QA} (A \cup B) \Leftrightarrow x_t \overline{QA}$ and $x_t \overline{QB}$.
- 8- $x_t \overline{QA} (A \cap B) \Leftrightarrow x_t \overline{QA}$ or $x_t \overline{QB}$.

2.2 Double Topological Space

Definition 2.2.1. [8] Let X be a non-empty set. Then:

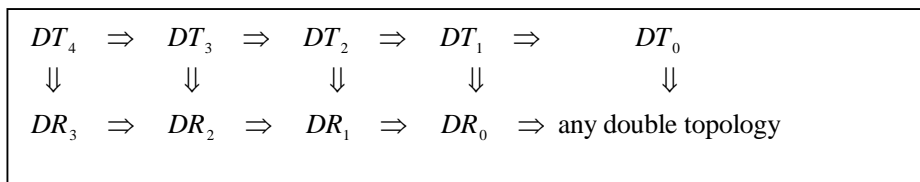
- 1- $\tau \subseteq D(X)$ is called a double topology on X if the following axioms are satisfied:
 $DT_1 \quad \phi, X \in \tau$.
 $DT_2 \quad$ if $A, B \in \tau$, then $A \cap B \in \tau$.
 $DT_3 \quad$ if $\{A_s : s \in S\} \subseteq \tau$, then $\bigcup_{s \in S} A_s \in \tau$.

The pair (X, τ) is called a double topological space and member of τ are called open double set.

2- $F \in D(X)$ is called a closed double set, if $F^c \in \tau$, and the family of all closed double sets is denoted by $\tau^c = \{F : F^c \in \tau\}$.

- 3- A double set Q_{x_t} is called a double neighborhood of the double point x_t if $x_t \in Q_{x_t} \in \tau$. The family of all double neighborhoods of x_t will be denoted by $\underline{N}(x_t)$.
- 4- If $A \in D(X)$, Then:

- (i) The closure of A is denoted by \overline{A} or $cL(A)$ and is defined by $\overline{A} = \bigcap \{F : A \subseteq F \in \tau^c\}$.



2.3 Completely normal spaces and paraproximity spaces

Definition 2.3.1. [king] An ordinary topological space (X, τ) is called completely normal space iff for every pair of separated sets $A, B \subset X$, there exist open sets $U, V \subset X$ such that $A \subset U, B \subset V$ and $U \cap V = \phi$.

- (ii) The interior of A is denoted by A° or $int(A)$ and $A^\circ = \bigcup \{V : V \in \tau, V \subseteq A\}$.
- (iii) The derived double set of A is denoted by A^d and is given by: $x_t QA^d \Leftrightarrow x_t Q(A - \{x_t\})$.

Definition 2.2.2. [6] A double topological space (X, τ) is called :

- 1- $D - R_0$ iff $x_t \overline{Q} y_r$ implies $y_r \overline{Q} x_t$.
- 2- $D - R_1$ iff $x_t \overline{Q} y_r$ implies there exist Q_{x_t}, Q_{y_r} such that $Q_{x_t} \overline{Q} Q_{y_r}$.
- 3- $D - R_2$ iff $x_t \overline{Q} F, F^c \in \tau$ implies that there exist Q_{x_t}, Q_F such that $Q_{x_t} \overline{Q} Q_F$.
- 4- $D - R_3$ iff $F \overline{Q} G$ and $F, G \in \tau^c$ implies that there exist Q_F, Q_G such that $Q_F \overline{Q} Q_G$.
- 5- $D - T_0$ iff $x_t \overline{Q} y_r$ implies $y_r \overline{Q} \overline{x_t}$ or $x_t \overline{Q} \overline{y_r}$.
- 6- $D - T_1$ iff $x_t \overline{Q} y_r$ implies $y_r \overline{Q} \overline{x_t}$ and $x_t \overline{Q} \overline{y_r}$.
- 7- $D - T_2$ iff $x_t \overline{Q} y_r$ implies that there exist Q_{x_t}, Q_{y_r} such that $Q_{x_t} \overline{Q} Q_{y_r}$.
- 8- $D - T_3$ iff it is $D - R_2$ and $D - T_1$.
- 9- $D - T_4$ iff it is $D - R_3$ and $D - T_1$.

Theorem 2.2.3. [6] The interrelation between the pervious axioms given in the following diagram:

Definition 2.3.2. [king] A mapping $\delta : P(X) \times P(X) \rightarrow \{0, 1\}$ is called a paraproximity on a set X if the following axioms are satisfied:

- 1. $\delta(A, \phi) = 1, \forall A \subseteq X$.
- 2. $\delta(A, B \cup C) = \delta(A, B) \cdot \delta(A, C), \forall A, B, C \subseteq X$.

3. For an arbitrary index set \wedge , $\delta (\bigcup_{\lambda \in \wedge} A_\lambda, B) = 0 \Leftrightarrow \delta (A_\mu, B) = 0$, for some $\mu \in \wedge$.
4. for any two points x, y of X , $\delta (x, y) = 0 \Leftrightarrow x = y$.
5. $\delta (A, B) = \delta (B, A) = 1 \Rightarrow \exists U, V \subseteq X$ with $U \cap V = \phi$, satisfying $\delta (A, U^c) = \delta (B, V^c) = 1$ and $\delta (U, U^c) = \delta (V, V^c) = 1$.

Theorem 2.3.3. [king] Let (X, δ) be a paraproximity space. Then the collection $\tau \delta = \{V \subseteq X: \delta (V, V^c) = 1\}$ is a completely normal topology on X .

Theorem 2.3.4. [king] Let (X, τ) be a completely normal ordinary topological space. Then the relation δ given by: $\delta (A, B) = 0 \Leftrightarrow A \cap \overline{B} \neq \phi$, is a paraproximity on X , for which $\tau_\delta = \tau$

3- Double complete normal spaces

Definition 3.1. Let (X, τ) be a double topological space, and let $\underline{A}, \underline{B} \in D(X)$. \underline{A} and \underline{B} are called double separated sets if $\underline{A} \overline{Q} \underline{B}$ and $\underline{B} \overline{Q} \underline{A}$.

Lemma 3.2. Let (X, τ) be a double topological space. Then:

- (i) \underline{A} and \underline{B} are double separated and $\underline{A}_1 \subseteq \underline{A}, \underline{B}_1 \subseteq \underline{B} \Rightarrow \underline{A}_1, \underline{B}_1$ are double separated.
- (ii) $\underline{A}, \underline{B} \in \tau^c$ and $\underline{A} \overline{Q} \underline{B} \Rightarrow \underline{A}$ and \underline{B} are double separated.
- (iii) $\underline{A}, \underline{B} \in \tau$ and $\underline{A} \overline{Q} \underline{B} \Rightarrow \underline{A}$ and \underline{B} are double separated.

Proof: Clear.

Definition 3.3. A double topological space (X, τ) is called DR_4 -space if for every two double separated sets $\underline{A}, \underline{B}$ in X , $\exists \underline{Q}_A, \underline{Q}_B$ such that $\underline{Q}_A \overline{Q} \underline{Q}_B$.

Definition 3.4. A double space (X, τ) is called double completely normal space (or DT_5 -space) if it is DR_4 and DT_1 .

Proposition 3.5. $(X, \tau) \in DT_5 \Rightarrow (X, \tau) \in DT_4$.

Proof: The result following from Definition 3.4 and Lemma 3.2.

Theorem 3.6 . Every closed double subspace of a DT_5 -space is DT_4 .

Proof: Let $(X, \tau) \in DT_5$ -space, Y be a double subspace of X , and $\underline{A}, \underline{B} \in \tau_Y^c$ such

that $\underline{A} \overline{Q} \underline{B}$. Then $\underline{A}, \underline{B} \in \tau^c \wedge \underline{A} \overline{Q} \underline{B}$
Lemma 3.2.5

$\Rightarrow \underline{A}, \underline{B}$ are double separated in X
 $X \in DT_5$
 $\Rightarrow \exists \underline{Q}_A, \underline{Q}_B$ such that $\underline{Q}_A \overline{Q} \underline{Q}_B$
 $\Rightarrow (\underline{Y} \cap \underline{Q}_A \overline{Q} \underline{Y} \cap \underline{Q}_B) \Rightarrow (Y, \tau_Y) \in DR_3$
 \wedge clearly $(Y, \tau_Y) \in DT_1 \Rightarrow (Y, \tau_Y) \in DT_4$.

4- Double Paraproximity Spaces

Definitions 4.1 Let $\delta : D(X) \times D(X) \rightarrow \{0,1\}$ be a relation on $D(X)$ that satisfies the following axioms:

- DH_1 $\delta (\phi, X) = \delta (X, \phi) = 1$.
 DH_2 $\delta (\underline{A}, \underline{B} \cup \underline{C}) = \delta (\underline{A}, \underline{B}) \cdot \delta (\underline{A}, \underline{C})$,
 $\forall \underline{A}, \underline{B}, \underline{C} \in D(X)$.
 DH_3 for an arbitrary index set \wedge ,
 $\delta (\bigcup_{\lambda \in \wedge} \underline{A}_\lambda, \underline{B}) = 0 \Leftrightarrow \delta (\underline{A}_\mu, \underline{B}) = 0$, for some $\mu \in \wedge$.

This δ is called a double H- proximity on X , and the pair (X, δ) is called a doubleH- proximity space (or an DHP- space, for short).

Definition 4.2. An DHP- space (X, δ) is called separated if δ satisfies the following

Axiom: DH_4 $\delta (x_r, y_r) = 0 \Leftrightarrow x_r \overline{Q} y_r, \forall x_r, y_r \in D(X)_r$.

If δ is a separated DH - proximity. Then (X, δ) is called a separated DHP- space (or an SDHP-space, for short).

Proposition 4.3. Let (X, δ) be an SDHP- space, then $\delta (\underline{A}, x_r) = 0 \Leftrightarrow \underline{A} \overline{Q} x_r$.

Proof: $\delta (\underline{A}, x_r) = \delta (\bigcup_{y_r \in \underline{A}} y_r, x_r) = 0 \Leftrightarrow$

$\delta (y_r, x_r) = 0$, for some $y_r \in \underline{A}$. $\Leftrightarrow y_r \overline{Q} x_r$, for some $y_r \in \underline{A} \Leftrightarrow \underline{A} \overline{Q} x_r$.

Definition 4.4. An SDHP- space (X, δ) is called a double paraproximity space (or a DPP-space, for short) if δ satisfies the following axiom.

DH_5 $\delta (\underline{A}, \underline{B}) = \delta (\underline{B}, \underline{A}) = 1 \Rightarrow \exists \underline{C}, \underline{D} \in D(X)$ Such that $\underline{C} \overline{Q} \underline{D}$, and $\delta (\underline{A}, \underline{C}) = \delta (\underline{C}, \underline{C}) = \delta (\underline{B}, \underline{D}) = \delta (\underline{D}, \underline{D}) = 1$.

Lemma 4.5. Let (X, δ) be a DPP-space. Then:

- i- If $\underline{\delta}(A, B) = 1$, then $\underline{\delta}(A, C) = 1$, for any $C \subseteq B$.
- ii- If $\underline{\delta}(A, B) = 1$, then $\underline{\delta}(C, B) = 1$, for any $C \subseteq A$.
- iii- If $\underline{\delta}(A, B) = 1$, then $A \overline{Q} B$.
- iv- $\underline{\delta}(x_i^c, x_i) = 1$, for any double point $x_i \in D(X)_p$.

Proof: (i) Since $B = B \cup C$ ($C \subseteq B$), and $\underline{\delta}(A, B) = 1$. $\underline{\delta}(A, B) = \underline{\delta}(A, B \cup C) = \underline{\delta}(A, B) \cdot \underline{\delta}(A, C) = 1$ by DH_2 . Then $\underline{\delta}(A, C) = 1$.

(ii) Proof of (ii) is similar to proof of (i).
 (iii) $\underline{\delta}(A, B) = 1 \Rightarrow \underline{\delta}(\bigcup_{x_i \in A} x_i, B) = 1$

$$\begin{aligned} DH_3 & \Rightarrow \underline{\delta}(x_i, B) = 1, \forall x_i \in A. \xrightarrow{Lema 4.5} \\ & \forall x_i \in A, \underline{\delta}(x_i, y_r) = 1, \forall y_r \in B \\ DH_4 & \Leftrightarrow x_i \overline{Q} y_r, \forall x_i \in A, y_r \in B \Leftrightarrow A \overline{Q} B. \end{aligned}$$

(iv) Since $x_i^c \overline{Q} x_i \Rightarrow y_r \overline{Q} x_i, \forall y_r \in x_i^c$
 $DH_4 \Leftrightarrow \underline{\delta}(y_r, x_i) = 1, \forall y_r \in x_i^c \xrightarrow{DH_3} \underline{\delta}(x_i^c, x_i) = 1$ (By proposition 4.3).

Theorem 4.6. Let $(X, \underline{\delta})$ be a DPP – Space. Then $\tau_{\underline{\delta}} = \{V \in D(X): \underline{\delta}(V, V^c) = 1\}$ is a double topology on X, induced by $\underline{\delta}$.

Proof: $DT_1 \quad \underline{\delta}(X, X^c) = \underline{\delta}(X, \phi) = \underline{\delta}(\phi, \phi^c) = \underline{\delta}(\phi, X) = 1 \Rightarrow X, \phi \in \tau_{\underline{\delta}}$.
 $DT_2 \quad U, V \in \tau_{\underline{\delta}} \Rightarrow \underline{\delta}(U, U^c) = 1$ and $\underline{\delta}(V, V^c) = 1$ and by (ii) in Lemma (4, 5), $\underline{\delta}(U \cap V, U^c) = 1$ and $\underline{\delta}(U \cap V, V^c) = 1$, Hence (by DH_2), $\underline{\delta}(U \cap V, U^c \cup V^c) = \underline{\delta}(U \cap V, (U \cap V)^c) = 1$. Consequently $U \cap V \in \tau_{\underline{\delta}}$.

$DT_3 \quad$ Let $V_i \in \tau_{\underline{\delta}}, \forall i \in I$, for some index set I . Then $\underline{\delta}(V_i, V_i^c) = 1, \forall i \in I \xrightarrow{DH_3} \underline{\delta}(\bigcup_{i \in I} V_i, V_i^c) = 1, \forall i \in I \xrightarrow{4.5(i)} \underline{\delta}(\bigcup_{i \in I} V_i, \bigcap_{i \in I} V_i^c) = 1 \Rightarrow \underline{\delta}(\bigcup_{i \in I} V_i, (\bigcup_{i \in I} V_i)^c) = 1 \Rightarrow \bigcup_{i \in I} V_i \in \tau_{\underline{\delta}}$.

Therefore, $\tau_{\underline{\delta}}$ is a double topology on X, generated by $\underline{\delta}$.

Corollary 4.7. $V \in \tau_{\underline{\delta}} \Leftrightarrow \underline{\delta}(x_i, V^c) = 1, \forall x_i \in V$.

Theorem 4.8. Let $(X, \underline{\delta})$ be a DPP- space. Then $\underline{\delta}(A, B) = 0 \Rightarrow A \overline{Q} B$.

Proof: Let $\underline{\delta}(A, B) = 0$ and suppose $A \overline{Q} B$
 $\Rightarrow A \subseteq \overline{B}^c$, if we choose all open double sets Q , which contain the closed double set \overline{B} , then $\bigcap_{\lambda} \overline{Q}_{\lambda} = \overline{B} \Rightarrow (A \subseteq \overline{B}^c) \overline{B}^c =$

$$\begin{aligned} (\bigcap_{\lambda} \overline{Q}_{\lambda})^c &= \bigcup_{\lambda} \overline{Q}_{\lambda}^c \text{ Since } \overline{Q}_{\lambda} \text{ is open } \forall \lambda, \\ \underline{\delta}(\overline{Q}_{\lambda}^c, \overline{Q}_{\lambda}) &= 1, \forall \lambda. \xrightarrow{DH_3} \\ \underline{\delta}(\bigcup_{\lambda} \overline{Q}_{\lambda}^c, \overline{Q}_{\lambda}) &= 1 \xrightarrow{4.5(ii)} \\ \underline{\delta}(\bigcup_{\lambda} \overline{Q}_{\lambda}^c, \bigcap_{\lambda} \overline{Q}_{\lambda}) &= 1 \Rightarrow \underline{\delta}(A, B) = 1. \end{aligned}$$

This contradicts our assumption that $\underline{\delta}(A, B) = 0$.

Corollary 4.9. Let $(X, \underline{\delta})$ be a DPP-space and let $x_i \in D(X)_p, A \in D(X)$, Then:

- (i) $\underline{\delta}(A, x_i) = 0 \Leftrightarrow x_i \in A$.
- (ii) $\underline{\delta}(x_i, A) = 0 \Rightarrow x_i \in \overline{A}$.

Theorem 4.10: Let $(X, \underline{\delta})$ be a DPP- space, Then: $(X, \tau_{\underline{\delta}}) \in DT_5$.

Proof: first, we prove that $\tau_{\underline{\delta}} \in DT_1$, for which we show that every double point of $D(X)_p$ is closed. Since $\underline{\delta}(x_i^c, x_i) = 1, \forall x_i \in D(X)_p \xrightarrow{4.6} \Rightarrow x_i^c \in \tau_{\underline{\delta}} \forall x_i \in D(X)_p \Rightarrow x_i \in \tau_{\underline{\delta}}^c, \forall x_i \in D(X)_p \Rightarrow (X, \tau_{\underline{\delta}}) \in DT_1$.

Now we show that for every separated double sets A, B in $X, \exists Q_A, Q_B$ such that $Q_A \overline{Q} Q_B$. Since $\underline{\delta}(\overline{A}^c, \overline{A}) = 1$, and A, B are separated, then $B \subseteq \overline{A}^c$. Consequently, $\underline{\delta}(B, \overline{A}) = 1$ and $\underline{\delta}(B, A) = 1$, (by Lemma 4.5 (ii), (i)). Similarly, we can show that $\underline{\delta}(A, B) = 1$. Now $\underline{\delta}(A, B) = \underline{\delta}(B, A) = 1$

DH₅
 $\Rightarrow \exists \underline{C}, \underline{D} \in D(X)$ Such that $\underline{C} \overline{Q} \underline{D}$ and
 $\underline{\delta}(\underline{A}, \underline{C}^c) = \underline{\delta}(\underline{C}, \underline{C}^c) = \underline{\delta}(\underline{B}, \underline{D}^c) =$
 $\underline{\delta}(\underline{D}, \underline{D}^c) = 1 \Rightarrow \underline{C}, \underline{D} \in \tau_{\underline{\delta}}$ (by 4.6), and
 $\underline{A} \subseteq \underline{C}, \underline{B} \subseteq \underline{D}$ (by 4.5 (iii)). Since $\underline{C} \overline{Q} \underline{D}$,
 then $(X, \tau_{\underline{\delta}}) \in DT_5$.

Theorem 4.11. Let (X, τ) be a double complete normal space. Then:
 $\underline{\delta} : D(X) \times D(X) \longrightarrow \{0, 1\}$, given by
 $\underline{\delta}(\underline{A}, \underline{B}) = 0 \Leftrightarrow \underline{A} \overline{Q} \underline{B}$, $\forall \underline{A}, \underline{B} \in D(X)$, is a SDH-proximity on X . Moreover, if $\underline{\delta}$ satisfies DH₅, then $\tau_{\underline{\delta}} = \tau$.

Proof: DH₁ $\underline{X} \overline{Q} \underline{\phi} \Rightarrow \underline{\delta}(\underline{X}, \underline{\phi}) = 1$,
 and $\underline{\phi} \overline{Q} \underline{X} \Rightarrow \underline{\delta}(\underline{\phi}, \underline{X}) = 1$.

DH₂ $\underline{\delta}(\underline{A}, \underline{B} \cup \underline{C}) = 0 \Rightarrow \underline{A} \overline{Q} (\underline{B} \cup \underline{C})$
 $\Leftrightarrow \underline{A} \overline{Q} (\underline{B} \cup \underline{C}) \stackrel{2.1.5}{\Leftrightarrow} \underline{A} \overline{Q} \underline{B}$ or $\underline{A} \overline{Q} \underline{C}$
 $\Leftrightarrow \underline{\delta}(\underline{A}, \underline{B}) = 0$ or $\underline{\delta}(\underline{A}, \underline{C}) = 0$.

DH₃ $\underline{\delta}(\bigcup_{i \in I} \underline{A}_i, \underline{B}) = 0 \Leftrightarrow (\bigcup_{i \in I} \underline{A}_i) \overline{Q} \underline{B} \stackrel{2.1.5}{\Leftrightarrow}$
 $\exists i_o \in I$ Such that $\underline{A}_{i_o} \overline{Q} \underline{B} \stackrel{2.1.5}{\Leftrightarrow}$
 $\underline{\delta}(\underline{A}_{i_o}, \underline{B}) = 0$ for some $i_o \in I$.

DH₄ $\underline{\delta}(x_p, y_r) = 0 \Leftrightarrow x_p \overline{Q} y_r \stackrel{(X, \tau) \in DT_1}{\Leftrightarrow}$
 $x_p \overline{Q} y_r, \forall x_p, y_r \in D(X)_p$. Thus $\underline{\delta}$ is SDH-Proximity on X . Moreover, if $\underline{\delta}$ satisfies DH₅,

then: $\tau_{\underline{\delta}} = \{\underline{V} \in D(X) : \underline{\delta}(\underline{V}, \underline{V}^c) = 1\}$
 $= \{\underline{V} \in D(X) : \underline{V} \overline{Q} \underline{V}^c\}$.

$$= \{\underline{V} \in D(X) : \underline{V} \subseteq \underline{V}^c = \underline{V}^o\}$$

$$= \{\underline{V} \in D(X) : \underline{V} \in \tau\} = \tau.$$

References:

- 1- M. Abdelhakem, Some Extended Forms of Fuzzy Topological Spaces via Ideals, Ph. D. thesis in Math., Fac. of Sci., Helwan Univ., Egypt (2011).
- 2- R. Engelking, General topology, Warszawa (1977).
- 3- E. Hayashi, on some properties of proximity, J. Math. Soc. Japan., 16 (4) (1964).
- 4- A. Kandil, O. A. E. Tantawy and M. Abdelhakem, Flou Topological Spaces via Flou Ideals, Int. J. App. Math., Vol. 23, No 5 (2010) 837-885.
- 5- A. Knadil, O. Tantawy and K. Barakat, Fuzzy Paraproximity Spaces, Nat. Math. and Comput. Sci., Vol. 4, No. 1, (2008) 13-22.
- 6- A. Kandil, O. A. E. Tantawy and M. Wafaie, Flou separation axioms, J. Egypt. Math. and Phys. Soc., accepted (2010).
- 7- A. Kandil, O. A. E. Tantawy and M. Wafaie, On flou (INTUITIONISTIC) compact space, J. Fuzzy Math., Vol. 17, No. 2, (2009), 275-294.
- 8- A. Kandil, O. A. E. Tantawy and M. Wafaie, On flou (INTUITIONISTIC) topological spaces, J. Fuzzy Math., Vol.15, No 2, 2007.
- 9- E. E. Kerre, "fuzzy sets and approximate reasoning", Lectures notes, University of Gent Belgium (1988).

Combined Effects of Temperature and Algal Concentration on Filtration and Ingestion Rates of *Crassostrea gigas*: Bivalvia

Mona, M. H.¹, Elkhodary, G.M.*² and Khalil, A.M

¹Zoology Department, Faculty of Science, Tanta University, Tanta, Egypt.

²Zoology Department, Faculty of Science, Damnhour University, Damnhour, Egypt.

³Zoology Department, Faculty of Science, Zagazig University, Zagazig, Egypt.

*gihankhodary@hotmail.com

Abstract: The effect of varying algal cell concentration, food items and temperature on the filtration and ingestion rates of the eyed larva of *Crassostrea gigas* were investigated under laboratory condition. The filtration and ingestion rates were measured according to the indirect method in which the flow of water into the passage cavity is inferred from the rate of removal of suspended particles. Cultures of the unicellular alga *Isochrysis galbana* and *Pavlovia lutheri* were used in the test solutions. Three different concentrations of the two algal species (100,50 and 25 cells/μl) and three temperature degrees (25 °C, 20 °C and 13 °C) were used to study the effect of these factors at different time intervals from starting the experiments (1, 6 and 12 days) on the filtration and ingestion rates of the eyed – larvae. The filtration and ingestion rates of the larvae of *C.gigas* that recorded by using *I. galbana* were large than that of *P. lutheri*. These results might depend on the size of the filtered particles. Moreover, the larvae of *C. gigas* regulate filtration rates according to the particle concentration in the surrounding medium, filtration was more actively in lower concentrations ($25 \times 10^6 \text{ L}^{-1} I. galbana$) than at the higher ones ($100 \times 10^6 \text{ L}^{-1} I. galbana$). The mean value of filtration and ingestion rates of *C.gigas* were significantly increased by the increase in temperature degree and 25°C were considerable the perfect temperature to achieve high values of both filtration and ingestion rates if it is compared by 20 °C and 13 °C. These results help to explain the feeding behavior of *C.gigas*.

[Mona, M. H., Elkhodary, G.M. and Khalil, A.M **Combined Effects of Temperature and Algal Concentration on Filtration and Ingestion Rates of *Crassostrea gigas*: Bivalvia**] Life Science Journal, 2011; 8(4):805-813] (ISSN: 1097-8135). <http://www.lifesciencesite.com>.

Key Words: Edible bivalve, *Crassostrea gigas*, Feeding behavior, Filtration rate, Ingestion rate-algal cell, Temperature.

1. Introduction

Filtration rate or clearance rate is defined as the volume of water filtered completely free of particles per unit of time and is also sometimes synonymously used as the pumping rate when all particles entering the mantle cavity are completely retained by gills (Winter, 1978). The ingestion rate or feeding rate is defined as the number of algal cells an organism consumes per unit time (Peters, 1984). Two principal methods are available to measure the rate of passage of water through the mantle cavity of a bivalve, the direct method on which the rate of pumping of water itself is measured, and the indirect method in which the flow is inferred from the rate of removal of suspended particles. The former method requires either a physical separation of the inhalant and the exhalant currents or a method of rendering visible the flow of water from the siphons by using dyes or other kinds of particles (Ali, 1970). Khalil, (1996) and Rajesh *et al.*, (2001) measured the filtration and ingestion rates in *Tapes decussatus*, *Perna viridis*, *Crassostrea madrasensis* and *Paphia malabarica* using *Isochrysis galbana* and *Pavlovia lutheri* as unicellular algal food. Christina and Hans (2005) measured clearance rate of *Rhodomonas sp.* in

Mytilus edulis. Luc *et al.*, (2008) studies the filtration rate of *Mytilus edulis* and *Crassostrea virginica* at low temperature using a mixed suspension of *Chaetoceros muelleri* and *Isochrysis galbana*. Filtration and ingestion rates of different larval stages of *Paphia malabarica* have been measured in relation to feeding on various species of unicellular algae (Raghavan, 2011).

Many countries in different regions of the world introduced the pacific oyster *Crassostrea gigas* into their water because of the over harvesting of their native oyster. *Crassostrea gigas* was introduced into Germany (Mexiner and Gerdener, 1976), Taiwan (Li & Yuan, 1981), Chile (Winter *et al.*, 1984) and Mexico (Cardenas, 1984).

The present work was planned to construct the basis of an ideal hatchery upon which the pacific oyster can be introduced and planted in Egypt. The selection of this animal was based on the following.

1. It's highly valuable as a food where it is considered one of the most important inexpensive and rich sources of protein.
2. Its high tolerance to the different environment parameters (e.g temperature, salinity and food requirement).

3. The recent technical advances that facilitate its cultivation and maintenance.

This work aims to assess the effect of temperature and algal cell concentration of *Isochrysis galbana* and *Pavlovia lutheri* on filtration and ingestion rates of *Crassostrea gigas* eyed – larvae. The technique that used provided a means of carrying out acute measurements of grazing rate, and hence of detecting short – term responses to changes in the environment.

2. Material and Methods

The filtration rates, swept-clear-volumes, (ml/h/individual) and the ingestion rates, number of algal cells filtered out, (cells/h/individual) of eyed-larvae were measured as a function of different ecological factors. Three different concentrations of the two algal species and three temperature degrees were used to study the effect of these factors at different time intervals from starting the experiments on filtration and ingestion rates of the eyed-larvae.

Experimental animals:

The swimming larvae of *Crassostrea gigas* were collected from coast oyster Hatchery of Quilcen, Washington to the laboratory. The artificial sea water was removed from the culture vessels through a screen of sufficiently fine mesh to retain these small larvae. Larvae were fed on a mixture of algae *Isochrysis galbana* and *Pavlovia lutheri*. The algal culture methods followed the techniques adopted by Guillard and Ryther (1962). A mixture of the antibiotics Streptomycin Sulphate; Erythromycin Lactobionate and Cefotaxime (200,150,200mg, respectively \l sea water) was added to the petri dishes of larval culture at each water change. This process is very important to keep the larvae healthy and in an active swimming condition. All larvae used in experiments, were acclimated in aerated fresh seawater for 7 days in order to settle down after the disturbance caused by shipping them to the lab. Investigated samples in good condition were chosen from bunches of similar size and age and cleaned from any mud particles and any epizoic growth. Measurements of filtration rates were made at three different temperature degrees 13°C, 20°C and 25°C, the required temperature was attained by holding the plastic dishes containing the algal cells and the larvae of *C. Gigas* in the analogous thermostat chambers. The larvae were brought to experimental temperature and left for 1 hour at this temperature before any readings of the filtration rates were begun.

Feeding:

Pure logarithmic phase from the cultures of the unicellular algae *Isochrysis galbana* and *Pavlovia*

lutheri were used. These were grown in f/2 medium (Guillard and Ryther, 1962) and centrifuged from the culture medium and suspended again in filtered sea water. Cell density was determined by means of a blood –cell counting chamber (Thoma, 0.1 mm depth). Three levels of food concentration were used through these experiments: 100, 50, 25 cells /µl of the cultural media. To reach the actual concentration required, these steps were followed:

- certain volume (v) of algal culture was poured in capped bottles.
- The suspension was centrifuged to get rid of the supernatant that causes high mortality among the larval cultures.
- Freshly prepared seawater was added to the algal cells that accumulated in the bottom of the bottles until reaching to the volume (v) again
- The algal cells/ µl (c) were counted by using the blood cell counting chamber.
- To deduce the required concentration (c) and volume (v) the following equation was applied

$$c \times v = c \times v$$

Experimental Design:

Groups of 10 larvae were placed in 25 ml plastic dishes (to avoid the settlement and metamorphosis of these larvae which might result in other substrata other than plastic) containing 10 ml of algal culture. These groups of dishes were classified to fulfill the purpose of the following experiments:

- Experiments to measure the effect of temperature on the filtration rate and the ingestion rate.
- Experiments to measure the effect of food concentration on both filtration and ingestion rates.
- Experiments to measure the effects of time on filtration rate and ingestion rate.

All previous experiments were carried out on the eyed – larvae of *Crassostrea gigas* to compare the effect of the different parameters on their filtration rates. Three 1 litre Pyrex dishes of the larval cultures were prepared where the density of the larvae were 100 larvae / L and kept in 13 °C, 20 °C and 25 °C thermostat chambers (one dish for each temperature) to be the stock of the different experiments.

To examine the effect of food concentrations (100, 50, 25 cells / µl) on the filtration and ingestion rates, three groups, A, B and C were prepared where each food density was represented by one of these groups. Each group composed of 7 dishes, whereas 10 larvae were held on 10 ml of algal suspension in 6 dishes while the seventh included only algae without animals as a control. This served to correct for any error which might result from sedimentation, flocculation or reproduction of the algae during the

experiments.

In clearance experiments, the larvae were continuously withdrawing particles and diluting the suspension with filtrate. To keep the initial concentration of the suspension nearly fixed, the suspension was exchanged with new one each 6 hours. To examine the effect of food items on the filtration rate, step 1 was repeated twice, one by using *pavlovia lutheri* and the other by using *Isochrysis galbana*. To examine the effect of temperature on the filtration rate step 2 was repeated three times for 13 °c, 20 °c, and 25 ° c. To examine the effect of time on filtration rate, 10 larvae were pipetted by using the automatic micropipette from the stock dishes to 25 ml plastic dishes (where the experiments were conducted after 1,6 and 12 days for starting the experiments) then steps 1,2 and 3 were repeated.

Calculation:

All calculations were operated by methods of Coughlan (1969) and Peters (1984) where the following formulae were applied because of their easiness and reliance:

$$\text{Ingestion rate} = \frac{(c_0 - c_t) V}{Nt} \text{ cells individual}^{-1} \text{ hour}^{-1}$$

$$\text{Filtration rate} = \frac{(Inc_0 - Inc_t) V}{Nt} \text{ ml. individual}^{-1} \text{ hour}^{-1}$$

Where:

C_0 = Initial cell concentration at time zero.

C_t = Final cell concentration at time (t)

t = Time interval (hours)

N = Number of individuals in container.

V = Volume of the algal culture used.

Statistical analysis:

The results are presented as mean \pm SD values. Two –way analysis of variance (ANOVA) was used to test the significance of filtration and ingestion rates in each food items. LSD test was used to analyze the mean comparisons among concentration of algal cell and temperature degree and paired T- test to compare between the different time intervals. All statistical analysis were preformed using the SPSS 17 soft ware (SPSS 2007)

3. Results

1.1. The effect of temperature, time and *I. galbana* concentration on filtration and ingestion rates of eyed larvae of *C. gigas*

By using 100 cells / μ l of *I. galbana*, the filtration rate decreased significantly from 0.078 ml/h/larva at 25°C to 0.005 \pm 0.001 ml/h/larva at 13 °c and the ingestion rate from 3558.4 \pm 8.502 cells/h/larva at 25 ° c to only 1402.79 \pm 5.645 cells /h/larva at 13°C (Tables,1&3). By comparing the

filtration and the ingestion rates in relation to the time of experiments, a highly significant decrease ($P \leq 0.001$) in these rates was observed by the passage of the time.

At the concentration 50 cells/ μ l (figures 1, 2) the rates continued to decline significantly ($P \leq 0.001$) after 1, 6 and 12 days at all tested temperatures.

Table 1 elucidate that at the concentration 25 cells/ μ l, the filtration rates were greatly affected by temperature after one day from starting the experiments measured under the effect of different temperatures. They always increased significantly by increasing the tested temperatures ($P \leq 0.001$). The rates were larger at 25 °c than that at 20 °c and 13 °c. At 25 °c and 20 °c, the filtration rate decreased significantly ($P \leq 0.001$) by increasing the duration of experiments and decreased not significantly at 13 °c.

On the other hand, the filtration rate of eyed –larva of *C. gigas* were significantly higher ($P \leq 0.001$) at concentration 25 cells/ μ l than concentration 100 cells/ μ l meanwhile, the ingestion rates decreased significantly by decreasing these concentrations (Table, 2)

1.2 The effect of temperature, time and *P.lutheri* concentration on filtration and ingestion rates of eyed larvae of *C. gigas*.

Figures 3 and 4 confine the predominance of 25°C as a perfect temperature to achieve high significant values of both filtration and ingestion rates if it is compared by 20 °c and 13°C by using 100 cells / μ l of *P.lutheri*. The highest values of these rates always recorded after one day from starting the experiments. At 20°C, the passage of time of experiments also decreased these rates significantly ($P \leq 0.001$) but there was no significant effect ($P \geq 0.05$) for the time on these rates at 13°C; the filtration (0.074 \pm 0.001 ml/h/larva) and the ingestion rates (1748.33 \pm 7.024 cells /h/larva) at the combination 25°C, 50 cells/ μ l and one day significantly decrease than that at the combination 13°C, 50cells/ μ l and 12 days, they were 0.003 \pm 0.001 ml/h/larva and 129.667 \pm 2.517 cells /h/ larva respectively.

Tables 5 the filtration rate recorded when 25cells/ μ l was used as a food concentration were significantly high ($P \leq 0.001$) than that measured with 100 and 50 cells/ μ l, yet these data were parallel to these of 100 and 50 cells/ μ l.

The previous data showed that the filtration rates and ingestion rates direct proportional with the temperature and inverse proportional with the time from starting the experiments. Meanwhile, the filtration rates inverse proportional with food concentration while ingestion rates direct proportional with the same parameter.

Table (1): The effect of different temperatures and different concentrations of *I. galbana* on the filtration rate (ml/h/larvae) of the eyed-larvae of *C.gigas*.

Time	Conc.	Temp.				LSD			
		Mean	25°C	20°C	13°C	Total	Comp.	P-value	
T1	100 cells/µl	Mean	0.078	0.066	0.005	0.050	100 cells/µl&50 cells/µl	0.000	
		SD	0.000	0.000	0.001	0.034	100 cells/µl&25 cells/ µl	0.000	
	50 cells/µl	Mean	0.093	0.063	0.005	0.054	50 cells/ µl &25 cells/ µl	0.000	
		SD	0.001	0.001	0.000	0.039	25°C&20°C	0.000	
	25 cells/µl	Mean	0.112	0.085	0.008	0.068	25°C&13°C	0.000	
		SD	0.000	0.001	0.001	0.047	20°C&13°C	0.000	
	Total	Mean	0.094	0.071	0.006	0.057			
		SD	0.015	0.010	0.001	0.039			
	T2	100 cells/µl	Mean	0.070	0.040	0.004	0.038	100 cells/ µl &50 cells/ µl	0.000
			SD	0.001	0.001	0.001	0.029	100 cells/ µl &25 cells/ µl	0.000
50 cells/µl		Mean	0.077	0.052	0.003	0.044	50 cells/ µl &25 cells/ µl	0.000	
		SD	0.001	0.001	0.001	0.033	25°C&20°C	0.000	
25 cells/µl		Mean	0.096	0.047	0.009	0.050	25°C&13°C	0.000	
		SD	0.001	0.001	0.001	0.038	20°C&13°C	0.000	
Total		Mean	0.081	0.046	0.005	0.044			
		SD	0.012	0.005	0.003	0.032			
T3		100 cells/µl	Mean	0.017	0.010	0.003	0.010	100 cells/ µl &50 cells/ µl	0.000
			SD	0.001	0.001	0.001	0.006	100 cells/ µl &25 cells/ µl	0.000
	50 cells/µl	Mean	0.024	0.019	0.002	0.015	50 cells/ µl &25 cells/ µl	0.000	
		SD	0.001	0.001	0.001	0.010	25°C&20°C	0.000	
	25 cells/µl	Mean	0.042	0.020	0.007	0.023	25°C&13°C	0.000	
		SD	0.001	0.002	0.000	0.015	20°C&13°C	0.000	
	Total	Mean	0.028	0.017	0.004	0.016			
		SD	0.011	0.005	0.002	0.012			

Table (2): Two way analysis for variance on filtration rate of eyed- larvae of *C.gigas* fed on *Isochrysis gabana*

ANOVA 2-way	T1		T2		T3	
	F	P-value	F	P-value	F	P-value
Conc.	3019.179	0.000	1393.263	0.000	748.742	0.000
Temp.	69006.385	0.000	52247.933	0.000	2460.712	0.000
Conc. *Temp.	827.977	0.000	633.125	0.000	198.458	0.000

T1: time after one day.

T1: time after 6days.

T3: time after 12 days.

Table (3): The effect of different temperatures and different concentrations of *Isochrysis gabana* on the ingestion rate (cells/h/larvae) of the eyed-larvae of *C.gigas* at different time intervals.

Time	Conc.	Temp.				LSD			
		Mean	25°C	20°C	13°C	Total	Comp.	P-value	
T1	100 cells/µl	Mean	3558.400	3340.800	497.333	2465.511	100 cells/ µl &50 cells/ µl	0.000	
		SD	8.502	6.239	7.024	1479.151	100 cells/ µl &25 cells/ µl	0.000	
	50 cells/µl	Mean	1845.067	1620.733	237.767	1234.522	50 cells/ µl &25 cells/ µl	0.000	
		SD	10.621	9.012	4.676	753.887	25°C&20°C	0.000	
	25 cells/µl	Mean	959.333	898.000	173.333	676.889	25°C&13°C	0.000	
		SD	4.041	7.550	4.509	378.630	20°C&13°C	0.000	
	Total	Mean	2120.933	1953.178	302.811	1458.974			
		SD	1144.311	1086.773	148.613	1213.278			
	T2	100 cells/µl	Mean	3397.600	2600.200	375.933	2124.578	100 cells/ µl &50 cells/ µl	0.000
			SD	5.503	5.632	4.002	1356.182	100 cells/ µl &25 cells/ µl	0.000
50 cells/µl		Mean	1760.367	1478.967	111.433	1116.922	50 cells/ µl &25 cells/ µl	0.000	
		SD	5.040	7.919	10.304	763.929	25°C&20°C	0.000	
25 cells/µl		Mean	955.000	715.667	178.000	616.222	25°C&13°C	0.000	
		SD	4.359	4.041	19.287	344.766	20°C&13°C	0.000	
Total		Mean	2037.656	1598.278	221.789	1285.907			
		SD	1077.937	820.935	119.665	1091.172			
T3		100 cells/µl	Mean	1402.767	925.933	240.667	856.456	100 cells/ µl &50 cells/ µl	0.000
			SD	5.645	6.001	4.041	505.916	100 cells/ µl &25 cells/ µl	0.000
	50 cells/ml	Mean	926.733	769.600	109.800	602.044	50 cells/ µl &25 cells/ µl	0.000	
		SD	6.513	6.089	9.702	375.459	25°C&20°C	0.000	
	25 cells/µl	Mean	645.667	388.000	152.667	395.444	25°C&13°C	0.000	
		SD	5.132	4.583	2.517	213.580	20°C&13°C	0.000	
	Total	Mean	991.722	694.511	167.711	617.981			
		SD	331.475	239.692	58.031	416.030			

Table (4): Two way analysis for variance on ingestion rate of eyed- larvae of *C.gigas* fed on *Isochrysis gabana*

ANOVA 2-way	T1		T2		T3	
	F	P-value	F	P-value	F	P-value
Conc.	144320.627	0.000	70343.022	0.000	13866.216	0.000
Temp.	173956.426	0.000	106971.294	0.000	45283.747	0.000
Conc. *Temp.	24044.330	0.000	13827.590	0.000	2926.363	0.000

T1: time after one day.

T1: time after 6days.

T3: time after 12 days

Table (5): The effect of different temperatures and different concentrations of *Pavlovia lutheri* on the filtration rate(ml/h/larvae) of the eyed-larvae of *C.gigas* at different time intervals.

Time	Conc.	Temp.					LSD	
		Mean	25°C	20°C	13°C	Total	Comp.	P-value
T1	100 cells/µl	Mean	0.061	0.037	0.003	0.034	100 cells/ µl & 50 cells/ µl	0.000
		SD	0.000	0.001	0.001	0.026	100 cells/ µl & 25 cells/ µl	0.000
	50 cells/µl	Mean	0.074	0.047	0.004	0.042	50 cells/ µl & 25 cells/ µl	0.000
		SD	0.001	0.001	0.001	0.031	25°C&20°C	0.000
	25 cells/µl	Mean	0.085	0.066	0.002	0.051	25°C&13°C	0.000
		SD	0.001	0.001	0.000	0.037	20°C&13°C	0.000
	Total	Mean	0.073	0.050	0.003	0.042		
		SD	0.010	0.013	0.001	0.031		
T2	100 cells/µl	Mean	0.055	0.025	0.002	0.028	100 cells/ µl & 50 cells/ µl	0.000
		SD	0.001	0.002	0.001	0.023	100 cells/ µl & 25 cells/ µl	0.000
	50 cells/µl	Mean	0.056	0.036	0.003	0.032	50 cells/ µl & 25 cells/ µl	0.002
		SD	0.001	0.001	0.001	0.023	25°C&20°C	0.000
	25 cells/µl	Mean	0.069	0.029	0.002	0.033	25°C&13°C	0.000
		SD	0.001	0.001	0.001	0.029	20°C&13°C	0.000
	Total	Mean	0.060	0.030	0.002	0.031		
		SD	0.006	0.005	0.001	0.024		
T3	100 cells/µl	Mean	0.013	0.008	0.003	0.008	100 cells/ µl & 50 cells/ µl	0.000
		SD	0.001	0.001	0.001	0.004	100 cells/ µl & 25 cells/ µl	0.000
	50 cells/µl	Mean	0.019	0.009	0.003	0.010	50 cells/ µl & 25 cells/ µl	0.000
		SD	0.001	0.001	0.001	0.007	25°C&20°C	0.000
	25 cells/µl	Mean	0.030	0.009	0.002	0.014	25°C&13°C	0.000
		SD	0.001	0.001	0.002	0.012	20°C&13°C	0.000
	Total	Mean	0.020	0.009	0.003	0.011		
		SD	0.007	0.001	0.001	0.009		

Table (6): Two way analysis for variance on filtration rate of eyed- larvae of *C.gigas* fed on *Pavlovia lutheri*

ANOVA 2-way	T1		T2		T3	
	F	P-value	F	P-value	F	P-value
Conc.	1204.619	0.000	159.124	0.000	167.163	0.000
Temp.	20680.027	0.000	16166.796	0.000	1645.347	0.000
Conc. *Temp.	341.999	0.000	196.341	0.000	170.796	0.000

T1: time after one day.

T1: time after 6days.

T3: time after 12 days

4. Discussion

The comparison of the previous record filtration rates of many bivalve larvae with the present ones reveals that much of the existing data fall in the range of filtration rates determined in the present work. According to the present study it was found that, the

colorimetric measurements for the initial and the final concentrations of the suspension tested by Ali (1970) were not exactly valid because the pseudofaeces rejected by the examined animals still have their own color and of course this will mislead to wrong reading. Although cell diameter of *P.lutheri* (6µm) was larger

than that of *I.galbana* (3um) (Bayne 1965), the filtration and the ingestion rates that recorded by using *I.galbana* were larger than that of *P.lutheri*. These results were in agreement with that of Débora *et al.*, (2009) who stated that, the differences in filtration rates of *Limnoperna fortunei* between the different types of food used (Algamac-2000® and *Scenedesmus sp.*) could be accounted for by the differences in algal cell size. Baker *et al.*,(1998) and Vanderploeg *et al.*,(2001) detected shifts in local phytoplanktonic communities following the introduction of the zebra mussel (*Dreissena polymoroha*). The mechanism underlying those shifts seemed to be the selective removal of particles of specific sizes; with the rejected

particles being returned to the water column in the form of unconsolidated pseudofaeces.

Moreover, This study also reported that the larvae of *C. gigas* regulate filtration rates according to the particle concentration in the surrounding medium, filtration was more actively in lower concentrations ($25 \times 10^6 L^{-1} I. galbana$) than at the higher ones ($100 \times 10^6 L^{-1} I. galbana$). Similar data were recorded by Gerdes (1983) in relation to *C. gigas*. While ,Rajesh *et al.*(2001) reported that the filtration rate of *Perna viridis* increased with increasing algal cell concentration until 10^5 cells.ml⁻¹, after which there was a rapid decline.

Table (7): The effect of different temperatures and different concentrations of *Pavlovia lutheri* on the ingestion rate(cells/h/larvae) of the eyed-larvae of *C.gigas*.

Time	Conc.	Temp.				LSD			
		25°C	20°C	13°C	Total	Comp.	P-value		
T1	100 cells/ µl	Mean	3203.667	2427.333	267.333	1966.111	100 cells/ µl & 50 cells/ µl	0.000	
		SD	6.028	7.506	5.686	1317.697	100 cells/ µl & 25 cells/ µl	0.000	
	50 cells/ µl	Mean	1748.333	1434.333	280.000	1154.222	50 cells/ µl & 25 cells/ µl	0.000	
		SD	7.024	5.132	7.000	669.639	25°C & 20°C	0.000	
	25 cells/ µl	Mean	925.000	845.000	60.000	610.000	25°C & 13°C	0.000	
		SD	5.568	6.557	3.000	413.977	20°C & 13°C	0.000	
	Total	Mean	1959.000	1568.889	202.444	1243.444			
		SD	999.276	692.585	107.080	1023.420			
	T2	100 cells/ µl	Mean	3074.000	1892.333	266.000	1744.111	100 cells/ µl & 50 cells/ µl	0.000
			SD	8.718	7.024	5.292	1220.987	100 cells/ µl & 25 cells/ µl	0.000
50 cells/ µl		Mean	1564.667	1225.000	153.000	980.889	50 cells/ µl & 25 cells/ µl	0.000	
		SD	5.132	5.568	6.000	638.117	25°C & 20°C	0.000	
25 cells/ µl		Mean	847.667	527.667	60.000	478.444	25°C & 13°C	0.000	
		SD	7.024	8.021	3.000	343.106	20°C & 13°C	0.000	
Total		Mean	1828.778	1215.000	159.667	1067.815			
		SD	984.190	590.996	89.443	949.421			
T3		100 cells/ µl	Mean	1093.000	766.667	300.333	720.000	100 cells/ µl & 50 cells/ µl	0.000
			SD	6.000	7.095	5.033	345.055	100 cells/ µl & 25 cells/ µl	0.000
	50 cells/ µl	Mean	775.000	448.000	129.667	450.889	50 cells/ µl & 25 cells/ µl	0.000	
		SD	5.568	6.000	2.517	279.479	25°C & 20°C	0.000	
	25 cells/ µl	Mean	541.667	172.333	86.667	266.889	25°C & 13°C	0.000	
		SD	8.505	62.740	7.024	211.804	20°C & 13°C	0.000	
	Total	Mean	803.222	462.333	172.222	479.259			
		SD	239.743	259.523	97.974	332.301			

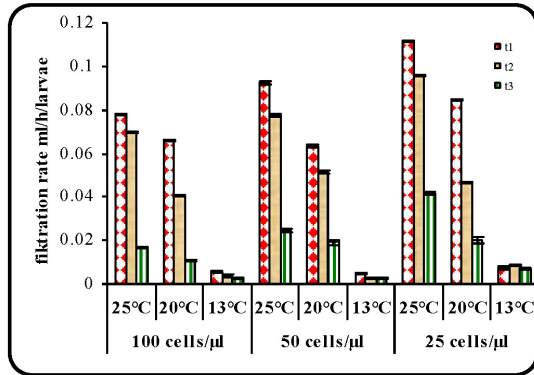
Table (8): Two way analysis for variance on ingestion rate of eyed- larvae of *C.gigas* fed on *Pavlovia lutheri*

ANOVA 2-way	T1		T2		T3	
	F	P-value	F	P-value	F	P-value
Conc.	113399.137	0.000	89073.342	0.000	991.378	0.000
Temp.	207160.524	0.000	156311.852	0.000	1904.352	0.000
Conc. *Temp.	23900.597	0.000	20078.818	0.000	70.093	0.000

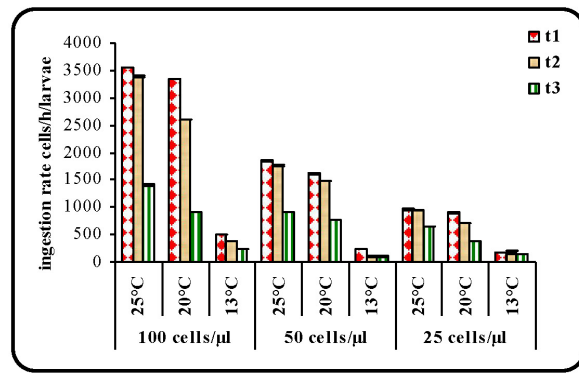
T1: time after one day.

T1: time after 6days.

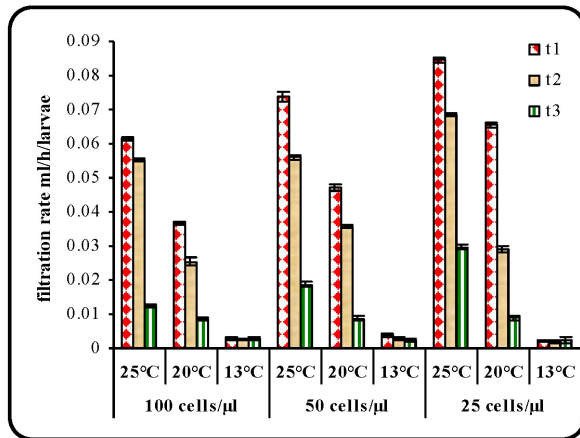
T3: time after 12 days



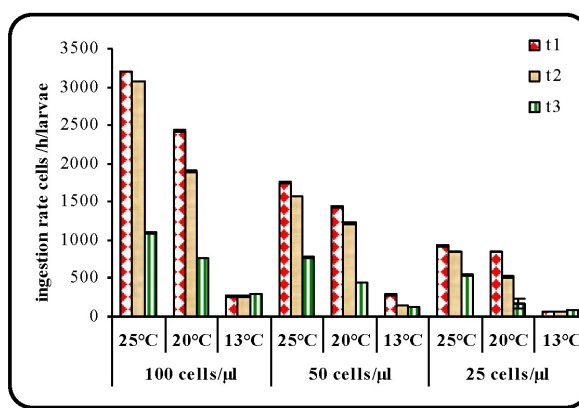
Fig(1): Mean \pm SD of filtration rate of eyed larvae of *C. gigas* under the effect of temperature and food concentrations of *I. galbana* at one day (t1), six days (t2) and twelve days (t3).



Fig(2): Mean \pm SD of ingestion rate of eyed larvae of *C. gigas* under the effect of temperature and food concentrations of *I. galbana* at one day (t1), six days (t2) and twelve days (t3).



Fig(3): Mean \pm SD of filtration rate of eyed larvae of *C. gigas* under the effect of temperature and food concentrations of *P. lutheri* at one day (t1), six days (t2) and twelve days (t3).



Fig(4): Mean \pm SD of ingestion rate of eyed larvae of *C. gigas* under the effect of temperature and food concentrations of *P. lutheri* at one day (t1), six days (t2) and twelve days (t3).

Many investigators elucidated the reduction rate on the basis of one of the following explanations: 1) the presence of the threshold concerning with the number of cells in suspension below which the oysters can not remove a maximum ration (Epifanio and Ewart, 1977), 2) the highly concentrated suspensions by which the gills of oysters became heavily covered with a mass of particles which would be rejected and removed as pseudofaeces (Ali, 1970), 3) the presence of inhibitory substances in the culture medium (Davids, 1964) and 4) the trying of the animals for adapting to food concentration to be typical of that of natural environments (Tenore and

Dunstan, 1973). Horgan and Mills (1997) indicated that there was a positive correlation between the amount of the food available and filtration rates.

The present investigations showed that, for each *I. galbana* and *P. lutheri* the filtration rates were direct proportional with the ingestion rates. By increasing the algal cell concentration, the ingestion rates decreased. Strychar and Macdonald (1999) reported that in *Crassostrea virginica* ingestion was regulated as the concentration of particles increased both by producing pseudofaeces and reducing clearance rates even at low particle concentrations. Pseudofaeces production is an important mechanism

to regulate ingestion and has typically been shown to increase with elevated seston concentrations in most of the bivalves studied.

The result of herein experiment showed, the filtration and ingestion rates of eyed larvae of *C. gigas* increased by the increase in temperature degrees. The filtration rate was increased by increasing the temperature up to 15 °C (Winter, 1969) and up to 15 °C – 17 °C (Theede, 1963, Ali, 1970). Working on *R. philippinarum*, Gouletquer *et al.* (1989) found that filtration of *R. philippinarum* was nearly constant between 12 and 20° C. Similarly, working on *R. philippinarum* and *T. decussatus*, Defosseze and Daguzan (1995) showed no significant changes in pumping rates from 19 to 29 °C. The data of Gerdes (1983) and the herein data partially agreed with the mentioned published data concerning with algal concentrations but fully contradicted with the data concerning with the maximum temperature where the highest filtration rate and the cells that filtered out occurred at 25°C. Moreover, in the present study, the combination of high food concentration and temperature positively affected on the feeding rates and this of course played an important role in putting an available interpretation to the growth rates in the same conditions.

Acknowledgment

The authors thank Dr. William K., Fitt, University of Georgia, U.S.A. for providing laboratory facilities, technique assistance discussion and experimental help throughout this study. Thanks are extended to Dr. Steeve Coon, University of Maryland, U.S.A. for kindly supplying larvae and the stock of algae.

Corresponding author

Mona, M.H.
Zoology Department, Faculty of Science, Tanta University, Tanta, Egypt.
monamm3@yahoo.com

References

Ali, R.M. (1970): The influence of suspension density and temperature on filtration rate of *Hiatella arctica*. *Marine Biology*, 6, 291 – 303
Baker, S. M.; Levinton, J. S; Kundziel, J. P. and Shumway, S. E. (1998): Selective feeding and biodeposition by zebra mussel and their relation to changes in phytoplankton composition and seston load. *Journal of Shellfish Research*, 17, 1207–1213.
Bayne, B.L. (1965). Growth and the delay of metamorphosis of the larvae of *Mytilus edulis* (L.), *Ophelia*, 2 (1):1-47.
Cardenas, E.B. (1984): Status of molluscan aquaculture on the Pacific coast of Mexico.

Aquaculture, 39, 83 – 93.
Christina K and Hans U. R. (2005): Effect of temperature on filtration rate in the mussel *Mytilus edulis*: no evidence for temperature compensation. *Marine Ecology Progress Series*, 305,147-152.
Coughlan, J. (1969): The estimation of filtering rate from the clearance of suspensions. *Marine Biology*, 2, 356 – 358.
Davids, C. (1964): The influence of suspensions of microorganisms of different concentrations on the pumping and ventilation of food by mussel (*Mytilus edulis* L.). *Netherland Journal of Sea Research*, 2, 233 – 249.
Débora P.; Antonio O.; Walter A.; P.Boeger and Marcio R. P. (2009): The effect of temperature and body size on filtration rates of *Limnoperna fortunei* (Bivalvia, Mytilidae) under laboratory conditions. *Brazilian Archives of biology and Technology*, 52 (1), 135:144.
Defosseze, J.M., Daguzan, J., (1995): Mesure comparative du débit palléal des bivalves *Tapes decussatus* et *Ruditapes philippinarum* lors de changements de température et de turbidité. *Cahiers de Biologie Marine*, 36, 299-307.
Epifanio, C.E. and Ewart. J. (1977): Maximum ration of four algal diets for the oyster *Crassostrea virginica* Gmelin. *Aquaculture*, 11, 13 – 29.
Gerdes, D. (1983): The pacific oyster *Crassostrea gigas* Part 1. Feeding behaviour of larvae and adults. *Aquaculture*, 31, 195-219.
Gouletquer, P., Heral, M., Deslous-Paoli, J.M., Prou, J., Garnier, J., Razet, D. and Boromthanasat, W., (1989): Ecophysiology et bilan énergétique de la palourde japonaise d'élevage *Ruditapes philippinarum*. *Journal of the Experimental Marine Biology and Ecology*, 132, 85-10.
Guillard, R.R. and Ryther, J.H. (1962): Studies on marine planktonic diatoms *I. Cyclotella nana* Hustedt and *Detonula confervacea* (Cleva) Gran. *Canadian Journal of Microbiology*, 8, 229 – 239.
Horgan, M. J. and Mills, E. L. (1997): Clearance rates and filtering activity of zebra mussel (*Dreissena polymorpha*): implications for freshwater lakes. *Canadian Journal of Fisheries and Aquatic Sciences*, 54, 249–255.
Kalil, A.M.(1996): The influence of algal concentration and body size on filtration and ingestion rates of the clam *Tapes decussatus* (L.) (Mollusca: Bivalvia). *Aquaculture Research*, 27 (8), 612-621.
Li, Y.P. and Yuan, P.W. (1981): Status of aquaculture in Taiwan. In: *Proceedings of ROC-US Cooperative Science Seminar on fish Diseases*. NSC Symposium 3, 1-6.
Luc A. C., Fabrice P., Réjean T., Stephen S. B. and Angeline L. (2008): Comparison of eastern oyster

- (*Crassostrea virginica*) and blue mussel (*Mytilus edulis*) filtration rates at low temperatures. Canadian Technical Report of Fisheries and Aquatic Sciences 2810.
- Meixner, R. and Gerdener, C. (1976): Untersuchungen über die Möglichkeit einer Fortpflanzung der eingeführten Pazifischen Auster *Crassostrea gigas* in deutschen Küstengewässern. Arch. Fischereiwiss., 26: 155-160.
- Peters, R.H. (1984). Methods for the study of feeding, grazing and assimilation by Zooplankton, P. 336-412. In: J.A. Downing and F.R. Rigler (eds), A manual on methods for the assessment of secondary production in fresh waters, 2nd ed. IBP Handbook 17, Blackwell Scientific Publications.
- Raghavan G. (2011): Influence of algal cell size on filtration and ingestion rates during different larval stages of the yellow neck clam, *Paphia malabarica* Chemnitz. Aquaculture Nutrition, 17(3), 327-331.
- Rajesh K.V., Mohamed K. S. and Kripa V. (2001): Influence of algal cell concentration, salinity and body size on filtration and ingestion rates of cultivable Indian bivalves. Indian Journal of Marine Science, 30, 87-92.
- SPSS (2007). SPSS Base 17.0 User's Guide. SPSS Inc., Chicago, USA.
- Strychar K B and Mac Donald B A, (1999): Impacts of suspended peat particles on feeding and absorption rates in cultured eastern oysters (*Crassostrea virginica*, Gmelin). J Shellfish Res 18: 437.
- Tenore, K.R. and Dunstan, W.M. (1973): Comparative of feeding and biodeposition of three bivalves at different food levels. Marine Biology 21,190 – 195.
- Theede, H. (1963): Experimentelle untersuchungen über die Filtrierleistung der Miesmuschel *Mytilus edulis* L. Kieler Meeresforsch, 19 (1): 20 - 41.
- Vanderploeg, H. A.; Liebig, J.A.; Carmichael, W. W.; Agy, M. A.; Johengen, T.H.; Fahnenstiel, G. L. and Nalepa T. F. (2001): Zebra mussel (*Dreissena polymorpha*) selective filtration promoted toxic *Microcystis* blooms in Saginaw Bay (Lake Huron) and Lake Erie. Canadian Journal of Fisheries and Aquatic Sciences, 58, 1208–1221.
- Winter, J.E. (1969): Über den Einfluss der Nahrungskonzentration und anderer Faktoren auf Filtrierleistung und Nahrungsausnutzung der Muscheln *Arctica islandica* und *Modiolus modiolus*. Marine Biology, 4, 87 – 135.
- Winter, J.E. (1978): A review on the knowledge of suspension- feeding in lamellibranchiate bivalves, with special reference to artificial aquaculture systems. Aquaculture, 13: 1-33.
- Winter, J.E., Toro, J.E., Navarro, J.M., Valenzuela, G.S. and Chaparro, O.R. (1984). Recent developments, status, and prospects of molluscan aquaculture on the Pacific coast of South America. Ibid., 39: 95 – 134.

11/22/2011

Leadership behavior as perceived by clinical teacher and nursing students

¹*Olfat A. Salem; ²Fatma M. Baddar and ³Gusrina Komara Putri

¹Female Nursing Administration and Education Department, College of Nursing, Riyadh, King Saud University, , Kingdom Saudi Arabia. Associate Professor Menofiya University

²Department of Nursing Administration, Faculty of Nursing, Alexandria University, Egypt. Administration and Education Department, College of Nursing, King Saud University

³Nursing Administration and Education Department, King Saud University, College of Nursing, Riyadh, Kingdom Saudi Arabia

osalem@ksu.edu.sa

Abstract: Leadership behavior of clinical teacher influences the effectiveness of clinical teaching. However, leader perception of their leadership behavior might be different with follower perception of it. Based on it, the study aim to describe the relationship between clinical teacher perception of leadership behavior and compared with student perception of it. 27 clinical teachers and 214 nursing students were participated in this study using Multifactor Leadership Questionnaire (MLQ). The results revealed statistically significance difference between leadership behaviour perception of clinical teacher and their students ($p < 0.05$).

[Olfat A. Salem; Fatma M. Baddar and Gusrina Komara Putri. **Leadership behavior as perceived by clinical teacher and nursing students**] Life Science Journal, 2011; 8(4):814-820] (ISSN: 1097-8135).

<http://www.lifesciencesite.com>.

Keywords: leadership, transformational leadership behaviours, transactional leadership behavior, clinical teaching

1. Introduction

Leadership in nursing education is essential for the quality of nursing curriculum. Particularly, for clinical teaching, clinical teachers act as the leader and nursing students act as their followers. Consequently, leadership behavior of clinical teacher influenced the quality of nursing education. In Saudi Arabia, nursing educator struggles to improve their graduate students in order to fulfill the needs of healthcare system in the Kingdom. Leadership behavior of clinical teachers influence the quality of clinical teaching. Concomitantly, deeper understanding of leadership behaviour of clinical teacher helping in creating framework of nursing education leadership studies in Saudi Arabia.

Leadership

The study of leadership started since the beginning of civilization. It goes parallel with organization study so when organization evolved to become a supportive and positive environment, the focus of leader also shifted 1. Sullivan E & Decker P (2005) 2 defined leadership as a process of uses interpersonal skills to influence others to accomplish specific goals. Leadership requires attending to and acknowledging others and being authentic and accountable 2. In addition, Yukl (1999) 3 defines leadership as an alternative perspective in a shared process of enhancing the collective and individual capacity for people to accomplish their work roles effectively.

Based on the literature, a lot of leadership style that consider popular. One of it is the transformational leadership style. The transformational leaders are proactive in many different and unique ways. These leaders attempt to optimize development, not just performance. Development encompasses the maturation of ability, motivation, attitudes, and values 4-6. Another approach by Yukl (2009) 3 stated that transformational leadership involves motivating individuals to do something different from before, or to do more than initially expected. In other words transformational leaders are change agents, visionaries and calculated risk-takers 6.

Nursing Education

In nursing education, particularly, clinical teacher is important factor in improving the quality of education. They are responsible for teaching and learning process. They are the key for nursing as a profession. Therefore, nurse educator effective leaderships are essential for the improvement of nursing education 7.

Many challenges that faced by the clinical teacher regarding the shortages of faculty number and changes roles. To cope with the increase number of students which is not proportionate pace with the faculty number, it is important to increase efficiency of faculty member. One of way to increase efficiency is through periodic career counseling regarding leadership development and interdisciplinary functioning 8. In scope of teacher role, currently, the

role of supervision in clinical teaching was not only to support students to gain their practical skills, but also to facilitate students to reach clinical proficiency by means that reflects along with students' peers and the supervisors able to display different attributes 8-9.

Sutkin, Wagner and Schiffer (2008) 10 stated that excellent clinical teaching, although multifactorial, transcends ordinary teaching, characterized by inspiring, supporting, actively involving, and communicating with students. Teachers who not only supervise students in their development of technical skills and applied knowledge but also serve as role models of the values and attributes of the profession for the life of a professional. As a result excellence teacher increases performance of student whereas bad teacher lead in low performance of student 11.

The relationship between clinical teacher and nursing student, it can be analogue like link between leader and follower. As stated by Theofanidis and Dikatanidou (2006) 12 that nursing tutors can act as leaders by generating student motivation. Nevertheless, Johnson-Farmer and Frenn (2009) 13 stated that teaching excellence was found to be a dynamic process, which includes active engagement of both students and faculties. Furthermore, Sawatzky, et al. (2009) 14 found that to become the best leader, it needs to be started with learning the basic understanding of what is leadership and how all the skills involved could be developed. Especially in academic setting, the leadership style academia plays an important role in student learning, they are responsible for preparation of the taskforce/manpower needed for the community development. They are the major factors that actualize the university roles; they are the cornerstones upon which any educational reforms are based whether updating or improving 14.

Particularly in Saudi, some leadership studies in Kingdom Saudi Arabia had been performed 15-18. The most recent study was conducted by Al-Kherb (1996) 15 which was about the relationship between principals length of administrative experience and organizational leadership behaviour in elementary schools in Saudi Arabia. This studied recommended the use of transformational leadership for schools in Saudi Arabia. The other researcher was conducted during 1980's by Al-Magidi (1989) 17 investigated the leadership behaviour of public elementary school principals as perceived by principals and their teacher in a selected school district in the south region of Saudi Arabia. The main important conclusion of the researcher was the principals perceived themselves as exhibiting leadership behaviour categories often to very often more than their teacher did. It showed the principals perceive themselves higher in positive

dimensions rather than teacher did (Al-Magidi, 1989) 17.

Significance of the study

Based on the all studies described, researchers have found that the leadership is one of the most significant factors affecting the quality of nursing education. However, in the Kingdom Saudi Arabia limited studies have been conducted regarding nursing leadership. Therefore, the goal of this study was to assess relationship between leadership behavior of clinical teacher from their own point of view (self-assessment) and also from the nursing student perception (observer-assessment).

Purpose

The objective of this study was to assess the relationship of clinical teacher leadership behaviour as perceived by themselves and by their students at CON.

2. Methods

Research design

Correlational design was used in this study

Setting and sample

The study was conducted at CON, King Saud University (KSU), Riyadh. The academic education departments (n=4), namely: 1) medical surgical nursing; 2) community health and psychiatric nursing; 3) maternity and pediatric nursing; 4) nursing administration and education. Concomitantly, the nursing student group was consisted of student from level 4th – 8th.

A non-probability, convenience sample was used in the present study. Inclusion criteria were established for both subject groups to control some variables. In the current study, for clinical teachers group, the inclusion criteria were have a direct contact with students at clinical settings and willing to participate in the study. Because of small number of clinical teachers, the inclusion criteria regarding year of experience was eliminated; total number of subject as clinical teacher was (n=27). For the second group who were nursing students, the inclusion criteria were having direct contact with clinical teachers and voluntary participation in the study; total number of nursing students(n= 214). Total number of clinical teacher was 31 so there were only 4 respondents not participated due to maternity leave. For the nursing student, total sample was 286 and it was distributed from fourth until eight level semesters. In average, the participant rate for the nursing student was approximately 75% whereas for the clinical teacher was 87%.

Instruments

In the current study, the questionnaire used as an instrument for data collection. Particularly, the tool used in this study was Multifactorial Leadership Questionnaire (MLQ) of 5x-short. This type of MLQ is for organizational survey and research purpose and for preparation of individual leader report. This questionnaire developed by Bass and Avolio (2005) it is used to measure leadership behaviours as perceived by nursing clinical teachers and nursing students through reference to "self" and "observers". Permission to use this questionnaire was obtained from Mind Garden as official institution for MLQ researchers.

The MLQ consists of three main components of leadership behaviour, namely: 1) transformational leadership behaviour consists of 20 item questions, it is divided into five main sub items, namely: idealized influence (attributed), idealized influence (behaviour), inspirational motivation, intellectual stimulation and, individualized consideration; 2) transactional leadership consist of 8 item questions. It is divided into two main types, namely: contingent reward and, active management by exception; 3) passive/avoidant behaviour grouped into two also, namely: passive management by exception and, laissez-faire. All those components in each sub grouping were consisted of four questions. Each questions assessed by likert rating scale ranging from 0 "Not at all" to 4 "Frequently, if not always".

In addition, demographic characteristics for nursing clinical teachers and nursing students were added. For clinical teachers, the demographic questions contain of six questions, which were: age, marital status, academic departments, years of experience, level of education and nationality. In other hand, for the demographic of nursing student consisted only from three questions, which were: age, marital status and level of education. Moreover, ethical consideration with a brief explanation about aim of the study and ensure anonymous of subjects was attached in each questionnaire. Instruction to the respondent was provided.

Procedures

After obtaining the official permissions from the CON administration and heads of academic departments, pilot study was carried out on 10% of clinical teachers who were previously affiliated to academic departments and nursing students in order to ensure clarity of tools and time consumption for filling the questionnaire. The decision was made to conduct the pilot study on those subjects in order not to contaminate the sample, for their limited number. Accordingly, they were excluded from the main study sample.

Directly after the pilot study and revision of it, the self-administered questionnaire was distributed to both subjects group. In this study, questionnaire for clinical teacher was distributed during their work hours in college. As well as for nursing student, questionnaire was given during their study activities in college and in clinical settings. Duration time for data collection was from May – July 2009.

Statistical analysis

The Statistical Packages for Social Science (SPSS 17) were used for performing the statistical analysis. A p-value <0.05 was considered statistically significant.

3. Results

The respondent consisted of 214 nursing students and 27 clinical teachers. All the respondents were female due to gender separation of education system in Saudi Arabia. Generally, the nationality of respondents for both clinical teachers and nursing students were Saudi. However, two clinical teachers were considered non-Saudi.

Table (1) illustrates that the mean score of teacher higher compared with students, except for the passive/avoidant domains. Management by exception active and passive not able to shows significance difference whereas other domains gives statistically significance difference (p<0.05). Whereas, in table (2) it is clearly seen that there predominant leadership style between nursing teachers and student with p-value < 0.001*.

For clinical teacher, idealized influence (behavior) with the intellectual stimulation, individual consideration and contingent reward give positive statistically significance difference correlation (p<0.05 and p<0.01). Consequently, contingent reward also positively statistically significance difference with idealized influence (behavior), intellectual stimulation and individualized consideration (p<0.01). Though most of the correlation is positive, in the other hand for leadership domain of intellectual stimulation, active and passive management by exception and laissez faire show some negative statistically significance difference correlation (table 3).

Following it, in nursing student group, the matrix table reflects that laissez-faire leadership statistically give significance difference when correlated with all leadership domains (p<0.05; p<0.01). The correlation between leadership domain become lesser as the leadership character become more transformational and it is show with idealized influence (attribute) that not have any correlation with other leadership domain (table 3).

Table 1. Comparison of leadership scores between nursing teachers and students

Leadership score domains	Group (mean±SD)		Mann Whitney Test	p-value
	Teachers (n=27)	Students (n=214)		
Transformational:				
Idealized Influence (Attributed)	2.8±0.6	2.0±0.8	27.46	<0.001*
Idealized Influence (Behavior)	2.7±0.6	2.1±0.6	22.28	<0.001*
Inspirational Motivation	3.0±0.4	2.1±0.8	33.48	<0.001*
Intellectual Stimulation	3.0±0.5	2.0±0.7	41.35	<0.001*
Individual Consideration	3.1±0.5	2.1±0.8	38.27	<0.001*
Total	2.9±0.3	2.1±0.6	45.77	<0.001*
Transactional:				
Contingent Reward	2.9±0.5	2.0±0.7	38.44	<0.001*
Management-by-Exception (Active)	2.1±0.7	2.1±0.8	0.00	0.97
Total	2.5±0.4	2.0±0.6	17.23	<0.001*
Passive/avoidant:				
Management-by-Exception (Passive)	1.5±0.8	1.8±0.7	2.75	0.10
Laissez-faire Leadership	1.2±0.6	1.8±0.7	17.80	<0.001*
Total	1.3±0.6	1.8±0.6	12.65	<0.001*

(*) Statistically significant at p<0.05

Table 2. Comparison of predominant leadership style between nursing teachers and students

	Group				X ² Test	p-value
	Teachers (n=27)		Students (n=214)			
	No.	%	No.	%		
Transformational	22	81.5	61	28.5	30.22	<0.001*
Transactional	2	7.4	71	33.2		
Laissez-faire (passive/avoidant)	2	7.4	72	33.6		
Mixed	1	3.7	10	4.7		

(*) Statistically significant at p<0.05

Table 3. Correlation matrix of leadership scores components for clinical teachers and nursing teachers

Leadership score domains	Pearson correlation coefficients (r)															
	Leadership score domains															
	IIA		IIB		IM		IS		IC		CR		MBEA		MBEP	
	CT	NS	CT	NS	CT	NS	CT	NS	CT	NS	CT	NS	CT	NS	CT	NS
IIA																
IIB	.305	.582**														
IM	.335	.622**	.043	.647**												
IS	.016	.540**	.412*	.585**	-.057	.548**										
IC	.340	.569**	.524**	.688**	.175	.647**	.449*	.670**								
CR	.299	.655**	.436*	.599**	.175	.611**	.514**	.572**	.574**	.530**						
MBEA	.053	.462**	.173	.433**	.246	.461**	.227	.410**	.072	.411**	-.009	.459**				
MBEP	-.185	.435	-.305	.453**	.296	.332**	-.121	.407**	-.170	.408**	-.346	.380**	.320	.311**		
LF	-.368	.202**	.060	.297**	-.188	.262**	.179	.248**	.033	.281**	-.374*	.208**	.278	.159*	.549**	.497**

(*) Statistically significant at p<0.05

(**) statistically significant at p<0.01

CT= Clinical teacher IM= Inspirational Motivation MBEP= Management by NS= Nursing Student

IS= Intellectual Stimulation Exception (Passive)

IIA= Idealized Influence (Attribute) CR= Contingent Reward LF= Laissez-Faire IIB= Idealized

Influence (Behavior) MBEA= Management by Exception (Active)

4. Discussion

One of important results in this study was the clinical teacher perceived their leadership behaviour to be more transformational rather than transactional and passive/avoidant behaviour. Different with it, their nursing student perceived the clinical teacher leadership behaviour transformational leadership behaviour not as highly as perception of clinical teacher. This result is similar to research by Faila and Stichler (2008) 19 and McGuire and Kennerly (2006) 20. On contrast with the result, study by Tapahe, Nyland and Eggett (2007) 21 found that student in dietetics education program perceived their instructor displayed more transformational leadership rather than transactional leadership behaviour.

As expected by researcher in the present study, the statistical analysis depicts significance difference among the two studied group. Different perception of self rated and other rated in leadership research was not surprising and research supported it (see table 1). Commonly self rated perceived themselves higher than other perceived themselves like occurred in this research 22. Specifically for transformational leadership, the tendency of self rated is to score themselves more with the transformational leadership style compared with transactional leadership style 21, 23-25. This is consistent with Bass and Yammarino (2000) 26 who reported same result that transformational leadership tended to be more aware of their own leadership abilities than observers.

Particularly to the current study, there are several reasons that might contribute to the highly statistical difference between the groups. First, clinical teacher already have knowledge regarding transformational leadership concept, however their behaviour has not reflect as a transformational leader. In other words, the self awareness of clinical teachers regarding importance of transformational leadership is not developed. Secondly, environment or organizational culture is one of essential factors as obstacles in conducting transformational leadership practice. When the institution still focused with the method of reward that focus with transactional leadership behaviour component such as productivity and cost management it will lead to low motivation in performing transformational leadership practice. Thirdly, high score of transformational leadership in this research might correlate with the gender of leader which was in here the clinical teacher that all female. Research by Hura (2005) 27 found that all female respondents have tendency to rated themselves higher in transformational leadership. Fourthly, the method of self report for the leader might create bias when it is conducted in correlational studies. In nature, people tend to perceive themselves in more positive way rather than negative.

In this context, Mc Guire and Kennerly (2006) 20 stated that perception of one's own leadership characteristic may have no relationship to the behaviours demonstrated by those who are direct reports. In addition, implication is the perceptions may have little or nothing to do with actual leader behaviour. In conclusion, it may suggest that actual leader behaviours differ for different subordinates, and so differing perceptions of subordinate are valid 28.

In contrast with those researchers, Barbuto and Burbach (2006) 29 found that leader self rated and other self rated not showed any significance difference. Nevertheless, research by Feinsimer and Frame (2001) 30 found the perception of transactional and transformational leadership behaviour do not differ across groups. Individuals within each group, however, do rate those same variables differently. Furthermore, research of Failla and Stichler (2008) 19 found no statistically significance difference were found between the nurse managers' perception of their leadership style as compared with their subordinates' perception of the managers' leadership style on the total scale scores for the MLQ, although the managers rated themselves slightly higher on the total transformational scale than did the subordinates

Passive management by exception and laissez faire leadership were not independent leadership subscales. They constitute a single construct, because these subscales correlated strongly each other 31. In this research, both of these leadership components confirms negative correlation which can be implied that score of leadership perception of clinical teacher was lower compared with their nursing student perception scores (see table 7 and 8). Strong reason for it because both of these leadership behaviours are considered to be more negative and leaders tend to perceive it lower compared with other leadership behaviour components that tend to be more positive.

Limitations

The study is limited by the sample, which was in one college. This does not allow for generalizability of the findings. In addition, the self-report questionnaire was used for data collection with research assumption of trustworthiness of the respondents. Furthermore, questionnaire addressed in English which is the second language of respondents.

Recommendations for further research

Greater sample size and various study settings are recommended for further studies. In addition, future research might see the applicability on MLQ in Arabic cultures.

Implications for nursing practice

Based on the study findings, recommendation are addressed into four main fields, namely: nursing administration, research, practice and education. In nursing administration, the university administrators need to continuously improve their efforts on developing transformational leadership behaviours. For nursing research, it is recommended to do further assessment in determining which leadership attributes causes nursing students to perceive their clinical teacher differently than the self-assessment and perception of leader. In addition, future research might see the applicability on MLQ in Arabic cultures. Greater sample size and various study settings are also recommended for further studies. In nursing practice, regular feedback of clinical teacher based from their student's point of view is suggested to create a smaller perception gap that occurred. Last, in nursing education, training and development in leadership, specifically for the transformational leadership is essential in increasing quality of education in college.

Conclusion

In conclusion, the current study could act as a preliminary study for leadership research in educational setting in Kingdom Saudi Arabia generally and specifically at College of Nursing, King Saud University. Particularly, main findings showed statistically significance difference perceptions of leadership behaviour between clinical teacher and their students which were supported by previous research in nursing leadership.

Acknowledgements

This research project was supported by a grant from the research center of the center for female scientific and medical colleges in King Saud University.

Corresponding Author:

Olfat Salem

College of Nursing, King Saud University, Kingdom of Saudi Arabia, P.O Box 642 Riyadh 11421
osalem@ksu.edu.sa / olfat99@yahoo.com

References

1. Stone AG, Russell RF, Patterson K. Transformational versus servant leadership: A difference in leader focus. *Servant Leadership Research Roundtable*. 2003. http://www.regent.edu/acad/sls/publications/conference_proceedings/servant_leadership_roundtable/2003pdf/stone_transformation_versus.pdf. Accessed May 20, 2009
2. Sullivan EJ, Decker PJ. *Effective Leadership and Management in Nursing*. 6th ed. New Jersey: Pearson Education;2005.
3. Yukl G. Leading organizational learning: Reflections on theory and research. *The Leadership Quarterly*, 2009; 20: 49-53.
4. Avolio BJ, Bass BM. *Multifactor Leadership Questionnaire*. 3rd ed manual and sampler set. Mind Garden; 2005.
5. Bolden R, et al. A review of leadership theory and competency frameworks. University of Exeter: Centre for Leadership Studies. 2003. http://centres.exeter.ac.uk/cls/documents/mgmt_standards.pdf. Accessed October 30, 2009.
6. Brennan MA, Moon MK, Pracht D. Understanding organizational leadership. University of Florida IFAS Extension. 2008. <http://edis.ifas.ufl.edu/fy1063>. Accessed Dec 10th, 2009.
7. Frank B, Eckrich H, Rohr J. Quality nursing care: leadership the difference. 2007. www.nursingcenter.com. Accessed May 15th, 2009.
8. McBride AB. Breakthroughs in nursing education: looking back, looking forward. *Nurs Outlook*. 1999; 47(3):114-119.
9. Barrett D. The clinical role of nurse lecturers: Past, present, and future. *Nurse Educ Today*. 2007; 27(5), 367-74.
10. Sutkin G, et al. What makes a good clinical teacher in medicine? A review of the literature. *Acad Med.*, 2008 83(5):452-66.
11. Irby DM, Papadakis M. Does good clinical teaching really make a difference? *Am J Med*. 2001; 110(3),231-232.
12. Theofanidis D, Dikapanidou S. Leadership in nursing. *ICUS Nurs Web J*. 2006; 25: 1-8. http://www.nursing.gr/protectedarticles/leadership_ip.pdf. Accessed May 10, 2009
13. Johnson-Farmer B, Frenn M. Teaching excellence: What great teachers teach us. *J Prof Nurs*. 2009; 25(5): 267-72.
14. Sawatzky JA, et al. Teaching excellence in nursing education: a caring framework. *J Prof Nurs*. 2009; 25(5):260-6.
15. Al-Kherb HA. The relationship between principals length of administrative experience and organizational leadership behavior in elementary schools in Saudi Arabia. PhD Dissertation: Western Michigan University. 1996.
16. Al-Knawy S. A study of leadership behavior as perceived and expected by deans, head of departments and faculty members in three elected institutions of higher learning in Saudi

- Arabia. PhD dissertation: Oklahoma University. 1985.
17. Al-Magidi A. Leadership behavior of public elementary school principals as perceived by principals and their teacher in a selected school district in the south region of Saudi Arabia. PhD dissertation: University of South Florida. 1989.
 18. Naji MA. Leadership behavior of secondary school principals and teacher morale in Southern Saudi Arabia', PhD dissertation: Graduate school University of Southern California. 1987.
 19. Failla KR, Stichler JF. Manager and staff perceptions of the manager's leadership style. *J Nurs Adm.* 2008; 38(11), 480-7.
 20. McGuire E, Kennerly SM. Nurse managers as transformational and transactional leaders. *Nurs Econ.* 2006; 24(4):179-185.
 21. Tapahe SJ, Nyland NK, Eggett DL. Instructor and student perceptions of instructor transformational leadership in dietetics education programs. *J Am Diet Assoc.* 2007; 107 (8).
 22. Hallinger P. Leading educational change: reflections on the practice of instructional and transformational leadership. *Cambridge Journal of Education.* 2003; 33 (3): 329-51.
 23. Corrigan PW, et al. Transformational leadership and the mental health team. *Adm Policy Ment Health.* 2002; 30(2), 97-108.
 24. Kleinman C. The relationship between managerial leadership behaviors and staff nurse. *Hosp Top.* 2004; 82(4):2-9.
 25. Reiss RG. A comparison of Leadership Styles of Occupational Therapy Education Program Directors and Clinic Administrators. PhD dissertation: University of North Texas. 2000.
 26. Bass B, Yammarino F. Transformational leader know them selves better. Office of Naval Research; 2000.
 27. Hura GM. The effects of rates and leader gender on ratings of leader effectiveness and attributes in a business environment. PhD dissertation: The Graduate Faculty of University of Akron. 2005.
 28. Yammarino FJ, Spangler WD, Dubinsky AJ. Transformational and contingent reward leadership: individual, dyad, and group levels of analysis. *Leadership Quarterly.* 1998; 9(1): 27-54.
 29. Barbuto JE, Burbach ME. The emotional intelligence of transformational leaders: A field study of elected officials. *J Soc Psychol.* 2006; 146(1), 51-64.
 30. Feinsimer BA, Frame MC. The relationship between transactional/transformational leadership and affective commitment: A multilevel analysis. *Illinois Institute of Technology.* 2001.
 31. Kanste O, Miettunen, J, Kyngas H. Psychometric properties of the Multifactor Leadership Questionnaire among nurses. *J Adv Nurs.* 2007; 57(2):201-12.

11/22/2011

Pneumonia and Impaired T Cell Function in Children with Down's Syndrome: Double Strike

Amany Abuelazm¹, Zeinab Galal^{*2} and Samia El Sahn³

Pediatric Department, Ahmed Maher Teaching Hospital¹, Clinical Pathology² and Pediatric Departments, Faculty of medicine, Ain Shams University³

^{*}dr_zgalal@hotmail.com

Abstract: Down's syndrome (DS) is the most common chromosomal abnormality in humans and is the most common known genetic cause of intellectual disability. DS is known for increased incidence of respiratory infections and autoimmune diseases, indicating impaired immunity. Subjects and methods: This study included sixty seven children; 49 preschool children with DS, with ages ranging from 2 to 6.5 years and 18 healthy, age- and gender-matched controls. Free T4, TSH, and thyroid autoantibodies (anti-thyroglobulin and anti-TSH receptor antibodies) were measured. Evaluation of total leucocytic count (TLC), lymphocytes, CD3+, CD4+, CD8+ and CD56+ cells was performed for each subject. Sputum specimens were collected from all DS subjects and controls for microscopic examination and culture. Results: Among 49 DS child 23 (46.9%) had signs and symptoms of respiratory tract infection, 11 of DS children (22.4%) were suffering from pneumonia. The culture results of sputum samples revealed that staphylococcus aureus was the most common organism; it represents 37.9% of the total bacterial pathogen isolates and 45.4% of the pneumonic patient's isolates. Nineteen DS subjects (38.78%) were hypothyroid according to the thyroid profile tests. Thyroid autoantibodies were detected in five (10.2%) of DS children, one euthyroid and four hypothyroid children. The values of TLC, lymphocyte, CD3+ and CD4+ cells ($5772.2 \pm 1861.1/\text{mm}^3$, 2234.2 ± 597.8 , 1774.2 ± 396.5 and 760.9 ± 298.4 respectively), were lower in DS children than healthy controls ($7908.0 \pm 1464.8/\text{mm}^3$, 3158.9 ± 722.5 , 2252.0 ± 636.8 and 1389.3 ± 379.4 respectively) and the differences were statistically significant. CD8+ and CD56+ cells were higher in DS children (979.4 ± 285.2 and 393.2 ± 102.9 respectively) than healthy controls (741.8 ± 170.6 and 175.5 ± 52.8 respectively) with significant statistical differences. CD4/CD8 ratio was reversed in DS children (0.78 ± 0.27). In conclusion, respiratory tract infection is very common in DS children and can easily complicate to pneumonia because of the complex impairment of T-lymphocytes which is one of the reasons of the defective immune responses among DS children. Staphylococcus aureus was the most common organism causing pneumonia in children with DS. Annual screening for thyroid function and thyroid autoantibodies in preschool DS children is very important to prevent further intellectual deterioration and improve overall development.

[Amany Abuelazm, Zeinab Galal and Samia El Sahn **Pneumonia and Impaired T Cell Function in Children with Down's Syndrome: Double Strike**] Life Science Journal, 2011;8(4):821-827] (ISSN: 1097-8135).

<http://www.lifesciencesite.com>.

Keywords: Pneumonia, T cell, children, Down's syndrome

1. Introduction

Down syndrome (DS) is the most common chromosomal abnormality among live-born infants and is the most frequent cause of mental retardation in man ^(3,16). Respiratory tract infections are the most important cause of mortality in individuals with DS at all ages ⁽⁴⁾. Acute respiratory tract infections especially pneumonia is a common reason for hospitalization and morbidity in children with DS ^(4,10,13).

In DS, non-immunological factors including structural abnormalities of the airways and lungs, glue ears, obstructive sleep apnoea and gastro-oesophageal reflux, may play a role in the increased frequency of respiratory tract infections ⁽²⁰⁾. Oropharyngeal aspiration (OPA) of food and fluids is known to be associated with pneumonia in dysphagic children with neurological disease and direct causality is often assumed ^(17,29). Secondary

immunodeficiency due to metabolic or nutritional factors in DS, particularly zinc deficiency, has been postulated ^(7,20).

Autoimmune phenomena such as acquired hypothyroidism, coeliac disease and diabetes mellitus occur at higher frequency compared with non-DS subjects. Leukemia is estimated to be 15–20 times more frequent in DS ^(11,16,24). The most common autoimmune disease in DS is related to the thyroid gland. Thyroid autoantibodies were found in 13–34% of subjects with DS ^(14,15,23,28). It is remarkable that the prevalence of thyroid autoantibody increases with age, being common after the age of 8 years ^(14,15). However, *Shalitin and Phillip (2002)* described two infants in whom chronic autoimmune thyroiditis was diagnosed at the age of 5 and 8 months with DS ⁽²³⁾.

The increased susceptibility to infection, malignancies, and autoimmune diseases, suggests that immunodeficiency is an integral part of DS ^(1,10).

In recent decades several studies have been performed to elucidate abnormalities of the immune system in DS ⁽⁴⁾. The abnormalities of the immune system associated with DS include: mild to moderate T and B cell lymphopenia, with marked decrease of naive lymphocytes, impaired mitogen-induced T cell proliferation, reduced specific antibody responses to immunizations and defects of neutrophil chemotaxis^(16,20). The molecular mechanisms leading to the immune defects observed in DS individuals and the contribution of these immunological abnormalities to the increased risk of infections require further investigation ⁽²⁰⁾.

In the current study we aimed to investigate some indicators of T cell immune response, such as white blood cells, total lymphocytes and some indicators of T helper and suppressor cells, to study thyroid function and the presence of thyroid autoantibodies; and above all the life threatening pneumonia infection in preschool DS children.

2. Subject and Methods

This study was conducted on sixty seven pediatric children divided into two groups: Group 1 comprised 49 children with Down's syndrome, 32 males and 17 females their ages ranged from 2 to 6.5 years (3.5 ± 1.6). DS children were present at the time of the researchers' visit to Early Detection & Intervention Unit of Ahmed Maher Teaching hospital and pediatric out-patient clinics of Ain Shams university Hospitals. They were participated in the study after getting written informed consent from parents of each child. The research was conducted between January 2009 and Desember 2010.

The diagnosis of DS children depends on clinical features and was confirmed by chromosomal analysis of Trisomy 21. Group II comprised 18 healthy children; 10 males and 8 females their ages ranged from 3 to 7.3 years (3.8 ± 1.7). Control subjects were from out-patient clinic coming for trivial symptoms, they were in good general conditions, and had no acute or chronic diseases affecting the immune system. The two groups were matching in age and sex, and they were all subjected to the following:

Complete medical history and clinical examination were done for DS children and control subjects with a special consideration for symptoms and signs of pneumonia like fever, chills, rigor, myalgia, malaise, diarrhoea, cough and dyspnoea. In addition to lake of air space (consolidation) on chest X-ray ⁽⁴⁾. And symptoms and signs of hypothyroidism, mainly constipation, dry skin, prolonged sleep and increased body weight; as identified by using Down's syndrome growth chart

⁽¹⁸⁾ and WHO child growth standards, height and weight for age ⁽³⁰⁾.

Specimen collection:

I-Blood specimens:

A convenience sample, not less than five ml of venous blood, was collected aseptically from each child. Blood samples were delivered to the laboratory in three aliquots. One ml of blood was anti-coagulated with disodium EDTA for processing in automated hematology cell coulter for blood count. Two ml were anti-coagulated with tripotassium EDTA to be analyzed by flowcytometry for the levels of CD3+, CD4+, CD8+ and CD56+ cells in a FACS Count Flow-cytometer (Becton & Dickinson, USA). And two ml of clotted blood for assay of TSH, free T4 and thyroid auto-antibodies (anti-thyroglobulin and anti-TSH receptor antibodies).

Total leucocytic count (TLC) and lymphocytic counts: were carried on Sysmex hematology coulter, Sysmex Corporation, Kobe, Japan.

Flowcytometric analysis of peripheral blood leucocytes:

Monoclonal bodies (MoAbs) directly conjugated with fluorescein isothiocyanate (FITC), phycoerythrin (PE), or phycoerythrin cyanin-5 (PC-5) were used to analyze the surface antigens of peripheral blood lymphocytes (PBL). The following monoclonal antibodies were used; anti-CD3 (anti-Leu4) recognizing all T cells, anti-CD8 (anti-Leu2a) recognizing cytotoxic T-cell subset, anti-CD4 (anti-Leu3) reactive with helper inducer T-cell subset, anti-CD56 (anti-Leu9) recognizing the N-CAM molecule reactive with resting and activated CD16+ cells, and with a small percentage of CD3+ lymphocytes, which are considered a subset of cytotoxic T lymphocytes that mediate non-major histocompatibility complex (MHC) restricted cytotoxicity. Four cytometry tubes were used for each subject in the study. About 100 μ L of EDTA treated blood was added to each of the previous tubes. (Becton Dickinson, San Jose, CA, USA).

TSH and free T4 assays were carried by chemiluminescence Kit (Roch Diagnostics, US). The chemiluminescence's immunoassay test utilizes a unique monoclonal antibody directed against a specific antigenic determinant on the hormone molecule. Hypothyroidism was diagnosed on the basis of a combination of a raised serum concentration of thyroid stimulating hormone (TSH) (reference values range from 0.2-4.2 IU/L) and or a marginally low concentration of free T4 (reference values range from 12-22 pmol/ ml) combined with

the presence of symptoms and signs associated with hypothyroidism.

Thyroid auto-antibodies detection: anti-thyroglobulin and anti-TSH receptor auto-antibodies were detected using a sensitive solid-phase immunosorbent radioassay kit (Biomedical diagnostic division, Solon, Ohio, US) based on binding the human ^{125}I -labeled antigens to the autoantibody. If antibodies were present in a titer of ≥ 5 , the sample was considered positive.

II-Sputum specimens:

Spontaneously expectorated sputum specimens were collected from the subjects in a sterile screw capped containers and transported as soon as possible within 2 hours of collection for culture. Sputum samples were processed by adding an equal volume of sputolysin (sputosol, Unipath, Hampshire, UK) and incubated for 30 minutes at 37°C during which they were vortexed for 5-10 seconds.

Microbiological examination of sputum specimens:(Cheesbrough 2000)⁽⁶⁾

(I) Microscopical examination :

- Wet preparation of the sputum examined microscopically by the low power to assess appropriateness of the sample. Only good quality samples were cultured. If large numbers of squamous epithelial cells were detected, the specimen was unsuitable for culturing as it was mostly saliva.
- Gram smear was done for pus cells and bacteria.
- Potassium hydroxide (KOH) preparation when fungal infections were suspected.
- Giemsa smears when pneumonic plaque or histoplasmosis was suspected
- Eosin preparation: to examine sputum for eosinophils.
- Ziehl-Neelsen smears to exclude acid fast bacilli.

(II) Culture on different media:

- Blood agar with optochin disc, incubated at 37 aerobically.
- Chocolate agar incubated in 5-10% CO₂ for *H. influenzae*.
- MacConkey agar for Gram-negative bacilli.
- Lowenstein Jensen media (Oxoid) was used to exclude *Mycobacterium tuberculosis (M.TB)*. The decontaminated specimens with N-acetylcysteine-sodium hydroxide (NALC-NaOH) were inoculated on the medium and incubated for 6-8 weeks before being discarded as negative. Media were incubated in a slant position with the screw cap loose for at least a week until the sediment has been adsorbed (Springer et al 1996).⁽²⁵⁾

Statistical analysis:

Statistical analysis of the data was performed with SPSS, version 11.0 software, and continuous variables were presented as means and SD. Comparison of qualitative variables of DS group and the control group were carried out using the Fisher's exact test. Student's t-test was used to compare quantitative variables. P value of ≤ 0.05 was considered significant.

3. Results

The present study was conducted on 67 children divided into 2 groups; Group 1 comprised 49 children with Down's syndrome, 32 males and 17 females their ages ranged from 2 to 6.5 years (3.5 ± 1.6). Group II comprised 18 healthy children; 10 males and 8 females their ages ranged from three to 7.3 years (3.8 ± 1.7). The two groups are matching in age and sex. Their weight and height data is represented in table 1. Weight of DS children was on 90th centile and 75th centile for males and females respectively on plotting on Down's chart in comparison with controls who lied on 50th centile for males and females. As regards to height, DS children were on 25th centile and 50th centile for males and females respectively while that of controls were on 50th centile for both males and females. (Table 1)

Among the 49 DS children, 23 (46.9%) had signs and symptoms of acute respiratory tract infection, 11 of the DS children suffering from pneumonia (22.4%). All of the pneumonic patients were admitted to the pediatric department of the university hospital. Regarding the culture results of sputum samples, 29 bacterial pathogens had been isolated from sputum samples of the 23 DS patients but none of the controls. *Staphylococcus aureus* was the most common organism; it represents 37.9% (11/29) of the total culture isolates and 45.4% (5/11) of the pneumonic patient's isolates. *Klebsiella pneumoniae* 24.1% (7/29) and 8.1% (2/11), *Candida albicans* represents 17.2% (5/29) and 18.1% (2/11), *Haemophilus influenzae* 10.3% (3/29) and 9.1% (1/11). While *Streptococcus pyogenes*, *Streptococcus pneumoniae* and *Pseudomonas aeruginosa* represent 3.4% (1/29) of the total isolates. The pathogenic organisms were isolated from sputum of 20 of the DS patients with acute respiratory tract infection; 10 of the pneumonic patients were included.

Atypical pneumonia was diagnosed in one child; he was suffering from severe signs and symptoms of pneumonia with abdominal pain, diarrhea and confusion, his sputum culture showed no growth on the used media and he did not respond to empirical antibiotic treatment. He was admitted to the

intensive care unit (ICU) in the university hospital but he passed away. (Table 2)

TLC /mm³ was lower in DS children (5772.2 ± 1861.1 /mm³) than in normal controls (7908.0 ± 1464.8/mm³) with significant statistical difference (P<0.005). Lymphocyte count/mm³ was lower in DS children (2234.2 ± 597.8 /mm³) than in healthy controls (3158.9 ± 722.5 /mm³) with significant statistical difference (P< 0.005). CD3+ lymphocytes absolute values were lower in DS children (1774.2 ± 396.5) than in healthy controls (2252.0 ± 636.8/mm³) with a significant statistical difference (P<0.05).

Absolute values and percents of CD4+ lymphocytes were found lower in DS children (760.9 ± 298.4 and 33.9 % ± 12.5) than in healthy controls (1389.1 ± 379.4 and 45.8% ± 4.6) and statistical difference were significant (P<0.005 for both absolute count and percents). CD8+ lymphocytes absolute values and percents were higher in DS children (979.4 ± 285.2 and 45.6% ± 15.6) than in

healthy controls (741.8 ± 170.6 and 23.5% ± 2.6) with statistical significant difference (P<0.05 and 0.0001 respectively). CD4/CD8 ratio was lower in DS children (0.78 ± 0.27) than healthy controls (1.8 ± 0.19) with significant statistical difference (P<0.0001). CD56+ cells count and percents were higher in DS subjects (393.2 ± 102.9 and 18.8% ± 6.8) than healthy controls (175.5 ± 52.8 and 5.2% ± 1.7) with significant statistical difference (P<0.0001) for both absolute count and percents). (Table 3, Figure 1)

On studying thyroid function, 19/49 (38.78%) of children with DS were hypothyroid, but none of the control group revealed any abnormality in thyroid function. Anti-thyroglobulin auto-antibodies were detected in five (10.2%) DS children; one euthyroid and four hypothyroid and in none of the control group and anti-TSH receptor auto-antibodies were not detected in any of DS children or the normal control group. (Table 4)

Table (1): Weight and height data of Down's syndrome children

Group	Down's syndrome children.		control children	
	Males (no.32)	Female (no.17)	Males (no.10)	Female (no.8)
Weight	13.9± 4.6 (90 th *)	10.9± 1 (75 th *)	14.7± 1.7(50 th *)	13±1.4 (50 th *)
Hight	83.2± 8 (25 th *)	80.1±5 (50 th *)	91.7± 10.1(50 th *)	88.3± 6.1(50 th *)

*centile

Table (2): Culture results of DS respiratory tract infection and pneumonia infection.

Group	Respiratory tract infection	Pneumonia infection
	(no. and %)	(no. and %)
Staphylococcus aureus	11(37.9%)	5 (45.4%)
Klebsiella pneumonia	7 (24.1%)	2 (18.1 %)
Candida albicans	5 (17.2%)	2 (18.1%)
Haemophilus influenza	3 (10.3%)	(9.1%)
Streptococcus pyogenes	1 (3.4%)	0 (0%)
Streptococcus pneumoniae	1 (3.4%)	0 (0%)
Pseudomonas aeruginosa	1 (3.4%)	0 (0%)

Table (3): Immunological profile of the studied subjects

Group	Down's syndrome No.49, (mm ³)	Healthy controls No.18, (mm ³)	t	P
TLC	5772.2 ± 1861.1	7908.0 ± 1464.8	3.150	<0.005**
Lymphocytes	2234.2 ± 597.8	3158.9 ± 722.5	3.563	<0.005**
CD3+ count	1774.2 ± 396.5	2252.0 ± 636.8	2.353	<0.05*
CD4+count	760.9 ± 298.4	1389.3 ± 379.4	4.716	<0.005**
CD4 %	33.9 ± 12.5	45.8 ± 4.6	2.969	<0.005**
CD8+ count	979.4 ± 285.2	741.8 ± 170.6	2.442	<0.05*
CD8 %	45.6 ± 15.6	23.5 ± 2.6	4.590	<0.0001**
CD4/ CD8	0.78 ± 0.27	1.8 ± 0.19	11.860	<0.0001**
CD 56 count	393.2 ± 102.9	175.5 ± 52.8	6.320	<0.0001**
CD56%	18.8 ± 6.8	5.2 ± 1.7	6.252	<0.0001**

TLC: Total leucocytic count. * = Significant. ** = Highly Significant. † Insignificant (P>0.05).

Table (4): Thyroid function in Down's syndrome children and healthy controls

Group	DS children (no.49)	Controls (no.18)
Hypothyroid	19 (38.78%)	0 (0%)
Anti-thyroglobulin	5 (10.2%)	0 (0%)
Anti-TSH receptor	0 (0%)	0 (0%)

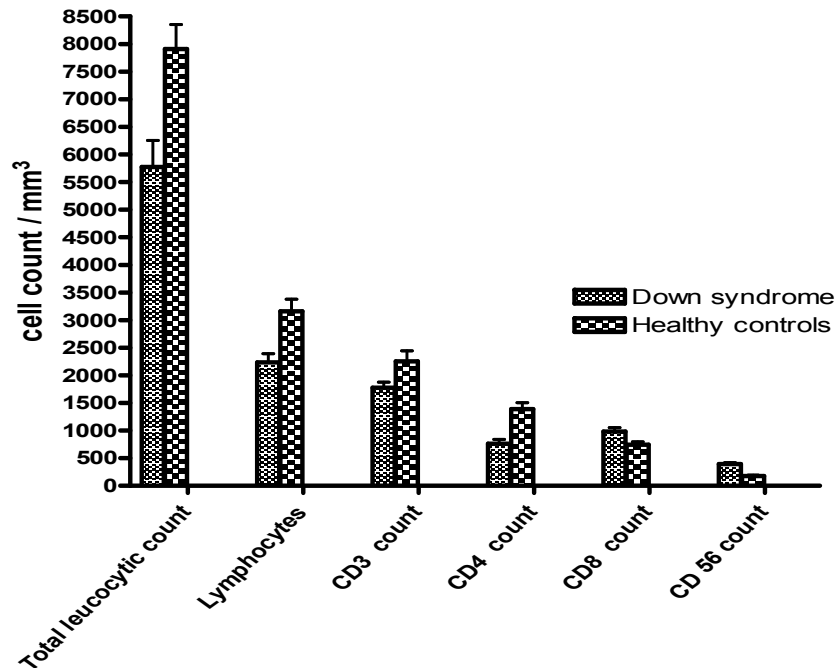


Figure (1): Total leucocytic count, lymphocytes, CD3+, CD4+, CD8+ and CD56+ cells in Down's syndrome children and healthy controls.

4. Discussion:

Down syndrome (DS) is the most common genetic disease and is presented with cognitive impairment, cardiac and gastrointestinal abnormalities, in addition to other miscellaneous clinical conditions ⁽²⁰⁾. DS individuals may have a high frequency of infections, usually of the upper respiratory tract, characterized by increased severity and prolonged course of disease, which are partially attributed to defects of the immune system ^(20,22).

The present study revealed the high incidence of respiratory tract infection among DS preschool children, 23/49 (46.9%), 11/49 (22.4%) of them were suffering from pneumonia. One child, with severe pneumonic condition, was admitted to the ICU, then passed away. It is widely accepted that children with multisystem involvement demonstrated a higher association with pneumonia than normals ⁽²⁹⁾. In agreement with our results, *Hilton et al. (1999)* ⁽¹³⁾ comprehensively reviewed 232 hospital admissions among DS children over 6 year period, and found that lower respiratory tract pathology was the most common cause for acute hospital admission. Based on age groups, the highest percentage of

admissions their studies were among 1–5-year-old children (45%). The predominant diagnosis of admission to the ICU was pneumonia (18%). It was found that *Staphylococcus aureus* was the most common organism; it represents 37.9% of our total culture isolates and 45.4% of the pneumonic patient's specimens. However, *Alonso et al.(2005)* ⁽²⁾ had reported bacterial pathogens isolates from tracheal secretion culture in 58 % of their DS studied group and the most common pathogen was *Staphylococcus aureus* (42 %). Three children (25 %) developed lobar pneumonia.

The increased frequency of haematological malignancies, autoimmune diseases and infections in DS, and the observed high frequency of hepatitis B surface antigen carriers, had already led to the hypothesis that DS is associated with abnormalities of the immune system ^(16,20). The basis of the immune defects is still unclear ⁽⁴⁾. The current study detected a significant decrease of the TLC in DS children. Some studies noted that in DS children, the immune cellular status is similar to the normal population ^(7,21). Peripheral blood mononuclear cells from DS subjects are characterized by several alterations leading to a

decreased response to infection, and a decreased killing ability of microorganisms. This may be one reason for the decreased immunity seen in children with DS ^(1,21).

In accordance with some earlier studies, we detected a significant decrease of the absolute number of circulating lymphocytes. In agreement with *Cossarizza et al. (1990)* ⁽⁹⁾, we confirmed the presence of a significant reduction of CD3+ lymphocyte absolute number in DS children. It has been noted that there is an inefficient release of mature T cells by the DS thymus, associated with selective failure of tyrosine phosphorylation ^(21,26).

We found that DS children had less T helper cells than the control group ^(8,21). Some studies documented a normal proportion of CD4+ T cells, whereas the percentage of suppressor-cytotoxic CD8+ lymphocytes is markedly increased and CD4/CD8 ratio of patients with DS and normal controls were similar ^(5,19). On the contrary, *Corsi et al. (2003)* ⁽⁸⁾ showed that peripheral CD4+ T cells were lower in children with DS, whereas mean values of cytotoxic CD8+ T cells were comparable with those from healthy children. *Cocchi et al. (2007)* ⁽⁷⁾ noted that the immune cellular status in DS children is similar to the normal population as far as white blood cell, lymphocyte, CD4+, CD8+, natural killer and immunoglobulins. *Guazzarotti et al. (2009)* ⁽¹²⁾ documented significant increase of both CD4+ and CD8. In our study, absolute values and percents of CD4+ lymphocytes were lower and CD8+ cells were higher in DS children than control group. This was concomitant with *Corsi et al. (2003)* ⁽⁸⁾, who reported a decrease in CD4+ and an increase in CD8+ cells with inverted CD4/CD8 ratio.

CD56+ cells are considered the cells capable of non MHC-restricted cytotoxicity, and appear to play an important role as tumor infiltrating lymphocytes ⁽⁵⁾. The current study showed that CD56+ cells percents and absolute values are higher in DS children than the control group. It was noted that the expansion of this small subset could be the consequence of an effort of DS immune system to compensate for the functional and numerical reduction of other cytotoxic subsets ^(5,9).

Many of immunological alterations in DS subjects are similar to those characteristic of chromosomally normal subjects of advanced age, DS subjects are aging fast ^(3,16). Reduced thymic endocrine activity ⁽²⁰⁾ and the zinc deficiency characteristic of DS ⁽⁷⁾ and molecular abnormalities due to gene over expression of loci located on chromosome 21 might be responsible for the derangement of T and NK subsets ^(10,12). It was suggested that zinc sulfate supplementation improves thyroid function in hypozincemic DS children ^(7,20).

Thyroid dysfunction, particularly hypothyroidism, is very common in DS. Interestingly, *Unachak et al. (2008)* ⁽²⁸⁾ claimed that sub-clinical hypothyroidism is very common in children with DS. *Tüysüz and Beker (2001)* ⁽²⁷⁾ reported prevalence of congenital hypothyroidism as 1.8% in children with DS, 25.3% of them had compensated hypothyroidism. The prevalence of hypothyroidism varies among different investigators from 3–54% in subjects with DS of all ages ^(14,15,23,28). In our work, we detected hypothyroidism in 38.8% of DS group and none of the controls. The variation in prevalence between different studies might be related to the age variation among the studied subjects and/or to differences in diagnostic criteria.

In the present work, thyroid autoantibodies were detected in 10.2% of DS children, four hypothyroid and one euthyroid. In contrast to our results, *Karlsson et al. (1998)* ⁽¹⁵⁾, reported hypothyroidism in 30 DS subjects, half of them acquired the condition before the age of 8 years, but only one of them displayed thyroid autoantibodies at diagnosis. They claimed that, autoimmune thyroid disease is uncommon in young children with DS but is common after 8 years of age.

Conclusion

Respiratory tract infection is very common in DS children and can easily complicate to pneumonia because of the complex impairment of T-lymphocytes subsets, which is one of the reasons of defective immune responses among DS children. *Staphylococcus aureus* was the most common organism causing pneumonia in children with DS. Annual screening for thyroid function and thyroid autoantibodies in DS preschool children is very important to prevent further intellectual deterioration and improve overall development. The awareness of the breadth of respiratory problems and a plan to monitor subjects with DS for their development have the potential to improve outcomes, as some of these conditions are readily identifiable and able to be treated.

A major re-appraisal in attitudes towards DS is required to ensure that the medical and social needs of people with the disorder are adequately met across their entire lifespan, accompanied by the provision of appropriate levels of care and management.

Corresponding author:

Zeinab A. Galal

Clinical Pathology Department, Faculty of medicine,
Ain Shams University

dr_zgalal@hotmail.com

5. References

1. **Abu Faddan N, Sayed D and Ghaleb F (2011).** T lymphocytes apoptosis and mitochondrial membrane potential in Down's syndrome. *Fetal Pediatr Pathol.*; 30(1):45-52.
2. **Alnoso M S, Menchon M N, Nunez RA, et al. (2005).** Bacterial tracheitis: an infectious cause of upper airway obstruction to be considered in children. *An Pediatr (Barc.)*; 63(2):164-8.
3. **Bittles AH, Bower C, Hussain R, et al. (2007).** The four ages of Down syndrome. *Eur J Public Health.*; 17(2):221-5.
4. **Bloemers BL, Broers CJ, Bont L, et al. (2010).** Increased risk of respiratory tract infections in children with Down syndrome: the consequence of an altered immune system. *Microbes Infect.* 12(11):799-808.
5. **Cetiner S, Demirhan O, Inal TC, et al. (2010).** Analysis of peripheral blood T-cell subsets, natural killer cells and serum levels of cytokines in children with Down syndrome. *Int J Immunogenet.*; 37(4):233-7.
6. **Cheesbrough, M (2000).** District laboratory practice in tropical countries, Cambridge University press, part 2, page 75.
7. **Cocchi G, Mastrocola M, Capelli M, et al. (2007).** Immunological patterns in young children with Down syndrome: is there a temporal trend? *Acta Paediatr.*; 96(10):1479-82.
8. **Corsi MM, Ponti W, Venditti A, et al. (2003).** Proapoptotic activated T-cells in the blood of children with Down's syndrome: relationship with dietary antigens and intestinal alterations. *Int J Tissue React.*; 25: 117-121.
9. **Cossarizza A, Monti D, Montagnani G, et al. (1990).** Precocious aging of the immune system in Down syndrome: alteration of B lymphocytes, T-lymphocyte subsets, and cells with natural killer markers. *Am J Med Genet Suppl.*; 7:213-8.
10. **De Hingh YCM, Van der Vossen PW, et al. (2005).** Intrinsic Abnormalities of Lymphocyte Counts in Children with Down Syndrome. *J Pediatr.*; 147:744-747
11. **Goldacre M, Wotton C, Seagroatt V, et al. (2004).** Cancers and immune related diseases associated with Down syndrome: a record linkage study. *Arch Dis Child.* ; 89:1014-17.
12. **Guazzarotti L, Trabattoni D, Castelletti E, et al. (2009).** T lymphocyte maturation is impaired in healthy young individuals carrying trisomy 21 (Down syndrome). *Am J Intellect Dev Disabil.*; 114(2):100-9.
13. **Hilton JM, Fitzgerald DA and Cooper DM (1999).** Respiratory morbidity of hospitalized children with Trisomy 21. *J Paediatr Child Health.*; 35(4):383-6.
14. **Ivarsson SA, Ericsson UB, orslund M, et al. (1997):** The impact of thyroid autoimmunity in children and adolescents with Down syndrome. *Acta Paediatr.*; (86)10: 1065-67.
15. **Karlsson B, Gustafsson J, Hedov G, et al. (1998).** Thyroid dysfunction in Down's syndrome: relation to age and thyroid autoimmunity. *Arch Dis Child.*; 79:242-5
16. **Kusters MA, Verstegen RH, Gemen EF, et al. (2009).** Intrinsic defect of the immune system in children with Down syndrome: a review. *Clin Exp Immunol.*; 156(2):189-93.
17. **Lazenby T. (2006).** The impact of aging on eating, drinking, and swallowing function in people with Down's syndrome. *Dysphagia.*; 23(1):88-97.
18. **Myreliid A, Gustafsson J, Ollars B, et al. (2002).** Growth charts for Down's syndrome from birth to 18 years of age. *Arch. Dis. Child.*; 87: 97-103.
19. **Nespoli L, Burgio GR, Ugazio AG, et al. (1993):** Immunological features of Down's syndrome: a review. *J Intellect Disabil Res.*; 37(6): 543-47.
20. **Ram G and Chinen J (2011).** Infections and immunodeficiency in Down syndrome. *Clin Exp Immunol.*; 164(1):9-16.
21. **Roat E, Prada N, Ferraresi R, et al. (2007).** Mitochondrial alterations and tendency to apoptosis in peripheral blood cells from children with Down syndrome. *FEBS Lett.* 6; 581(3):521-5.
22. **Sherman SL, Allen EG, Bean LH, et al. (2007).** Epidemiology of Down syndrome. *Ment Retard Dev Disabil Res Rev.*; 13(3):221-7.
23. **Shalitin S and Phillip M (2002).** Autoimmune thyroiditis in infants with Down's syndrome. *J Pediatr Endocrinol Metab.*; 15(5):649-52
24. **Söderbergh A, Gustafsson J, Ekwall O, et al. (2006):** Autoantibodies linked to autoimmune polyendocrine syndrome type I are prevalent in Down syndrome. *Acta Paediatr.*; 95(12):1657-60
25. **Springer B, Stockman L, Teschner K, et al. (1996).** Two-laboratory collaborative study on identification of mycobacteria: molecular versus phenotypic methods. *J Clin Microbiol.*; 34(2):296-303.
26. **Tamiolakis D, Venizelos I, Kotini A, et al. (2003).** Prevalence of CD8/CD4 ratio in the fetal thymic parenchyme in Down's syndrome. *Acta Medica (Hradec Kralove).*; 46(4):179-82.
27. **Tüysüz B and Beker DB (2001).** Thyroid dysfunction in children with Down's syndrome. *Acta Paediatr.* ; 90(12):1389-93.
28. **Unachak K, Tanpaiboon P, Pongprot Y, et al. (2008).** Thyroid functions in children with Down's syndrome. *J Med Assoc Thai.* ; 91(1):56-61.
29. **Weir K, McMahon S, Barry L, et al. (2007).** Oropharyngeal aspiration and pneumonia in children. *Pediatr Pulmonol.*; 42(11):1024-31.
30. **WHO Child Growth Standards, heigth and weight for age (2006)** at the WHO website www.who.int/childgrowth.

Bayesian censored data viewpoint in Weibull distribution

Abd-Elfattah A.M¹ and Marwa O. Mohamed²

¹King Abdul-Aziz University, Statistics Department, Faculty of Science, Saudi Arabia

²Department of Mathematics, Zagazig University, EGYPT

mo11577@yahoo.com

Abstract: The time of failure and average life of a component, measured from some specified time until it fails, is represented by a continuous random variable. Extensively in recent years, one distribution that has been used as a model to deal with such problems for product life is the Weibull distribution. The objective of this paper is to consider the estimation problem of the probability $P(Y < X)$ for Weibull distribution. Based on Classical Type I censored samples. The maximum-likelihood estimators (MLE) are obtained for stress–strength reliability. Bayes estimates under various loss functions are researched. Some computational results from intensive simulations are presented. In the end, in order to investigate the accuracy of estimations, an illustrative example is examined numerically by means of Monte Carlo simulation.

[Abd-Elfattah A.M. and Marwa O. Mohamed. **Bayesian censored data viewpoint in Weibull distribution**]. Life Science Journal, 2011; 8(4):828-837] (ISSN: 1097-8135). <http://www.lifesciencesite.com>.

Key-Words: Weibull distribution, Bayesian estimator, LINEX loss function, Reliability function, stress-strength model, Risk function and squared error loss function, Type-I censored data.

1. Introduction

When modeling data under classical stress–strength analysis, the reliability (R) there is a system subject to a stress Y and strength X . Both Y and X are assumed random variables with known probability distributions. In this system, (R) represents the probability (P) that Y exceeds and X , i.e. $P(Y < X)$. This model has many applications in various areas. For example, if Y represents the maximum pressure caused by flooding and X represents the strength of the leg of a bridge on a stream, then P is the probability that the bridge will be solid. Another example, if Y and X represent the control and treatment groups respectively, then P measures the treatment effect. In this regard, the estimation of P will be important in making inferences.

Several authors have considered different choices for stress and strength distributions, including, [1]-[7]. All of those choices were based on the complete sample study. The monograph by **Kotz et al.** [8] provided an excellent review of the development of this model. However, may not be unrealistic in experimenters often employ censoring schemes in life tests to shorten the test time or to reduce the test cost. However, censoring restricts the ability to exactly observe failure times. Two censored tests (type I and type II), are commonly used in industrial engineering applications. Type I censored test is conducted with a time censored scheme, in which the life test is terminated. The determination could be either occurs at time t_0 . Or certain number of failures before the

time t_0 . Alternatively, the type II censored test is conducted with a failure censored scheme, in which the life test is terminated if the first r smallest failure lifetimes are collected, where the number of failure lifetimes is predetermined. Survived units at the termination time of test are considered as censoring. **Lawless** [9] provides detailed discussions for life tests with two censoring schemes, Based on censoring samples.

Although, extensive work has been done on the developments of the stress–strength models under

Complete samples, not much attention has been paid to when the data are censored (. Jiang and Wong [10] studied inference for stress-strength with truncated exponential distribution). Abd-Elfattah and Marwa ([11], [12]) studied inference for the stress- strength under exponentially and Weibull distributed type II censoring data. Recently, Statistical inference for the stress–strength parameter based on progressively type II exponentially censored data was discussed in Saracoglu, *et al.* [13]. While Lio and Tsai [14] studied $P(Y < X)$ under progressively first failure censored samples when X and Y have two parameters Burr type XII distributions.

In this paper, we consider the statistical inference of the reliability stress–strength parameter $R = P(X < Y)$ when X and Y are independent Weibull random variables. Based on type-I censored Weibull distribution for both X and Y .

The comparison between Bayes estimate for $R = P(Y < X)$ under LINEX and square error loss functions is the main target for this paper.

The rest of the paper organized as follows: In Section 2, the Bayes estimate of R under mean square errors is derived. The Bayes estimate of R under LINEX loss function is provided in Section 3. The risk function is provided in Section 4. Simulation results and data analysis are presented in Section 5. A numerical example is given for illustration in Section 6. Some concluding remarks are given in Section 7.

2. Bayes Estimation Of θ_1 and θ_2 Under Type-I Censored Data

Recently, the Bayesian approach has received large attention for analyzing failure data or time-to-event data, and has been often proposed as a valid alternative to traditional statistical perspectives. The Bayesian approach to reliability analysis allows prior subjective knowledge on lifetime parameters and technical information on the failure mechanism, as well as experimental data, to be incorporated into the inferential procedure. Hence Bayesian methods usually require less sample data to achieve the same quality of inferences than methods based on sampling theory, which becomes extremely important in case of expensive testing procedures. In this section we are concerned on the estimation of the unknown parameters θ_1 and θ_2 of the Weibull distribution based on a type-I censored random sample of size n and m . Suppose that X_1, \dots, X_n a random sample of n units is testes until the test is terminating at time Z_1 . Times to failure for Q_1 observations are observed where Q_1 is random. Where these lifetimes observed only if $x_i \leq Z_1, i = 1, \dots, n$. Therefore

$$\omega_i = \begin{cases} 1 & \text{if } x_i \leq Z_1 \\ 0 & \text{if } x_i > Z_1 \end{cases} \quad (1)$$

Where $Q_1 = \sum_{i=1}^n \omega_i$, in the case of Y_1, \dots, Y_m the test will terminate at Z_2 . Times to failure for Q_2 observations are observed where Q_2 is random. Where these lifetimes observed only when $x_j \leq Z_2, j = 1, \dots, m$. Therefore

$$\varepsilon_j = \begin{cases} 1 & \text{if } y_j \leq Z_2 \\ 0 & \text{if } y_j > Z_2 \end{cases} \quad (2)$$

Where $Q_2 = \sum_{j=1}^m \varepsilon_j$, The likelihood function

$$L(x_1, \dots, x_n | \theta_1) = \frac{\theta_1^{Q_1}}{\theta_1^k} \prod_{i=1}^n x_i^{(k-1)\omega_i} e^{-\frac{\sum_{i=1}^n x_i^k \omega_i}{\theta_1}} e^{-Z_1^k (n-Q_1)} \quad (3)$$

and

$$L(y_1, \dots, y_m | \theta_2) = \frac{\theta_2^{Q_2}}{\theta_2^k} \prod_{j=1}^m y_j^{(k-1)\varepsilon_j} e^{-\frac{\sum_{j=1}^m y_j^k \varepsilon_j}{\theta_2}} e^{-Z_2^k (m-Q_2)} \quad (4)$$

Put $S_1 = \sum_{i=1}^n x_i^k \omega_i + Z_1^k (n - Q_1)$,

$$S_2 = \sum_{j=1}^m y_j^k \varepsilon_j + Z_2^k (m - Q_2).$$

Because $X_i, Y_j, i = 1, \dots, n$ and $j = 1, \dots, m$ are independent and identically distributed Weibull random variables with Parameters θ_1 and θ_2 .

We will use linear transformation in some steps that to study the distributions of S_1 and S_2 , where x is Weibull random variable with parameter θ_1 , then

$$\psi = X^k \omega + Z_1^k (n - Q_1) \quad (5)$$

equation (5) is distributed as exponential with parameter $\omega \theta_1$ to prove that, put $C = Z_1^k (n - Q_1)$ then

$$\psi = X^k \omega + C \quad (6)$$

$$\text{and } \left(\frac{\psi - C}{\omega}\right)^{\frac{1}{k}} = X \quad (7)$$

by using technique of linear transformation

$$\frac{dX}{d\psi} = \frac{1}{\omega_i^k} \left(\frac{\psi - C}{\omega_i}\right)^{\frac{1}{k}-1} \quad (8)$$

then

$$f(\psi) = \frac{1}{\theta_1 \omega_i} e^{-\frac{\psi - C}{\theta_1 \omega_i}}, \psi > C \quad (9)$$

by substitute with the value of C in equation, then

$$f(\psi) = \frac{1}{\theta_1 \omega_i} e^{-\frac{\psi - Z_1^k (n - Q_1)}{\theta_1 \omega_i}}, \psi > Z_1^k (n - Q_1) \quad (10)$$

This has truncated exponential distribution with

parameter $\omega \theta_1$.

So

$$\sum_{i=1}^n x_i^k \omega_i + Z_1^k (n - Q_1) \tag{11}$$

has gamma distribution with $(n + 1, \omega \theta_1)$.

also, for the case Y ,

$$\sum_{j=1}^m y_j^k \varepsilon_j + Z_2^k (m - Q_2) \tag{12}$$

has gamma distribution with $(m + 1, \varepsilon \theta_2)$.

Then, The distribution of S_1 and S_2 are:

$$g(S_1) = \frac{1}{\Gamma(n+1)(\omega_i \theta_1)^{n+1}} S_1^n e^{-\frac{S_1}{\omega_i \theta_1}}, S_1 > 0 \tag{13}$$

and

$$g(S_2) = \frac{1}{\Gamma(m+1)(\varepsilon_j \theta_2)^{m+1}} S_2^m e^{-\frac{S_2}{\varepsilon_j \theta_2}}, S_2 > 0 \tag{14}$$

Combining the prior distributions, with the likelihood functions using Bayes' theorem, the posterior density of

θ_1 and θ_2 are as follows:

$$\pi_1(\theta_1 | x) = \frac{e^{-\frac{(a+S_1)}{\theta_1}} (Q_1 + c + 1)}{(a + S_1)^{Q_1 + c + 1}} \tag{15}$$

$$\pi_2(\theta_2 | y) = \frac{e^{-\frac{(b+S_2)}{\theta_2}} (Q_2 + d + 1)}{(b + S_2)^{Q_2 + d + 1}} \tag{16}$$

By using (15), (16) under squared error loss, the Bayes estimator of θ_1 and θ_2 are the posterior mean denoted by $\hat{\theta}_{MSE1}$ and $\hat{\theta}_{MSE2}$.

The posterior mean $E_{\pi_1}(\theta_1)$ and $E_{\pi_2}(\theta_2)$:

$$\hat{\theta}_{MSB1} = \frac{a + S_1}{Q_1 + c} \tag{17}$$

And

$$\hat{\theta}_{MSB2} = \frac{b + S_2}{Q_2 + d} \tag{18}$$

3. Bayes Estimator of θ_1 and θ_2 Based on LINEX Loss Function

The loss function plays a critical role in Bayesian perspective. Most authors use the simple quadratic (symmetric) loss function and obtain the posterior mean as the Bayesian estimate. However, in practice, the real loss function is often not symmetric. For example, Feynman [15] remarks that in the disaster of a space shuttle, the management may have overestimated the average life or reliability of solid fuel rocket booster. The consequences of overestimates, in loss of human life, are much more serious than the consequences of underestimates. In this case, an asymmetric loss function might be more appropriate. Varian [16] introduced LINEX (Linear-Exponential) loss function, which is the simple generalization of squared error (SE) loss function and can be used in almost every situation (Zellner[18]).

The LINEX loss function is defined as follows:

$$L(\Lambda) = e^{u\Lambda} - u\Lambda - 1; u \neq 0 \tag{19}$$

In this section, the Bayes estimators of θ_1 and θ_2 will be derived, using LINEX as follows: Since

$$f(x) = \frac{k}{\theta_1} x^{k-1} e^{-(x^k/\theta_1)}, x > 0; k, \theta_1 > 0 \tag{20}$$

and

$$f(y) = \frac{k}{\theta_2} y^{k-1} e^{-(y^k/\theta_2)}, y > 0; k, \theta_2 > 0 \tag{21}$$

are probability density function of X and Y.

Suppose $\Lambda_1 = \hat{\theta}_1 / \theta_1 - 1$, where $\hat{\theta}_1$ an estimate of θ_1 . Consider the following LINEX loss function.

$$L(\Lambda_1) = e^{u_1 \Lambda_1} - u_1 \Lambda_1 - 1; u_1 \neq 0 \tag{22}$$

The sign and magnitude of ‘ u_1 ’ represent, respectively, the direction and degree of asymmetry. A positive value of ‘ u_1 ’ is used when overestimation is more costly than underestimation; while a negative value of ‘ u_1 ’ is used in the reverse situation for ‘ u_1 ’ close to zero.

Also, the same definition for θ_2 where $\Lambda_2 = \hat{\theta}_2 / \theta_2 - 1$ and $\hat{\theta}_2$ is an estimate of θ_2 . Again consider the following LINEX loss function.

$$L(\Lambda_2) = e^{u_2 \Lambda_2} - u_2 \Lambda_2 - 1; u_2 \neq 0 \quad (23)$$

The sign of u_2 treats like the sign of u_1 . Using the LINEX loss function (22), the posterior expectation of the loss function $L(\Lambda_1)$ with respect to $\pi_1(\theta_1/x)$ for θ_1 is

$$E[L(\Lambda_1)] = \int_0^\infty (e^{u_1(\hat{\theta}_1/\theta_1 - 1)} - u_1(\frac{\hat{\theta}_1}{\theta_1} - 1) - 1) \pi_1(\theta_1 | x) d\theta_1$$

$$= e^{-u_1} E(e^{u_1(\hat{\theta}_1/\theta_1)} - u_1(\frac{\hat{\theta}_1}{\theta_1}) - 1) \quad (24)$$

The value of $\hat{\theta}_1$ that minimizes the posterior expectation of the loss function $L(\Lambda_1)$ denoted by $\hat{\theta}_{LB1}$ is obtained by solving the following equation

$$\frac{\partial E[L(\Lambda_1)]}{\partial \hat{\theta}_1} = e^{-u_1} E(\frac{u_1}{\theta_1} e^{u_1(\hat{\theta}_1/\theta_1)} - u_1 E(\frac{1}{\theta_1})) = 0 \quad (25)$$

That is, $\hat{\theta}_{LB1}$ is the solution of the equation:

$$E(\frac{1}{\theta_1} e^{u_1(\hat{\theta}_1/\theta_1)}) = e^{-u_1} E(\frac{1}{\theta_1}) \quad (26)$$

Provided that all expectations exist and finite, we get the optimal estimate of $\hat{\theta}_1$ relative to $L(\Lambda_1)$

$$E(\frac{1}{\theta_1} e^{u_1(\frac{\hat{\theta}_{LB1}}{\theta_1})}) = \frac{(a+S_1)^{(Q_1+c+1)}}{\Gamma(Q_1+c+1)} \int_0^\infty \frac{e^{-\frac{(a+S_1)+u_1\hat{\theta}_{LB1}}{\theta_1}}}{\theta_1^{Q_1+c+1}} d\theta_{LB1} \quad (27)$$

$$= \frac{(a+S_1)^{(Q_1+c+1)} (Q_1+c+1)}{((a+S_1)+u_1\hat{\theta}_{LB1})^{Q_1+c+2}}$$

For the right hand side of equation (27)

$$e^{u_1} E(\frac{1}{\theta_1}) = e^{u_1} \int_0^\infty \frac{e^{-\frac{(a+S_1)}{\theta_1}} (a+S_1)^{(Q_1+c+1)}}{\theta_1^{Q_1+c+1} \Gamma(Q_1+c+1)} d\theta_1 \quad (8)$$

$$= e^{u_1} \frac{(a+S_1)^{(Q_1+c+1)} (Q_1+c+1)}{(a+S_1)^{(Q_1+c+2)}}$$

$$= e^{u_1} \frac{(Q_1+c+1)}{(a+S_1)}$$

Now, from (18) and (19) in (28)

$$\frac{(a+S_1)^{(Q_1+c+1)} (Q_1+c+1)}{((a+S_1)+u_1\hat{\theta}_{LB1})^{Q_1+c+2}} = e^{u_1} \frac{(Q_1+c+1)}{(a+S_1)} \quad (29)$$

Then $\hat{\theta}_{LB1}$ can be expressed as follow

$$(a+S_1)^{Q_1+c+2} = e^{u_1} ((a+S_1)+u_1\hat{\theta}_{LB1})^{Q_1+c+2} \quad (30)$$

then

$$\hat{\theta}_{LB1} = \frac{(a+S_1)}{u_1} (1 - e^{-u_1/Q_1+c+2}) \quad (31)$$

Let the loss function of θ_2 is $L(\Lambda_2)$. The posterior expectation of the loss function $L(\Lambda_2)$ with respect to $\pi_2(\theta_2/y)$ of $\hat{\theta}_2$ is the value of $\hat{\theta}_2$ that minimizes the posterior expectation of the loss function $L(\Lambda_2)$ denoted by $\hat{\theta}_{LB2}$

$$\hat{\theta}_{LB2} = \frac{(b+S_2)}{u_2} (1 - e^{-u_2/Q_2+d+2}) \quad (32)$$

4. The Joint Risk Efficiency

The risk functions of estimators $\hat{\theta}_{LB1}$ and $\hat{\theta}_{LB2}$ which relative to $L(\Lambda_1)$ and $L(\Lambda_2)$ are of interest. These joint risk functions are denoted by $R_L(\hat{\theta}_{LB1}, \hat{\theta}_{LB2})$ and $R_L(\hat{\theta}_{MSB1}, \hat{\theta}_{MSB2})$, where subscript L denotes risk relative to $L(\Lambda_1)$ and $L(\Lambda_2)$. Let us study the joint risk efficiency of $\hat{\theta}_{LB1}$ and $\hat{\theta}_{LB2}$, we will find $R_L(\hat{\theta}_{LB1}, \hat{\theta}_{LB2})$ from equations (31) and (32) as the following:

$$R_L(\hat{\theta}_{LB1}, \hat{\theta}_{LB2}) = [e^{-u_1} \int_0^\infty e^{u_1 \hat{\theta}_{LB1} / \theta_1} g(S_1) dS_1 - \int_0^\infty u \frac{\hat{\theta}_{LB1}}{\theta_1} g(S_1) dS_1 + \int_0^\infty u g(S_1) dS_1 - \int_0^\infty u g(S_1) dS_1] \\ [e^{-u_2} \int_0^\infty e^{u_2 \hat{\theta}_{LB2} / \theta_2} g(S_2) dS_2 - \int_0^\infty u \frac{\hat{\theta}_{LB2}}{\theta_2} g(S_2) dS_2 - \int_0^\infty u g(S_2) dS_2 + \int_0^\infty u g(S_2) dS_2 - \int_0^\infty u g(S_2) dS_2] \quad (33)$$

$$+ \int_0^\infty u g(S_2) dS_2 - \int_0^\infty u g(S_2) dS_2] \\ \frac{a(1-e^{-\frac{u_1}{Q_1+c+2}})}{\theta_1}^{-u_1}$$

$$R_L(\hat{\theta}_{LB1}, \hat{\theta}_{LB2}) = [\frac{e}{\Gamma(n+1)\theta_1^{n+1}\omega_i^{n+1}} \\ \frac{-u_1}{-S_1(1-e^{-\frac{u_1}{Q_1+c+2}})\alpha_j} \frac{-u_1}{Q_1+c+2} \\ \int_0^\infty e^{\frac{-u_1}{\alpha_j\theta_1}} S_1^n dS_1 - \frac{a(1-e^{-\frac{u_1}{Q_1+c+2}})}{\Gamma(n+1)\theta_1^{n+2}\omega_i^{n+1}}]$$

$$\int_0^\infty S_1^n e^{\frac{-S_1}{\alpha_j\theta_1}} dS_1 - \frac{\frac{-u_1}{Q_1+c+2}}{(1-e^{-\frac{u_1}{Q_1+c+2}})} \\ \frac{1}{\Gamma(n+1)\theta_1^{n+2}\omega_i^{n+1}}$$

$$\int_0^\infty S_1^{n+1} e^{\frac{-S_1}{\alpha_j\theta_1}} dS_1 + u_1 - 1] [\frac{e}{\Gamma(m+1)\theta_2^{m+1}\epsilon_j^{m+1}} \\ \frac{-u_2}{-S_2(1-e^{-\frac{u_2}{Q_2+d+2}})\alpha_j} \frac{-u_2}{Q_2+d+2} \\ \int_0^\infty e^{\frac{-u_2}{\epsilon_j\theta_2}} S_2^m dS_2 - \frac{b(1-e^{-\frac{u_2}{Q_2+d+2}})}{\Gamma(m+1)\theta_2^{m+2}\epsilon_j^{m+1}}]$$

$$\int_0^\infty e^{\frac{-u_2}{\epsilon_j\theta_2}} S_2^m dS_2 \\ - \frac{b(1-e^{-\frac{u_2}{Q_2+d+2}})}{\Gamma(m+1)\theta_2^{m+2}\epsilon_j^{m+1}} \int_0^\infty S_2^m e^{\frac{-S_2}{\epsilon_j\theta_2}} dS_2 \\ - \frac{(1-e^{-\frac{u_2}{Q_2+d+2}})}{\Gamma(m+1)\theta_2^{m+1}\epsilon_j^{m+1}} \int_0^\infty S_2^{m+1} e^{\frac{-S_2}{\epsilon_j\theta_2}} dS_2 + u_2 - 1]. \quad (34)$$

$$- \frac{(1-e^{-\frac{u_2}{Q_2+d+2}})}{\Gamma(m+1)\theta_2^{m+1}\epsilon_j^{m+1}} \int_0^\infty S_2^{m+1} e^{\frac{-S_2}{\epsilon_j\theta_2}} dS_2 + u_2 - 1].$$

Then

$$R_L(\hat{\theta}_{LB1}, \hat{\theta}_{LB2}) = [\frac{e^{-\frac{u_1}{Q_1+c+2}}}{\theta_1}^{-u_1} \\ \frac{e}{(1+(1-e^{-\frac{u_1}{Q_1+c+2}})\omega_i)^{n+1}} \\ - (1-e^{-\frac{u_1}{Q_1+c+2}})^{-1} (\alpha_j \theta_1^{n+1} + (n+1) + u_1 - 1)]$$

$$[\frac{e^{-\frac{u_2}{Q_2+d+2}}}{\theta_2}^{-u_2} \\ \frac{e}{(1+(1-e^{-\frac{u_2}{Q_2+d+2}})\epsilon_j)^{m+1}} \\ - (1-e^{-\frac{u_2}{Q_2+d+2}})^{-1} (\epsilon_j \theta_2^{m+1} + (m+1) + u_2 - 1)].$$

In the same manner, we get

$$R_L(\hat{\theta}_{MSB}, \hat{\theta}_{MSB}) = E_{XY}(L(\Lambda_1), L(\Lambda_2)) \\ = \int_0^\infty \int_0^\infty L(\Lambda_1)L(\Lambda_2)g(S_1)g(S_2)dS_1dS_2 \\ = \int_0^\infty e^{u_1(\hat{\theta}_{MSB}/\theta_1-1)} - u_1(\frac{\hat{\theta}_{MSB}}{\theta_1} - 1) - 1]g(S_1)dS_1 \quad (36)$$

$$\int_0^\infty e^{u_2(\hat{\theta}_{MSB}/\theta_2-1)} - u_2(\frac{\hat{\theta}_{MSB}}{\theta_2} - 1) - 1]g(S_2)dS_2.$$

Then

$$R_L(\hat{\theta}_{MSB}, \hat{\theta}_{MSB}) = [e^{-u_1} \int_0^\infty e^{u_1 \hat{\theta}_{MSB} / \theta_1} g(S_1) dS_1 \\ - u_1 \int_0^\infty \frac{\hat{\theta}_{MSB}}{\theta_1} g(S_1) dS_1 + u_1 - 1] \\ [e^{-u_2} \int_0^\infty e^{u_2 \hat{\theta}_{MSB} / \theta_2} g(S_2) dS_2 \\ - u_2 \int_0^\infty \frac{\hat{\theta}_{MSB}}{\theta_2} g(S_2) dS_2 + u_2 - 1]. \quad (37)$$

by using the equations (13),(14),(17) and (18) in(37)

$$\begin{aligned}
 R_L(\hat{\theta}_{MSB}, \hat{\theta}_{MSB}) &= \left[\frac{e^{u_1(\frac{a}{\theta_1(Q+c)}-1)}}{\Gamma(n+1)\omega_1^{n+1}\theta_1^{n+1}} \right. \\
 \int_0^\infty \int_0^\infty S_1\left(\frac{u_1\omega_1-(Q+c)}{\theta_1(Q+c)\omega_1}\right) dS_1 & \left. - \frac{u_1^a}{\Gamma(n+1)(Q_1+c)\theta_1^{n+2}\omega_1^{n+1}} \right. \\
 \int_0^\infty \int_0^\infty S_1\left(\frac{S_1}{\omega_1\theta_1}\right) dS_1 & \left. - \frac{u_1}{\Gamma(n+1)(Q_1+c)\theta_1^{n+2}\omega_1^{n+1}} \right. \\
 \int_0^\infty \int_0^\infty S_1\left(\frac{S_1}{\omega_1\theta_1}\right) dS_1 & \left. + u_1 - 1 \right] \left[\frac{e^{u_2(\frac{b}{\theta_2(Q_2+d)}-1)}}{\Gamma(m+1)\varepsilon_j^{m+1}\theta_2^{m+1}} \right. \\
 \int_0^\infty \int_0^\infty S_2\left(\frac{u_2\varepsilon_j-(Q_2+d)}{\theta_2(Q_2+d)\varepsilon_j}\right) dS_2 & \left. - \frac{u_2^b}{\Gamma(m+1)(Q_2+d)\theta_2^{m+2}\varepsilon_j^{m+1}} \right. \\
 \int_0^\infty \int_0^\infty S_2\left(\frac{S_2}{\varepsilon_j\theta_2}\right) dS_2 & \left. - \frac{u_2}{\Gamma(m+1)(Q_2+d)\theta_2^{m+2}\varepsilon_j^{m+1}} \right. \\
 \int_0^\infty \int_0^\infty S_2\left(\frac{S_2}{\varepsilon_j\theta_2}\right) dS_2 & \left. + u_2 - 1 \right].
 \end{aligned} \tag{38}$$

Then

$$\begin{aligned}
 R_L(\hat{\theta}_{MSE}, \hat{\theta}_{MSE}) &= \left[\frac{(Q+c)^{m+1} e^{u_1(\frac{a}{\theta_1(Q+c)}-1)}}{(Q+c-u_1\omega)^{m+1}} \right. \\
 - \frac{u_1}{(Q_1+c)} & \left. \frac{1}{(\omega_1^{(n+1)+u_1-1})} \left[\frac{(Q_2+d)^{m+1} e^{u_2(\frac{b}{\theta_2(Q_2+d)}-1)}}{(\varepsilon_j^{(Q_2+d)-u_2\varepsilon_j})^{m+1}} \right. \right. \\
 - \frac{u_2}{(Q_2+d)} & \left. \left. \frac{1}{(\theta_2^{(m+1)+u_2-1})} \right] \right].
 \end{aligned} \tag{39}$$

The risk efficiency of $R_L(\hat{\theta}_{LB1}, \hat{\theta}_{LB2})$ with respect to $R_L(\hat{\theta}_{MSB1}, \hat{\theta}_{MSB2})$ under LINEX Loss

$L(\Lambda_1)$ and $L(\Lambda_2)$ may be defined as follows:

$$RE3_L(\hat{\theta}_{LB1}, \hat{\theta}_{LB2}, \hat{\theta}_{MSB1}, \hat{\theta}_{MSB2}) = \frac{R_L(\hat{\theta}_{MSB1}, \hat{\theta}_{MSB2})}{R_L(\hat{\theta}_{LB1}, \hat{\theta}_{LB2})} \tag{40}$$

4. Simulation Study

We needed to check whether an estimator is inadmissible under some loss function or not. If so, the estimator would not be used for the losses specified by that loss function. For this purpose the risks of the estimators and risk efficiency have been computed $RE3$. So we will obtain the MLE for the unknown parameters of the Weibull distribution then use them to obtain Bayes estimators under LINEX loss function and Bayes estimator under square errors. The following steps will be considered to obtain the estimators:

Step (1): Generate random samples X_1, \dots, X_n from Weibull distribution with sample sizes 5, 10, 15 and 20, the shape parameters θ_1 , for each value of the sample size of n we will generate 1000 random samples from Weibull distribution in the case of time=30.

Step (2): Similarly, we can obtain the generate samples for y_1, \dots, y_m from Weibull distribution with parameters θ_2 , for each value of the sample size of m we will generate 1000 random samples from Weibull distribution.

Step (3): Using the Equation (35) to find the $R_L(\hat{\theta}_{LB1}, \hat{\theta}_{LB2})$ and use Equation (39) to find $R_L(\hat{\theta}_{MSB1}, \hat{\theta}_{MSB2})$ and Finally, Supply the values of risk function $RE3_L$ from equation (40).

Step (4): we take the average of there 1000 values then calculate risk function $RE3_L$.

Step(5): repeat steps (1-4)in the case of time=50.

Table (1) $u_1 = 0.8, u_2 = 0.8, \theta_1 = 2, \theta_2 = 2$ and $R = 0.4$

(n,m)	MSE1	MSE2	LB1	LB2	R_{LB}	R_{MSE}	RE3
(5,5)	1.784	2.975	1.438	2.399	2.05E-03	8.38E-04	0.409
(10,10)	2.498	2.93	2.153	2.526	8.03E-04	3.98E-04	0.496
(15,15)	2.651	2.767	2.367	2.471	4.12E-04	2.32E-04	0.562
(20,20)	2.587	3.433	2.36	3.132	2.472E-04	1.51E-04	0.613
(5,4)	2.079	2.88	1.676	2.56	2.32E-03	9.34E-04	0.404
(10,8)	2.095	2.426	1.805	2.547	9.552E-04	4.62E-04	0.484
(10,9)	2.16	2.397	1.862	2.34	8.72E-04	4.27E-04	0.49
(20,18)	2.134	2.766	1.947	2.504	2.73E-04	1.64E-04	0.603
(20,19)	2.1	3.092	1.99	2.811	2.591E-04	1.5E-04	0.608

Table (2) $u_1 = 0.8, u_2 = 0.8, \theta_1 = 1, \theta_2 = 2$ and $R = 0.333$

(n,m)	MSE1	MSE2	LB1	LB2	R_{LB}	R_{MSE}	RE3
(5,5)	1.136	1.597	0.916	1.45	5.29E-04	5.40E-04	1.017
(10,10)	1.33	2.371	1.146	2.044	3.37E-04	3.41E-04	1.011
(15,15)	1.283	1.089	1.145	1.698	2.067E-04	2.076E-04	1.004
(20,20)	1.12	2.32	0.998	2.119	1.4E-04	1.4E-04	1.001
(5,4)	0.688	1.566	0.555	1.78	7.058E-04	5.905E-04	0.978
(10,8)	1.314	1.864	1.132	2.042	3.945E-04	3.831E-04	0.971
(10,9)	1.22	1.805	1.052	1.541	3.637E-04	3.606E-04	0.992
(20,18)	1.1	2.115	1.21	1.915	1.522E-04	1.499E-04	0.985
(20,19)	1.325	1.95	1.013	2.285	1.453E-04	1.443E-04	0.993

Table (3) $u_1 = 1, u_2 = 1, \theta_1 = 1, \theta_2 = 2$ and $R = 0.333$

(n,m)	MSE1	MSE2	LB1	LB2	R_{LB}	R_{MSE}	RE3
(5,5)	1.273	2.47	1.167	1.975	1.54E-03	1.60E-03	1.045
(10,10)	1.254	2.192	1.037	1.813	1.13E-03	2.00E-03	1.764
(15,15)	1.626	2.247	1.417	1.958	5.35E-04	9.58E-04	1.51
(20,20)	1.3	2.233	1.18	2.005	4.05E-04	5.60E-04	1.381
(5,4)	0.982	2.077	0.785	2.328	1.811E-03	3.397E-03	1.005
(10,8)	1.474	2.104	1.136	2.001	9.589E-04	9.527E-04	0.993
(10,9)	1.609	1.836	1.379	1.557	8.842E-04	8.974E-04	1.015
(20,18)	1.325	2.363	1.244	2.131	3.7E-04	3.705E-04	1.001
(20,19)	1.415	2.571	1.324	2.328	3.5E-04	3.567E-04	1.01

Table (4) $u_1 = -1, u_2 = -1, \theta_1 = 1, \theta_2 = 2$ and $R = 0.333$

(n,m)	MSE1	MSE2	LB1	LB2	R_{LB}	R_{MSE}	RE3
(5,5)	1.156	1.764	1.004	1.533	1.55E-03	1.38E-03	0.893
(10,10)	1.356	1.957	1.232	1.779	8.51E-04	7.63E-04	0.896
(15,15)	1.256	2.212	1.02	2.057	5.23E-04	4.75E-04	0.909
(20,20)	1.114	2.6	1.12	2.453	3.50E-04	3.22E-04	0.919
(5,4)	1.343	1.652	1.167	1.417	1.744E-03	1.507E-03	0.819
(10,8)	1.12	2.254	1.245	2.02	1.002E-03	8.691E-04	0.867
(10,9)	1.364	2.304	1.232	2.094	9.205E-04	8.126E-04	0.883
(20,18)	1.17	2.554	1.017	2.603	3.845E-04	3.489E-04	0.908
(20,19)	1.253	2.664	1.24	2.507	3.667E-04	3.350E-04	0.914

Table (5) $u_1 = 0.8, u_2 = 0.8, \theta_1 = 2, \theta_2 = 3$ and $R = 0.4$

(n,m)	MSE1	MSE2	LB1	LB2	R_{LB}	R_{MSE}	RE3
(5,5)	1.502	2.49	1.835	2.3	5.071E-03	2.95E-03	0.486
(10,10)	2.025	2.95	1.735	2.16	1.932E-03	9.53E-04	0.493
(15,15)	2.351	3.396	2.09	3.018	9.97E-04	5.57E-04	0.559
(20,20)	2.354	2.751	2.139	2.501	5.98E-04	3.65E-04	0.61
(5,4)	1.823	3.345	1.457	3.158	5.54E-03	2.22E-03	0.4
(10,8)	2.234	2.99	1.914	3.011	2.302E-03	1.10E-03	0.48
(10,9)	2.701	3.0247	1.955	3.089	2.10E-03	1.02E-03	0.487
(20,18)	2.123	2.798	2.455	2.533	5.61E-04	3.97E-04	0.6
(20,19)	2.373	3.1	2.165	2.818	2.59E-04	1.58E-04	0.608

Table (6) $u_1 = 0.8, u_2 = 0.8, \theta_1 = 1, \theta_2 = 2$ and $R = 0.333$

(n,m)	MSE1	MSE2	LB1	LB2	R_{LB}	R_{MSE}	RE3
(5,5)	0.991	1.83	0.799	1.475	5.2911E-04	5.40E-04	1.017
(10,10)	1.471	2.325	1.268	2.405	3.37E-04	3.4E-04	1.011
(15,15)	0.132	1.923	1.222	1.717	2.1E-04	2.2E-04	1.004
(20,20)	0.999	2.36	1.011	2.153	1.41E-04	1.4E-04	1.001
(5,4)	0.923	1.635	0.744	1.717	7.12E-04	5.9E-04	0.978
(10,8)	1.775	2.669	1.53	2.253	3.934E-04	3.8E-04	0.971
(10,9)	1.7	1.929	1.245	1.647	3.6E-04	3.6E-04	0.992
(20,18)	1.333	2.454	1.111	2.222	1.5E-04	1.5E-04	0.985
(20,19)	1.532	2.478	1.212	2.323	1.5E-04	1.4E-04	0.993

Table (7) $u_1 = 1, u_2 = 1, \theta_1 = 1, \theta_2 = 2$ and $R = 0.333$

(n,m)	MSE1	MSE2	LB1	LB2	R_{LB}	R_{MSE}	RE3
(5,5)	0.725	1.784	0.579	1.524	1.54E-03	1.60E-03	1.045
(10,10)	0.888	1.967	0.657	1.685	8.20E-04	8.48E-04	1.034
(15,15)	0.965	2.452	0.875	2.179	5.03E-04	5.15E-04	1.024
(20,20)	1.121	2.314	0.924	2.014	3.38E-04	3.44E-04	1.017
(5,4)	1.149	2.131	0.899	1.704	1.720E-03	1.729E-03	1.005
(10,8)	1.1545	2.553	0.983	2.141	9.589E-04	9.527E-04	0.993
(10,9)	1.254	2.178	0.999	1.866	8.842E-04	8.974E-04	1.015
(20,18)	1.222	2.236	1.021	2.017	3.701E-04	3.705E-04	1.088
(20,19)	1.235	2.353	1.0222	2.131	3.533E-04	3.567E-04	1.01

Table (8) $u_1 = -1, u_2 = -1, \theta_1 = 1, \theta_2 = 2$ and $R = 0.333$

(n,m)	MSE1	MSE2	LB1	LB2	R_{LB}	R_{MSE}	RE3
(5,5)	1.533	1.841	1.332	1.6	1.55E-03	1.3E-03	0.893
(10,10)	1.232	2.031	1.222	1.846	8.51E-04	7.6E-04	0.896
(15,15)	1.325	2.194	1.25	2.041	5.23E-04	4.7E-04	0.909
(20,20)	1.424	2.015	1.24477	2.145	3.50E-04	3.2E-04	0.919
(5,4)	1.254	2.159	1.33	1.876	1.744E-03	1.5E-03	0.864
(10,8)	1.111	2.162	1.145	1.937	1.002E-03	8.6E-04	0.867
(10,9)	1.675	1.831	1.522	1.654	9.205E-04	8.1E-04	0.883
(20,18)	1.254	2.428	1.425	2.279	3.845E-04	3.4E-04	0.908
(20,19)	1.92	2.921	1.811	2.749	3.667E-04	3.3E-04	0.914

We can study the different between the cases of the risk functions in the different case of sample sizes equal sample sizes and not equals ,in different times; it will be clear from figures mentioned below:

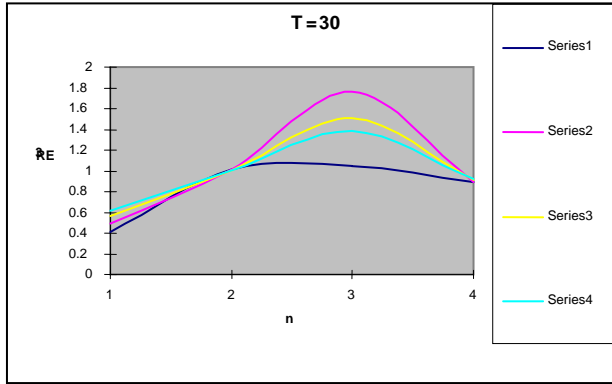


Figure (1): to Compare between the proposed estimators of RE_3 in different cases of the sample sizes $n, m = 5, 10, 15$ and 20 and for different values of u_1, u_2 in case of time =30 hours.

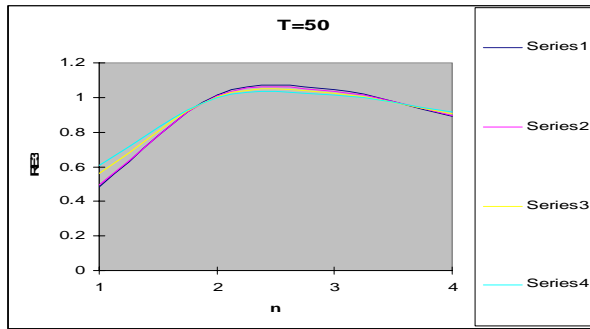


Figure (2): to Compare between the proposed estimators of RE_3 in different cases of the sample sizes $n, m = 5, 10, 15$ and 20 and for different values of u_1, u_2 in case of time =50 hours.

5. Illustrative Example

The simulation study shows that $R_L(\hat{\theta}_{LB1}, \hat{\theta}_{LB2})$ is preferable than $R_L(\hat{\theta}_{MSB1}, \hat{\theta}_{MSB2})$. This section will provide a true example on the life test from Weibull distribution with type-I censored data for failure terminated data given in blow tables come. These T_1, \dots, T_{10} failure times corresponding to devices x_1, \dots, x_{10} , and U_1, \dots, U_{10} failure times corresponding to devices y_1, \dots, y_{10}

Table 9. Numbers.

77.668	16.263	116.729	399.071
118.077	182.737	102.947	6.17
87.592	12.411	49.022	72.435
6.171	7.400	12.411	21.49
89.601	272.005	199.458	50.668

Using the statistics of total time. we obtain the following point estimator of the mean life:

$$\text{Mean life} = \frac{\text{Total test time}}{\text{sample number}} \tag{41}$$

Then for x and y the mean life will be:

$$\text{Meanlife}_x = \frac{\sum T}{n} = \frac{859925}{10} = 85.992 \tag{42}$$

and

$$\text{Meanlife}_y = \frac{\sum U}{m} = \frac{1030402}{10} = 103.04 \tag{43}$$

The reciprocal of mean life, yields the point estimate of the device failure rate for x and y :

$$\text{failure rate} = \frac{1}{\text{mean life}} \tag{44}$$

Then the failure rate for x and y will be:

$$\text{failurerat}_x = \frac{1}{85.9925} = 0.0116 \tag{45}$$

and

$$\text{failurerat}_y = \frac{1}{103.0402} = 0.0097 \tag{46}$$

We then use the appropriate statistical reliability to calculate the CI in the Weibull case .The formula to obtain a Weibull CI for true , but unknown mean for x and y indexed by $\hat{\theta}_1$ and $\hat{\theta}_2$ respectively with a confidence level $100(1 - \alpha)\%$,is given by.

$$\left[F_{1-\alpha/2}^{-1}(2n, 2m) \left(\frac{\sum T}{n} + F_{1-\alpha/2}^{-1}(2n, 2m) \right)^{-1}, F_{\alpha/2}^{-1}(2n, 2m) \left(\frac{\sum T}{n} + F_{\alpha/2}^{-1}(2n, 2m) \right)^{-1} \right] \tag{47}$$

From the last equation we find the CL is 0.9999 and we use it to obtain 90%confidence bound for the Weibull mean, the 90% upper bound for unknown mean:

$$\hat{\theta}_1 = 2.195 \text{ and } \hat{\theta}_2 = 2.195 \tag{48}$$

Then the failure rate is

$$\hat{R} = \frac{\hat{\theta}_1}{\hat{\theta}_1 + \hat{\theta}_2} = 0.499 \tag{49}$$

Now we find the failure rate for mean square error loss function case and LINEX loss function case: I-for mean square error loss function:

Before finding the value of failure rate $R_L(\hat{\theta}_{MSB1}, \hat{\theta}_{MSB2})$, we should find the value of $\hat{\theta}_{MSB1}$ and $\hat{\theta}_{MSB2}$ from equations (17) and (18), so:

$$\hat{\theta}_{MSB1} = 0.304 \text{ and } \hat{\theta}_{MSB2} = 0.0158 \tag{50}$$

Where $a, b, c, d > 0, u_1, u_2 \neq 0$, and for S_1, S_2 calculated by MATHCAD program and we get their values as the following

$$S_1 = -2.604, S_2 = -2.794. \quad (51)$$

Now from equation (39) we can find the value of

$$R_L(\hat{\theta}_{MSB1}, \hat{\theta}_{MSB2}) = 0.9505 \quad (52)$$

II-for LINEX loss function:

Before finding the value of failure rate $R_L(\hat{\theta}_{LB1}, \hat{\theta}_{LB2})$, we should find the value of $\hat{\theta}_{LB1}$ and $\hat{\theta}_{LB2}$ from equations (31) and (32), so:

$$\hat{\theta}_{LB1} = 0.0235 \text{ and } \hat{\theta}_{LB2} = 0.01244. \quad (53)$$

By using equation (35) we can find the value of

$$R_L(\hat{\theta}_{LB1}, \hat{\theta}_{LB2}) = 0.653 \quad (54)$$

Using equation (40) to find failure rate for mean square error loss function case and LINEX loss function case:

$$RE = \frac{0.9505}{0.653} = 1.4555 \quad (55)$$

RE is greater than one which indicates that the proposed estimators $R_L(\hat{\theta}_{LB1}, \hat{\theta}_{LB2})$ are preferable

to $R_L(\hat{\theta}_{MSB1}, \hat{\theta}_{MSB2})$.

4. Conclusion

In this paper, the Bayes estimation of stress-strength parameter for two Weibull distributions under type-I censoring has been considered. The LINEX loss function and square error loss function have been proposed. Extensive simulations are performed to check the performance of the two estimators, and it's observed that the LINEX loss function is preferable to the square errors loss function. Also, for the illustrative example which demonstrated agreed with the paper results.

Corresponding author

Marwa O. Mohamed
Department of Mathematics, Zagazig University,
EGYPT
mo11577@yahoo.com

References:

- [1] Kundu D., and R.D. Gupta (2005)., "Estimation of $P(Y < X)$ for Generalized Exponential Distribution," *Metrika*, vol. 61(3), pp. 291-308.
- [2] Surles J.G., and W.J. Padgett, (1998) Inference for $P(Y < X)$ in the Burr Type X, model," *Journal of Applied*

- Statistical Science*, (1998), pp. 225-238.
- [3] Panahi H. and S. Asadi (2010), "Estimation of $R=P[Y < X]$ for two-parameter Burr Type XII Distribution," *World Academy of Science, Engineering and Technology*, (2010) vol. 72, pp. 465-470.
- [4]. AwadA.M., and M.K. Gharraf (1986), "Estimation of $P(Y < X)$ in the Burr Case: A Comparative Study," *Communications in Statistics-Simulation and Computation*, vol, 15, pp. 389- 402.
- [5]. RaqabM.Z., and D. Kundu(2005), "Comparison of different estimators of $P(Y < X)$, for a scaled Burr Type X distribution," *Communications in Statistics - Simulation and Computation*, vol. 34(2), , 465-483.
- [6]. Mokhlis N.A(2005)., "Reliability of a Stress-Strength Model with Burr Type III Distributions," *Communications in Statistics—Theory and Methods*, vol. 34, , pp. 1643-1657.
- [7]. Surles J.G., and W. J. Padgett (2001), "Inference for $P(Y < X)$ in the Burr type X model," *Applied Statistics Science*, vol, 7), pp. 225-238.
- [8]. Kotz,Y. Lumelskii, and M. Pensky (2003), *The Stress–Strength Model and Its Generalization: Theory and Applications*, World Scientific, Singapore, (
- [9] Lawless(1982), *J. F. Statistical Models and Methods for Lifetime Data*. John Wiley & Sons, New York.
- [10] JiangL. and A.C.MWong (2008). A note on inference for $P(X < Y)$ for right truncated exponentially distributed data, *Statist. Papers* 49, pp. 637–651.
- [11] Abd-Elfattah, A. M. and Marwa O(2009). Mohamed, Estimating system reliability of competing Weibull failures with censored samples. *Selcuk Journal of applied Mathematics*, Vol. 10, No. 2, pp. 53-65.
- [12] Abd-Elfattah, A. M. and Marwa O. Mohamed(2008), Estimation of $P(Y < X)$ in Exponential Case based on type II censored samples. The 43 th Annual Conference on Statistics, Computer Science and Operation Research).
- [13]. SaracogluB., I. Kinaci, and D. Kundu(2011), On estimation of $R = P(Y < X)$ for exponential distribution under progressive type-II censoring, *J. Stat. Comput. Simul.* , accepted for publication,
- [14]. Lio & Tzong-Ru Tsai (2011), Estimation of $\delta=P(X < Y)$ for Burr XII distribution based on the progressively first failure-censored samples. *Journal of Applied Statistics*, accepted for publication,).
- [15] Feynman (1987), Mr. Feynman goes to Washington. In: *Engineering and Science*. California Institute of Technology, Pasadena, CA), pp. 6-22.
- [16]. Varian (1975), A Bayesian approach to real state assessment In: Stephen, E. F., Zellner, A. (Eds.), *Studies in Bayesian Econometrics and Statistics in Honor of Leonard J. Savage*. North-Holland, Amsterdam, pp.195-208. *Statist. Assoc.* 81) 446-451.

11/22/2011

Histopathological and Immunohistochemical Studies on the Prognostic Significance of Angiogenesis in Renal Cell Carcinoma

Samia, M. Sanad¹, Mahmoud, A. El-Baz² and Mohamed, A. Erfan³

¹Zoology Department, Faculty of Science, Zagazig University, Egypt.

²Pathology Department, Faculty of Medicine, Mansoura University, Egypt

³Urology and Nephrology Center, Mansoura University, Egypt.

Abstract: In the present study, evaluation of tumour angiogenesis has been carried out in a group of patients with renal cell carcinoma. The retrospective study included 97 patients for whom radical nephrectomy was carried out between 1997 and 1999 in the Urology and Nephrology Center belonging to Mansoura University, Egypt. Patients were stratified according to grade, stage, age, lymph node status, tumour size and angiogenesis. Angiogenesis was evaluated by measuring the mean microvessel density (MVD). Microvessels were immunohistochemically stained using monoclonal antibody that reacted with endothelial cells lining the wall of blood vessels and was called CD34. Microvessels were counted in active areas of angiogenesis (hot spots) under magnification of X250 and the mean of 3 counts (MVD) was used for univariate and multivariate statistical analysis. The results of the present study indicated that, evaluation of microvessel density is of no appreciable value in the assessment of prognosis for renal cell carcinoma. Tumour stage could provide more objective tool for better judgment on the patient survival and might help in choice of the more convenient therapy for the individual patient.

[Samia, M. Sanad, Mahmoud, A. El-Baz and Mohamed, A. Erfan **Histopathological and Immunohistochemical Studies on the Prognostic Significance of Angiogenesis in Renal Cell Carcinoma**] Life Science Journal, 2011; 8(4):838-851] (ISSN: 1097-8135). <http://www.lifesciencesite.com>.

Key words: Histopathological, Immunohistochemical, Angiogenesis, Renal cell carcinoma.

1. Introduction

Renal cell carcinoma (RCC) is a relatively rare tumour affecting six of every 100,000 people and accounting for approximately 3% of adult malignancies and 1.4 of cancer related deaths. It is more common among urban population and among males with a male-to-female ratio of approximately 2:1. The tumour arises from the proximal convoluted tubules of the kidney and is characterized by abundant neovascularization and arteriovenous-venous fistula formation. Growth of solid tumours requires angiogenesis. The new proliferating vessels supply oxygen and nutrition for the tumour cells and promote their growth. Experimental evidence shows that, the dynamics of hematogenous metastasis are dependant on the access of the tumour cells to the microvasculature. RCC is a tumour with unpredictable behavior (Dekel *et al.*, 2002). Radical nephrectomy is the curative treatment option for renal cell carcinoma. If the tumour is small and nephron sparing is required, partial nephrectomy is the procedure of choice (Dekel *et al.*, 2002). Clearly there is a need for more precise prognostic markers for predicting the risk of developing metastatic RCC.

Because RCC is one of the most highly vascularized solid malignancies, it seems logical that factors that regulate the process of angiogenesis and invasion would be correlated to its pathogenesis (Slaton *et al.*, 2001). The prognostic of RCC remains poor. One third of the patients already have

metastasis when first consulting the hospital. Another 30-40% of patients develop metastases after surgical excision of the primary tumour. RCC are radioresistant and more than 8% are chemoresistant (Stassar *et al.*, 2001). Angiogenesis is the growth of new vessels from the existing vasculature, a process central to tumour growth and metastasis (Jones and Fujima, 1999). The measurement of intratumoural microvessel density (MVD) has been proved to be an important prognostic indicator for many malignant neoplasms. The value of MVD as a predictor of patient prognosis in RCC is controversial. Certain reports revealed a direct correlation between MVD and survival, others revealed an inverse correlation and one report showed no correlation (Sabo *et al.*, 2001).

There is considerable experimental evidence that angiogenesis plays a crucial role in the growth of solid tumours over 1 to 2 mm. in diameter (about 10⁶ cells), and in gaining access to the existing vasculature. A multitude of new angiogenesis inducers and inhibitors have been isolated and characterized, and attempts to control tumour growth by inhibiting angiogenesis have generated much interest. The results of early clinical trials are just now becoming available (Fujioka *et al.*, 1998).

The aim of the present study is:

1. To determine whether the degree of vascular complexity has a predicative value in the prognosis of RCC or not.

2. To evaluate the relationship between angiogenesis and the different clinical and pathologic parameters such as age, sex grade and lymph node status.
3. To perform multivariate analysis to detect the independent prognostic factors that can affect the patients survival.

2. PATIENTS AND METHODS

1. Patients:

Between January 1997 and December 1999, 97 patients were diagnosed as renal cell carcinoma and were admitted to Mansoura Urology and Nephrology Center. The study group consisted of these patients for whom radical nephrectomy was performed for the treatment of renal tumour. The patients of this retrospective study were chosen on the basis of availability of complete archival material. At the time of nephrectomy, all specimens were examined according to the same pathological protocol. Tissue sections were obtained from the tumour.

1. a. Age:

Patients' age ranged from 5 to 76 years for the whole study population. For men (mean \pm SD = 49 \pm 12.2 years) but for women (mean \pm SD= 50.7 \pm 13.3 years).

1. b. Sex:

There were 69 (71.1%) men and 28 (28.9%) women and the male to female ratio 2.46: 1.

2. Histopathology:

The hematoxylin and eosin stained slides were reviewed to confirm the diagnosis. Conventional type of renal cell carcinoma was diagnosed in 42 patients (43.3%), chromophobe type in 19 patients (19.6%), papillary type in 33 patients (34.0%) and unclassified type in 3 patients (3.1%).

2. a. Grade:

Tumours were graded using Fuhrman's grading system (Fuhrman *et al.*, 1982) into four grades 1, 2, 3 and 4. The percents of grades of our study were found to be (41.2%), (40.2%), (15.5%) and (3.1%) respectively.

2. b. Stage:

The International Union Against Cancer and the American Joint Committee on Cancer proposed a revision of TNM system that is now the recommended staging system for RCC (Guinan *et al.*, 1997). This system was used in the present study for pathological staging of the tumours where:

Stage I: Tumour within capsule.

Stage II: Tumour invasion of perinephric fat (confined to Gerota's fascia).

Stage III: Tumour involvement of regional lymph nodes and/or renal vein and cava.

Stage IV: Adjacent organs or distant metastases.

The percents of the stages of the patients were found to be (67.0%), (16.5%), (13.4%) and (3.1%) respectively.

3. Tumour size:

By reviewing the pathological reports, the tumour size was assessed by determination of the largest diameter. The tumours were categorized according to size into 2 groups, equal and less than 7 cm and more than 7 cm.

4. Histopathological examination:

After radical nephrectomy, the tumour was immediately fixed in 10% neutral buffer formalin for 24 hours. Several pieces of 3-5 mm thickness were taken from the tumour and fixed tissues were chemically processed through the tissue processor (VIP Tissue-Tek apparatus, Japan). These processed tissues were embedded in molten paraffin wax and the paraffin blocks were sectioned at 3 μ m for hematoxylin and eosin staining and at 4 μ m for immunohistochemical staining with Reichert Jung 2030 microtome (West Germany) using disposable blades.

5. Tumour angiogenesis:

Angiogenesis of the tumours was assessed after highlighting the microvessels using the immunohistochemical staining technique.

5. a. Immunohistochemistry:

The avidin-biotin immunoperoxidase technique was applied (Guesdon, 1979). Four micron thick sections from retrieved tumour blocks were dewaxed and rehydrated through graded alcohols. These sections were mounted on coated slides by Histo-Grip (Zymed, USA) and were washed in water. Antigen sites were unmasked using microwave antigen retrieval technique (Kok and Boon, 1995). After their cooling, the slides were rinsed with phosphate buffered saline (PBS). Endogenous peroxidase activity was removed by submersing slides in blocking solution which was prepared by adding one part of 30% H₂O₂ to nine parts of methanol. Non-specific binding was blocked with blocking serum (reagent A of Histostain®- plus bulk kit, Zymed, USA). It was left for 10 minutes in contact with the slides. After removing the excess blocking serum, the monoclonal mouse anti-CD34 which is an antibody concentrate that will provide qualitative demonstration of the CD34 protein in formalin-fixed paraffin embedded human tissue sections was applied.

CD34 was applied at a dilution of 1: 100 in phosphate buffer saline (PBS, 10 mM sodium phosphate, 140 mM sodium chloride, PH 7.2) and was incubated for 60 min. The slides were rinsed well

with PBS for 3 minutes. Biotinylated secondary antibody solution (reagent B of Histostain[®] - plus bulk kit, Zymed, USA) was incubated with the slides for 10 minutes. This was followed by a further wash in PBS. Enzyme conjugate solution (ready to use streptavidin-peroxidase HRP which is reagent C of Histostain[®] plus bulk kit, Zymed, USA) was applied to the slides for 10 minutes. The slides were washed with buffer solution, then the final steps of this procedure i.e. addition of chromogen substrate di-amino-benzidine (DAB) [Sigma chemical company, UK] and light counter-stain with haematoxylin were performed. The result is brown stain to the microvessels:

5. b. Assessment of microvessel density:

The microvessel density, defined as capillaries and small venules, was assessed in areas with a solid tumour morphology away from any artifact or necrosis and without prior knowledge of patient outcome. The vessel counting was performed in three areas of maximal neovascularization where the highest number of discrete microvessels was stained (hot spots) (Dickinson *et al.*, 1994). Low power light microscopy at X40 magnification was used to scan the often heterogeneous tumour sections for these areas. At X250 magnifications, counts were made of all distinct brown staining endothelial cells or cell clumps. Sclerotic areas within the tumour which showed less neovascularization, and adjacent benign tissue were not considered in vessel counts. Microvessels found in unaffected areas adjacent to tumour infiltrated tissue were not counted but were used as an internal control in assessing quality (Jaeger *et al.*, 1995). To be defined as an individual vessel, cell nests showing immunostaining had to be clearly separate from adjacent microvessels, tumour cells or connective tissue elements. Vessel lumina, or intratumoural red blood cells were not necessary to define microvessels. Larger muscular walled vessels were excluded from the assessment. The microvessel density (MVD) was defined as the mean of the highest 3 counts.

6. Follow-up:

Patients were kept under regular clinical review. Follow-up, including mortality data, were obtained for all patients except one patient. They were followed regularly and examined for treatment failure depending on clinical findings and radiological evidence. The mean follow-up was 62.34±35.87 months (range =106) for the whole study groups. It was 61±37 (range=105), 63.87±35.04 (range =105), 69.94±32.53 (range= 93) and 12±10.81 (range= 21) for conventional, papillary, chromophobe and unclassified renal cell carcinoma (RCC) types respectively.

7. Prognostic variables:

The following clinical, morphologic, and biologic variables were studied with respect to prognosis: age, sex, histopathologic grade, tumour stage and lymph node status, beside tumour angiogenesis.

8. Statistical analysis:

The statistical analysis was performed using SPSS (Statistical Package of Social Science) program version 11(SPSS inc., Chicago, IL, USA). The quantitative data were presented in the form of mean, standard deviation and range. Student-t-test and one way-ANOVA (Analysis of variance) were used in the analysis. Kaplan-Miere survival curves were plotted and the log-rank test was used to determine statistical differences between life table curves (Kaplan and Meier, 1958). The period of disease-free survival was defined as the time between the date of surgery and death (from cancer) or the development of local recurrence or distant metastasis. Death from unknown cause was considered death from cancer. Censored survival values represent patients who were alive without clinical evidence of disease at the time of last follow-up. To simplify the statistical analysis, the patients were divided into groups according to age, tumour size and MVD.

Cox's proportional hazard analysis was used to study the simultaneous effects of the different factors in survival (Cox, 1972). The included variables were only those which were significant with log rank test. This multivariate analysis was performed to study the effect of one factor on survival, while the influence of others was controlled.

To simplify the statistical analysis in Kaplan-Meire survival curves and because of the little number of cases in both stage 4, grade 4 and unclassified type, we concluded them with stage 3, grade 3 and papillary type respectively.

3. Results

In the present study, the clinico-pathologic features of the study population are enlisted in table (1). Total cases were 97; conventional type accounted 43.3% of cases, papillary type 34%, chromophobe type 19.6% and unclassified type 3.1%.

Types:

1.a. Conventional renal cell carcinoma:

There were 42 patients with conventional type renal cell carcinoma included in this study. Most of them were men (69%). Age ranged from 5 to 76 years (mean ± SD=50.76 ± 13.27). The median follow up period was 82 months (range=105). The

regional lymph nodes were positive in 12 cases and negative in 30 cases.

1.b. Papillary renal cell carcinoma:

There were 33 patients with papillary type renal cell carcinoma included in this study, most of them were men (78.78%). Age ranged from 24 to 75 years (mean \pm SD=48.81 \pm 11.32 years). The median follow up period was 69 months (range=105). The regional lymph nodes were positive in 8 cases and negative in 25 cases.

1.c. Chromophobe renal cell carcinoma:

There were 19 cases with chromophobe renal cell carcinoma included in this study. Most of them were men (68.42%). Age ranged from 33 to 62 years (mean \pm SD= 50.36 \pm 9.05). The median follow up period was 82 months (range=29). The regional lymph nodes were positive in 5 cases and negative in 14 cases.

1.d. Unclassified renal cell carcinoma:

There were 3 cases only with unclassified renal cell carcinoma. Two females and one male. The first female was 24 years old with follow up period 21 months and died of disease. The second female was 68 years old with follow up period 15 months and died of disease. The male case was 14 years old and unfollowed.

2- Lymph node status:

For all cases, there were 25 cases with positive lymph nodes, and 72 cases with negative lymph nodes as shown in table (2).

3- Angiogenesis in renal cell carcinoma:

The slides of 97 patients were suitable for pathological interpretation after immunohistochemical staining for tumour angiogenesis (figs. 1-12) Descriptive analysis of microvessel density (MVD) for the four types of renal cell carcinoma which were included in our study are shown in table (3).

4- Angiogenesis and Clinicopathologic characteristics:

There was no significant relationship between MVD and age, sex, grade, stage, and tumour size. Type had a significant relationship with MVD (Table 4). Conventional type had significantly higher MVD than that of papillary type and chromophobe type. Unclassified type had a median vascularity. A significant relationship between MVD and lymph node status was obtained too. Negative cases had higher MVD mean than positive cases.

Correlation between angiogenesis (MVD) and age was slightly positive (increasing in age increased MVD slightly) as shown in fig. (13). Correlation coefficient (R)= -0.07 ($-1 \leq R \leq 1$).

Correlation between angiogenesis (MVD) and tumour size was slightly negative (increasing in

tumour size decreased MVD slightly) as shown in fig (14). Correlation coefficient (R) = 0.117 ($-1 \leq R \leq 1$).

5- Other significant relations:

5-a. Relations between age and stage was significant (P value=0.004). High ages had significantly higher stages.

5-b. Relation between tumour size and stage was significant (P value=0.03). Increasing in tumour size increased tumour stage.

5-c. Relation between tumour size and grade was significant (P value=0.01). Increasing in tumour size increased tumour grade.

5-d. Relation between stage and grade was significant (P value=0.0001).

Most stages had low grades and vice versa.

5-e. Relation between tumour size and survival time was significant (P value=0.009) (Fig. 15). As the tumour size increased the survival time decreased. Correlation coefficient (R)= -0.265 ($-1 \leq R \leq 1$).

6. Survival of patients with renal cell carcinoma (Table 5):

6. a. Overall survival:

The 5-year survival rate was 72.16%. The risk of treatment failure (tumour recurrence or death from tumour) was high in the first 2 years of follow up (Fig. 16).

6.b. Survival and sex:

Males had better survival than females. This difference reached statistical significance ($p=0.02$). The 5-year survival for males 79.71% while it was 53.57 for females (Fig. 17).

6. c. Survival and age:

Age was categorized in four groups to simplify the statistical analysis: <40 years, 40-50 years, 50-60 years and >60 years. The number of patients in each group was 16, 36, 26 and 19 patients respectively. There was no significant relationship between age and the survival of the patients ($P=0.28$) (Fig. 18).

6. d. Survival and stage:

Tumour stage had a significant impact on patients survival ($P < 0.0001$). There were only 3 cases in stage four, therefore we categorized stages 3 and 4 in one group. The 5-year survival rate was 83.08%, 68.75% and 31.25% for stage 1, 2 and 3 and 4 respectively (Fig. 19).

6.e. Survival and grade:

A significant relationship was observed between tumours grade and survival ($P=0.001$). As in stage, the number of grade four patients were 3 cases, thus we categorized grade 3 and 4 in one group. The 5-year survival rates for patients with grade 1, 2 and (3 and 4) were 80.00%, 76.92% and 44.44% respectively (Fig. 20).

6. f. Survival and type:

There was no significant relationship between the type and survival of the patients ($P=0.65$). Unclassified type was 3 cases only, thus we added them to papillary type to simplify statistical analysis. The 5-year survival rates were 69.05%, 78.95% and 72.22% for conventional, chromophobe and (papillary and unclassified) types respectively (Fig. 21).

6. g. Survival and lymph node status:

There was a significant relationship between the lymph node status and the survival of patients ($P=0.04$). The 5-year survival rates for patients with negative and positive lymph nodes were 77.78% and 56.00% respectively (Fig 22). The presence of regional positive lymph nodes which led to metastasis to the patients decreased the survival rates to these patients.

6. h. Survival and tumour size:

Tumour size of the patients was divided into 2 groups: >7 cm and ≤ 7 cm. The first group (> 7 cm) number was 65 patients and had a 5-year survival rate 63.08% and the second group (≤ 7 cm) number was 32 patients and had a 5-year survival rate 90.63%.

There was a significant relationship between lymph node status and survival of the patients ($P=0.004$) (Fig. 23).

6. i. Survival and microvessel density (MVD):

Microvessel density (MVD) was divided into 3 groups: < 20 , 20-30 and >30 . The number of patients in the 3 groups were 49, 37 and 11 patients respectively. The 5-year survival rates for the 3 groups were 77.55%, 62.16% and 81.82% respectively. There was no significant relationship between MVD and survival of the patients ($P=0.157$) (Fig. 24).

6. j. Multivariate analysis:

Multivariate analysis was performed, using Cox's proportional hazard analysis, for the significant variables in univariate analysis (sex, stage, grade, lymph node status and tumour size). Sex and lymph node status could not sustain its significance, while stage proved to be independent variable for prognosis and sustained its significance (Table 6). Grade and tumour size were considered as dependent variables, although their (P value) slightly increased above the critical value 0.05.

Table (1): Characteristics of the study population

	Total cases	Conventional type	Papillary type	Chromophobe type	Unclassified type
Number	97	42	33	19	3
Male to female ratio	69:28	29:13	26:7	13:6	1:2
Mean age \pm SD range	49.54 \pm 12.56 71 (5-76)	50.76 \pm 13.27 71 (5-76)	48.81 \pm 11.32 51 (24-75)	50.36 \pm 9.05 29 (33-62)	35.33 \pm 28.72 54 (14-68)
Grade:					
1	40	24	6	10	-
2	39	11	20	8	-
3	15	7	7	1	-
4	3	-	-	-	3
Stage:					
1	65	29	19	17	-
2	16	4	9	1	2
3	13	8	4	1	-
4	3	1	1	-	1
Lymph node status					
Negative	72	30	25	14	3
Positive	25	12	8	5	-
Tumour size					
≤ 7 cm	32	18	8	6	-
> 7 cm	65	24	25	13	3

Table (2): Positive and negative lymph node percents.

	Frequency	Percent	Valid Percent	Cumulative percent
Positive	25	25.8	25.8	25.8
Negative	72	74.2	74.2	100.0
Total	97	100.0	100.0	

Table (3): Descriptive analysis of MVD for types of RCC

Type	Minimum MVD	Maximum MVD	Range	SUM	Mean	SD
Conventional	17	42	25	1101	26.21	6.919
Papillary	14	29	15	621	18.81	3.58
Chromophobe	15	32	17	372	19.57	3.93
Unclassified	18	29	11	71	23.66	5.50

Table (4): Clinico-pathological characteristics of RCC and their relation to the tumour angiogenesis.

Variable	No. of patients	Microvessel density mean (MVD)	P value
1) Type			
Conventional	42	26.21	0.001
Papillary	33	18.81	
Chromophobe	19	19.57	
Unclassified	3	23.66	
2) Age	97	22.3	0.25
3) Sex			
- Male	69	22.13	0.9
- Female	28	22.78	
4) Grade			
- G1	40	23.9	0.19
- G2	39	21.25	
- G3	15	20.6	
- G4	3	23.66	
5) Stage			
- S1	65	22.75	0.76
- S2	16	20.87	
- S3	13	21.92	
- S4	3	22.33	
6) Lymph node			
- positive	25	20.36	0.03
- negative	72	23.18	
7) Tumour size	97	22.3	0.48

Table (5): Kaplan-Meier estimate of 5-year disease-free survival in relation to patient and tumour characteristics.

Characteristic	No. of patients	Mean survival	5 year survival rate%	95% confidence interval (95% CI)	P value
1- Total	97	6.70	72.16	6.00, 7.91	
Sex					
Male	69	7.16	79.71%	6.42, 7.91	0.02
Female	28	5.48	53.57%	4.10, 6.86	
Stage					
- 1	65	7.46	83.08%	6.76, 8.15	<0.0001
2	16	5.94	68.75%	3.94, 7.93	
3, 4	16	3.87	31.25%	2.04, 5.69	
Grade					
1	40	7.27	80.00%	6.31, 8.24	0.0001
2	39	7.19	76.92%	6.24, 8.15	
3, 4	18	3.60	44.44%	1.83, 5.36	
Age					
< 40	16	7.23	81.25%	5.78, 8.69	0.28
40-50	36	7.18	77.78%	6.13, 8.22	

50-60	26	6.54	69.23%	5.23, 7.86	
> 60	19	5.02	57.89%	3.43, 6.60	
Type					
Conventional	42	6.41	69.05%	5.34, 7.48	0.65
Papillary and unclassified	36	6.60	72.22%	5.45, 7.74	
Chromophobe	19	7.23	78.95%	5.83, 8.63	
Lymph node status					
Positive	25	5.80	56.00%	4.31, 7.28	0.04
Negative	72	7.00	77.78%	6.24, 7.75	
Tumour size					
> 7 cm	65	5.95	63.08%	5.04, 6.87	0.004
≤ 7 cm	32	8.03	90.63%	7.25, 8.81	
MVD					
< 20	49	7.12	77.55%	6.21, 8.03	0.157
20-30	37	5.91	62.16%	4.69, 7.12	
> 30	11	7.40	81.82%	5.71, 9.09	

Table (6): Results of the proportional hazard analysis (Cox's regression) of disease free survival in RCC

Characteristics	Regression	Standard error	Relative risk (95% CI) Exp (B) (lower, upper)	P value
Grade				0.0515
G1				
G2	-0.4088	0.5092	0.6645 (0.2449, 1.8024)	0.4220
G3,4	0.7612	0.5272	2.1409 (0.7618, 6.0170)	0.1488
Stage				0.0232
S1				
S2	0.6935	0.5498	2.0007 (0.6811, 5.8767)	0.2071
S3,4	1.2752	0.4654	3.5794 (1.4377, 8.9115)	0.0061
Tumour size	1.2628	0.6530	3.5353 (0.9831, 12.7130)	0.0531

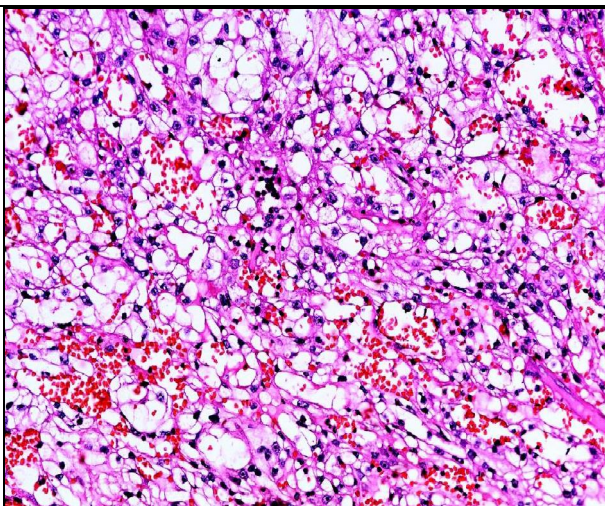


Fig. (1): Conventional type of renal cell carcinoma (RCC) (H&E X250).

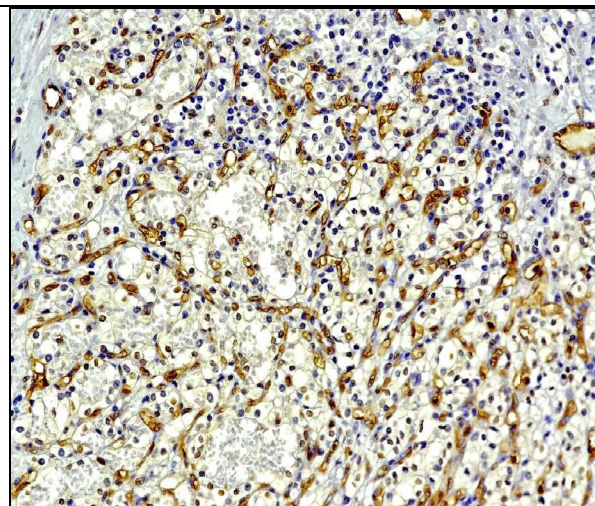


Fig. (2): Conventional renal cell carcinoma showing high vascularity stained with anti-CD34 monoclonal antibody using avidin-biotin immunoperoxidase technique (X250).

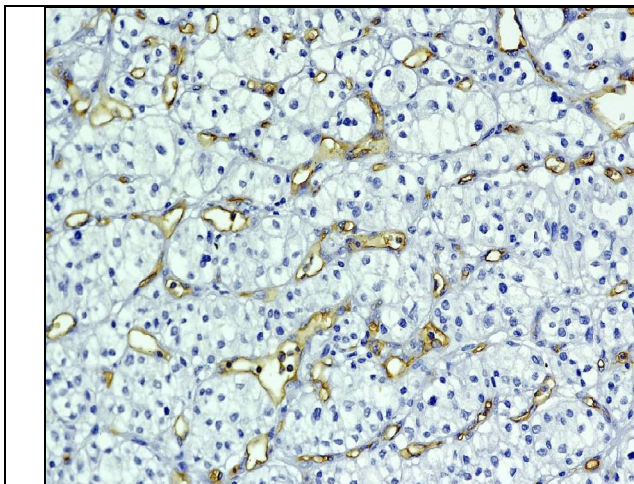


Fig. (3): Conventional renal cell carcinoma showing median vascularity stained with anti-CD34 monoclonal antibody using avidin-biotin immunoperoxidase technique (X250).

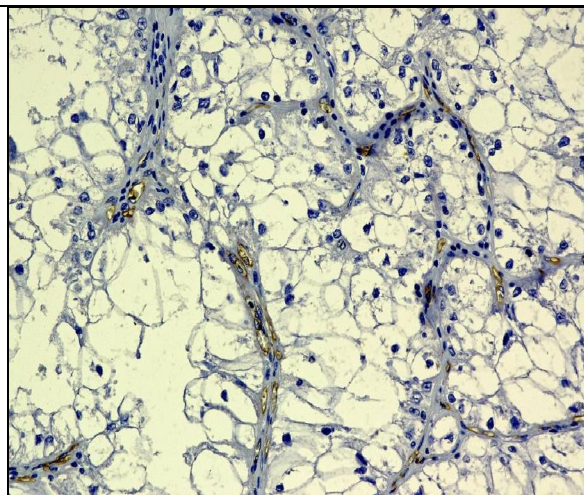


Fig. (4): Conventional renal cell carcinoma showing low vascularity stained with anti-CD34 monoclonal antibody using avidin-biotin immunoperoxidase technique (X250).

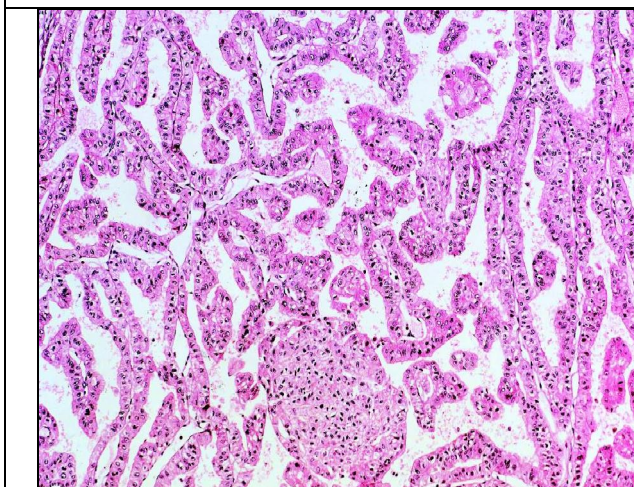


Fig. (5): Papillary type of RCC (H&E X100).

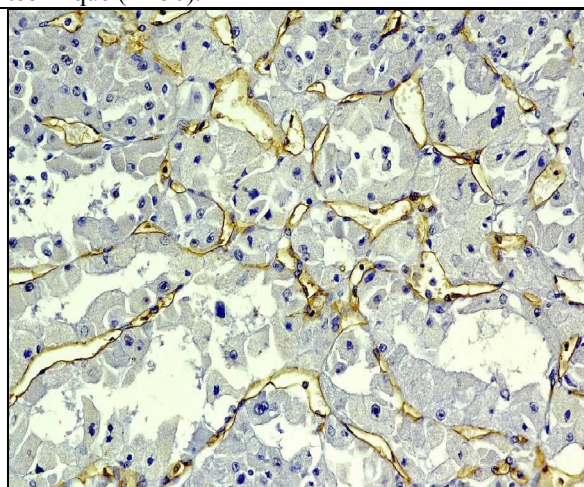


Fig. (6): Papillary renal cell carcinoma showing median vascularity stained with anti-CD34 monoclonal antibody using avidin-biotin immunoperoxidase technique (X250).

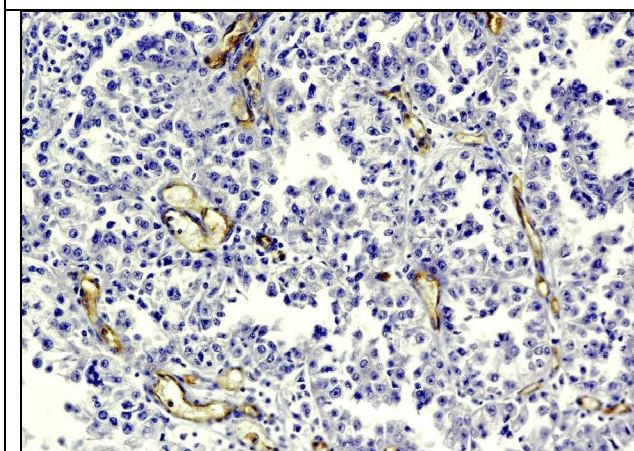


Fig. (7): Papillary renal cell carcinoma showing low

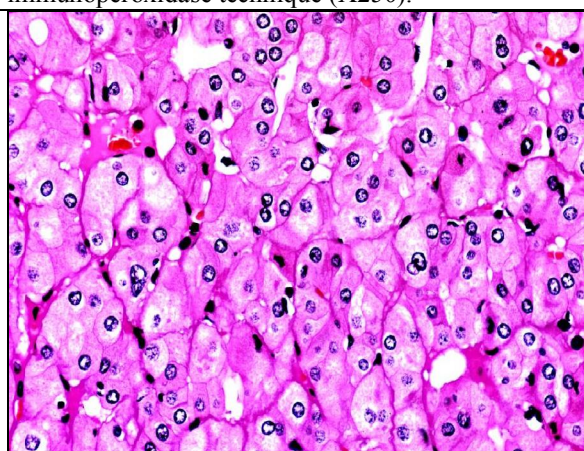


Fig. (8): Chromophobe type of RCC (H&E X250).

vascularity stained with anti-CD34 monoclonal antibody using avidin-biotin immunoperoxidase technique (X250).

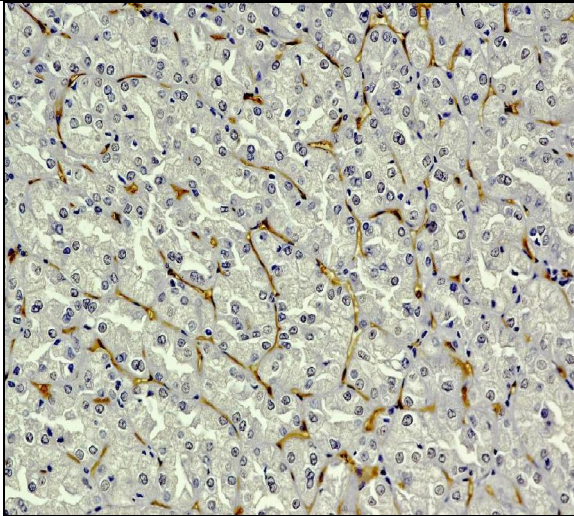


Fig. (9): Chromophobe renal cell carcinoma showing high vascularity stained with anti-CD34 monoclonal antibody using avidin-biotin immunoperoxidase technique (X250).

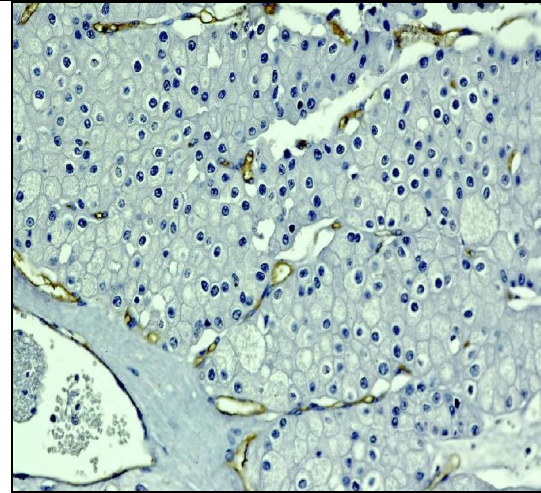


Fig. (10): Chromophobe renal cell carcinoma showing low vascularity stained with anti-CD34 monoclonal antibody using avidin-biotin immunoperoxidase technique (X250).

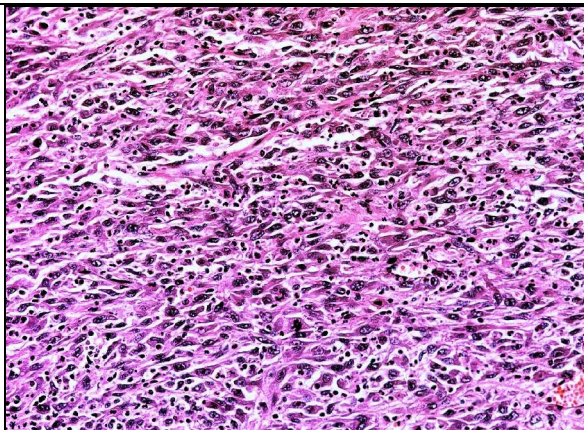


Fig. (11): Unclassified type of RCC (H&E X250).

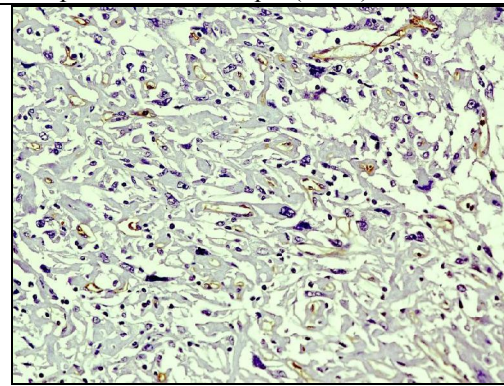


Fig. (12): Unclassified renal cell carcinoma showing median vascularity stained with anti-CD34 monoclonal antibody using avidin-biotin immunoperoxidase technique (X250).

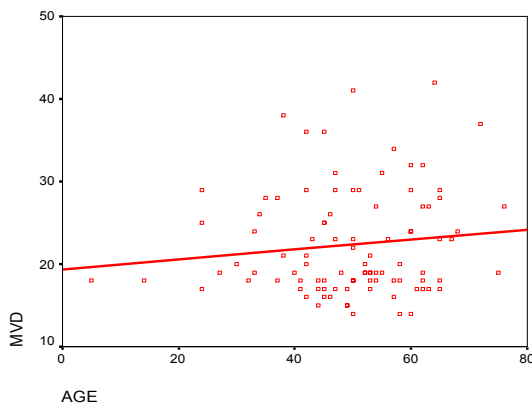


Fig. (13): Correlation between MVD and age. MVD (vessels/X 250 field)

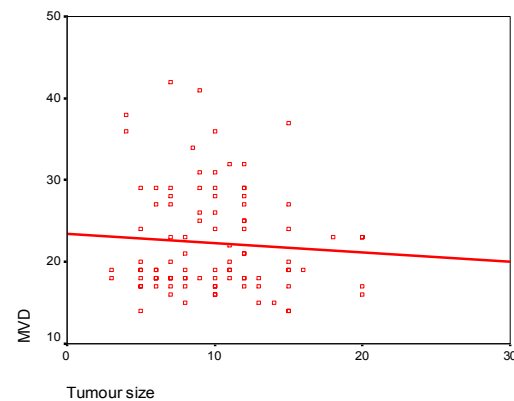


Fig. (14): Correlation between MVD and tumour size. MVD (vessels/ X 250 field)

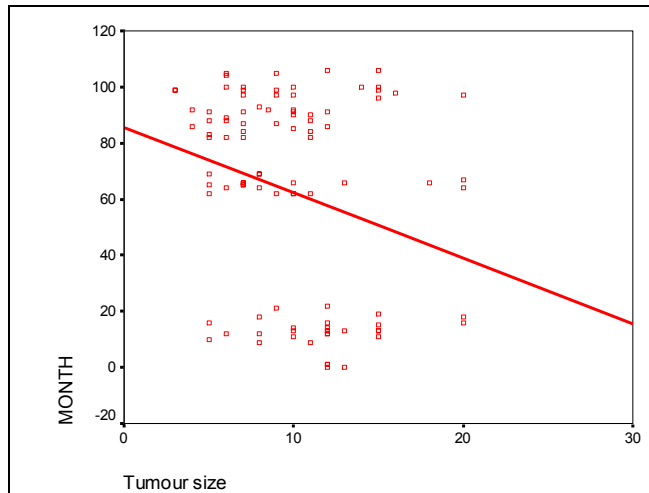


Fig. (15): Relation between tumour size and survival time

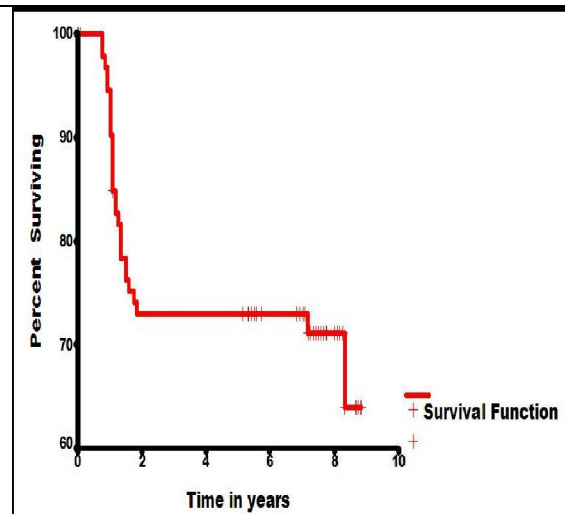


Fig. (16): The overall survival of 97 patients with RCC.

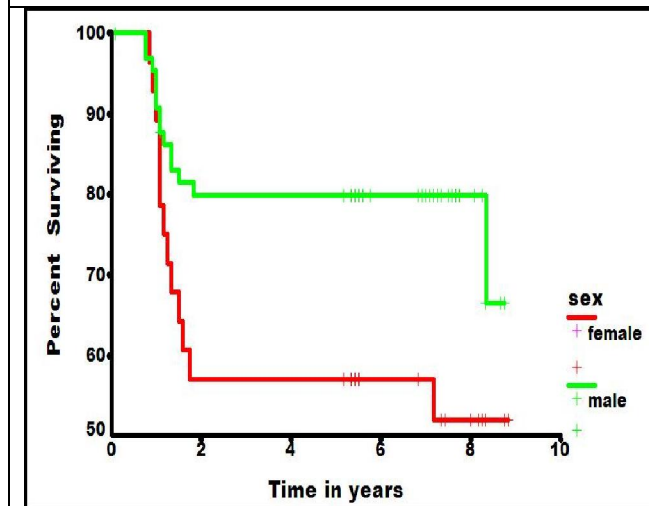


Fig. (17): Survival of 97 patients with RCC in relation to sex (P value=0.02).

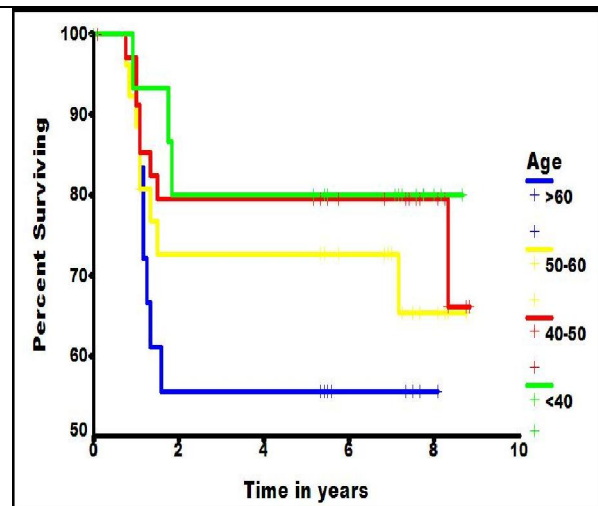


Fig. (18): Survival of 97 patients with RCC in relation to age (P value=0.28)

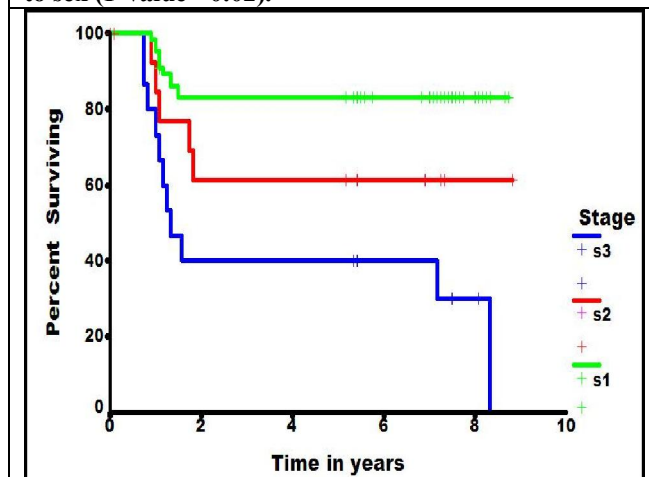


Fig. (19): Survival of 97 patients with RCC in relation to stage (P value=0.28)

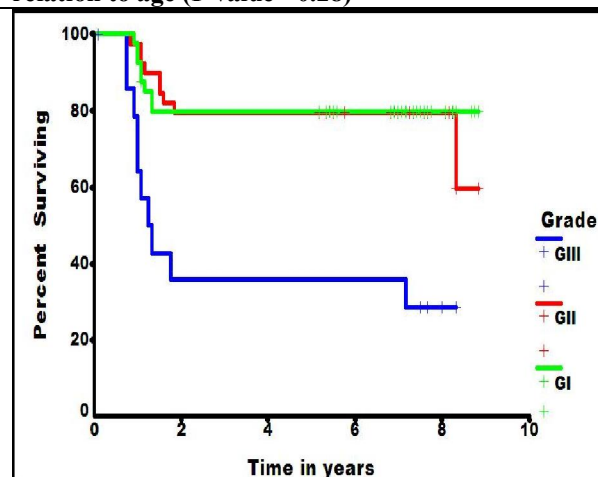


Fig. (20): Survival of 97 patients with RCC in relation to grade (P value=0.0001).

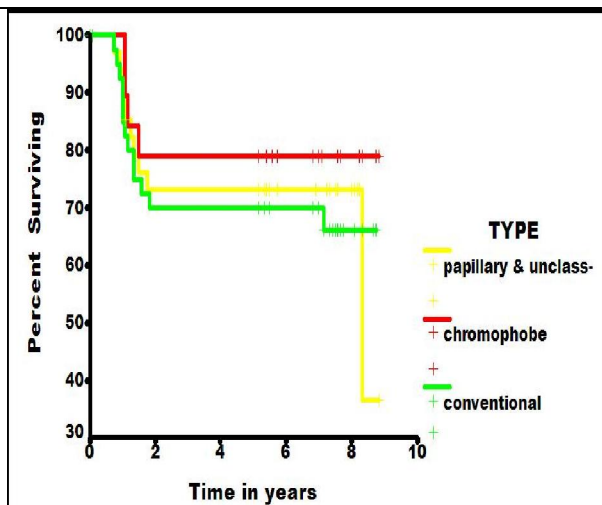


Fig. (21): Survival of 97 patients with RCC in relation to type (P value= 0.65).

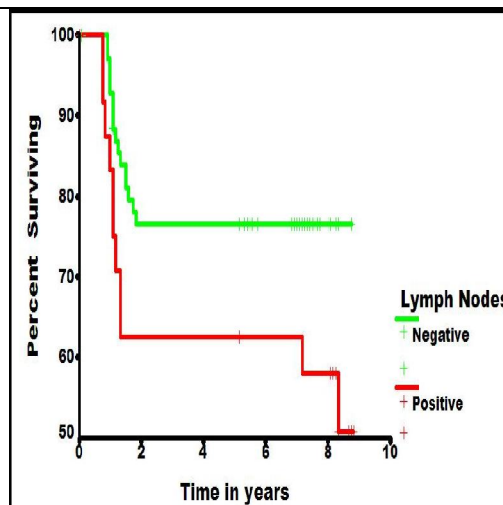


Fig. (22): Survival of 97 patients with RCC in relation to lymph node status (P value= 0.04).

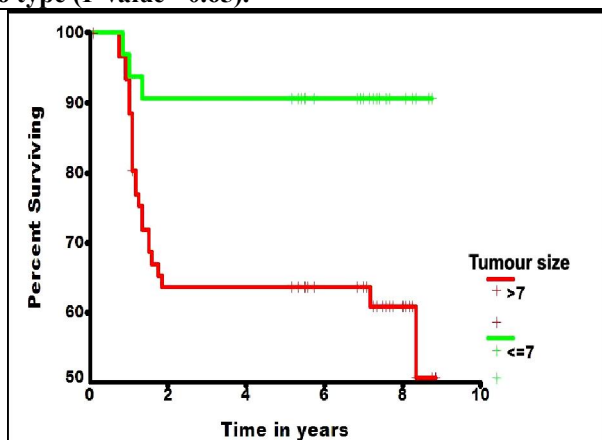


Fig. (23): Survival of 97 patients with RCC in relation to tumour size (P value= 0.004).

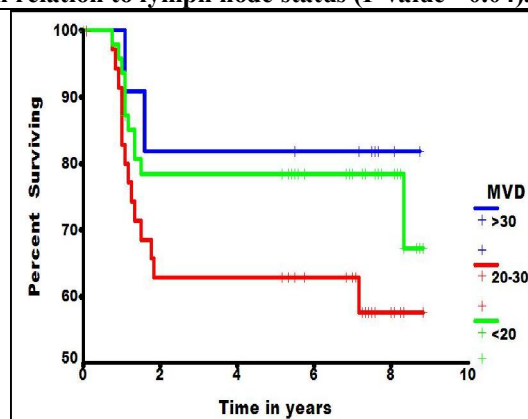


Fig. (24): Survival of 97 patients with RCC in relation to microvessel density (MVD) (P value= 0.157)

4. Discussion

In the present study, the male to female ratio is 2.46:1 which is nearly similar to most studies. The average age of the study group was 49.5 ± 12.57 years. In the west, mean age is higher, for example 65.3 years (Roosen *et al.*, 1994) and 65.1 years (Dekel *et al.*, 2002). The overall 5-year survival in 97 patients in this report is 72.16%, with a mean survival 6.70 years, while the overall 5 and 10-year survival rates for patients with RCC were rather similar among the different series and ranged from 50 to 70% and 30 to 50% respectively (Giuliani *et al.*, 1990; Sene *et al.*, 1992 and Giberti *et al.*, 1997). In the present retrospective study, we analyzed various parameters with the aid of univariate and multivariate analysis with survival rate to determine the most effector prognostic indicators.

The prognostic role of microvessel density as assessed by microscopy for renal cell carcinoma in our study is to determine the relationships between

microvessel density and other parameters such as age, stage, grade, type, sex, lymph node status and tumour size, and comparing our results with other results. Male to female ratio in our study was 2.46:1. This ratio differed in most studies but males number in most studies was higher than females number. In some studies, male to female ratio was high such as 4.6:1 (Suzuki *et al.*, 2001) and 4:1 (Kinouchi *et al.*, 2003), and in some other studies this ratio decreased such as 1.9:1 (Sabo *et al.*, 2001) and 1.5:1 (Dekel *et al.*, 2002).

Methods for the quantification of blood vessels in previous studies of angiogenesis have usually involved some element of subjectivity, mainly in the selection of the area of highest vascularity (hot spot area). Joo *et al.* (2004) found that, individual microvessels were counted in the area of highest vascularity at (X200) in three selected microscopic fields. Any brown staining endothelial cell or cluster that was separated from the other nearby

microvessels was counted. Large anastomosing sinusoidal vessels were counted as a single vessel. Large vessels with thick muscular walls were excluded from the count. The microvessel count was expressed as the mean number of vessels in the selected area. **Sabo et al. (2001)** found that the five most vascularized microscopic fields (hot spots) of the RCC tumours were selected for analysis using medium-sized magnifying lens (X100). (**Nativ et al., 1998**) found that, in all tumour sections, individual microvessels were counted in the area of highest vascularity at (X400) magnification of five randomly selected microscopic fields. In our study we counted microvessels using magnifying lens (X250) we compared our results with other results according to the relationships between MVD and other prognostic factors in RCC.

In the present study we found that there was no significance in the correlation between stage and MVD (P value=0.794). Similar results were previously reported (**Mac Lennan et al., 1995; Slaton et al., 2001 and Joo et al., 2004**). Other results found that there was a significant relationship between stage and MVD (**Sabo et al., 2001 and Kinouchi et al., 2003**). The 5-year survival rates of stages I, II, III and IV were 83.08%, 68.75% and 31.25% respectively in our study. The 5-year survival following nephrectomy in some studies was 60% to 80% in stage I, 40% to 70 % in stage II, 10% to 40% in stage III and 5 % or less in stage IV (**Sene et al., 1992 and Thrasher and Paulson, 1993**). These results are in agreement with our results.

Univariate analysis in our study identified tumour stage as a significant prognostic factor for cancer specific survival (P< 0.00001); Multivariate analyses indicated that T. stage was an independent prognostic factor. Similar results were reported in some other studies (**Miyata et al., 2003**). Some studies reported a significant relationship in univariate analyses but not in multivariate analyses (**Joo et al., 2004**).

In our study we found that, there was no significance (P value= 0.061) between grade and microvessel density. Similar results were previously reported (**Mac Lennan et al., 1995; Slaton et al., 2001 and Joo et al., 2004**). Some other studies found that, there was a significant relationship between grade and MVD (**Nativ et al., 1998 and Kinouchi et al., 2003**). **Sabo et al. (2001)** found that although MVD was higher in low-grade as opposed to high grade tumour, the difference was not statistically significant (P value = 0.12).

The 5-year survival rates for grades I, II, III and IV were 80.00%, 76.92% and 44.44% respectively in our results. **Medieros et al. (1997)** found that, the 5-year survival rates for grade 1 through 4 were 76%,

72%, 51% and 35% respectively, with significant differences observed between tumours of grade 1 and 2 and those of grades 3 and 4 in survival rates.

In our results we found that, there was significant differences between tumours of grades 1 and 2 and those of grades 3 and 4 in survival rates (P value= 0.0001) in univariate analyses. Multivariate analyses identified tumour grade as a dependent prognostic factor. Similar results were reported in some other studies (**Miyata et al., 2003**). **Joo et al. (2004)** found that, there was no significance between grade and survival rates in both univariate and multivariate analysis.

Our results revealed that there was no significance in the correlation between MVD and tumour size (P value= 0.481). Similar results were previously reported (**Nativ et al., 1998 and Joo et al., 2004**). **Kinouchi et al. (2003)** found that there was a significant relationship between MVD and tumour size.

The 5-year survival rates for patients with tumour size ≤ 7 and > 7 were 90.63% and 63.08% respectively. **Giuliani et al. (1990)** reported 5-year survival rates of 84% for patients with tumour size less than 5 cm, 50% for tumours between 5 and 10 cm, and 0% for tumours more than 10 cm in diameter. Such tumours have been associated with more than 90% 5-year survival rates, whether they are managed with nephron-sparing surgery or radical nephrectomy (**Butler et al., 1994 and Lerner et al., 1996**).

In our study we found that, there was significant differences between tumours ≤ 7 and > 7 in 5-year survival rates (P value= 0.004) in the univariate analysis. Multivariate analysis indicated that tumour size was a dependent factor (P value = 0.0531). Similar results were reported in some other studies, **Joo et al. (2004)** found that, there was significantly differences between tumour size groups in survival rates by univariate analyses (P value= 0.0105), but multivariate analyses indicated that tumour size was a dependent factor (P value = 0.415). **Roosen et al. (1994)** found that, there was insignificant differences in tumour size groups in univariate analyses (P value = 0.65), and identifies tumour size as a dependent factor in multivariate analyses (P value=0.97).

In our study we found that, there was insignificant relationship between sex and microvessel density (MVD) (P value=0.997). Similar results were previously reported by **Nativ et al. (1998)** who found that, there was no significant relationship between MVD and sex.

The 5-year survival rates for males and females were 79.71% and 53.57% respectively in our study. There was significantly differences between males and females using univariate analyses (P value=

0.0243) when multivariate analyses was performed, the survival difference between males and females disappeared.

In Western, studies have contested and supported the adverse impact of male gender in patients with RCC. **Ljungbery et al. (1988)** and **Green et al. (1989)** found no significant difference in survival between 81 men and 55 women with RCC. **Lieber and associates (1981)** reported that men had poorer survival rate than women. Many investigations found that, there was an insignificant relationship between sex and survival using univariate analyses and sex was identified as dependent factor using multivariate analyses (**Roosen et al., 1994** and **Suzuki et al., 2001**). **Lieber and associates (1981)** found that, there was significant differences between males and females using univariate analyses, but when multivariate analyses were performed, the survival difference disappeared.

Many investigations have evaluated the prognostic value of age of the patients with RCC. Our results indicated that, there was no significance relationship between age and MVD (P value =0.254). Although increasing in age increased MVD as shown in the results, this relationship was statistically insignificant. Similar results were noted between angiogenesis and age by **Nativ et al. (1998)**.

The 5-year survival rates for age < 40, between 40 and 50, between 50 and 60 and > 60 are 81.25%, 77.78%, 69.23% and 57.89% respectively. Univariate analyses indicated that there were no significant differences between age groups (P value=0.2828). Similar results were obtained using univariate and multivariate analysis (**Roosen et al., 1994**). Opposite results reported that, differences between age groups were significant using univariate analysis (P value =0.019), but when multivariate analyses was performed significantly differences between age groups disappeared and age became a dependent factor (**Suzuki et al., 2001**). **Dehner et al. (1970)** reported 64.3% year actuarial survival rate for 15 children treated with nephrectomy. **Lieber et al. (1981)** found no significant differences in survival according to age at diagnosis. The overall 3-year survival, 5-year survival and 10-year survival were 60%, 55% and 47% respectively.

The present study indicated that, there was a significant relationship between lymph node status and MVD (P value= 0.03). Similar results were reported by **Dekel et al. (2002)** and **Joo et al. (2004)**. Opposite results were obtained by **Slaton et al. (2001)** who found that, there was no significant differences between the two groups of lymph node status in microvessel density. The 5-year survival rates for positive and negative lymph nodes were 56% and 77.78% respectively, this difference was

significant using univariate analyses (P value= 0.04), but multivariate analyses indicated that lymph node status was a dependent factor. Lymph node involvement had long been recognized as a dire prognostic sign as it is associated with 5-year and 10-year survival rates of 5% to 30% and 0% to 5% respectively (**Bassil et al., 1985**). **Gusliani and associates (1990)** reported 52% 5-year survival for 25 patients with nodal positive disease managed with radical nephrectomy and extensive lymph node dissection which was better than historical controls. Other studies suggested improved survival in patients with pathologic stage NO disease managed with lymph dissection (**Golimbu et al., 1986** and **Herrlinger et al., 1991**).

The present study indicated that, there was a significant correlation between the histological type and microvessel density (P value= 0.001). There was significant differences between conventional type and both of papillary and chromophobe types. The mean microvessel count in conventional type was higher than that in both papillary and chromophobe types. **Mac Lennan and Bostwick (1995)** found that, there was a positive correlation of clear cell pattern and chromophobe pattern with increased MVD (P value= 0.047). **Kinouchi and his associates (2003)** found that, there was a significant correlation between type and MVD (P value= 0.009). The clear type was significantly higher than non clear type in the mean microvessel density. **Nativ et al. (1998)** found that, there was no significance between angiogenesis and cell type or histologic architecture. The 5-year survival rates for conventional type, chromophobe type and papillary and unclassified types were 69.05%, 78.95% and 72.2% respectively. There were no significant differences between all types in survival rates using univariate analyses (P value = 0.6539). **Dekel et al. (2002)** found that, the vessel count in papillary type was lower than in other histologic types. **Giuliani et al. (1990)** found that, there was not any statistical differences in survival between different types. **Suzuki et al. (2001)** found that, the correlation between survival and histologic examination was unclear.

The value of MVD as a predictor for patient prognosis in RCC is controversial because certain reports revealed a direct correlation between MVD and survival. Others revealed an inverse correlation and one report showed no correlation (**Sabo et al., 2001**). The 5-year survival rates for patients with low MVD < 20, median (20-30) and high > 30 were 77.55%, 62.16 and 81.82% respectively in our study. The differences between groups were insignificant using univariate analyses (P value= 0.1571).

Regarding prognosis and angiogenesis in RCC, reports showed that MVD is an independent

prognostic factor, MVD is a risk factor for distant metastasis (Suzuki *et al.*, 2001). They found that there was no correlation between angiogenesis and survival (P value= 0.112). Similar studies classified MVD into few, moderate and large amounts like our study and found no correlation between MVD and survival using univariate and multivariate analysis (Roosen *et al.*, 1994). Nativ *et al.* (1998) found that, there was a significant relationship between MVD and survival in univariate analysis (P value=0.041) and in multivariate analysis. For patient survival they found that the only significant and independent predictors were MVD (P value= 0.00014). The 10-year survival rate for patients with low and high microvessel count was 91% and 46% respectively.

References

- BASSIL, B.A., DOSORETZ, D.E. AND PROUT, G.R. (1985): Validation of the tumour, nodes, and metastasis classification of renal cell carcinoma. *J. Urol.*, 134: 450-454.
- BUTLER, B.P., NOVICK, A.C., MILLER, D.P., *et al.* (1994): Management of small unilateral renal cell carcinomas: radical versus nephron-sparing surgery. *Urology*, 45: 34-41.
- COX, D.R. (1972): Regression models and life tables. *J. Roy. Stat. Soc. Ser. B.*, 34: 187-220.
- DEHNER, L.P., LEESTMA, J.E. AND PRICE, E.B. (1970): Renal cell carcinoma in children: A clinicopathologic study of 15 cases and review of the literature (abstract). *J. Pediatr.*, 76:358.
- DEKEL, Y., KOREN, R., KUGEL, V., LIVINE, P.M. AND GAL, R. (2002): Significance of angiogenesis and microvascular invasion in renal cell carcinoma. *Path. Oncol. Res.*, 8: 129-130.
- DICKINSON, A.J., FOX, S.B., PERSAD, R.A., HOLLYER, J., SIBLEY, G.N.A. AND HARRIS, A.L. (1994): Quantification of angiogenesis as an independent predictor of prognosis in invasive bladder carcinoma. *B. J. U.*, 74: 762-766.
- FUHRMAN, S.A., LASKY, L.C. AND LIMAS, C. (1982): Prognostic significance of morphologic parameters in renal cell carcinoma. *Am. J. Surg. Pathol.*, 6: 655-663.
- FUJIOKA, T., HASEGAWA, M., ISHIKURA, K., MATSUSHITA, Y., SATO, M. AND TANJI, S. (1998): Inhibition of tumour growth and angiogenesis by vitamin D3 agents in murine renal cell carcinoma. *J. Urology*, 160: 247-251.
- GIBERTI, C., ONETA, F., MARTORANA, G., ROVIDA, S. AND CARMIGNANI, G. (1997): Radical nephrectomy for renal cell carcinoma: Long term results and prognostic factors on a series of 328 cases. *Eur Urol.*, 31: 40-48.
- GIULIANI, L., GIBERTI, C., MARTORANA, G. AND ROVIDA, S. (1990): Radical extensive surgery of renal cell carcinoma: Long term results and prognostic factors. *J. Urol.*, 143: 468-474.
- GOLIMBU, M., TESSLER, A., AL-ASHARI, S., *et al.* (1986): Renal cell carcinoma. Survival and prognostic factors. *Urology*, 27: 291-301.
- GREEN, L.K., AYALA, A.G., RO, J.Y., SWANSON, D.A. AND GUINEE, V.H. (1989) Role of nuclear grading in stage I renal cell carcinoma. *Urology*, 34: 310-315.
- GUESDON, J.L., *et al.* (1979): The use of avidin-biotin interaction in immunoenzymatic techniques. *J. Histochem. Cytochem.*, 27: 1131-1139.
- GUINAN, P., SOBIN, L.H., ALGABA, F., *et al.* (1997): TNM staging of renal cell carcinoma: Workgroup no.3. Union Internationale Contre le Cancer and the American Joint Committee on Cancer. *Cancer*, 80: 992-993.
- HERRLINGER, A., SCHROTT, K.M., SCHOTT, G. AND SIGEL, A. (1991): What are the benefits of extended dissection of the regional renal lymph nodes in the therapy of renal cell carcinoma? *J. Urol.*, 146: 1224-1227.
- JAEGER, T.M., WEIDNER, N., CHEW, K., MOORE, D.H., KERSCHMANN, R.L., WALDMAN, F.M. AND CARROLL, P.R. (1995): Tumour angiogenesis correlate with lymph node metastasis in invasive bladder cancer. *J. Urol.*, 154: 69-71.
- JONES, A. AND FUJIMAMA, C. (1999): Angiogenesis in urological malignancy: Prognostic indicator and therapeutic target. *B.J.U. International*, 83: 535-556.
- JOO, H.J., OH, D.K., KIM, Y.S., LEE, K.B. AND KIM S.J. (2004): Increased expression of caveolin-1 and microvessel density correlates with metastasis and poor prognosis in clear cell renal cell carcinoma. *B.J.U. International*, 93: 291-296.
- KAPLAN, E.L. AND MEIER, P. (1958): Nonparametric estimation from incomplete observations. *J. Am. Stat. Ass.*, 53: 457-481.
- KINOUCI, T., MANO, M., MATSOUKA, I., *et al.* (2003): Immature tumour angiogenesis in high grade and high stage renal cell carcinoma. *Urology*, 62: 765-770.
- Kok, L. and Boon, M. (1995): Microwave cookbook for microscopists: Art and Koleske A J, Baltimore D and Lisanti M B: Reduction of caveolin and caveolae in oncogenically transformed cells. *Proc. Natl. Acad. Sci. USA*, 92: 1381-1385.
- LERNER, S.E., HAWKINS, C.A., BLUTE, M.L., *et al.* (1996): Disease outcome in patients with low stage renal cell carcinoma treated with nephron sparing or radical surgery. *J. Urol.*, 155: 1868-1873.
- LIEBER, M., TOMERA, F., TAYLOR, W. AND FARROW, G. (1981): Renal adenocarcinoma in young adults: Survival and variables affecting prognosis (abstract). *J. Urol.*, 125:146.
- LJUNGBERY, B., DACHEK, M., HIETALA, S., *et al.* (1988): Renal cell carcinoma in a solitary kidney: Late nephrectomy after 35 year and analysis of tumour DNA content. *J. Urol.*, 139:350-352.
- MAC LENNAN, G.T. AND BOSTWICK, D.G. (1995): Microvessel density in renal cell carcinoma: Lack of significance. *Urology*, 46: 27-30.
- MEDEIROS, L.J., JONES, E.C., AIZAWA, S., *et al.* (1997): Grading of renal cell carcinoma: Workgroup no.2 Union Internationale Contre le Cancer and the American Joint Committee on Cancer. *Cancer*, 80: 990-991.
- MIYATA, Y., KOGA, S., TAKEHARA, K., *et al.* (2003): Expression of thrombospondin- derived 4N1K peptide, containing proteins in renal cell carcinoma tissues is associated with a decrease in tumour growth and angiogenesis. *Clin. Cancer Res.*, 9: 1734-1740.
- NATIV, O., SABO, E., REISS, A., WALD, M., MADJAR, S. AND MOSKOVITZ, B. (1998): Clinical significance of tumour angiogenesis in patients with localized renal cell carcinoma. *Urology*, 51: 693-696.
- ROOSEN, J.U., ENGEL, U., JENSEN, R.H., KVIST, E. AND SCHOU, G (1994): Renal cell carcinoma: Prognostic factors. *B. J. U.*, 74: 160-164.
- SABO, E., BOLTENKO, A., SOVA, Y., STEIN, A., KLEINHAUS, S. AND RESNICK, M.B. (2001): Microscopic analysis and significance of vascular architectural complexity in renal cell carcinoma. *Clin Cancr Res.*, 7: 533-537.
- SENE, A.P., HUNT, L., MC MAHON, R.F.T. AND CARROLL, R.N.P. (1992): Renal carcinoma in patients undergoing nephrectomy. Analysis of survival and prognostic factors. *B.J.U.*, 70: 125-134.
- SLATON, J., INOUE, K., PERROTTE, P., EL-NAGGAR, A., SWANSON, D.A., *et al.* (2001): Expression levels of genes that regulate metastasis and angiogenesis correlate with advanced pathological stage of renal cell carcinoma. *Amer. J. Path.*, 58: 735-743.
- STASSAR, M., DEVITT, G., BROSIUS, M., RINNAB, L., *et al.* (2001): Identification of human renal cell carcinoma associated genes by suppression subtractive hybridization. *B. J. Cancer*, 85: 1372-1382.
- SUZUKI, K., MORITA, T., HASHIMOTO, S. AND TOKUE, A. (2001): Thymidine phosphorylase/ platelet- derived endothelial cell growth factor (PD- ECGF) associated with prognosis in renal cell carcinoma. *Urol. Res.*, 29: 7-12.
- THRASHER, J.B. AND PAULSON, D.F. (1993): Prognostic factors in renal cancer. *Urol. Clin. North Am.*, 20:247-262.

11/22/2011

Construction of a HSV-1 strain HF Based Replication Defective Vector with LR-Recombination Sites

Qingzhi Wang, Bo Song, Xinjing Liu, Zhiqiang Han, Jiameng Lu, Ting Yang, Chenyang Jiang, Xiaolu Zhang, Chandra Avinash, Shilei Sun, Yuming Xu*

Department of Neurology, the First Affiliated Hospital of Zhengzhou University, Zhengzhou, Henan 450052, China

Corresponding author: Yuming Xu, yumingxu@zzu.edu.cn; Co-first author: Bo Song, songbo76@sina.com;

Co-corresponding author: Shilei Sun, sunshilei@hotmail.com

Abstract: In this study, we incorporated the lambda phage based specific recombination sites attR into HSV-1 replication-defective vector by using Red recombineering, and constructed the HSV-1 replication-defective vector BAC-HSV1-HF- Δ ICP27-attR-GK. In addition, a red fluorescence reporter gene DsRed was introduced to the vector to construct the BAC-HSV1-HF- Δ ICP27-attB-DsRed by LR recombination approach. To conduct research on the expression of exogenous gene integrated to the vector, the plasmid BAC-HSV1-HF- Δ ICP27-attB-DsRed was transfected to the 2-2 Vero cells, 72hr later, CPE and the red fluorescence protein were observed. These results indicated that we successfully constructed HSV-1 replication-defective vector BAC-HSV1-HF- Δ ICP27-attR-GK which carrying LR recombination specific sites attR, and the vector can incorporate exogenous gene by a one-step LR recombination in vitro. This method simplified the procedure of site-directed integration of exogenous gene into HSV-1 replication-defective vectors, and greatly facilitated the research of HSV-1 derived vectors for gene therapy. [Qingzhi Wang, Bo Song, Xinjing Liu, Zhiqiang Han, Jiameng Lu, Ting Yang, Chenyang Jiang, Xiaolu Zhang, Chandra Avinash, Shilei Sun, Yuming Xu. **Construction of a HSV-1 strain HF Based Replication Defective Vector with LR-Recombination Sites**. Life Science Journal, 2011; 8(4):852-857] (ISSN: 1097-8135). <http://www.lifesciencesite.com>.

Keywords: HSV-1, Red recombineering, LR recombination, replication defective vectors, site-directed integration

Introduction

Herpes simplex virus type 1 (HSV-1) is an enveloped, double-strand (ds) DNA virus, could cause serious infection diseases in humans, including infection of skin, mucous membranes and nervous system, is an important human pathogen^[1-2]. Due to its features, such as natural cell tropism, lowly immunogenicity and inability of integration of genome to host chromosomes, HSV-1 derived vectors have been exploited^[3-4]. HSV-1 Replication-defective vectors^[5-6] are kind of mutant virus with deletions in one or more genes essential for the lytic cycle, such as ICP4 and ICP27, these defective virus could be packaged in the complementary cell lines. With a neurotropic property and the ability of establishing latent infection, replication-defective vectors could steadily and long-termly express the exogenous gene in neurons, have become a good candidate for gene therapy^[5-6]. However, because of the huge genome of HSV-1, It's still a question of how to integrate the target gene into replication-defective HSV-1 vectors simply and rapidly.

Typical methods to clone exogenous gene into replication-defective HSV-1 vectors are mainly based on homologous recombination in eukaryocyte, owing to its disadvantages such as multiple manipulation, difficulties in screening recombinant clones, it's not suitable for simple and rapid cloning of target genes. The appearance of recombineering technology^[7-8] and

development of bacteria artificial chromosome (BAC) technology^[9-11] greatly facilitated the research of HSV-1 genome function and HSV-1 derived vectors, and the target gene can be integrated into replicate-defective HSV-1 vectors simply by the recombineering technology in *Escherichia coli*. Although this system simplified the procedure of target mutagenesis HSV-1, it still needs to accomplish recombination with the help of recombinase in *Escherichia coli*, which has low efficacy and long screening cycle. How to integrate target gene into HSV-1 derived vectors simply and rapidly in vitro has become a new research area for us.

LR recombination system^[12] is a kind of site-specific recombination system based on λ phage, which contains two starting DNAs: an entry clone (attL1-gene-attL2), and a destination vector (attR1-cm-ccdB-attR2). The target DNA fragment flanked by attL in the entry clone could exchange with the DNA fragment between the attR sites in the destination vector with the action of LR recombinase. There hasn't been a report about LR recombination system applied in integrating exogenous DNA fragment into replication-defective HSV-1 vectors so far yet.

We previously^[13] constructed the HSV-1 replication-defective vector BAC-HSV1-HF- Δ ICP27 with Red recombineering technology successfully. In this study, we incorporate the attR recombination sites based on λ phage to the BAC-HSV1-HF- Δ ICP27 vector to construct a replication-defective HSV-1

vector BAC-HSV1-HF- Δ ICP27-attR-GK. In addition, we cloned the red fluorescence reporter gene DsRed into BAC-HSV1-HF- Δ ICP27-attR-GK by the one-step LR recombination in vitro. In this paper we provide a new approach for site-directed integration of exogenous gene into replication-defective HSV-1 vectors.

Materials

Cells: African green monkey kidney (Vero) cells were purchased from Shanghai Institute of Biochemistry and Cell Biology, Chinese Academy of Sciences. The 2-2 cell line was kindly provided by Dr Jia laboratory in The Prostate Centre at Vancouver General Hospital, Vancouver, British Columbia, Canada. All cells were grown in Dulbecco's Modified Eagle Medium (DMEM), supplement with 10% fetal calf serum in humidified 37°C, 5% CO₂ incubator.

Plasmid and bacteria: The plasmid pYD-C255, a GalK-kan (galactokinase-kanamycin) dual-expression cassette and a recombineering *E. coli* strain SW105 were gifted by Dr YU, Washington University in St.Louis. The DH10B electroporation competent cells were conserved by our laboratory. The plasmid BAC-HSV1-HF- Δ ICP27 was constructed by our laboratory as described previously^[13], which is able to produce infectious viral particle when transfected into 2-2 complement cell lines. The plasmid pGM-T was purchased from TIANGEN. The plasmid pAd/BLOCK-iTTM-DEST (DEST), pENTRTM/U6 and a *E. coli* strain *E. coli* DB3.1 cells were purchased from Invitrogen. The plasmid pDsRed2-C1 was purchased from Clontech.

Enzyme and primers: All the restriction enzyme were purchased from Takara. All the primers were synthesized by Sangon Biotech.

Methods

1 Construction of BAC-HSV1-HF- Δ ICP27-attR-GK replication-defective vector by Red recombineering

1.1 Procure of recombinant UL47-UL48 homology arms

To construct pGM-T-UL47-UL48 vector, UL47-UL48 homology arms were amplified by PCR using the follow primers: P1: 5'-GACGCGGCCGCGGTAGTCGTCCTCCTCGTA-3' and P2: 5'-CGGAGCTAAACCACATTCGCGAGCACC-3', and HSV-1 HF virus genome DNA as the template. The 1.5 kb PCR products were cloned to pGM-T vector via TA cloning method.

1.2 Procure of LR recombination specific sites attR

The vector pGM-T-attR1-cm-ccdB-attR2 is a derivative of pGM-T, modified by the insertion of a

gene cassette containing attR recombination sites acquired from DEST into the multiple cloning region of the pGM-T. To achieve that, pGM-T was digested with Sall and NotI, and treated with calf intestinal phosphatase (CIP). The plasmid DEST was digested with NheI and SphI to obtain a 1.9kb fragment harboring attR1-cm-ccdB-attR2. The T4 DNA polymerase-blunted fragment was ligated into the linear pGM-T, and transformed into *E. coli* DB3.1 cells.

1.3 Procure of Red recombination selection gene GalK-kan

GalK-kan cassette was amplified by PCR using the P3: 5'-CCTGTTGACAATTAATCATCG-3' and P4: 5'-CTCAGCAAAAGTTCGATTTA-3' as primers, and pYD-C255 plasmid as the template. The PCR products were digested with DpnI and then the 2.3kb PCR products GalK-kan cassette was inserted to the BamHI/PstI sites of pGM-T-attR1-cm-ccdB-attR2 vector by blunt end, with the cm-ccdB DNA sequence deleted.

1.4 Construction of pGM-T-UL47-attR-GK-UL48 vector

The vector pGM-T-UL47-attR-GK-UL48 is a derivative of pGM-T-UL47-UL48, modified by the insertion of a DNA fragment attR1-GalK-kan-attR2. To achieve that, a 2.8kb fragment harboring attR1-GalK-kan-attR2 was acquired by the NcoI/SacI digestion of plasmid pGM-T-attR1-GK-attR2, and then cloned to the BstBI site of pGM-T-UL47-UL48 by blunt end.

1.5 Procure of Red recombination fragment UL47-attR-GK-UL48

The 3.6kb UL47-attR-GK-UL48 DNA fragment was obtained through digesting pGM-T-UL47-attR-GK-UL48 vector with KpnI, SacI and XmnI respectively.

1.6 Transduction of UL47-attR-GK-UL48 DNA fragment into BAC-HSV1-HF- Δ ICP27 recombineering bacteria and identification of recombinant colonies

As shown in Figure 1, to induce a homology recombination, electrocompetent SW105 bacteria harboring BAC-HSV1-HF- Δ ICP27 was electroporated with UL47-attR-GK-UL48 DNA fragment, after 5 hr resuscitation in the LB, the recombinant bacteria was applied on a MacConkey + cm⁺ + kana⁺ plate over night at 31°C in a cabinet-type incubator. After incubation, four red colonies were picked and identified by PCR with two pairs of primers, UL47-F/GalK-R: CCTGAATGGTGTGAGTGG/GACATGGTGGCGATAGA and Kan-F/UL48-R: CACGAGCACATACATTACAA/GTTGGACGAGTCGGAATC.

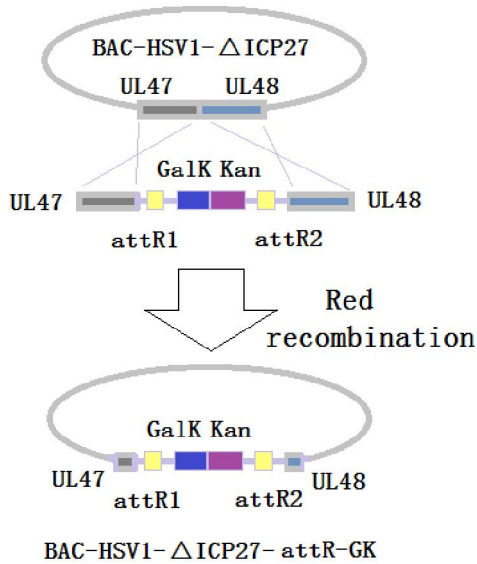


Fig.1. Outline of Red recombination

2 Functional analysis of BAC-HSV1-HF-ΔICP27-attR-GK replication-defective vector

2.1 Construction of BAC-HSV1-HF-ΔICP27-attB-DsRed by LR recombination technique

1) Procure of reporter gene DsRed

To introduce the reporter gene to the entry vector pENTR™/U6 with attL sites, a 1.5kb reporter gene DsRed cassette was obtained by AseI/MluI digestion of plasmid pDsRed2-C1 and then cloned to the SmaI site of pENTR™/U6 by blunt end to produce a new entry vector pENTR-attL1-DsRed-attL2 with DsRed reporter gene.

2) LR recombination integrate reporter gene to BAC-HSV1-HF-ΔICP27-attR-GK and identification of recombinant clones

As shown in Figure 2, plasmids pENTR-attL1-DsRed-attL2 and BAC-HSV1-HF-ΔICP27-attR-GK were incubated at 25°C with the help of LR recombinase for 5 hr, followed by being digested with protease K for 10min, the LR recombination system was electroporated into DH10B competent cells, and the recombinant bacteria was applied on Cm⁺ LB plate over night at 37°C in a cabinet-type incubator. After incubation, some recombinant colonies were picked and streaked onto a Kana⁺ LB plate and a Cm⁺ LB plate respectively for another 24hr, four colonies which could grow on Cm⁺ but not Kana⁺ LB palte were picked and identified by PCR with primers DsRed-F/DsRed-R: CGGCTGCTTCATCTACAA/ACCACCTGTTCTGA GA T.

2.2 Functional analysis of testing infective

BAC-HSV1-HF-ΔICP27-attB-DsRed vector virus generation and reporter gene expression in Vero and 2-2 cells

Vero cells and 2-2 cells (5.0×10⁵ cells/well) grown on the 6-well plate were respectively transfected with 2 μg of BAC-HSV1-HF-ΔICP27-attB-DsRed and BAC-HSV1-HF-ΔICP27-attR-GK plasmid DNA using lipofectamin 2000 following the manufacturer's protocol. 72 hr later, observing the CPE and the expression of red fluorescence protein under the fluorescence microscope.

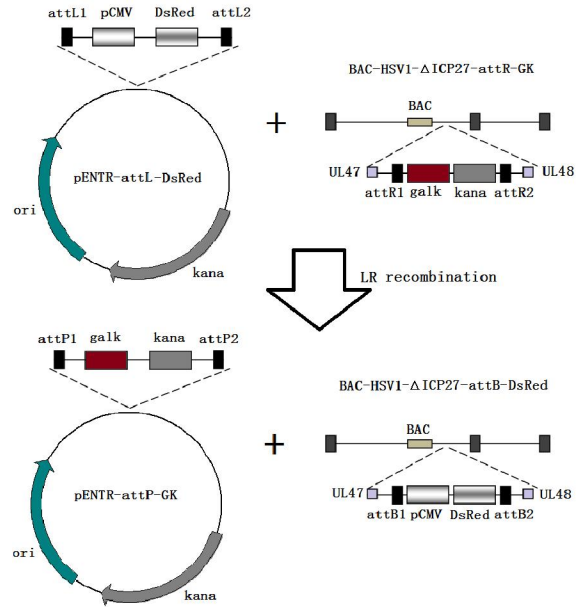


Fig.2. Outline of LR recombination

Results

1. Construction of BAC-HSV1-HF-ΔICP27-attR-GK replication-defective vector by Red recombineering

Through positive selection of the Red recombination in SW105 bacteria strain, we obtained the recombinant bacteria colonies, which were grown on MacConkey + Cm⁺ + Kan⁺ indicator plate. In Figure 3, recombinant bacteria colonies were shown in red color.

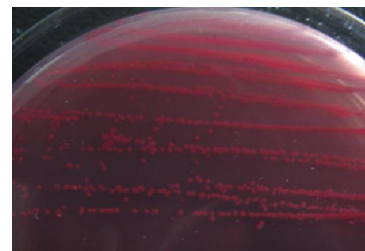


Fig.3. Recombinant bacteria colonies showing in red color on MacConKey + Cm⁺ + Kana⁺ indicator plate

PCR analysis of Galk-kan gene from the selected recombinant colonies showed the Galk-kan gene was integrated to BAC-HSV1-HF- Δ ICP27 genome at the right sites. As shown in Figure 4, agarose gel

electrophoresis showed the correct PCR products of Galk-kan gene with the primers of Kan-F/UL48-R in A1 and UL47-F/Galk-R in A2.

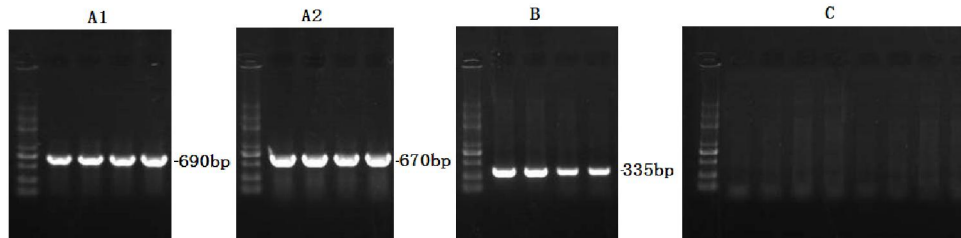


Fig.4. Agarose gel electrophoresis of PCR products

A1 primers: Kan-F/UL48-R; A2 primers: UL47-F/Galk-R;

B primers: DsRed-F/DsRed-R; C primers: Kan-F/UL48-R and UL47-F/Galk-R

2. Construction of BAC-HSV1-HF- Δ ICP27-attB-DsRed replication-defective vector by LR recombination

After LR recombination between pENTR-attL1-DsRed-attL2 and BAC-HSV1-HF- Δ ICP27-attR-GK, the recombination reaction was electroporated into DH10B competent cells, and the recombinant bacteria was applied on Cm⁺ LB plate over night at 37°C in a cabinet-type incubator. We obtained recombinant bacteria colonies, which could grow on Cm⁺ but not Kana⁺ LB plate were picked. PCR analysis of DsRed gene and the Galk-kan gene from the selected recombinant colonies showed the DsRed gene was inserted and Galk-kan gene was replaced from BAC-HSV1-HF- Δ ICP27-attR-GK genome. In Figure 4, agarose gel electrophoresis showed the correct PCR products of DsRed gene with the primers of DsRed-F/DsRed-R in B, Kan-F/UL48-R and UL47-F/Galk-R in C.

3. Functional identification of BAC-HSV1-HF- Δ ICP27-attB-DsRed replication-defective vector

As shown in Figure 6, after transfection of the Vero cells and 2-2 cells with BAC-HSV1-HF- Δ ICP27-attR-GK and BAC-HSV1-HF- Δ ICP27-attB-DsRed plasmid DNA, CPE was observed in 2-2 cells, but not in Vero cells; red fluorescence was observed in both Vero and 2-2 cells transfected with BAC-HSV1-HF- Δ ICP27-attB-DsRed plasmid DNA, but not the cells transfected with BAC-HSV1-HF- Δ ICP27-attR-GK plasmid DNA.

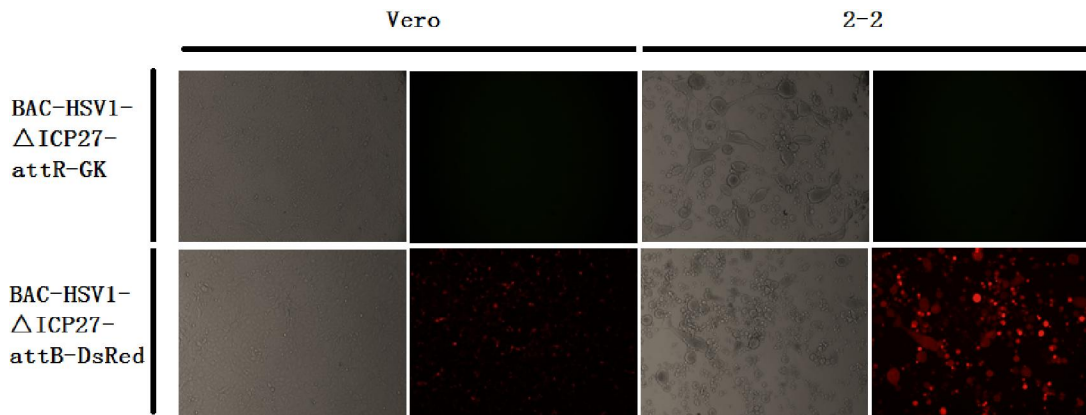


Fig.5. CPE and red fluorescence observation in Vero and 2-2 cells transfected with plasmids 72hr later(X 100)

Discussions

Insertion of exogenous DNA sequences into HSV-1 genome can be achieved in a number of ways. PHILIP J^[14] and coworkers utilized the cre-loxP site-specific recombination system based on P1 phage, and lacZ (Escherichia coli β -galactosidase) as reporter gene, successfully inserted exogenous DNA sequences into HSV genome in vitro. DM Krisky^[15] and coworkers used homologous recombination technology

and lacZ cassette flanked by PacI restriction recognition sites as the reporter gene, made any modification of HSV-1 genome to be possible. However, the two methods mentioned above still need to screen recombinant clones in eukaryotic cells, the procedure remained complex. The emergence of recombinering technology and development of BAC technology further simplified the process of targeting mutation of HSV-1 genome. Our previous study^[6]

successfully knockout the HSV-1 replication essential gene ICP27 from BAC-HSV1-HF plasmid and constructed the HSV-1 replication-defective vector BAC-HSV1-HF- Δ ICP27. However, the integration of exogenous genes still need to be carried out in *E. coli* with a two-step recombination and selection, the process remained complex.

In this study, we constructed HSV-1 replication-defective vector BAC-HSV1-HF- Δ ICP27-attR-GK by recombining the specific sites attR with selection gene galactokinase and kanamycin into the HSV-1 replication-defective vector BAC-HSV1-HF- Δ ICP27 through Red recombineering. As the integration site was between HSV-1 late gene UL47 and UL48, without deleting any gene, it will not affect the gene function. And then, to identify the function of HSV-1 replication-defective vector BAC-HSV1-HF- Δ ICP27-attR-GK, we integrated the reporter gene DsRed into BAC-HSV1-HF- Δ ICP27-attR-GK by a one-step LR recombination in vitro. After transfection 2-2 cells with plasmid DNA BAC-HSV1-HF- Δ ICP27-attB-DsRed, infectious virus particle was generated, and red fluorescence protein was expressed. These results indicated that the method of using LR recombination to integrate exogenous gene into HSV-1 replication-defective vector was feasible.

The advantages of BAC-HSV1-HF- Δ ICP27-attR-GK are: (i) The target genes can be site-directed integrated into HSV-1 replication-defective vector with only one-step recombination in vitro; (ii) Any DNA fragment flanked by specific sites attL can be integrated into HSV-1 replication-defective vector rapidly and efficiently, and it is promising in gene therapy research; (iii) This method can be applied to the studies of other viral related vectors and gene function in theory.

The establishment of this method further simplifies the procedure of integration of target gene into HSV-1 related vectors; it is a good candidate for research of target gene therapy and viral gene function. In addition, this method will play a great role in the development of commercial viral vectors in view of its features such as highly efficiency, site-directed integration and recombination in vitro. Although this study provides a new idea for construction of HSV-1 and other viral vectors, it still has some shortages, such as integration of the target gene can only be inserted to the sites between attR1 and attR2. We believe that with the development of recombineering technology, target modification of the virus genome will become increasingly simple, and further facilitate the development of HSV-1 and other virus related vectors in gene therapy.

Conclusion

We constructed a HSV-1 HF derived replication-defective vector carrying the lambda phage based specific recombination sites attR. Through using this vector, site-directed integration of exogenous gene could be achieved by a simple one-step LR recombination in vitro. It simplified the procedure to integrate exogenous gene into HSV-1 replication-defective vector.

Corresponding author:

Dr. Yuming Xu, yumingxu@zzu.edu.cn. Mailing address: 1 East jianshe Road, Zhengzhou, Henan province, 450052, China

References

1. Watanabe D. Medical application of herpes simplex virus. *J Dermatol Sci.* 2010; 57(2): 75-82.
2. Fraefel C, Marconi P, Epstein AL. Herpes simplex virus type 1-derived recombinant and amplicon vectors. *Methods Mol Biol.* 2011; 737: 303-43.
3. E Berto, A Bozac, P Marconi. Development and application of replication-incompetent HSV-1-based Vectors. *Gene Therapy.* 2005;12: S98-S102.
4. De Silva S, Bowers WJ. Herpes Virus Amplicon Vectors. [J]. *Viruses.* 2009;1(3):594- 629.
5. Toma HS, Murina AT, Areaux RG Jr, et al. Ocular HSV-1 latency, reactivation and recurrent disease. [J]. *Semin Ophthalmol.* 2008; 23(4): 249-73.
6. Roberto Manservigi. HSV Recombinant Vectors for Gene Therapy. *The Open Virology Journal.* 2010; 4:123-156.
7. Ellis H M, Yu D, DiTizio T, et al. High efficiency mutagenesis, repair, and engineering of chromosomal DNA using single-stranded oligonucleotides. [J]. *Proc Natl Acad Sci USA,* 2001; 98(12): 6742-6746.
8. Donald L, James A, Lynn C. Genetic Engineering Using Homologous Recombination. *Annu. Rev. Genet.* 2002; 36:361-388.
9. Gierasch WW, Zimmerman DL, et al. Construction and characterization of bacterial artificial chromosomes containing HSV-1 strains 17 and KOS. [J]. *J Virol Methods,* 2006, 135(2):197-206.
10. Liu X, Song B, Lu J, et al. The Construction of BAC-HSV-1 Strain HF with GFP Reporter Gene and the research of Its Infectious Progeny Virus. *Chinese journal of virology,* 2011; 27(3): 238-243.
11. Brune W, Messerle M, Koszinowski UH. Forward with BACs. *TIG.* 2000;16:254-259.
12. James L, Gary F, Michael A. DNA cloning Using in vitro site-specific Recombination. *Genome Res.* 2000; 10:1788-1795.

- 13 Li Xiang, Xinjing Liu, Huitao Liu, et al. Construction of HSV-1 HF based replication defective vector. Life Science Journal. 2011; 8(3):547-553.
- 14 Philip J, Brian Sauer, Myron Levine, et al. A Cell-Free Recombination System for Site-Specific Integration of Multigenic Shuttle Plasmids into the Herpes Simplex Virus Type 1 Genome. J Virol. 1992;66:5509-5515.
- 15 DM Krisky, PC Marconi, T Oligino, et al. Rapid method for construction of recombinant HSV gene transfer vector. Gene Therapy. 1997; 4:1120-1125.

11/28/2011

Evaluation of Different Immunological Techniques for Diagnosis of *Schistosomiasis haematobium* in Egypt

¹ Mahfouz, A., ¹ Mahana, N., ^{*2} Rabee, I., ¹ El Amir, A.

¹ Zoology Department, Faculty of Science, Cairo University, Cairo, Egypt

² Theodore Bilharz Research Institute, Giza, Egypt

^{*} noha_mahana@yahoo.com

Abstract: The detection of soluble egg antigen (SEA) in serum and urine could be more valuable in diagnosis; hence early treatment would be applied before irreparable damage occurs. In this study, *Schistosoma* (*S.*) eggs were isolated from the intestine of infected hamsters and purified by Sodium Dodecyl Sulfate-Polyacrylamide Gel Electrophoresis (SDS-PAGE). The purified SEA was injected in rabbits to raise specific polyclonal antibodies (pAb) against *S. haematobium*. The purified pAb was further used as a primary capture to coat ELISA plates. The secondary capture of pAb was by conjugation with horse-raddish peroxidase (HRP). According to parasitological examination, this study included 150 *S. haematobium* infected patients, 50 other parasites infected patients and 30 negative control samples. Latex agglutination technique (LAT) was performed for both serum and urine in comparison to sandwich and dot-ELISA on 150 infected individual. Comparison was evaluated between LAT, sandwich and Dot-ELISA in serum samples, it showed 92%, 98% and 98.66% sensitivity and 92.50%, 96.25% and 98.75% specificity, respectively, while in urine samples showed 88.66%, 90.66% and 94.66% sensitivity and 91.25%, 93.75% and 96.25% specificity, respectively. It was clear that, the sensitivity of LAT in urine was significantly higher than the parasitological examinations. From the obtained results and with consideration to sandwich and Dot-ELISA assays, LAT assay have an important value as an applicable, fast and accurate diagnostic technique for schistosomiasis in the field.

[Mahfouz, A., Mahana, N., Rabee I., and El Amir A **Evaluation of Different Immunological Techniques for Diagnosis of Schistosomiasis haematobium in Egypt.** Life Science Journal, 2011; 8(4):858-867] (ISSN: 1097-8135). <http://www.lifesciencesite.com>.

Keywords: *Schistosoma*, LAT, Sandwich ELISA, Dot-ELISA

1. Introduction

Schistosomiasis is one of the most prevalent parasitic diseases in the world, second behind malaria (WHO, 2005; 2006). It affects 207 million of the world's poorest people through 74 countries in several parts of the world (King, 2009), 85% of them live in sub-Saharan Africa (Chitsulo *et al.*, 2004). It is estimated that schistosomiasis causes about 200,000 deaths per year. There are five main *Schistosoma* species (*S. spp.*) that affect humans which are: *S. haematobium*, *S. mansoni*, *S. japonicum*, *S. mekongi* and *S. intercalatum* (Chitsulo *et al.*, 2000; 2004).

During schistosome infection, many of the eggs laid by the female worms become trapped in the tissues. The liver is particularly affected in *S. mansoni* and *S. japonicum* infections, while, the bladder and ureters are the main organs of egg deposition by *S. haematobium* worms. As the major factor in the pathogenesis of schistosomiasis is the host granulomatous response to antigens secreted from the trapped eggs in host tissues (Pearce, 2005). Furthermore, early diagnosis is not possible because

eggs are not found in feces and urine until flukes reach maturity (Armour *et al.*, 1997).

Despite advances in control via snail eradication and large-scale chemotherapy, the level of incidence has shown no significant decrease and continues to spread to new geographic areas particularly in sub-Saharan Africa (Patz *et al.*, 2000; Siddiqui *et al.*, 2005). So, early diagnosis is necessary for prompt treatment before irreparable damage to the liver occur (Hillyer *et al.*, 1992). Schistosomiasis was diagnosed by many ways or methods as parasitological methods such as microscopic detection of eggs (Van Lieshout *et al.*, 2000). But these methods, however, are labor-intensive, time consuming, and somewhat messy due to low worm burden and/or high day to day fluctuation in egg counts (Corachan, 2002).

Several immunological tests using crude or purified egg and adult worm antigens have been developed in the last decades to detect anti-*S. haematobium* antibodies (Chen and Mott, 1989; Feldmeier, 1993). Therefore, several immunodiagnostic methods have been developed for the diagnosis of light infections, which developed on either detection of antibodies specific to schistosome

antigens or the presence of schistosome circulating antigens (CSA) in patients' serum or urine (Salah *et al.*, 2006). Commonly used assays is enzyme linked immunosorbent assay (ELISA) (Whitty *et al.*, 2000; Amorosa *et al.*, 2005), Western blotting (WB), or immunofluorescence (Thors *et al.*, 2006). Although ELISA typically is a laboratory-based tool useful for large-scale operations, its application in the field is difficult (Xue *et al.*, 1993).

The latex agglutination test (LAT) is one of the simplest slide agglutination tests available in a diagnostic parasitology laboratory. LAT has been used to detect antibodies in a variety of parasitic diseases such as visceral leishmaniasis (Arya, 1997; Bagchi *et al.*, 1998), toxoplasmosis (Mazumder *et al.*, 1988), schistosomiasis *japonicum* (Wang *et al.*, 2006) and echinococcosis *granulosus* (Barbieri *et al.*, 1993). Ibrahim *et al.* (2010) used LAT in detecting circulating schistosome antigens in urine and serum samples of *S. mansoni* infected patients, the sensitivity was 90% and 87.1%, and specificity of the assay was 88.7% and 93.5%, respectively.

This study aimed at the development of pAb-based LAT as a simple, rapid and field applicable screening test for soluble egg antigen in serum and urine samples of human schistosomiasis *haematobium*

2. Materials and Methods

2.1 Animals

Newzealand white male rabbits, weighing approximately 1.5 Kg and about 1.5 months age, were examined before the experiments (free from *Schistosoma* and other parasitic infections), and maintained at the Schistosome Biological Supply Program, Theodor Bilharz Research Institute, Giza, Egypt (SBSP/TBRI). They were kept under standard laboratory care (at 21°C, 45-55% humidity), filtered drinking water, 24% protein and 4% fat diet. Animal experiments have been carried out according to the internationally valid guidelines and ethical conditions (Nessim *et al.*, 2000).

2.2 Patients' Samples

This study was conducted on 230 individuals from highly endemic areas in Fayoum Governorate and from out patients clinic and hospital at TBRI and El-kaser El-Aine University Hospital. By parasitological examination (urine analysis) they were divided into 150 *S. haematobium* infected patients with the main age 38±11.7 years, 50 infected with other parasites (*S. mansoni*, *Fasciola*, *Echinococcus*, *Ancylostoma* and *Ascaris*) with mean age to 28±10.1 years, in addition, 30 individuals of the medical staff at TBRI served as parasite free-healthy negative control with mean age 33±9.9 years.

Urine and blood samples were collected from all cases and sera were separated, aliquoted and kept at -70°C until used.

According to the intensity of infection, *S. haematobium* infected group (the number of ova count/10ml urine) was subdivided into light, moderate and high infection using Neucleopore technique.

Light infection: included 50 patients with egg count ranging from 10-90 egg/10ml urine with mean of 54.1±20.8.

Moderate infection: included 30 patients with egg count ranging from 100-400 egg/10ml urine with mean of 209.5±79.3.

High infection: included 70 patients with egg count ranging from 200-1000 egg/10ml urine with mean of 738.5±176.2.

2.3 Antigen Preparation

Viable *S. haematobium* adult worms were purchased from the SBSP/TBRI. *S. haematobium* (Egyptian strain) SEA was prepared as previously described by Deelder *et al.* (1976) and used for ELISA standard curves. Antigen was identified by 12% SDS-PAGE (1mm) under reducing condition according to Bio-Rad Lab. Model 595, Richmond, CA, USA manufacturer.

2.4 Reactivity and Specificity of *S. haematobium* SEA by Indirect ELISA

ELISA test based on the original method of Engvall and Perlman (1971) was used with some modifications. Wells of polystyrene microtiter plates (Costar, Corporate Headquarters, Cambridge, MA, USA) were coated with 1 µg/well of *S. haematobium* SEA in coating buffer (carbonate-bicarbonate buffer), then incubated overnight at 4°C. Plates were washed 5 times with the washing buffer, blocked by dispensing 200 µl/well of 1% bovine serum albumin (BSA) in PBS and left for 1 hr at room temperature. Following washing the wells 5 times, 100 µl/well labeled primary antibody diluted in the washing buffer was added and then incubated for 1 hr at room temperature. Then, the plates were washed 5 times with the washing buffer and 100 µl/well of the diluted conjugate (secondary antibody) was dispensed with incubation for 1 hr at 37°C. After 5 times washing, 100µl from the freshly prepared substrate solution was added in each well till color appearance. After that, stopping buffer 50µ/well was added to stop the over enzyme-substrate reaction. The absorbance was measured at 492 nm in case of peroxidase conjugates or 405 nm in case of alkaline phosphatase conjugates.

2.5 Production and Purification of Polyclonal Antibody (pAb)

One mg of *S. haematobium* SEA product was mixed with an equal vol. of complete Freund's adjuvant (CFA) and injected intramuscularly (i.m.) into each of 2 rabbits according to Guobadia and Fagbemi (1997). Booster doses [0.5 mg mixed with an equal vol. of incomplete FA (IFA)] were i.m. administered at weeks 2, 3 and 4 after the initial dose according to (Fagbemi and Guobadia, 1995). Blood samples were examined from the rabbit's ear before injection and before each boosting injection to detect the titer of antibodies produced. When the titer became high (~4 days post last injection), the animals were sacrificed and blood samples were collected. Antisera were pooled and heat-inactivated then stored as aliquots at -20°C till used (Pelley and Hillyer, 1978). Proteins in solutions form hydrogen bonds with water which increase its solubility, so ammonium sulfate precipitation methods was used to remove these water molecules (Harlow and Lane, 1988). The gamma protein was further purified from serum proteins (IgG) by caprylic acid treatment (Mckinney and Parkinson, 1987; Sheehan and FitzGerald, 1996). Protein content was estimated after each purification according to Bradford (1976). The purity of the produced IgG was identified by 12% SDS-PAGE (1mm) under reducing conditions (Laemmli, 1970).

2.6 Testing for Reactivity and Specificity of pAb to *S. haematobium* SEA Antigen by Indirect ELISA

As described above. microtitre plate was coated overnight at 4°C with 30 µg/ml SEA in carbonate coating buffer, blocked with 0.1% BSA in PBS then 100 µl/well of serially diluted pAb (1:50 to 1:3200) in washing buffer was added. Hundred µl/well of anti-rabbit IgG peroxidase conjugate (Sigma) diluted in washing buffer (1/1000) was dispensed. Fifty µl/well of 8N H₂SO₄ was added to stop the enzyme substrate reaction. The absorbance was measured at 492 nm using ELISA reader (Bio-Rad microplate reader, Richmond, Ca). After each step, there were washing 5 times and the incubation was 1hr at 4°C.

2.7 Reactivity of *S. haematobium* pAb SEA in sera and urine by Sandwich ELISA

Labeling of pAb with HRP was performed by periodate method according to Tijssen and Kurstak (1984). Sandwich ELISA, originally described by Engvall and Perlmann (1971), was performed. Wells of microtitre plates were coated with 100 µl/well of purified 10 µg/ml pAb IgG in carbonate buffer, pH 9.6. The plates were washed 3 times with washing buffer 0.1 M PBS/T, pH 7.4. Then blocked with 200 µl/well 2.5% fetal calf serum (FCS) (Sigma)/0.1 M

PBS/T for 2 hr and incubated at 37°C. The plates were washed with washing buffer 3 times. Hundred µl of pooled positive and negative sera, was added individually to each well, and incubated for 2 hr at 37°C. The plates were washed trice with washing buffer. Hundred µl/well of peroxidase-conjugated IgG antibodies of dilution 1/50, 100, 250, 500 and 1000 was dispensed and plates were incubated for 1 hr at 37°C, and then were washed 5 times with washing buffer. Color appearance was done by addition of 100 µl/well substrate buffer and the plates were kept in dark at room temperature for 30 min., then the enzyme reaction was stopped by 50 µl/well of 8 NH₂So₄. The absorbance was measured at 492 nm using ELISA reader.

2.8 Dot-ELISA (Antigen Detection Assay)

Dot-ELISA was performed according to Boctor *et al.* (1987), the pre-wetted NC membrane was transferred to the Bio-Dot apparatus and washed once with 0.6 carbonate coating buffer for 5 min. After removing the excess solution, by suction, the membrane coated with 10-50 µl/well IgG pAb diluted in carbonate buffer (1/250, 500 and 1000), from original concentration (8 mg/ml), then incubated for variable times. Excess solution was removed, and then membrane was washed 3 times with 100 µl PBS-T/well. Then blocking solution was applied (10-50 µl/well), incubated at room temperature for 15-45 min. Positive and negative control reference samples were added diluted 1/1-1/32 in the diluent-blocking buffer then incubated for variable times (15-45 min.) and washed 3 times with 100 µl PBS-T/well. HRP conjugated pAb was used in 3 dilutions (1/100, 250 and 500) diluted in the diluent-blocking solution and incubated for variable times, then the NC membrane was removed from the Bio-Dot apparatus and washed 5 times with 100 µl PBS-T/well each time, followed by 2 times washing with PBS only. DAB substrate was applied by immersing NC membrane in substrate solution. The reaction was stopped, just after development of the color, with cold dist. H₂O.

2.9 Latex Agglutination Test (LAT)

1% standardized polystyrene latex suspension (0.81 µm; Sigma, St. Louis, MO) was prepared by mixing 0.1 ml of latex suspension with 9.9 ml of 0.02 M glycine-buffered saline (GBS), pH 8.4. This was stored at 4°C until used. One ml of 1% latex suspension was mixed with 1 ml of purified pAb (1.0 mg/ml). The mixture was incubated at 37°C for 2 hr in a water bath. After incubation, antibody-sensitized latex particles were washed two times with GBS, pH 8.4, and centrifuged at 3000 x g for five min. The pellet of pAb-sensitized latex particles was emulsified with 1% BSA/GBS, pH 8.4 to make a 2%

suspension. The particles were stored at 4°C until used. Latex particles coated with normal rabbit serum were used as negative control.

The test was performed on a clean two halves slide. A drop of test serum or urine (50 µl) was placed on each half of the slide. An equal vol. of sensitized latex reagent was added to the serum or urine on one half. The same vol. of control latex suspension was added to the serum or urine on the other half as a negative control. The slide was then manually rotated for two min. then inspected. Agglutination with sensitized latex reagent and not with the control latex reagent was considered a positive result. Appropriate controls were examined in parallel in each test.

Interpretation of results: According to the intensity of agglutination accumulated around the edge of the reaction zone, the positivity was classified into high (+++), moderate (++) , low (+). When no agglutination was seen, the result was considered negative (-).

3. Results

3.1 Characterization of Antigen

The SEA products were found to contain 8 mg/ml of total protein as measured by Bio-Rad protein assay

3.2 Antigen profile

The eluted protein gained from the different purification methods was analyzed by 12% SDS-PAGE under reducing conditions showing different bands ranged from 18.5 -106 kDa (Fig. 1).

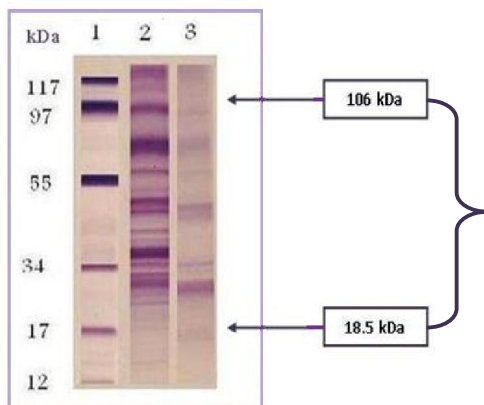


Figure 1: SDS-PAGE of SEA eluted from affinity chromatography columns. Lane 1: Low molecular weight standard; Lane 2: Crude SEA product; Lane 3: Purified SEA.

3.3 Reactivity of target antigen by indirect ELISA

The antigenicity of the purified SEA was tested by indirect ELISA technique. Serum samples from *S. haematobium* human-infected gave a strong

reaction against *S. haematobium* SEA with OD reading equal to 1.31 and no cross reactivity was recorded with sera of patients infected with other parasites e.g., fascioliasis, echinococcosis, ancylostomiasis and ascariasis (Table 1).

Table 1: Reactivity of purified *S. haematobium* SEA by indirect ELISA

Serum Samples	OD readings at 492 nm (M ± SD)
Schistosomiasis	1.31±0.342
Fascioliasis	0.26±0.201
Echinococcosis	0.11±0.094
Ancylostomiasis	0.18±0.082
Ascariasis	0.20±0.105

OD= optical density, SD= standard deviation

3.4 Characterization of pAb

The total protein content of crude rabbit serum containing anti-*S. haematobium* SEA antibody was 12.5 mg/ml, and 5.9 mg/ml after 50% ammonium sulfate precipitation method, while following 7% caprylic acid precipitation method the content dropped to 3.1 mg/ml. Finally, the protein content of highly purified anti- *S. haematobium* SEA IgG pAb subjected to ion exchange chromatography method (DEAE Sephadex A-50 ion exchange column chromatography) was 2.3 mg/ml.

3.5 pAb profile

The purity of IgG pAb after each purification step was assayed by 12% SDS-PAGE under reducing conditions. Analysis of 50% ammonium sulfate-precipitated proteins showed several bands. While the purified IgG pAb after 7% caprylic acid was represented by only 2 bands, L and H-chain bands at 31 and 53 kDa, respectively. The pAb appears free from other proteins (Fig. 2).

3.6 Reactivity of pAb against *S. haematobium* SEA

The sera of rabbit injected with *S. haematobium* SEA were tested for the presence of specific anti-*S. haematobium* SEA antibodies by indirect ELISA. An increasing antibody level started 1 wk after the 1st booster dose. Three days after the 2nd booster dose, immune sera gave a high titer against *S. haematobium* SEA with OD of 2.97 at 1/200 dilution (Fig. 3).

These sera were also found to be strongly reacting to *S. haematobium* SEA compared to other parasitic antigens (Table 2).

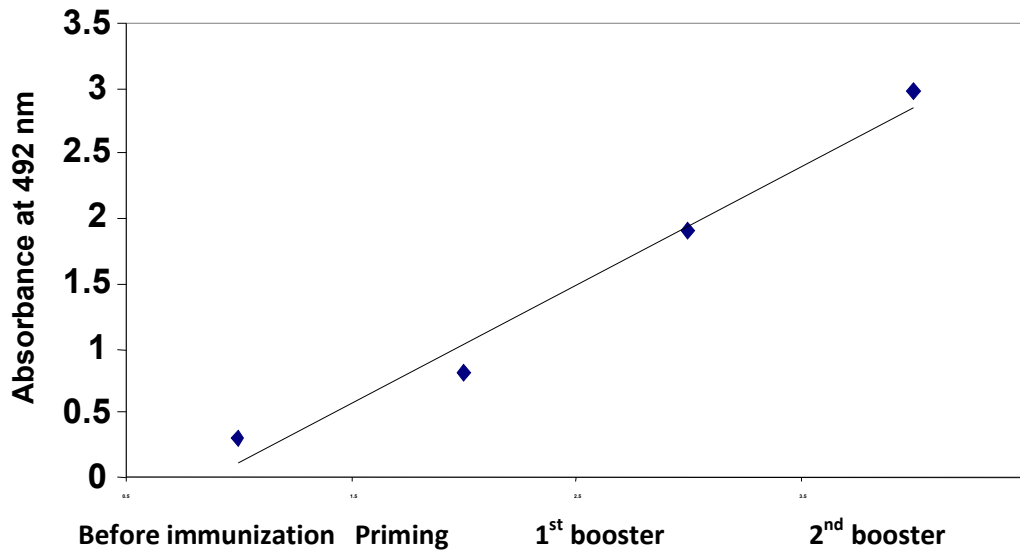


Figure 2: 12% gel (1mm) under reducing condition of anti-*S. haematobium* SEA IgG antibody before and after pAb purification stained with commassie blue. Lane 1: Molecular weight of standard protein; Lane 2: Crude anti-*S. haematobium* SEA IgG pAb; Lane 3: Precipitated proteins after 50% ammonium sulfate treatment; Lane 4: Purified IgG antibodies after 7% caprylic acid treatment.

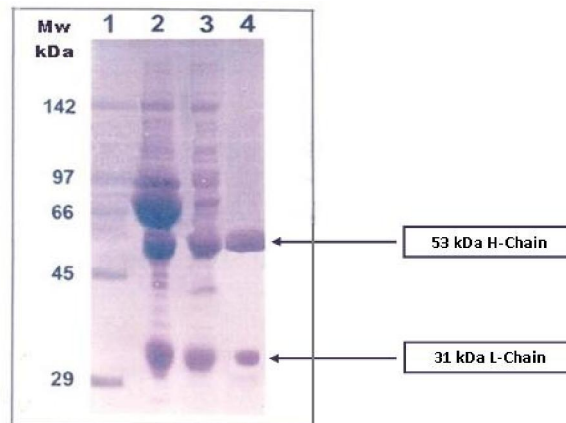


Figure 3: Reactivity of immunized rabbit anti-*S. haematobium* SEA antisera (diluted 1/250) against *S. haematobium* SEA by indirect ELISA.

Table 2: Specificity of rabbit anti-*S. haematobium* SEA pAb against different parasitic antigens by indirect ELISA

Parasitic antigen	OD readings at 492 nm (M ± SD)
<i>S. haematobium</i>	2.98±0.21
<i>Fasciola</i>	0.24±0.13
<i>Echinococcus</i>	0.19±0.11
<i>Ancylostoma</i>	0.31±0.14
<i>Ascaris</i>	0.41±0.10

3.7 Detection of *S. haematobium* SEA in human serum and urine by:

3.7.1 Sandwich ELISA

In order to measure the incidence of positivity for *S. haematobium* SEA in the studied sera and urine, the cut off point for positivity was measured as mean OD reading of negative controls +2SD. Tested samples showing OD values more than cut off value were considered positive for *S. haematobium* SEA. In sera of schistosomiasis group, the highest mean OD readings were observed in 70 cases with heavy intensity infection out of 70 (100% positivity),

followed by moderate (29 cases out of 30, 96.7% positivity), while the lowest readings were observed in those of light intensity of infection (48 cases out of 50, 96% positivity) (Table 3).

In other parasites-infected groups, the highest positivity was observed with fascioliasis (2 cases out of 15, 13.3% positivity), followed by echinococcosis group, the SEA was detected in only 1 case out of 15 (6.6% positivity). While, ancylostomiasis and

ascariasis groups were completely negative (0% positivity).

The results in urine of schistosomiasis infected group were the same as those in sera, where the mean OD hence the percent of positivity was directly proportional increased with the intensity of infection.

In other parasites-infected groups, fascioliasis and echinococcosis cases showed a highest positivity, followed by ancylostomiasis group. On the other hand, ascariasis group recorded 0% positivity.

Table 3: Detection of *S. haematobium* SEA in human sera and urine infected with *S. haematobium* and other parasites-infected groups by sandwich ELISA in comparison to healthy control sera

Groups	Positive cases		Negative cases	
	M (OD) ± SD		M (OD) ± SD	
	Sera	Urine	Sera	Urine
Healthy control (n=30)	-----	-----	0.215±0.02	0.287± 0.03
<i>S. haematobium</i> (n=150)				
Light infection (n=50)	0.764±0.22	0.811±0.24	0.355±0.12	0.371±0.14
Moderate infection (n=30)	1.155±0.26	1.020±0.21	0.435±0.18	0.411±0.12
Heavy infection (n=70)	2.411±0.19	2.121±0.23	-----	0.459±0.12
Other parasites (n=50)				
Fascioliasis (n=15)	0.444±0.22	0.521±0.30	0.211±0.13	0.191±0.11
Echinococcosis (n=15)	0.379±0.11	0.429±0.17	0.178±0.23	0.201±0.20
Ancylostomiasis (n=10)	-----	0.413±0.18	0.199±0.29	0.193±0.21
Ascariasis (n=10)	-----	-----	0.210±0.09	0.233±0.13

Cut off value= 0.312

m= mean

OD= Optical density SD= standard deviation

3.7.2 Dot-ELISA

Using Dot-ELISA for identification of SEA in sera of schistosomiasis group that classified according to the intensity of infection and experimental color intensity score range into heavy, moderate and light infection groups. In schistosomiasis group, the color intensity score was ranged from 2 to 4.

The color intensity score was directly proportional increased with the intensity of infection where the score was 4, 3 and 2 in sera of heavy, moderate and light infection group, respectively. In other parasites groups, the fascioliasis gave the highest positivity (6.6%), while echinococcosis, ancylostomiasis and ascariasis groups were completely negative (0% positivity).

The same results were obtained in urine of schistosomiasis infected group while in other parasites-infected group, SEA was detected in 13.3% of the fascioliasis and decreased to only 6.7% in echinococcosis group and still completely absent in urine of ancylostomiasis and ascariasis groups (0% positivity) (Table 4).

Table 4: Detection of *S. haematobium* SEA in human sera and urine infected with *S. haematobium* and other parasites-infected groups by Dot-ELISA in comparison to healthy control

Groups	Positive cases	
	Score of the color range	
	Sera	Urine
Healthy control (n=30)	-	-
<i>S. haematobium</i> (n=150)		
Light infection (n=50)	++	++
Moderate infection (n=30)	+++	+++
Heavy infection (n=70)	++++	++++
Other parasites (n=50)		
Fascioliasis (n=15)	+	+
Echinococcosis (n=15)	-	-
Ancylostomiasis (n=10)	-	-
Ascariasis (n=10)	-	-

3.7.3 LAT

Agglutination was detected in 68 cases out of 70 of heavy infected patients, while in the moderate and light infection group was recorded in 27 cases out of 30 and 43 out of 50, respectively. On the other

hand, 20%, 13.3%, 10% and 0% patient sera infected with fascioliasis, echinococcosis, ancylostomiasis and ascariasis were positive.

S. haematobium SEA was detected in the urine of 65 cases out of 70 heavy infected patients, while in the moderate infection group was 26 cases out of 30, whereas, in light infection group was 42 out of 50. In the groups infected with other parasites, the fascioliasis and echinococcosis gave the highest positivity (20%), whereas, ancylostomiasis group gave only 10% positivity and ascariasis was completely negative (0% positivity) (Table 5).

3.8 Sensitivity and specificity

Table (6) summarizes the sensitivity, specificity, PPV and NPV of sandwich ELISA, Dot-ELISA and LAT which are used for detection of *S. haematobium* SEA in human sera and urine. It was found that, the sensitivity of LAT in comparison to sandwich ELISA and Dot-ELISA in human sera, were 92%, 98% and 98.66%, respectively, while the specificity are 92.50%, 96.25% and 98.75%, respectively. On the other hand, in human urine the sensitivity were 88.66%, 90.66% and 94.66%, respectively, while the specificity were 91.25%, 93.75% and 96.25%, respectively. Thus, from the above data we can conclude that, the LAT and Dot-ELISA specificity and sensitivity were much close to that of sandwich ELISA.

For all techniques (sandwich ELISA, Dot-ELISA and LAT), detection of SEA in urine recorded a slightly lower results than that detected in serum. But, these detectable values have a highly satisfied sensitivity, specificity, PPV and NPV which are respective and reasonable values for diagnosis of *S. haematobium* in all degrees of infection.

4. Discussion

Early diagnosis of schistosomiasis is necessary for prompt treatment before irreparable damage to the liver occurs (Hillyer *et al.*, 1992). So that, development of early sensitive, specific as well as low-cost immunodiagnosics for detection of infected individuals would be an important step towards reaching the goal in schistosomiasis. Detection of *S. haematobium* ova in urine of infected

individuals remains the leading routine method for direct diagnosis of the disease. However, a homogeneous distribution of *S. haematobium* ova in urine is difficult to achieve (Braun-Munzinger and Southgate, 1992), but due to many obstacles, it is not of valuable sensitivity (Hillyer, 1998). Sensitivity of all fecal examination methods is found to be poor and immunodiagnosis is considered essential for correct diagnosis (Agrawal, 2004). Many attempts have been made to identify the egg antigens which are responsible for inducing those reactions and which proved also to be useful immunodiagnostic reagents (McManus and Loukas, 2008).

Table 5: Detection of *S. haematobium* SEA in human sera and urine infected with *S. haematobium* and other parasites-infected groups by LAT in comparison to healthy control

Groups	Positive cases		Negative cases	
	Score of the agglutination		Score of the agglutination	
	Sera	Urine	Sera	Urine
Healthy control (n=30)	-	-	-	-
<i>S. haematobium</i> (n=150)				
Light infection (n=50)	++	++	+	+
Moderate infection (n=30)	+++	+++	++	++
Heavy infection (n=70)	++++	++++	+++	+++
Other parasites (n=50)				
Fascioliasis (n=15)	+	+	-	-
Echinococcosis (n=15)	+	+	-	-
Ancylostomiasis (n=10)	+	+	-	-
Ascariasis (n=10)	-	-	-	-

Table 6: Sensitivity, specificity, PPV and NPV percentage of LAT versus sandwich ELISA and Dot-ELISA for detection of *S. haematobium* SEA in sera and urine

Type of experiment	%Sensitivity		%Specificity		PPV		NPV	
	Serum	Urine	Serum	Urine	Serum	Urine	Serum	Urine
Sandwich ELISA	98%	90.66%	96.25%	93.75%	96.08%	87.74%	92.77%	79.78%
Dot-ELISA	98.66%	94.66%	98.75%	96.25%	98.01%	92.81%	96.34%	87.50%
LAT	92%	88.66%	92.50%	91.25%	88.46%	84.71%	80.43%	75.25%

In this study, *S. haematobium* eggs were isolated from the intestine of 8-wk infected hamster and SEA was purified by affinity chromatography then SDS-PAGE with 8 mg/ml total protein by Bio-Rad protein assay. The purified SEA was reasonable in comparison with that of purified antigen from any biological fluid following similar purification procedures (Ibrahim *et al.*, 2010).

The antigenicity of the purified SEA was tested by indirect ELISA, detecting the highly antigenicity as the major factor in the pathogenesis of schistosomiasis. The pathology of schistosomiasis reflects the host granulomatous response to antigens secreted from the trapped eggs in host tissues (Pearce, 2005). Bosompem *et al.* (1996) precipitated proteins in urine of *S. haematobium* infected individuals and found that such antigen could be used to elicit specific antibodies which could bind SEA, so, it will be useful in *S. haematobium* diagnosis.

So male New Zealand white rabbits were immunized with purified *S. haematobium* SEA and the reactivity of anti-*S. haematobium* SEA pAb against SEA of *S. haematobium* and other parasites (*Fasciola*, *Echinococcus*, *Ancylostoma* and *Ascaris*) were determined by indirect ELISA. The IgG fraction of rabbit anti-*S. haematobium* SEA pAb was purified using ammonium sulphate precipitation method followed by 7% caprylic acid treatment and finally by using ion exchange chromatography method (DEAE Sephadex A-50) according to Goding (1986),

The sensitivity and specificity of LAT for the detection of *S. haematobium* SEA were evaluated in both human sera and urine. In serum, the sensitivity and specificity were 92% and 92.50%, respectively, compared to 98% and 96.25% by sandwich ELISA. While in urine, they recorded 88.6% and 91.25%, respectively, compared to 90.66% and 93.75% by sandwich ELISA.

Our results are in agreement with those of Demerdash *et al.* (1995) who used anti-*S. mansoni* SEA mAb in sandwich ELISA for detection of CSA in serum and urine samples and reported a sensitivity of 90% and 97%, respectively, while in mixed *S. mansoni* and *S. haematobium* infection, it was 91% in sera and 100% in urine samples. The overall specificity of the assay was 98%. On the other hand, Hanallah *et al.* (1995) who used different mAb and reported a sensitivity and specificity of 90.0% and 94.8% in urine, while in serum it was 97.0% and 98.4%, respectively. Also, El-Bassiouny *et al.* (2005) used a pair of mAb and found 96.7% sensitivity and 92% specificity, respectively.

There is a considerable degree of cross reactivity was revealed in the present study between *S. haematobium* and other parasites with varying degrees. This was obvious in case of detection of

human serum by sandwich ELISA, where cross reactivity show 13.3% positivity in fascioliasis and 6.6% in echinococcosis while in detection of human urine, the cross reactivity show 13.3% positivity in echinococcosis and 10% in ancylostomiasis, so that, the best sensitivity and specificity obtained from using serum in detection of *S. haematobium* SEA in case of sandwich ELISA.

However, patients infected with parasites other than *Schistosoma* (3 patients in serum and 5 patients in urine) showing detectable levels of SEA were coming from endemic areas of *S. haematobium* infection and missed urine diagnosis of light infection is a possibility.

The negative results observed in ELISA were found in patients with low number of egg/10 ml urine and this could be due to the possibility that the intact ova of *S. haematobium* may release only small undetectable amounts of antigen into the circulation. Another possibility is that the antigen released from the parasite form immune complexes with circulating antibodies (Carlier *et al.*, 1983; Nash, 1984). Additionally, the disappearance of CSA could be due to the effect of successful chemotherapy denoting the reliability of CSA assay as a cure monitor (Van lieshout *et al.*, 1993; Demerdash *et al.*, 1995).

Although, the sandwich ELISA was specific and sensitive method, but Dot-ELISA was more sensitive and specific technique than sandwich ELISA (El-Missiry *et al.*, 1990; Shaheen *et al.*, 1994; Parija, 1998; Montenegro *et al.*, 1999; El-Amir *et al.*, 2008).

In accordance, the sensitivity and specificity of Dot-ELISA assay in the present study for the detection of *S. haematobium* SEA in serum and urine were 98.66%, 98.75% and 94.66%, 96.25%, respectively. These results were also confirmed by Rokni *et al.* (2006), who used Dot-ELISA in detection of E/S antigens of *F. hepatica* and found the sensitivity, specificity, PPV and NPV were 96.8%, 96.1%, 96.8% and 96.1%, respectively.

Moreover, in this study, a significant correlation was observed between the level of SEA detected by ELISA and LAT in both serum and urine and the number of eggs excreted in urine of schistosomiasis patients denoting the reliability of SEA detection as an indication for intensity of infection. These results were in parallel with those of Hendawy *et al.* (2006).

In conclusion, the use of LAT for SEA assay could be a valuable applicable screening diagnostic technique in field survey. A confirmatory sandwich ELISA for SEA assessment in sera is recommended for query false negative results. At the same time, more studies have to be performed to improve the sensitivity and specificity of LAT and hence encourage its use on a large scale for diagnosis of multiple parasitic infections in field surveys.

Corresponding author

Mahana, N

Theodore Bilharz Research Institute, Giza, Egypt

noha_Mahana@yahoo.com**References**

- Agrawal, M.C. (2004): Problems of human schistosomiasis in India-status and strategy. Abstracts and Program, 3rd Global meeting on parasitic diseases, Bangalore, India, PL., 1: 2-3.
- Amorosa, V.; Kremens, D.; Wolfe, M.S.; Flanigan, T.; Cahill, K.M.; Judy, K.; Kasner, S.; Blumberg, E. (2005): *Schistosoma mansoni* in family 5 years after safari. *Emerg Infect Dis.*, 11: 339-341.
- Armour, J.; Urquhart, G.M.; Ductan, J.L. (1997): *Veterinary Parasitology*, 2nd ed. Oxford: Blackwell Science Ltd., p. 64.
- Arya, S.C. (1997): Latex agglutination test for the visceral leishmaniasis (letter). *Trans R Soc Trop Med Hyg.*, 91: 366.
- Bagchi, A.; Tiwari, S.; Gupta, S.; Katiyar, J. (1998): Latex agglutination test. Standardization and comparison with direct agglutination and Dot ELISA in the diagnosis of visceral leishmaniasis in India. *Ann Trop Med Parasitol.*, 92: 159-163.
- Barbieri, M.; Steria, S.; Battisoni, J.; Nieto, A. (1993): High performance latex reagent for hydatid serology using an *Echinococcus granulosus* lipoprotein antigen purified from cyst fluid in one step. *Int J Parasitol.*, 23: 565-572.
- Boctor, F.N.; Stek, M.J.; Peter, J.B.; Kamal, R. (1987): Simplification and standardization of Dot-ELISA for human schistosomiasis *mansoni*. *J Parasitol.*, 73: 589-592.
- Bosompem, K.; Arishima, T.; Yamashita, T.; Ayi, I.; Anyan, W.; Kojima, S. (1996): Extraction of *S. haematobium* antigens from infected human urine and generation of potential diagnostic monoclonal antibodies to urinary antigens. *Acta Trop.*, 62: 91-103.
- Bradford, M.M. (1976): A rapid and sensitive method for the quantitation of microgram quantities of protein utilizing the principle of protein-dye binding. *Anal Biochem.*, 72: 248-254.
- Braun-Munzinger, R.A.; Southgate, B.A. (1992): Repeatability and reproducibility of egg counts of *Schistosoma haematobium* in urine. *Trop Med Parasitol.*, 43: 149-154.
- Carlier, Y.; Nzeyimana, H.; Boul, D.; Capron, A. (1983): Evaluation of circulating antigens by a sandwich radioimmunoassay, and of antibodies and immune complex, in *Schistosoma mansoni*-infected African parturients and their newborn children. *Am J Trop Med Hyg.*, 29: 74-81.
- Chen, M.G.; Mott, K.E. (1989): Progress in the assessment of morbidity due to *Schistosoma haematobium* infections: in a review of the recent literature. *Trop Dis Bull.*, 48: 2643-2648.
- Chitsulo, L.; Engels, D.; Montresor, A.; Savioli, L. (2000): The global status of schistosomiasis and its control. *Acta Trop.*, 77: 41-51.
- Chitsulo, L.; Loverde, P.; Engels, D. (2004): Schistosomiasis. *Nat Rev Microbiol.*, 2: 12-23.
- Corachan, M. (2002): Schistosomiasis and international travel. *Clin Infect Dis.*, 35: 446-450.
- Deelder, A.M.; Klappe, H.T.M.; Van den Aardweg, G.J.M.J.; Van Meerbeke, E.H.E.M. (1976): *Schistosoma mansoni* demonstration of two circulating antigens in infected hamsters. *Exp Parasitol.*, 40: 189-197.
- Demerdash, Z.; Mohamed, S.; Shaker, Z.; Hassan, S.; El Attar, G.; Saad el Din, H.; Abadeer, N.; Mansour, M. (1995): Detection of circulating schistosome antigens in serum and urine of schistosomiasis patients and assessment of cure by a monoclonal antibody. *Egy Soc Parasitol.*, 25: 471-484.
- El-Amir, A.; Rabia, I.; Kamal, N.; El-Deeb, S. (2008): Evaluation of the diagnostic potential of different immunological techniques using polyclonal antibodies against *Fasciola gigantica* excretory/secretory antigens in sheep. *Egypt J Immunol.*, 15: 65-74.
- El-Bassiouny, A.; Salah, F.; Kamel, M.; Rabia, I. (2005): Effective diagnosis of active schistosomiasis by a pair of IgG monoclonal antibodies against *Schistosoma mansoni* soluble egg antigen. *Egypt J Med Sci.*, 26: 369-382.
- El-Missiry, A.G.; El-Serougi, A.O.; Salama, M.M.; Kamal, A.M. (1990): Evaluation of Dot-ELISA technique in the serodiagnosis of schistosomiasis in Egypt. *J Egypt Soc Parasitol.*, 20: 639-645.
- Engvall, E.; Perlman, P. (1971): Enzyme-linked immunosorbent assay. Quantitative assay of IgG. *Immunochem.*, 8: 871-874.
- Fagbemi, B.O.; Guobadia, E.E. (1995): Immunodiagnosis of fascioliasis in ruminants using a 28-kDa cysteine protease of *Fasciola gigantica* adult worm. *Vet Parasitol.*, 57: 309-318.
- Feldmeier, H. (1993): Diagnosis. Jordan P, Webbe G, Sturrock RF., eds. *Human Schistosomiasis*. Oxon: CAB Internat., p. 217-304.
- Goding, J.W. (1986): *Monoclonal antibodies: Principles and Practice*. Alden Press Oxford, London and Northampton, p. 112-116.
- Guobadia, E.E.; Fagbemi, B.O. (1997): The isolation of *F. gigantica*-specific antigens and their use in the serodiagnosis of fascioliasis in sheep by the detection of circulating antigens. *Vet Parasitol.*, 68: 269-282.
- Hanallah, S.B.; Shaker, Z.A.; Kaddah, M.A. (1995): Monoclonal antibodies specifically directed to urinary schistosomal antigens detect antigenaemia and antigenuria in human schistosomiasis *mansoni*. *Egypt J Bilh.*, 17: 27-49.
- Hendawy, M.A.; Mohamed, S.H.; Ibrahim, R.A. (2006): Nitrocellulose cassettes (NCC) as a field applicable technique for rapid and effective diagnosis of schistosomiasis and fascioliasis. *New Egypt J Med.*, 35: 86-92.
- Hillyer, G.V. (1998): Immunodiagnosis of human and animal fascioliasis. In: *Fascioliasis* Ed JP Dalton CABI Publishing Oxon Wallingford UK., p. 435-448.
- Hillyer, G.V.; Soler de Galanes, M.; Rodriguez-Perez, J.; Bjorland, J.; Silva de Lagrava, M.; Ramirez Guzman, S.; Bryan, R. (1992): Use of the Falcon assay screening test-enzyme linked immunosorbent assay (FAST-ELISA), the enzyme linked immunoelectrotransfer blot (EITB) to determine the prevalence of human Fascioliasis in the Bolivian Altiplano. *Am J Trop Med Hyg.*, 46: 603-609.
- Ibrahim, R.B.; Mohamed, S.H.; Demerdash, Z.A.; Diab, T.M.; Maher, K.; Safwat, W.; Shaker, Z.A. (2010): Anti-*Schistosoma mansoni* mAb-based latex agglutination: A reliable field applicable

- immunodiagnostic test for screening of active Human Schistosomiasis. *J Amer Sci.*, 6: 19-27.
31. King, C.H. (2009): Toward the elimination of schistosomiasis. *N Engl J Med.*, 360: 106-109.
 32. Laemmli, V.K. (1970): Cleavage of structural proteins during assembly of the head of the bacteriophage T4. *Nature*, 227: 630-634.
 33. Mazumder, P.; Chuang, H.Y.; Wentz, M.W.; Wiedbrauk, D.L. (1988): Latex agglutination test for the detection of antibodies to *Toxoplasma gondii*. *J Clin Microbiol.*, 26: 2444-2446.
 34. McKinney, M.M.; Parkinson, A. (1987): A simple, non-chromatographic procedure to purify immunoglobulins from ascites fluid. *J Immunol Meth.*, 96: 271-278.
 35. McManus, D.P.; Loukas, A. (2008): Current status of vaccines for schistosomiasis. *Clin Microbiol Rev.*, 21: 225-242.
 36. Montenegro, S.M.; Miranda, P.; Mahanty, S.; Abath, F.G.; Teixeira, K.M.; Coutinho, E.M.; Brinkman, J.; Gonçalves, I.; Domingues, L.A.; Domingues, A.L.; Sher, A.; Wynn, T.A. (1999): Cytokine production in acute versus chronic human Schistosomiasis *mansoni*: the crossregulatory role of interferon-gamma and interleukin-10 in the responses of peripheral blood mononuclear cells and splenocytes to parasite antigens. *J Infect Dis.*, 179: 1502-1514.
 37. Nash, T.E. (1984): Immune complex size for determines the clearance rate of circulating antigen in schistosome infected mice. *Am J Trop Med Hyg.*, 33: 621-626.
 38. Nessim, N.G.; Hassan, S.I.; William, S.; El-Baz, H. (2000): Effect of the broad spectrum anthelmintic drug flubendazole upon *Schistosoma mansoni* experimentally infected mice. *Arzneimittelforschung*, 50: 1129-1133.
 39. Parija, S.C. (1998): Urinary antigen detection for diagnosis of parasitic infections. *Parasitol Today*, 14: 5-6.
 40. Patz, J.; Graczyk, T.; Geller, N.; Vittor, A. (2000): Effects of environmental changes on emerging parasitic diseases. *Int J Parasitol.*, 30: 1395-1405.
 41. Pearce, E.J. (2005): Priming of the immune response by schistosome egg. *Parasite Immunol.*, 27: 265-270.
 42. Pelley, R.P.; Hillyer, G.V. (1978): Demonstration of a common antigen between *Schistosoma mansoni* and *Fasciola hepatica*. *Am J Trop Med Hyg.*, 27: 1192-1194.
 43. Rokni, M.B.; Samani, A.; Massoud, J.; Babaei Nasr, M. (2006): Evaluation of Dot-ELISA method using excretory-secretory antigens of *Fasciola hepatica* in laboratory diagnosis of human fasciolosis. *Iranian J Parasitol.*, 1: 26-30.
 44. Salah, F.; El Bassiouny, A.; Kamel, M.; Rabia, I.; Mansour, W.; Hassan, S.; Siam, M.; Demerdash, Z. (2006): Effective diagnosis of active schistosomiasis by a pair of IgG monoclonal antibodies against *Schistosoma haematobium* soluble egg antigen. *Parasitol Res J.*, 5: 528-533.
 45. Shaheen, H.; al Khafif, M.; Farag, R.; Kamal, K.A. (1994): Serodifferentiation of human fascioliasis from schistosomiasis. *Trop Geog Med.*, 46: 326-327.
 46. Sheehan, D.; FitzGerald, R. (1996): Ion-exchange chromatography. *Methods Mol Biol.*, 59: 145-150.
 47. Siddiqui, A.A.; Pinkston, J.R.; Quinlin, M.L.; Kavikondala, V.; Rewers-Felkins, K.A.; Phillips, T.; Pompa, J. (2005): Characterization of protective immunity induced against *Schistosoma mansoni* via DNA priming with the large subunit of calpain (Sm-p80) in the presence of genetic adjuvants. *Parasite*, 12: 3-8.
 48. Thors, C.; Holmblad, P.; Maleki, M.; Carlson, J.; Linder, E. (2006): Schistosomiasis in Swedish travelers to sub-Saharan Africa: can we rely on serology? *Scand J Infect Dis.*, 38: 794-799.
 49. Tijssen, P.; Kurstak, P. (1984): Highly efficient and simple methods for the preparation of peroxidase and active peroxidase-antibody conjugate for enzyme immunoassays. *Anal Biochem.*, 136: 451-457.
 50. Van Lieshout, L.; De Jonge, N.; Mansour, M.M.; Bassily, S.; Krijger, F.W.; Deelder, A.M. (1993): Circulating cathodic antigen levels in serum and urine of schistosomiasis patients before and after chemotherapy with praziquantel. *Trans R Soc Trop Med Hyg.*, 87: 311-312.
 51. Van Lieshout, L.; Polderman, A.M.; Deelder, A.M. (2000): Immunodiagnosis of schistosomiasis by determination of the circulating antigens CAA and CCA, in particular in individuals with recent or light infections. *Acta Trop.*, 77: 69-80.
 52. Wang, H.; Zhang, Y.; Yan, B.; Liu, L.; Wang, S.; Shen, G.; Yu, R. (2006): Rapid, simple, and sensitive immunoagglutination assay with SiO₂ particles and quartz crystal microbalance for quantifying *Schistosoma japonicum* antibodies. *Clin Chem.*, 52: 2065-2071.
 53. Whitty, C.; Mabey, D.; Armstrong, M.; Wright, S.; Chiodini, P. (2000): Presentation and outcome of 1107 cases of schistosomiasis from Africa diagnosed in a non-endemic country. *Trans R Soc Trop Med Hyg.*, 94: 531-534.
 54. WHO. Report of the third global meeting of the partners for parasite control Deworming for Health and Development. 2005.
 55. WHO. Schistosomiasis. 2006.
 56. Xue, C.; Taylor, M.; Bickle, Q.; Savioli, L.; Renganathan, A. (1993): Diagnosis of *Schistosoma haematobium* infection: evaluation of ELISA using keyhole limpet haemocyanin or soluble egg antigen in comparison with detection of eggs or haematuria. *Trans Roy Soc Trop Med Hyg.*, 87: 654-658.

12/12/2011

Effect of Intratympanic Dexamethasone Administration on Cisplatin-Induced Ototoxicity in Adult Guinea Pigs, Is It Time-Dependent? Audiological and Histological Study

Mirahan T. Thabet¹, Rasha Elkabarity¹, Nevine Bahaa E. Soliman², Nagwa Kostandy Kalleney² and Amr Gouda³

Audiology¹, Histology² and Otolaryngology³ Departments, Faculty of Medicine, Ain Shams University, Cairo, Egypt.

nbahaasoliman@gmail.com

Abstract: Introduction: Cisplatin is a cornerstone chemotherapeutic drug often dose-limited by ototoxicity. Many trials have been introduced for a complete cure or prevention of cisplatin-induced ototoxicity but unfortunately, with un-satisfactory results. Intratympanic steroids have been recently tried and shown competitive results in terms of reduction of ototoxicity. However, perfect timing of drug administration remains controversial.

Aim of the work: To evaluate the effect and safety of intratympanic dexamethasone administration on cisplatin-induced ototoxicity in adult male guinea pigs and to assess the differences between early and late protection from this ototoxicity.

Materials and methods: Forty eight adult male guinea pigs were divided as follows: Group I served as control group. Group II was subjected to intratympanic saline (subgroup IIa) or dexamethasone (subgroup IIb) injection. Group III was intraperitoneally injected with cisplatin. Groups IV and V were subjected first to intratympanic dexamethasone administration in both ears for 5 days starting 1 day and 1 hour -respectively- before cisplatin intraperitoneal injection.

Results: Dexamethasone intratympanic injection revealed similar functional and structural results compared with control. Cisplatin intraperitoneal injection resulted in a profound cochlear functional and structural damage in group III. Limited otoprotection resulted from intratympanic dexamethasone administration one day before cisplatin. Intratympanic dexamethasone injection one hour before cisplatin treatment resulted in a significant preservation of the functional and structural properties of the cochlea.

Conclusion: Intratympanic dexamethasone administration is a safe, easy and efficient way to protect from cisplatin ototoxicity especially when administered one hour before cisplatin treatment.

[Mirahan T. Thabet, Rasha Elkabarity, Nevine Bahaa E. Soliman, Nagwa Kostandy Kalleney and Amr Gouda **Effect of Intratympanic Dexamethasone Administration on Cisplatin-Induced Ototoxicity in Adult Guinea Pigs, Is It Time-Dependent? Audiological and Histological Study**] Life Science Journal, 2011;8(4):868-882] (ISSN: 1097-8135). <http://www.lifesciencesite.com>.

Key words: dexamethasone, cisplatin, ototoxicity, guinea pigs.

1. Introduction:

Cisplatin is a common chemotherapeutic agent essentially used to treat many different types of cancer including neuroblastoma, osteosarcoma, testicular, ovarian, cervical, bladder, lung, and head & neck cancers. It has several side effects stemming from its non-specific cytotoxic action. The most striking dose-limiting side effect of cisplatin therapy is ototoxicity (1). Cisplatin-induced ototoxicity generally manifests as tinnitus and sensorineural hearing loss which starts in the high frequencies. Nevertheless, it extends into lower frequencies that are important for speech perception. This hearing impairment is dose related, cumulative, bilateral and usually permanent (2). Moreover, ototoxicity caused by cisplatin may occur within hours to days after drug administration (3). Dozens of experimental studies have attempted to find an ideal otoprotectant by administration of antioxidants at an early stage in the ototoxic pathways. Unfortunately, many of these

agents have been found to inhibit the tumoricidal effects of cisplatin (4).

Systemic glucocorticoids are currently in use for treatment of hearing loss in a variety of cochlear disorders such as autoimmune inner ear, Meniere's disease, tinnitus and cases of sudden or idiopathic hearing loss when etiology is unclear (5). Unfortunately, corticosteroids also down-regulate apoptosis genes in tumor cells. Therefore, their systemic application to protect against cisplatin-induced ototoxicity may result in decreased efficacy of cisplatin's tumoricidal properties (6).

Intratympanic administration of drugs is a contemporary method of locally treating inner ear disorders, allowing diffusion across the round window into the inner ear where it can exert its effect. Specifically, steroids placed into the middle ear have been shown to diffuse across the round window into the inner ear and bathe the inner ear structures (7). This method allowed concentration of steroid to much higher levels within the inner ear

compared to oral or parenteral routes (5). Also, local administration prevented systemic absorption avoiding the common systemic side effects of steroids including hyperglycemia, peptic ulcers, hypertension and osteoporosis. Most importantly it prevented the more problematic reduced efficacy of chemotherapeutic agents (6). Intratympanic administration of steroids has been used to safely treat other inner ear disorders such as sudden sensorineural hearing loss (8) and Ménière's disease for many years (9).

So, our desired goal is to evaluate the safety of the intratympanic dexamethasone therapy, from both audiological and histological points of view as a steroid-protectant from cisplatin ototoxicity and to assess the ultimate timing of drug application for satisfactory protective results.

2. Materials and Methods:

Animals

Forty eight adult male guinea pigs were used in this study. They were housed under standard conditions of boarding in wire mesh cages with food and water *ad libitum*. The experiment was done in the Medical Research Center and in the Audiology Department, Faculty of Medicine, Ain Shams University.

Experimental groups

Guinea pigs were allocated into five groups, 8 animals each; except for group II it consisted of 16 animals:

Group I (Control):

Guinea pigs received single intraperitoneal injection of 1 ml of saline and served as a control group.

Group II:

After the first Auditory Brainstem Response (ABR) measuring, this group was divided into 2 subgroups each consisted of 8 animals:

Subgroup IIa: (Saline)

Guinea pigs were subjected to intratympanic saline injection in both ears once daily for 5 days.

Subgroup IIb: (Dexamethasone):

Guinea pigs were subjected to intratympanic dexamethasone injection in both ears once daily for 5 days (10).

Group III (Cisplatin):

A single intraperitoneal injection of cisplatin at a dose of 8 mg/kg (11) was administered to guinea pigs of this group. It was purchased as Cytoplatin-50 Aqueous, CIPLA LTD, Verna Industrial Estate, India.

Group IV (Dexamethasone 1 day before cisplatin):

Guinea pigs were subjected to intratympanic dexamethasone injection in both ears once daily for 5 days, starting 1 day before a single cisplatin injection at a same dose and route as group III.

Group V (Dexamethasone 1 hour before cisplatin):

Guinea pigs were subjected to same doses of dexamethasone as group IV, in both ears for the same period, starting 1 hour before a single cisplatin injection at the same dose and route as group III.

Procedure of Intra-tympanic injection:

Prior to injection, the animals were examined for any evidence of tympanic membrane perforation, middle ear infection, effusion, and/or debris in the external auditory canals. Intratympanic injections of dexamethasone (with a concentration of 4 mg/ml) or 0.9% saline in guinea pig ears were carried out under light ether anesthesia using a 30 degree pediatric nasal endoscope. After the tympanic membrane was visualized, a sterile 22-gauge canula connected to a 1ml syringe was passed through the inferior portion of the tympanic membrane. About 0.5 - 0.7 ml (enough to fill the middle ear) of either solution was injected into the middle ear space (10). Dexamethasone was purchased as dexamethasone sodium phosphate ampoules (Amriya pharmaceutical industries, Alexandria- Egypt).

I-Audiological study:

Auditory Brainstem Response (ABR) was measured in all guinea pigs before injection of cisplatin or intra-tympanic saline or dexamethasone. Moreover, ABR was repeated after saline or dexamethasone intratympanic injection in guinea pigs of subgroup IIa and subgroup IIb, respectively. All recordings were conducted under anesthesia by ketamine hydrochloride (Sigma), 40 mg/kg (12) in a soundproof chamber.

Stimulus parameters:

The ABRs were generated in response to 100 μ s alternated clicks at a range of 2-4 KHz. The stimulus was presented at a rate of 21 pulses / second. Monaural thresholds were obtained via headphone at 10 dB steps between 100 dB SPL down to threshold.

Recording parameters:

The ABRs were recorded by means of three platinum-iridium needle electrodes, placed subdermally over the vertex (positive), the mastoid (negative) and the contra-lateral mastoid (ground). The recording window included a 10-millisecond post-stimulus times. ABRs were amplified 20000-fold and filtered from 30 Hz to 3000 Hz. At least two

repeatable traces with approximately 1000 response sweeps for each trace were collected for each subject. The test session including electrode application and evoked response recording for each subject lasted for about 30 minutes.

Response analysis:

The ABRs were defined by three positive peaks (I, III, V) at supra-threshold intensity (100 dB SPL). Three recording parameters were analyzed. Absolute and inter-peak latencies for wave I, III and V measured and threshold. Threshold was defined as the lowest intensity capable of producing a visually detectable, reproducible wave V.

Eight days post cisplatin injection; ABR in all guinea pigs in groups III, IV and V were re-measured by the same procedure. Moreover, ABR was repeated simultaneously in subgroups IIa and IIb. Hearing loss induced by single-dose cisplatin in guinea pig has been found to be stabilized by 5-7 days after cisplatin injection (13, 14).

II- Histological study:

At the end of the final ABR recording session, all animals were anesthetized with ketamine hydrochloride 40 mg/kg (12). The animals were decapitated, the temporal bone was taken, and the cochleae were dissected carefully. The right cochleae of all groups were processed for light microscopic examination (LM). Moreover, the left cochleae of all groups were processed for scanning electron microscopic examination (SEM). A tiny opening was made in the apical turn of the cochleae by a curved stapes pick. The proper fixative was gently forced through the preformed apical opening by a fine needle fitted onto a tuberculin syringe allowing for good fixation.

A-Light microscopic study (LM):

The cochleae were fixed in 10% formalin for 2 days. Decalcification was done using the chelating agent, ethylene-diamine-tetra-acetic acid (EDTA) in the form of its disodium salt (5.5 g EDTA in 90 ml distilled water and 10 ml formaldehyde, 37:40%). Decalcification was done for 4 weeks with daily change of the solution until softening of specimens was obtained. Specimens were processed to form paraffin blocks. Serial longitudinal sections passing parallel to the modiolus were cut at sections of 5µm thickness and subjected to Haematoxylin and Eosin (H&E) stain (15).

B- Scanning electron microscopic study (SEM):

The cochleae were fixed in 1.5% glutaraldehyde in Phosphate buffered saline (pH=7.4) for 2 hours at room temperature. The

cochleae were then washed in Phosphate buffered saline, transferred to 1% osmium solution. Longitudinal micro-dissection of the cochleae was done using extra sharp forceps and microsurgical scissors. They were then dried and gold-coated using sputter coated SCD/005. Tissues were mounted in copper stub and viewed using scanning electron microscope (XL30) in the Anatomy Department, Faculty of Medicine, Ain Shams University (16).

III-Morphometric and Statistical study:

A- Auditory brainstem response (ABR) thresholds and threshold shifts were expressed as mean ± SEM.

B- The cochleae were examined in serial H&E-stained sections from all guinea pigs in each group (five high power fields /section) to measure the thickness of the central part of the fibrous connective tissue meshwork underneath the stria vascularis. The measurements were performed using Image Analyser (Olympus Image J, NIH, 1.41b, USA) in the Oral Pathology Department, Faculty of Dentistry, Ain Shams University. The mean values of different fields from serial cochlear sections were estimated.

The standard error of means (SEM) of all data was calculated and statistical analysis was carried out using SPSS statistical program version 17; IBM Corporation, Route 100 Somers, NY 10589. Data were evaluated by using the one-way analysis of variance test (ANOVA). Comparison of measurements between all groups was done by post hoc least significant difference. As regard the probability, the least significant level used was at P value less than 0.05.

3. Results:

I-Audiological results:

Forty eight adult guinea pigs were enrolled in the present study (groups I, II, III, IV and V). Prior testing, all animals showed normal mobile tympanic membranes together with normal ABR morphology and thresholds (Diagram 1).

As shown in table (1), all Animals of all groups showed normal mean hearing thresholds with normal mean absolute latencies of waves I, III and V & normal inter-peak latencies (I-III, III-V and I-V). There was non-significant statistical difference (p>0.05) in all groups of the study prior to cisplatin intraperitoneal injection and prior to saline or dexamethasone intratympanic injection. This emphasized that all animals were normal hearers before any intervention.

Cisplatin injection resulted in a death rate of 2 animals (25%) in each of groups III, IV and V,

leaving 6 animals in each of these groups continuing the experiment.

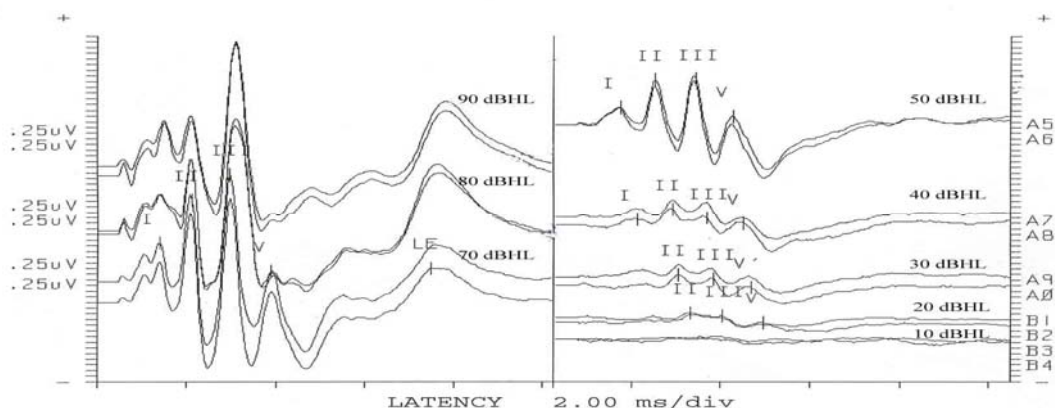


Diagram 1: showing different ABR parameters of a control guinea pig.

Table (1): Showing the Mean \pm SEM of different ABR parameters and comparison between all groups: (Before administration of drugs)

	Group I	Group II	Group III	Group IV	Group V
Threshold	11.25 \pm 2.39 (8)	10.00 \pm 2.89 (16)	10.00 \pm 2.04 (8)	13.75 \pm 1.25 (8)	10.00 \pm 2.04 (8)
I Lat.	1.48 \pm 0.14 (8)	1.46 \pm 0.13 (16)	1.57 \pm 0.15 (8)	1.43 \pm 0.14 (8)	1.58 \pm 0.13 (8)
III Lat.	2.73 \pm 0.13 (8)	2.74 \pm 0.15 (16)	2.80 \pm 0.23 (8)	2.65 \pm 0.13 (8)	2.73 \pm 0.17 (8)
V Lat.	3.90 \pm 0.11 (8)	4.10 \pm 0.18 (16)	3.80 \pm 0.31 (8)	3.95 \pm 0.12 (8)	4.00 \pm 0.11 (8)
V Lat Ths	4.90 \pm 0.17 (8)	4.48 \pm 0.17 (16)	4.77 \pm 0.29 (8)	4.78 \pm 0.19 (8)	4.73 \pm 0.18 (8)
I-III	1.25 \pm 0.06 (8)	1.35 \pm 0.08 (16)	1.47 \pm 0.27 (8)	1.20 \pm 0.07 (8)	1.23 \pm 0.09 (8)
III-V	1.18 \pm 0.08 (8)	1.25 \pm 0.09 (16)	1.10 \pm 0.06 (8)	1.28 \pm 0.09 (8)	1.18 \pm 0.08 (8)
I-V	2.38 \pm 0.13 (8)	2.58 \pm 0.19 (16)	2.60 \pm 0.31 (8)	2.53 \pm 0.18 (8)	2.40 \pm 0.16 (8)

-Values are mean \pm SEM. - Number in parenthesis indicates the number of guinea pigs.

Table (2): Showing the Mean \pm SEM of different ABR parameters and comparison between all groups: (After administration of drugs)

	Group I (Control)	Group IIa (Saline)	Group IIb (Dexa)	Group III (Cisplatin)	Group IV (Dexa 1 day before Cisplatin)	Group V (Dexa 1 hour before Cisplatin)
Threshold	11.25 \pm 2.39 (8)	11.25 \pm 1.25 (8)	12.50 \pm 1.44 (8)	58.33 \pm 4.41 ^a (6)	26.67 \pm 3.33 ^{ab} (6)	11.67 \pm 1.67 ^{bc} (6)
I Lat.	1.48 \pm 0.14 (8)	1.45 \pm 0.12 (8)	1.58 \pm 0.14 (8)	1.43 \pm 0.03 (6)	1.23 \pm 0.03 (6)	1.47 \pm 0.09 (6)
III Lat.	2.73 \pm 0.13 (8)	2.78 \pm 0.05 (8)	2.75 \pm 0.17 (8)	2.70 \pm 0.06 (6)	2.73 \pm 0.09 (6)	2.90 \pm 0.26 (6)
V Lat.	3.90 \pm 0.11 (8)	4.23 \pm 0.20 (8)	3.98 \pm 0.13 (8)	3.90 \pm 0.00 (6)	3.90 \pm 0.21 (6)	4.03 \pm 0.28 (6)
V Lat Ths	4.90 \pm 0.17 (8)	4.43 \pm 0.15 (8)	4.83 \pm 0.17 (8)	4.83 \pm 0.23 (6)	4.93 \pm 0.24 (6)	5.03 \pm 0.47 (6)
I-III	1.25 \pm 0.06 (8)	1.33 \pm 0.08 (8)	1.18 \pm 0.09 (8)	1.27 \pm 0.03 (6)	1.37 \pm 0.09 (6)	1.43 \pm 0.19 (6)
III-V	1.18 \pm 0.08 (8)	1.45 \pm 0.18 (8)	1.30 \pm 0.11 (8)	1.20 \pm 0.06 (6)	1.17 \pm 0.22 (6)	1.13 \pm 0.12 (6)
I-V	2.38 \pm 0.13 (8)	2.78 \pm 0.19 (8)	2.65 \pm 0.17 (8)	2.47 \pm 0.03 (6)	2.33 \pm 0.12 (6)	2.57 \pm 0.23 (6)

-Values are mean \pm SEM. - Number in parenthesis indicates the number of guinea pigs. -Dexa=Dexamethasone

- a: significance of difference by LSD from Group I (Control) at least $p < 0.05$.

- b: significance of differences by LSD from Group III (Cisplatin) at least $p < 0.05$.

- c: significance of differences by LSD from Group IV (dexamethasone 1 day before cisplatin) at least $p < 0.05$

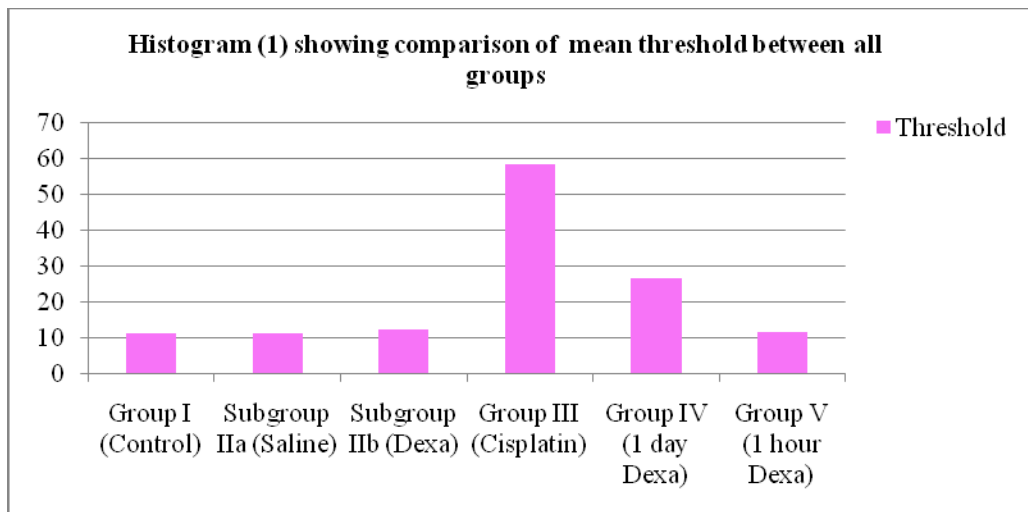
As shown in table (2) and histogram (1), guinea pigs of subgroups IIa and IIb given either saline or dexamethasone intratympanically respectively, showed non-significant statistical difference ($p>0.05$) in mean threshold and all other parameter means of ABR testing compared with group I (control). This documented that intratympanic dexamethasone is safe.

On the other hand, both groups III and IV showed statistically significant elevated mean threshold parameter only ($p<0.05$) with non-significant statistical difference ($p>0.05$) as regards the other parameters means of ABR testing compared with group I (control). Moreover, group IV (administered dexamethasone 1 day before cisplatin) showed significant statistical difference in mean threshold parameter only ($p<0.05$) with non-significant statistical difference as regards the other parameters means of ABR testing ($p>0.05$) compared with group III (not protected from cisplatin ototoxicity). This documented the limited protective effect of dexamethasone (injected 1 day prior to cisplatin administration) on cisplatin ototoxicity in both ears in group IV.

On the other hand, group V (administered dexamethasone 1 hour before cisplatin) showed non-

significant statistical difference ($p>0.05$) in mean threshold and all other parameters means of ABR testing compared with group I (control). Moreover, group V (administered dexamethasone 1 hour before cisplatin) showed significant statistical difference in mean threshold parameter only ($p<0.05$) with non-significant statistical difference as regards the other parameters means of ABR testing ($p>0.05$) compared with group III (not protected from cisplatin ototoxicity). This documented the marked protective effect of dexamethasone (injected 1 hour prior to cisplatin administration) on cisplatin ototoxicity in group V.

Additionally, group V (administered dexamethasone 1 hour before cisplatin) showed significant statistical difference in mean threshold parameter only ($p<0.05$) with non-significant statistical difference as regards the other parameters means of ABR testing ($p>0.05$) compared with group IV (administered dexamethasone 1 day before cisplatin). This result pointed to better protection achieved by administration of dexamethasone one hour (total protection) prior cisplatin administration than one day (partial protection).



Dexa= Dexamethasone

II-Histological results:

No histological differences were found in the structure of the cochleae of the control group (given single intraperitoneal saline injection) and in both subgroups of group II (given either intratympanic saline or dexamethasone injections).

A) Light microscopic results:

Group I (Control):

Examination of H&E-stained sections of control group showed the wedge-shaped cochlear duct housed in the bony cochlea. Reissner's membrane was noticed with its two layers of simple squamous epithelium roofing the cochlear duct and separating it from the scala vestibuli, while the basilar membrane made its floor separating it from

the scala tympani. The basilar membrane extended from the spiral lamina medially to the spiral ligament on the lateral wall, supporting the organ of Corti (Figure 1). Neuroepithelial cells of the organ of Corti were seen as three outer hair cells (OHCs) with acidophilic cytoplasm and basal rounded vesicular nuclei and one inner hair cell (IHC) with central rounded vesicular nucleus. Outer pharyngeal cells supported the OHCs and the inner pharyngeal cell was seen supporting the IHC. Outer and inner pillars surrounded the tunnel of Corti. Other supporting cells as Hensen, Claudius, Böttcher cells laterally and border cells medially could be recognized. The tectorial membrane was seen hanging over the hair cells as homogenous acidophilic structure (Figure 2). Stria vascularis covered the lateral wall of the cochlear duct and was made of three layers of epithelium; marginal, intermediate and basal with obvious capillaries, melanin pigments and fibrous connective tissue meshwork underneath (Figure 3).

Group III (Cisplatin):

Cisplatin intraperitoneal injection resulted in cytoplasmic vacuolization and degeneration of OHCs in most of the sections in this group (Figures 4 & 5). Widely spaced OHCs were also seen in most of those sections (Figure 6). Absent OHCs was noticed in some sections, especially in the third row, with degeneration of the remaining OHCs (Figure 7). The IHCs were seen apparently less affected compared with OHCs showing slight cytoplasmic vacuolization in some sections (Figure 6). Most of the supporting cells in all sections examined were highly vacuolated, swollen and showed pyknotic nuclei (Figures 4, 5, 6 & 7). Regarding the stria vascularis, vacuolated epithelial cells could be seen involving the three layers. Dilated congested intraepithelial capillaries could be easily noticed. The fibrous connective tissue meshwork underneath the stria vascularis showed apparent increase in thickness as compared with the control sections (Figure 8). It is noteworthy that most of these findings were seen in the basal and middle turns of the cochlea with little affection of the apical turns.

Group IV (Dexamethasone 1 day before cisplatin):

Intratympanic administration of dexamethasone, one day before intraperitoneal cisplatin injection, H&E-stained sections of the cochleae showed moderate protection against cisplatin ototoxicity. Widely spaced OHCs with slightly vacuolated cytoplasm were detected (Figure 9). Other sections showed degenerated OHCs with pyknotic nuclei together with slight vacuolization of the IHC (Figure 10). Vacuolization of the cytoplasm

of the supporting cells was also observed (Figures 9 & 10). The fibrous connective tissue meshwork underneath the stria vascularis showed apparently decreased thickness as compared with Group III (Cisplatin group). Cytoplasmic vacuolization was also noticed in the epithelial cells of the stria, especially in the intermediate and basal layers (Figure 11).

Group V (Dexamethasone 1 hour before cisplatin):

Intratympanic administration of dexamethasone, one hour prior to cisplatin intraperitoneal injection markedly protected the hair cells from cisplatin ototoxicity. The OHCs and IHCs structure was seen comparable to the control. The supporting cells were slightly vacuolated (Figure 12), while stria vascularis and the thickness of its underlying fibrous connective tissue meshwork were seen comparable to the control group (Figure 13).

Scanning electron microscopic results:

Group I (Control):

Examination of the organ of Corti of the control group showed the stereocilia of OHCs arranged in three rows as W-shaped organized structures. The IHCs were arranged in one row with their U-shaped organized stereocilia (Figure 14).

Group III (Cisplatin):

After cisplatin intraperitoneal injection, the arrangement of the three rows of OHCs showed disarray in some specimens (Figure 15). The stereocilia of OHCs were seen lost in many places. Most of the remaining stereocilia showed disarrangement, fusion and loss of their regular W-shaped pattern (Figure 16). Many of stereocilia of OHCs showed formation of membrane blebs and others were lost (Figure 17). On the other hand, no loss of IHCs stereocilia was noticed in this group. However, disarrangement, backward deflection and membrane blebs of some IHCs' stereocilia were obvious (Figure 17). Moreover, membrane blebs were seen on the top surface of the supporting cells (Figures 16 & 17). Again these findings were mostly seen in the basal and middle turns of the cochlea.

Group IV (Dexamethasone 1 day before cisplatin):

Dexamethasone intratympanic administration, one day before cisplatin injection in this group showed loss of some stereocilia of OHCs. Stereocilia of some IHCs were seen disarrayed. The top surface of some supporting cells showed few blebblings (Figure 18).

Group V (Dexamethasone 1 hour before cisplatin):

Intratympanic administration of dexamethasone, one hour before cisplatin

intraperitoneal injection in this group, resulted in protection of the hair cells and their stereocilia as they appeared similar to the control group (Figure 19

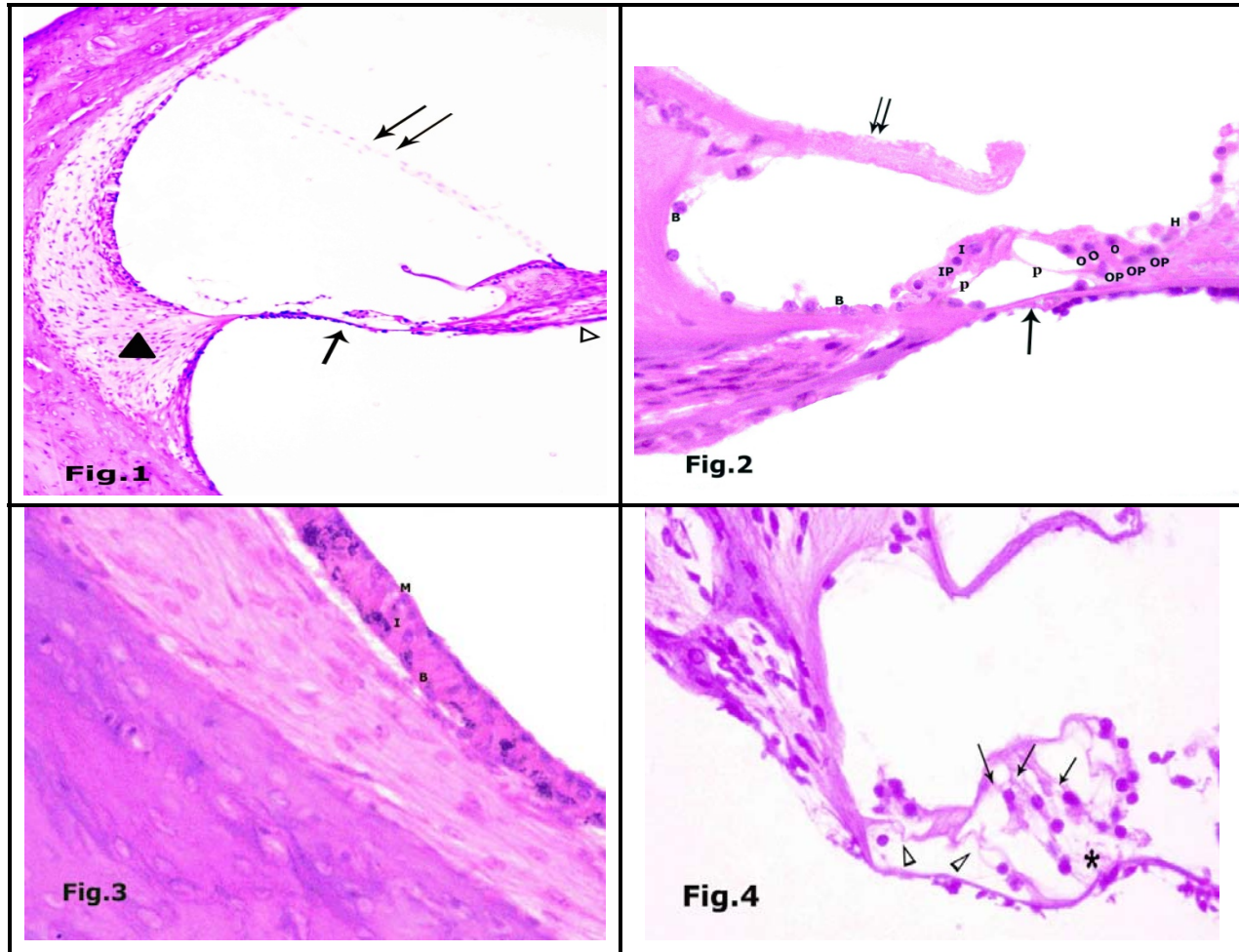


Fig. 1: Showing the wedge-shaped cochlear duct with scala vestibuli above and scala tympani below it. Basilar membrane (↑) is seen extending between spiral ligament (▲) and the spiral lamina (Δ). Reissner's membrane is clearly seen as 2 layers of simple squamous cells (↑↑).

(Group I: H&E × 250)

Fig. 2: Showing the organ of Corti resting on the basilar membrane (↑). OHCs (O), IHC (I), pillar cells (P) can be seen. Other supporting cells as outer phalyngeal (OP), inner phalyngeal (IP), border cells (B), Hensen cells (H) can be noticed. Notice the homogenous acidophilic tectorial membrane hanging over the hair cells (↑↑).

(Group I: H&E × 640)

Fig. 3: Showing the marginal cells (M), intermediate cells (I) and basal cells (B) of stria vascularis epithelium. Notice the fibrous connective tissue meshwork underneath.

(Group I: H&E × 640)

Fig. 4: Showing cytoplasmic vacuolization of OHCs (↑). Notice the vacuolated pillar cells (Δ) and outer phalyngeal cells (*).

(Group III: H&E × 640)

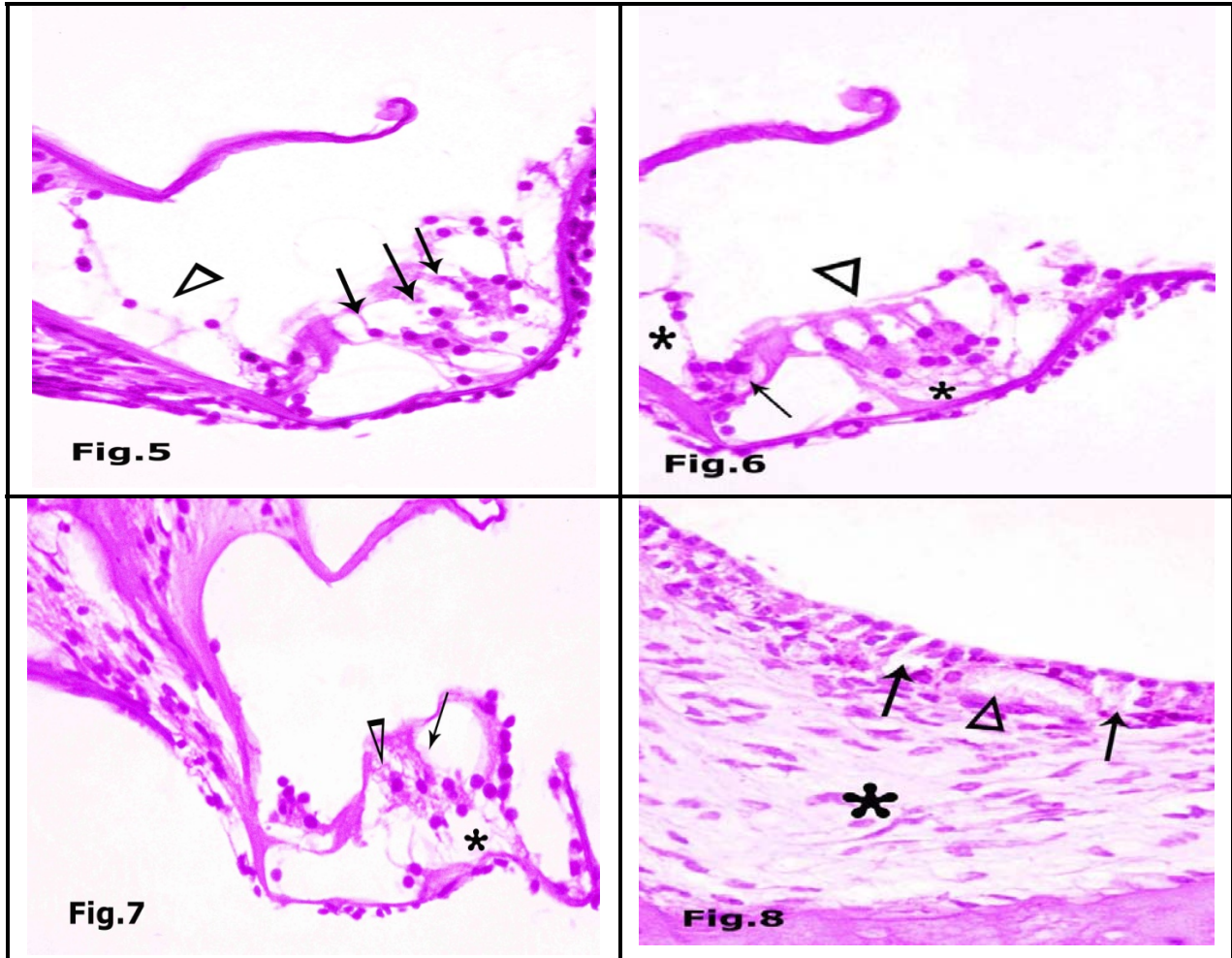


Fig. 5: Showing degenerated OHCs (↑) and swollen vacuolated supporting cells with pyknotic nuclei (Δ).
(Group III: H&E × 640)

Fig. 6: Showing widely-spaced OHCs (Δ) and slightly vacuolated IHC (↑). Vacuolated supporting cells can also be seen (*).
(Group III: H&E × 640)

Fig. 7: Showing absent OHC in the third row (↑) and degeneration of the other OHCs (Δ). Notice the vacuolated supporting cells (*).
(Group III: H&E × 640)

Fig. 8: Showing vacuolated cells in the stria vascularis (↑). Apparently thickened fibrous connective tissue meshwork (*) compared with control and dilated congested intraepithelial capillaries (Δ) can be seen.
(Group III: H&E × 640)

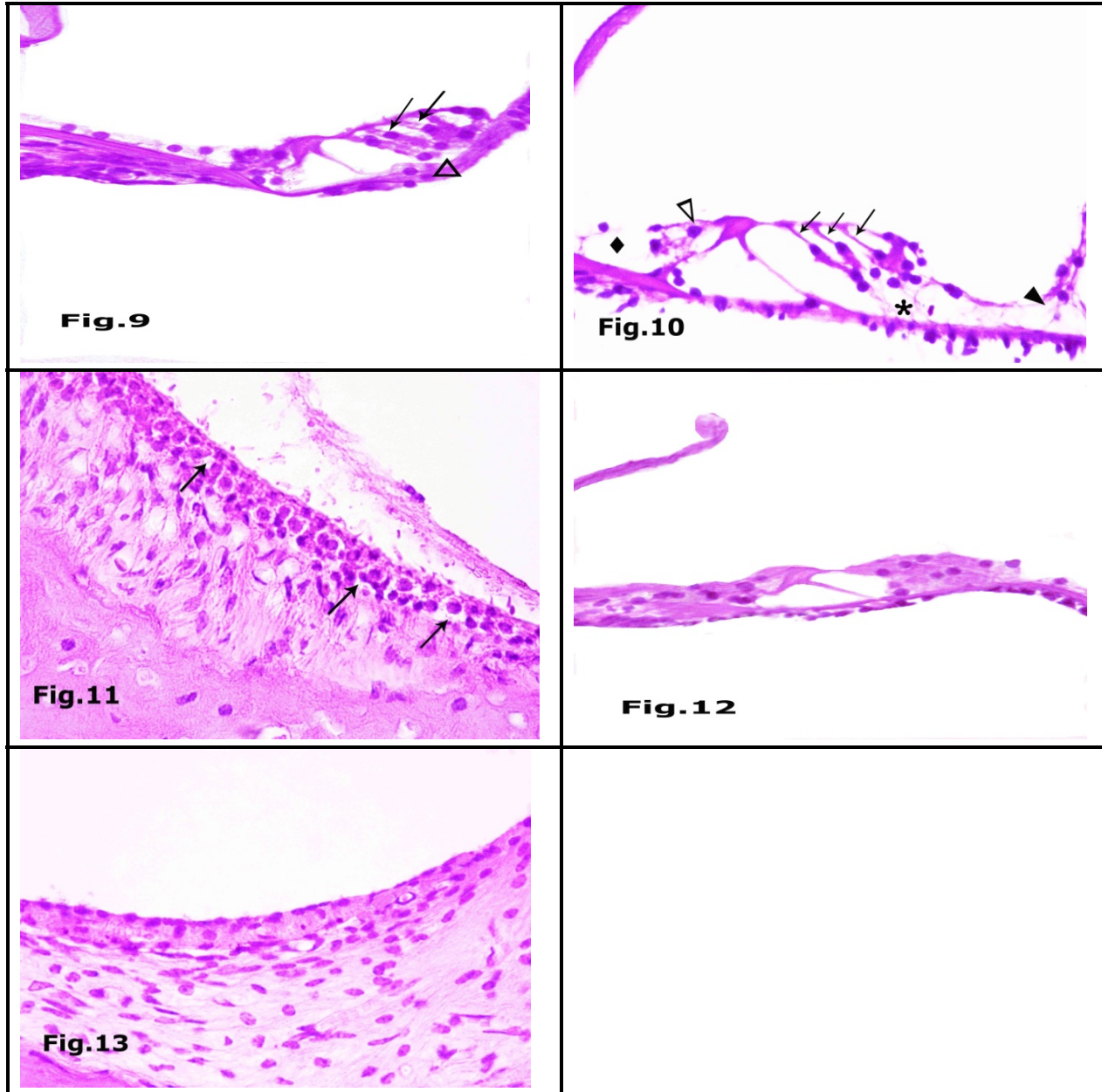


Fig. 9: Showing widely spaced and slightly vacuolated OHCs (↑). Slightly vacuolated supporting cells can be seen (Δ).
(Group IV: H&E × 640)

Fig. 10: Showing degenerated OHCs with pyknotic nuclei (↑). Notice the vacuolated IHC (Δ), outer pharyngeal cells (*), Hensen cells (▲) and border cells (◆).
(Group IV: H&E × 640)

Fig. 11: Showing apparently decreased thickness of the fibrous connective tissue meshwork underneath the stria vascularis compared with group III. Cytoplasmic vacuolization can be seen in the cells of the intermediate and basal layers (↑).
(Group IV: H&E × 640)

Fig. 12: Showing the OHCs and IHC comparable to the control group.
(Group V: H&E × 640)

Fig. 13: Showing apparently normal stria vascularis as compared with the control group.
(Group V: H&E × 640)

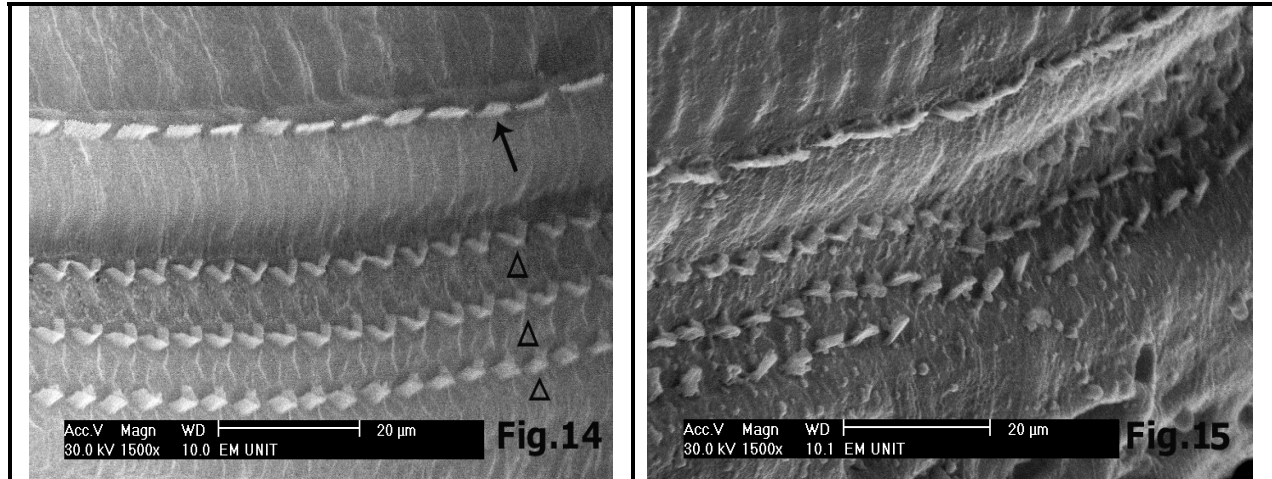


Fig. 14: Showing the W-shaped arrangement of the stereocilia of the three rows of OHCs (Δ). The stereocilia of the IHC row is seen as U-shape (↑). (Group I: SEM × 1500)

Fig. 15: Showing disarray of the three rows' arrangement of OHCs. (Group III: SEM × 1500)

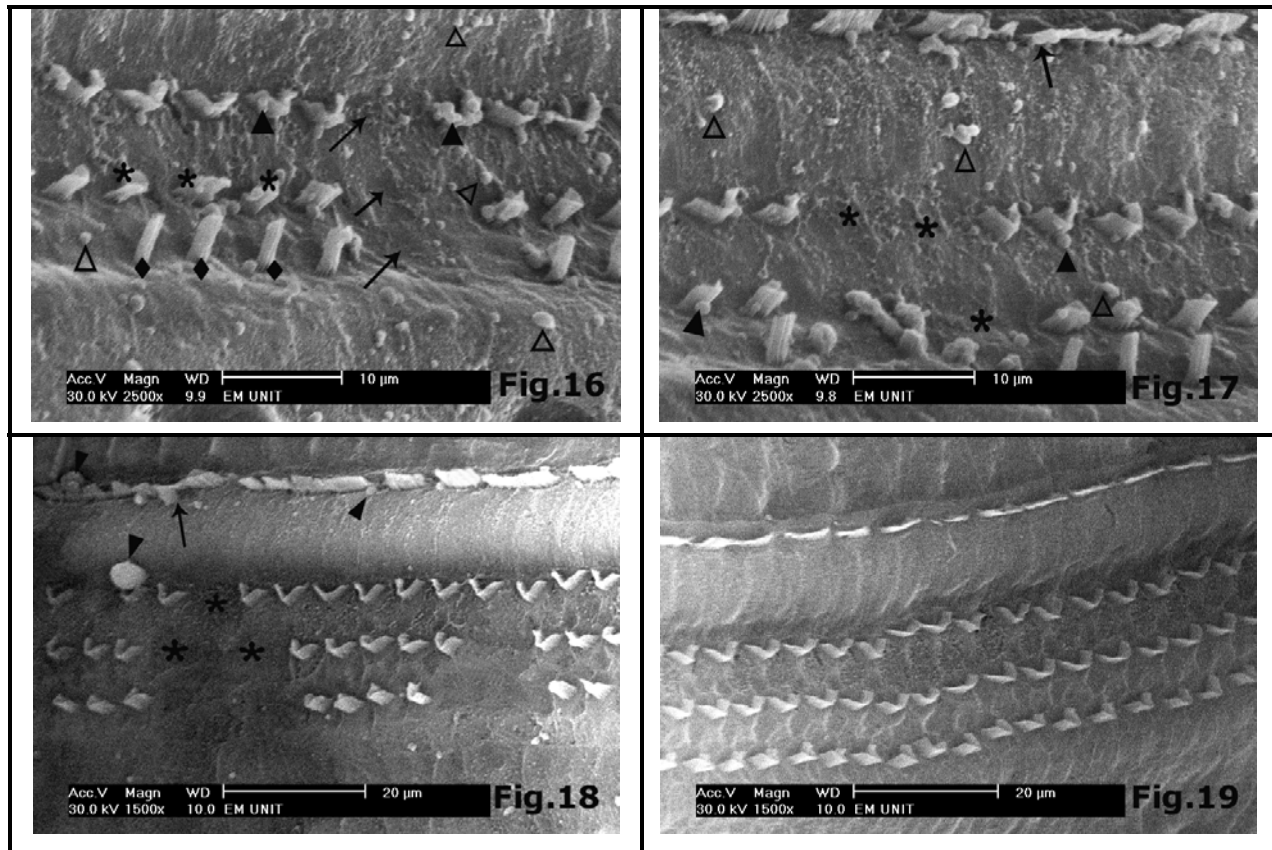


Fig. 16: Showing lost (↑), disarranged (*) and fused (◆) stereocilia of some OHCs. Multiple blebs can be easily seen in the stereocilia of hair cells (▲) and in the top of supporting cells (Δ). (Group III: SEM × 2500)

Fig. 17: Showing backward deflection and blebbing (↑) of IHC stereocilia. Some stereocilia of OHCs show blebs (▲), whereas others are lost (*). Notice the blebbing in the top of the supporting cells (Δ). (Group III: SEM × 2500)

Fig. 18: Showing loss of stereocilia of some OHCs (*). Disarray (↑) of stereocilia of some IHCs can be seen. Notice the few blebs in the top of some supporting cells (▲). (Group IV: SEM × 1500)

Fig. 19: Showing apparently normal organization of stereocilia of OHCs and IHCs. (Group V: SEM × 1500)

B) Morphometric and Statistical histological results:**Table (3): Showing the Mean \pm SEM of thickness of the central part of the fibrous connective tissue meshwork underneath the stria vascularis in μm and comparison between all groups: (After administration of drugs)**

	Group I (control)	Subgroup IIa (Saline)	Subgroup IIb (Dexa)	Group III (Cisplatin)	Group IV (Dexa 1 day before Cisplatin)	Group V (Dexa 1 hour before Cisplatin)
Thickness Of meshwork	24.05 \pm 0.85 (8)	25.81 \pm 1.47 (8)	25.40 \pm 1.56 (8)	53.71 \pm 2.02 ^a (6)	24.06 \pm 1.55 ^b (6)	23.78 \pm 1.44 ^b (6)

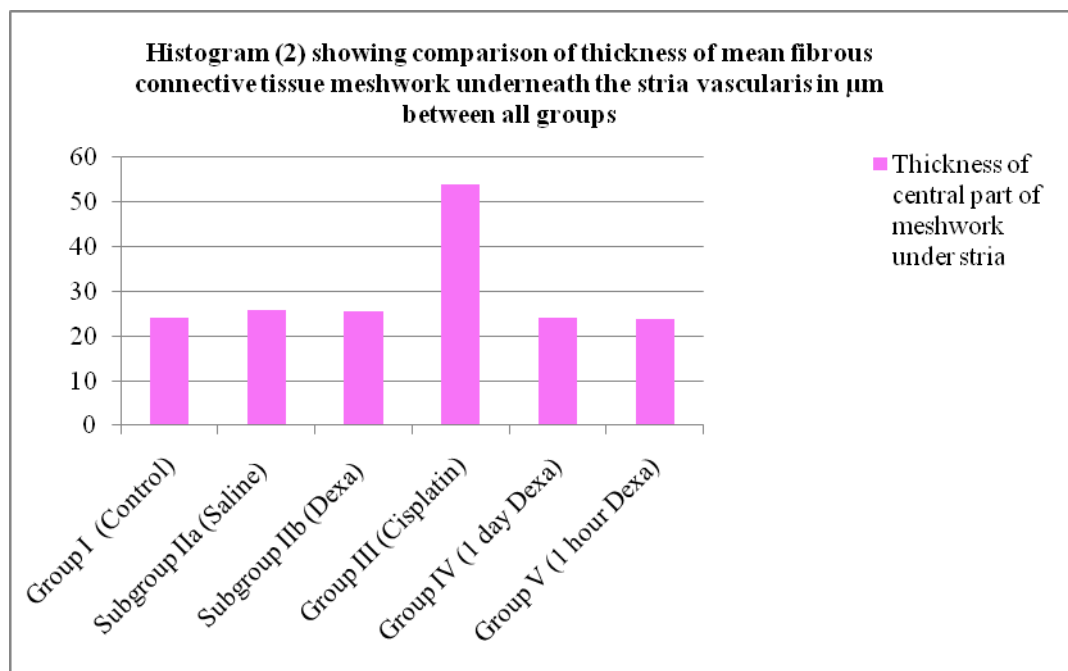
-Values are mean \pm SEM. - Number in parenthesis indicates the number of guinea pigs. Dexa= Dexamethasone

- a: significance of difference by LSD from Group I (Control) at least $p < 0.05$.

- b: significance of differences by LSD from Group III (Cisplatin) at least $p < 0.05$.

As shown in table (3) and histogram (2), both subgroups of group II showed statistically non-significant difference in the mean thickness of the fibrous connective tissue meshwork underneath the stria vascularis ($p > 0.05$) compared with the control. On the other hand, group III (Cisplatin group) showed significant increase in the mean thickness of the fibrous connective tissue meshwork underneath the stria vascularis ($p < 0.05$) compared with the control. However, each of groups IV (administered dexamethasone 1 day before cisplatin) and group V (administered dexamethasone 1 hour before

cisplatin) showed non-significant statistical difference in the mean thickness of the fibrous connective tissue meshwork underneath the stria vascularis ($p > 0.05$) compared with the control. On the other hand, each of groups IV (administered dexamethasone 1 day before cisplatin) and group V (administered dexamethasone 1 hour before cisplatin) showed significant decrease in the mean thickness of the fibrous connective tissue meshwork underneath the stria vascularis ($p < 0.05$) compared with group III (cisplatin group).



Dexa= Dexamethasone

4. Discussion:

Cisplatin ototoxicity continues to be a challenging side effect affecting a majority of cancer patients receiving it as chemotherapy (17). The present study tried to investigate the cisplatin ototoxicity using a dose equivalent to that used in humans undergoing cisplatin chemotherapy worldwide (18, 19). On the other hand, the concentration of dexamethasone used in the current study is the only one available in the Egyptian market and used by clinicians in a variety of diseases.

In the present study, before administration of cisplatin and any intratympanic injection, all guinea pigs were evaluated using ABR to ensure normal hearing. On the other hand, cisplatin presented its ototoxic effect detected in the significant increase in the mean ABR threshold compared with the control. This coincides with the presence of histological degenerative changes in group III in this study particularly in the basal turns of the cochlea.

The OHCs were the most affected by cisplatin ototoxicity in group III in this study especially in the lower turns. This agreed with recent studies reporting similar findings in OHCs, spiral ganglion cells and neurons in the auditory brainstem nuclei. The damage was noticed primarily in the high frequency region of the cochlea (10, 20, 21). This may be due to a progression of drug ototoxicity in a base to apex gradient (10). This could be attributed to lower levels of antioxidants found in the base, hence, increased this zone's susceptibility to free radicals (22). Coinciding with the results of the present study, some authors reported that the most important finding after cisplatin administration was the loss of OHCs' stereocilia starting in the third row at the basal turn (23). They added that the stereocilia were disarrayed and fused which agrees with the results of group III in the present study. This might be caused by loss of lateral cross links connecting the tips of stereocilia of the same or adjacent rows to make them function as a unit (24).

The IHCs were far less intensely affected by cisplatin ototoxicity in group III in the present work. This was in agreement with a number of studies reporting that IHCs were noticeably less affected by cisplatin ototoxicity (23, 25).

Vacuolization of supporting cells of the organ of Corti was noticed in cisplatin group (group III) in the present study. This extends the results of some investigators who attributed this finding to swelling of mitochondria (26). Others reported that the supporting cells were more sensitive than hair cells that the ultrastructural changes preceded any detectable affection of OHCs (18).

The thickness of the fibrous connective tissue meshwork underneath the stria vascularis was also found apparently increased after cisplatin injection in group III of the present work. This was confirmed by the significant increase in its mean thickness in group III compared with group I. This could be attributed to edema formation in this tissue. In agreement, a previous study reported edema formation in the connective tissue underneath the stria vascularis followed by severe atrophy after cisplatin therapy (27). This might be secondary to immune-mediated cochlear destruction induced by ototoxic drugs, leading to cochlear inflammatory process as reported in a recent study (28). Other investigators reported that proinflammatory cytokines as tumour necrosis factor-alpha (TNF- α), interleukin-1beta, and interleukin-6 and nuclear factor kappa B (NF κ B) are upregulated by cisplatin treatment in vitro and in the rat cochleae (29). Other authors reported injury of stria vascularis in a time course paralleling OHCs loss, suggesting that cisplatin targets it directly (30). Coinciding, group III in this study showed that cisplatin-induced vacuolar degeneration in the epithelial cells of the stria vascularis and showed dilated congested intraepithelial capillaries.

Several mechanisms might be involved in cisplatin-induced ototoxicity. Recent studies showed that a trans-membrane trimer localized in the hair cells (copper transporter; ctr1) enhanced the cellular uptake and influx of cisplatin, hence increasing its cytotoxicity (31, 32). Upon entering the cells, cisplatin integrates into the DNA causing its cross linking and damage that result in accumulation of dysfunctional protein and inefficient enzyme synthesis (33). Progressively, the cochlea becomes unable to flush out the accumulated toxins at a rapid rate, thus reactive oxygen species (ROS) overloads. Combined with the expected depletion of antioxidants, cell injury and apoptosis is the result (34). Cisplatin-mediated ROS generation depends on induction and activation of a permeant channel used by cisplatin called "the transient receptor potential vanilloid 1 (TRPV1) channel. This activation might enhance Ca⁺⁺ influx and overload (35). The resulting increase in intracellular Ca⁺⁺ might inhibit a group of ATPases known as aminophospholipid translocases (APTLs) that maintain the normal asymmetrical distribution of phosphatidylserine and phosphatidylethanolamine across the plasma membrane (36, 37). At the same time, this activates phospholipid scramblases that randomize all membrane phospholipids between leaflets resulting in a complete loss in cell membrane lipid asymmetry (38). This might cause disturbance of cell membrane and consequently formation of membrane blebs that

was noticed by SEM examination in the stereocilia of OHCs, IHCs and in the top surfaces of several supporting cells in the present study.

Furthermore, cisplatin was found to activate big conductance K^+ channels (BK) in the fibrocytes of the spiral ligament of cochlear lateral wall. This led to disruption of the electrochemical gradient by K^+ efflux, decreasing intracellular K^+ levels causing disturbance of the ionic concentration essentially needed for hair cell function. The final expected result is triggering apoptosis and cell death (39).

To our knowledge, few investigators tried the intratympanic way of steroid administration for protection from cisplatin-induced ototoxicity. They suggested that this way of local drug application was safe and feasible, avoiding systemic side effects without compromising the tumoricidal efficacy of chemotherapy (10, 28).

Recently, a study reported that intratympanic injection ensured a high concentration of the protective drug to enter the inner ear directly aiming the target organ (40). These authors added that steroids injected into the middle ear could reach scala tympani within minutes, mainly through the round window membrane and minimally through oval window membrane. It then quickly reaches scala vestibuli through the spiral ligament laterally or Rosenthal canal medially. The communication routes between scala tympani and the organ of Corti and spiral ganglion assure that hair cells and nerve cells will rapidly be exposed to drugs delivered through the round window. The presence of drug within the scala media demonstrated transport into the endolymphatic spaces as well (41). Dexamethasone, after its intratympanic injection, had a higher rate of endocytosis, hence greater intracellular efficacy in contrast to other steroids as methyl prednisolone (42). This was the reason behind our choice of dexamethasone in particular in the present work.

In the present study, intratympanic dexamethasone alone (subgroup IIb) had non-significant statistical difference in comparison with the saline administration (subgroup IIa) and with control animals (group I) in relation to ear functional assessment by ABR. This also matched the histological finding as no apparent structural abnormality was observed in the structure of the cochleae by either H&E stain or by SEM examination of dexamethasone treated cochleae of subgroup IIb compared with control. Moreover, subgroup IIb showed non-significant statistical difference in the mean thickness of the fibrous connective tissue meshwork underneath the stria vascularis compared with group I. All these results revealed the safety of dexamethasone on cochlear function and structure. This coincides with other

study that reported no change in the cochlear construction and function after intratympanic dexamethasone application in guinea pigs (43).

The results of the present study showed that intratympanic dexamethasone played a protective role against cisplatin-induced ototoxicity by reducing ABR threshold shifts and improving the histological structure. Prior to this study, there were no combined histological and audiological investigations concerning the time dependent effect in better cochlear protection. As shown in the audiological and histological results of the present study, administration of dexamethasone one hour prior to cisplatin intake (Group V) showed much better protection than one day (Group IV). This might be explained by the findings of another study that observed significant levels of dexamethasone in the perilymph within one hour, and decreased by 50-100 folds within 12 hours in guinea pigs (44).

Dexamethasone had multiple effects as an otoprotectant, acting on ion homeostasis and immune suppression (45). Regarding ion homeostasis, dexamethasone increased the expression of Na^+/K^+ channels (46) and of active water channels (aquaporins) in the endolymphatic sac and the tissues surrounding endolymphatic spaces (47). It was documented that the stria vascularis pumps K^+ into the endolymph to maintain the endolymphatic potential critical for normal hearing. This process requires K^+ recycling from the base of hair cells through the spiral ligament via intercellular gap junctions (28). Any pathologic process that interferes with this movement of K^+ or stria vascularis function will cause hearing loss. Through both Na^+/K^+ and aquaporins channels, dexamethasone could effectively maintain the tightly regulated ion transport mechanisms critically needed for auditory and vestibular hair cell functions (46). As for immune suppression, intratympanic dexamethasone down regulated greater number of proinflammatory cytokine genes in the cochlear tissues than if delivered systemically (48). Immune-mediated cochlear tissue destruction resulting from ototoxic drugs usually initiated cochlear inflammatory processes that are responsive to glucocorticoid treatments. Therefore, immune suppression is a key factor in protecting the ear or reversing hearing loss (28). This may explain the absence of edema noticed in the cochleae of groups IV and V, administered intratympanic dexamethasone one day and one hour respectively before cisplatin in the present study. This was reflected by the significant decrease in the mean thickness of the fibrous connective tissue meshwork underneath the stria vascularis compared with group III (cisplatin group). However, each of groups IV and V showed non-significant statistical

difference in the mean thickness of the fibrous connective tissue meshwork underneath the stria vascularis compared with the control. In addition, dexamethasone reported to act as a slowly-acting free radical scavenger greatly accounting for cisplatin ototoxicity (49). Thus, all these functions (ion homeostasis, immune suppression and free radical scavenging) seem to be quite interlinked as regard to maintenance of the endolymphatic potential of fluids around auditory and vestibular hair cells.

Conclusion:

It is concluded that cisplatin ototoxic insult is planned and predictable that possible protection by intratympanic dexamethasone administration should be given precisely in good timing before the insult. Giving the drug as early as one hour yielded marvelous protective effect and turned to be a perfect timing of interference before cisplatin chemotherapy treatment session begins. We recommend following this way of protection as it proved to be safe, easily performed by an otolaryngologist in the same clinic in which cisplatin injection is to be performed.

Acknowledgement:

We dedicate this work to the soul of our beloved, most respectable colleague Mirahan Thabet, lecturer of audiology, Faculty of medicine, Ain Shams University. Without her great participation as a main author in this study, this work was never to be done.

Corresponding author:

Nevine Bahaa E. Soliman
Histology Department, Ain Shams University,
Cairo, Egypt. nbahaasoliman@gmail.com

References

- 1- Rybak L, Whitworth C (2005). Ototoxicity: therapeutic opportunities. *Drug Discov Today*;10:1313-21.
- 2- Bokemeyer C, Berger CC, Hartmann JT, Kollmannsberger C, Schmoll HJ, Kuczyk MA, Kanz L (1998). Analysis of risk factors for cisplatin-induced ototoxicity in patients with testicular cancer. *Br J Cancer*;77:1355-62
- 3- Rybak L, Mukherjea D, Jajoo S, Ramkumar V (2009). Cisplatin ototoxicity and protection: clinical and experimental studies. *Tohoku J Exp Med*; 219(3): 177-86.
- 4- Rybak L, Whitworth C, Mukherjea D, Ramkumar V (2007). Mechanisms of cisplatin-induced ototoxicity and prevention. *Hear Res*; 226:157-67.
- 5- Bird PA, Murray DP, Zhang M, Begg EJ (2011). Intratympanic versus intravenous delivery of dexamethasone and dexamethasone sodium phosphate to cochlear perilymph. *Otol Neurotol*;32(6):933-6.
- 6- Herr I, Ucur E, Herzer K, Okouoyo S, Ridder R, Krammer PH, von Knebel Doeberitz M, Debatin KM (2003). Glucocorticoid cotreatment induces apoptosis resistance toward cancer therapy in carcinomas. *Cancer Res*;63:3112-20.
- 7- Hargunani C, Kempton J, DeGagne J, Trune D (2006). Intratympanic injection of dexamethasone: time course of inner ear distribution and conversion to its active form. *Otol Neurotol*; 27:564-69.
- 8- Kara E, Cetik F, Tarkan O, Sürmelioglu O (2010). Modified intratympanic treatment for idiopathic sudden sensorineural hearing loss. *Eur Arch Otorhinolaryngol*; 267(5):701-7.
- 9- Barrs DM (2004). Intratympanic corticosteroids for Meniere's disease and vertigo. *Otolaryngol Clin North Am*; 37: 955-72.
- 10- Hill G, Morest D, Parham K (2008). Cisplatin-Induced Ototoxicity: Effect of Intratympanic Dexamethasone Injections. *Otol Neurotol* October; 29(7): 1005-11.
- 11- Ekborn A, Laurel G, Ehrsson H, Miller J (2003). Intracochlear administration of thiourea protects against cisplatin-induced outer hair cell loss in the guinea pig. *Hear Res*; 181(1-2): 109-15.
- 12- Dang V, Bao S, Ault A, Murray C, Mills JM, Chiedi C, Dillon M, Todd JP, DeTolla L, Rao S (2008). Efficacy and safety of five injectable anesthetic regimens for chronic blood collection from the anterior vena cava of guinea pigs. *Journal of the American Association for Laboratory Animal Science* November;47(6):56-60
- 13- Kalcioğlu MT, Kizilay A, Gulec M, Karatas E, Iraz M, Akyol O, Egri M, Ozturan O (2005). The protective effect of erdosteine against ototoxicity induced by cisplatin in rats. *Eur Arch Otorhinolaryngol* Oct;262(10):856-63.
- 14- Ramírez-Camacho R, Citores MJ, Trinidad A, Verdaguera JM, García-Berrocal JR, Marero AM, Puente A, González-García JA, Vargas JA (2007). HSP-70 as a nonspecific early marker in cisplatin ototoxicity. *Acta Otolaryngol Jun*;127(6):564-7.
- 15- Bancroft JD and Gamble M (2008). *Theory and Practice of Histological Techniques*. 6th edition. Churchill Livingstone Elsevier;126.
- 16- Kaltenbach J, Rachel J, Mathog A, Zhang J, Falzarano P, Lewandowski M (2002). Cisplatin-Induced hyperactivity in the dorsal cochlear nucleus and its relation to outer hair cell loss: relevance to tinnitus. *J neurophysiol*; 88(2): 699-714.
- 17- Zuur CL, Simis YJ, Lansdaal PE, Hart AA, Schornagel JH, Dreschler WA, Rasch CR, Balm AJ (2007). Ototoxicity in a randomized phase III trial of intraarterial compared with intravenous cisplatin chemoradiation in patients with locally advanced head and neck cancer. *J Clin Oncol*; 20;25(24):3759-65
- 18- Blakley BW, Hochman J, Wellman M, Gool A, Hussain AE (2008). Differences in ototoxicity across species. *J Otolaryngol Head Neck Surg* Oct; 37(5): 700-3
- 19- Ramirez-Camacho R, Garcia-Berrocal J, Bujan J, Martin-Marero A, Trinidad A (2004). Supporting cells as a target of cisplatin-induced inner ear damage: therapeutic implication. *Laryngoscope*; 114(3): 533-7
- 20- De Freitas MR, Figueiredo AA, Brito GA, Leitao RF, Carvalho Junior JV, Gomes Junior RM, Ribeiro Rde A (2009). The role of apoptosis in cisplatin-induced ototoxicity in rats. *Braz J otorhinolaryngol* Sept-Oct ;75(5) :745-52
- 21- Salt AN (2008). Dexamethasone concentration gradients along scala tympani after application to the round window membrane. *Otol Neurotol* April; 29(3): 401-6.
- 22- Sha SH, Taylor R, Forge A, Schacht J (2001). Differential vulnerability of basal and apical hair cells is based on intrinsic susceptibility to free radicals. *Hear Res*; 155:1-8.

- 23- Garcia-Berrocal JR, Nevado J, Ramirez-Camacho R, Sanz R, Gonzalez-Garcia JA, Sanchez-Rodriguez C, Cantos B, Espana P, Verdague JM, Trinidad A (2007). The anticancer drug cisplatin induces an intrinsic apoptotic pathway inside the inner ear. *British Journal of Pharmacology*;152: 1012-20
- 24- Osborne M, Comis S (1990). High resolving scanning electron microscopy of stereocilia in the course of normal, postmortem and drug-treated guinea pigs. *Electron Microscop Tech*; 15(3): 245-60
- 25- Wang J, Ladrech S, Pujol R, Brabet P, Van De Water TR, Puell JL (2004). Caspase inhibitors, but not c-Jun NH2-terminal kinase inhibitor treatment, prevent cisplatin-induced hearing loss. *Cancer Res*; 64(24):9217-24.
- 26- Cardinaal RM, de Groot JCMJ, Huizing EH, Smoorenburg GF, Veldman JE (2004). Ultrastructural changes in the adult guinea pig cochlea at different survival times following cessation of 8 day cisplatin administration. *Otolaryngol*; 124(2): 144-54
- 27- Lee JE, Nagakawa T, Kita T, Kim TS, Iguchi F, Endo T, Shiga A, Iguchi F, Lee SH, Ito J (2004). Mechanisms of apoptosis induced by cisplatin in marginal cells in mouse stria vascularis. *ORL J Otorhinolaryngol Relat Spec*; 66:111-18.
- 28- Daldal A, Odabasi O, Serbetcioglu B (2007). The protective effect of intratympanic Dexamethasone on cisplatin-induced ototoxicity in guinea pigs. *Otolaryngol Head Neck Surg*; 137:747-52.
- 29- So H, Kim H, Kim Y, Kim E, Pae HO, Chung HT, Kim HJ, Kwon KB, Lee KM, Lee HY, Moon SK, Park R (2008). Evidence that cisplatin-induced auditory damage is attenuated by downregulation of proinflammatory cytokines via Nrf2/HO-1. *J. Assoc. Res. Otolaryngol*; 9:290-306.
- 30- Van Ruijven MWM, de Groot JCMJ, Klis SFL, Smoorenburg G (2005). Cochlear targets of cisplatin: an electrophysiological and morphological time-sequence study. *Hear Res*; 205: 241-48.
- 31- More SS, Akil O, Ianculescu AG, Geier EG, Lustig LR, Giacomini KM (2010). Role of the copper transporter, CTR1, in platinum-induced ototoxicity *J Neurosci* July 14; 30(28): 9500-9
- 32- Ding D, He J, Allman BL, Yu D, Jiang H, Seigel GM, Salvi RJ (2011). Cisplatin ototoxicity in rat cochlear organotypic cultures. *Hear Res* Aug; 12 [Epub ahead of print].
- 33- Caronia D, Patino-Garcia A, Milne RL, Zalacain-Diez M, Pita G, Alonso MR, Moreno LT, Sierrasesumaga-Arznabarreta L, Benitez J, Gonzaler-Neira A (2009). Common variations in ERCC2 are associated with response to cisplatin chemotherapy and clinical outcome in osteosarcoma patients. *Pharmacogenomics J*; 9: 347-53.
- 34- Rybak LP, Husain K, Morris C, Whitworth C, Somani S (2000). Effect of protective agents against cisplatin ototoxicity. *Am J Otol*; 21:513-20
- 35- Mukherjea D, Jajoo S, Whitworth C, Bunch JR, Turner JG, Rybak LP, Ramkumar V (2008). Short interfering RNA against transient receptor potential vanilloid 1 attenuates cisplatin-induced hearing loss in the rat. *J. Neurosci*; 28:13056-13065.
- 36- Devaux PF (1992). Protein involvement in transmembrane lipid asymmetry. *Annu Rev Biophys Biomol Struct*; 21: 417-439.
- 37- Bitbol M, Fellmann P, Zachowski A and Devaux PF (1987). Ion regulation of phosphatidylserine and phosphatidylethanolamine outside-inside translocation in human erythrocytes. *Biochim Biophys Acta*; 904: 268-282.
- 38- Zhou Q, Zhao J, Stout JG, Luhm RA, Wiedmer T and Sims PJ (1997). Molecular cloning of human plasma membrane phospholipid scramblase. A protein mediating transbilayer movement of plasma membrane phospholipids. *J Biol Chem*; 272: 18240-18244.
- 39- Liang F, Schulte BA, Qu C, Hu W, Shen Z (2005). Inhibition of the calcium- and voltage-dependent big conductance potassium channel ameliorates cisplatin-induced apoptosis in spiral ligament fibrocytes of the cochlea. *Neuroscience*; 135:263-71.
- 40- Salt AN, Plontke SK (2009). Principles of local drug delivery to the inner ear *Audiol Neurotol*;14:350-360
- 41- Banerjee A, Parnes LS (2004). The biology of intratympanic drug administration and pharmacodynamics of round window drug absorption. *Otolaryngol Clin North Am Oct*; 37(5):1035-51.
- 42- Parnes LS, Sun AH, Freeman DJ (1999). Corticosteroid pharmacokinetics in the inner ear fluids: an animal study followed by clinical application. *Laryngoscope*;109:1-17
- 43- Liu HJ, Dong MM, Chi FL (2005). Structure and function influence of cochlear after dexamethasone intratympanic application. *Zhonghua Er Bi Yan Hou Tou Jing Wai Ke Za Zhi Jun*; 40(6):440-3. Abstract
- 44- Wang X, Fernandez R, Dellamary L, Harrop A, Ye Q, Lichter J, Lau D, Lebel C, Piu F (2010). Pharmacokinetics of Dexamethasone solution following Intratympanic Injection in Guinea Pig and Sheep. *Audiol Neurotol Oct* 28; 16(4):233-41.
- 45- Ahn JH, Yoo MH, Yoon TH, Chung JW. Can intratympanic dexamethasone added to systemic steroids improve hearing outcome in patients with sudden deafness? *Laryngoscope* 2008; 118:279-82
- 46- Pondugula SR, Raveendran NN, Ergonul Z, Deng Y, Chen J, Sanneman JD, Palmer LG, Marcus DC (2006). Glucocorticoid regulation of genes in the amiloridesensitive sodium transport pathway by semicircular canal duct epithelium of neonatal rat. *Physiol Genomics*; 24:114-23.
- 47- Ishiyama G, Lopez IA, Ishiyama A (2006). Aquaporins and Meniere's disease. *Curr Opin Otolaryngol Head Neck Surg*; 14:332-36.
- 48- Hamid M, Trune D (2008). Issues, indications, and controversies regarding intratympanic steroid perfusion. *Curr Opin Otolaryngol Head Neck Surg October*; 16(5): 434-40
- 49- Paksoy M, Ayduran E, Sanli A, Eken M, Aydın S, Oktay ZA (2011). The protective effects of intratympanic dexamethasone and vitamin E on cisplatin-induced ototoxicity are demonstrated in rats. *Med Oncol Jun*; 28(2):615-21.

12/12/2011

**Extracellular Metabolites Produced by a Novel Strain, *Bacillus alvei* NRC-14:
3. Synthesis of a Bioflocculant that has Chitosan-Like Structure**

Shadia M. Abdel-Aziz*¹, Hoda A. Hamed¹, Foukia E. Mouafi² and Nayera A. M. Abdelwahed³

Microbial Chemistry Dept.¹, Microbial Biotechnology Dept.², Chemistry of Natural and Microbial Products Dept.³,
National Research Centre Dokki, Cairo, Egypt.

*abdelaziz.sm@gmail.com

Abstract: An extracellular biopolymer flocculant (BPF) was produced by a novel strain, *Bacillus alvei* NRC-14, cultivated in low nutritional medium. Effect of carbon and nitrogen sources as well as the initial pH and medium components, on production of the BPF were studied. Production of this BPF is induced in presence of chitosan or chitosan-containing substrate as carbon source, suggesting a correlation between the activities of several key enzymes involved in the pathway with the yield of the BPF. Therefore, biosynthetic pathway of this BPF may starts with an aminosugar as a precursor which was then, presumably, polymerized and converted to a bioflocculant. The highest production was achieved in low nutrition medium containing: dried mycelium of the fungus *Mucor rouxii* (10g/L), (NH₄)₂SO₄ (1.5g/L) and MgSO₄·7H₂O (0.5g/L). The flocculating activity reached 98% in less than 48 hr of growth. The produced bioflocculant is a polysaccharide consisting of aminosugars and has good flocculating activity in charcoal or kaolin clay suspension, without any cation addition. IR-spectra elucidate that, the BPF has chitosan-like structure with a molecular weight of 6.9 x 10⁴ Da. Surprisingly, shelf-life studies of this BPF revealed that it retained 94% of its flocculating activity after keeping at room temperature for up to 6 months period, indicating its higher stability. This is the first report about a bioflocculant that has chitosan-like structure produced by a novel strain, *Bacillus alvei* NRC-14.

[Shadia M. Abdel-Aziz, Hoda A. Hamed, Foukia E. Mouafi and Nayera A. M. Abdelwahed. **Extracellular Metabolites Produced by a Novel Strain, *Bacillus alvei* NRC-14: 3. Synthesis of a Bioflocculant that has Chitosan-Like Structure**/Life Science Journal, 2011; 8(4): 883-890] (ISSN: 1097-8135).
<http://www.lifesciencesite.com>.

Key words: Extracellular metabolites, *Bacillus alvei* NRC-14, biopolymer flocculant, *Mucor rouxii*, chitosan.

1. Introduction

Bioflocculation is a dynamic process resulting from the synthesis of extracellular polymers by microorganisms during their growth. Flocculation was first reported, in 1876, by Louis Pasteur (Salehizadeh and Shojaosadati, 2001) and has been extensively investigated update. A correlation was established between the accumulation of extracellular bioflocculants and cell aggregation (Tenny and Verhoff, 1973). The term flocculation is used to describe the aggregation of microbial cells to form flocs with other sediments in the culture. Bioflocculants are useful in aggregation of colloids, cells, cell debris, sediments, etc. The predominant components of bioflocculant are extracellular polymeric substances such as polysaccharides, proteins, glycoproteins, or nucleic acids (Lazarova and Manem 1995; Gao et al. 2006; Leonard et al. 2011). Flocculating agents can be classified into three groups: 1) inorganic flocculants such as aluminium sulfate and polyaluminium, 2) Organic synthetic high-polymer flocculants such as polyacrylamide and polyetheleneamine, and 3) naturally occurring flocculants such as chitosan, and the microbial flocculants (Shih et al. 2001). Organic

synthetic flocculants are widely applied in industrial fields nowadays because they are highly effective, however, their use is environmentally harmful and some of their degraded monomer such as acrylamide, are neurotoxic and even strong human carcinogens (Kwon et al. 1996) and can induce Alzheimer's disease (Arezo 2002) caused by aluminum salts. Moreover, when iron coagulants (such as ferric chloride) are used excessively they may cause corrosion and staining of appurtenances and give rise to unpleasant aesthetic concerns such as odor, color, and metallic taste (Lijun et al.2009). The usage of synthetic flocculants has been restricted mainly in European countries because of their hazardous effects (Ho et al. 2010). Compared with synthetic flocculants, bioflocculants have special advantages such as safety, strong effects, biodegradable, and harmlessness to the environment and human, so they may potentially applied in drinking and wastewater treatment, downstream processing as well as fermentation processes (Mao et al. 2011). Furthermore, flocculation is an industrially accepted practice used in many food processing and pharmaceutical operations, demonstrating that many of the polymers are generally regarded as safe when

the product is intended for human or animal consumption (Cartier et al.1997, Wang et al. 2011). However, a major bottleneck for the commercialization of bioflocculants is the higher production cost compared with inorganic and synthetic flocculants.

In the present study, attention was focused on the bioflocculant produced by a novel strain, *B. alvei* NRC-14. During a study for production of chitosanase by this strain, using mycelium of the fungus *Mucor rouxii* as a carbon source, it was noticed that a culture broth of the strain was highly viscous and displayed high flocculating properties, i.e. the particles of the mycelium were extremely aggregated to the cells of the strain and other sediments. The progress and extent of flocculation were followed by an obvious decrease in turbidity of the culture broth, and the medium seemed very clear. Therefore, in the present study attention was turned for isolating this biopolymer flocculant (BPF). Optimization of the culture conditions, nutritional requirements for maximum production, and some properties of the produced BPF are reported herein. To our knowledge, production of a bioflocculant by a newly isolated, *B.alvei* NRC-14, is reported for the first time.

2. Materials and methods

Microorganism and growth conditions

The strain *B. alvei* NRC-14, used in this study, is a local bacterial strain isolated from the Egyptian soil. Identification and taxonomic studies on the isolate were carried out by methods described in *Bergey's Manual of Systematic Bacteriology* (Juni, 1986). The strain was maintained on nutrient agar slants, stored at 4°C, and subcultured at intervals. To study the effect of growth conditions on production of the bioflocculant, the organism was grown in a broth medium (Tabata and Terui, 1962), containing (g/L): 10, flaked chitosan; 2, K₂HPO₄; 1, KH₂PO₄; 0.5, MgSO₄.7H₂O; 0.1, CaCl₂; 0.5, yeast extract; and 0.1, NaCl. The medium was supplemented with different carbon and nitrogen sources, and the pH was adjusted to different pH values. Flasks were incubated for 5d at 30°C, under shaking conditions (130 rpm).

Production of the bioflocculant

To study the effect of medium components on production of the BPF, the organism was grown in a minimal medium (MM) containing (g/L):10.0, fungal mycelium (FM) of *Mucor rouxii*; 1.5, (NH₄)₂SO₄ and 0.5, MgSO₄.7H₂O. For comparison, an enriched medium (EM) was used, which contained (g/L): 10.0, FM; 1.5, (NH₄)₂SO₄; 2.0, K₂HPO₄; 1.0, KH₂PO₄; 0.1,

NaCl; 0.1, CaCl₂; 0.02, FeSO₄; 0.05, MnSO₄; and 0.5, MgSO₄.7H₂O. The pH value of both medium was adjusted to 5.5. Experiments were done in 1L conical flasks containing 400 ml of each medium. Flasks were inoculated with a pre-culture (4%, v/v) and incubated at 30°C for 5d under shaking conditions (130rpm). Samples were taken at different time intervals and monitored for cell growth, pH, and detection of flocculating activity (FA). Cell-free supernatant was used as the test BPF to determine the flocculating activity (FA).

Preparation of fungul mycelium

The fungus, *M. rouxii*, was grown in potato-dextrose broth and incubated at 30°C for 7d. The pellets were harvested, washed with distilled water, and dried at 50°C. The dried mycelium was homogenized, and used as a carbon source for the production of the BPF.

Calculation of molecular weight

The molecular weight (MW) of the produced BPF in relation to viscosity was calculated according to the method of Il'ina et al. (2001).

Determination of flocculating activity

The FA was measured according to the method of Kurane et al. (1986) using a suspension of charcoal (5g/L, in distilled water) as a test material. To 9.5 ml of charcoal suspension in a test tube, 0.5 ml of cell-free supernatant was added. The reaction mixture was stirred with a vortex mixture and allowed to stand for 5 min. The absorbance of the upper phase was measured at 550 nm, using spectrophotometer. A control sample without the bioflocculant was used. The FA was calculated according to the following equation: Flocculating activity (%) = [(A- B)/ B] x100%, where A and B are the optical densities of the control and the sample, respectively.

Extraction and purification of the crude bioflocculant

The BPF of strain NRC-14 was purified by the method of Shih et al. (2001) as follows: the viscous culture broth (400 ml) was mixed with three volumes of cold distilled water and centrifuged at 7000xg for 20 min. The resultant supernatant was poured into two volumes of cold ethanol to precipitate the bioflocculant. The precipitate was collected by centrifugation at 7000xg for 20 min, and kept at 4°C.

Characterization and some properties of the bioflocculant

The culture supernatant together with the purified BPF was used as test bioflocculants to estimate the effect of flocculant dosage, pH, and temperature on the FA. The culture broth and the purified flocculant were obtained at the same time of cultivation. A control sample was prepared and the FA was measured and calculated as described above. To estimate the influence of the pH value on the FA, a reaction mixture containing charcoal suspension and the bioflocculant was adjusted to pre-determined pH values using HCL or NaOH, and then the FA was measured. The temperature dependence of both flocculants was determined at different degrees of temperature followed by measuring the residual FA of charcoal suspension (Gao et al. 2006).

Analytical methods

Protein content was assayed by the method of Lowry, using bovine serum albumin as standard (Lowry et al. 1951). Amino-sugars were determined by the Elson-Morgan method (Chaplin & Kennedy 1986).

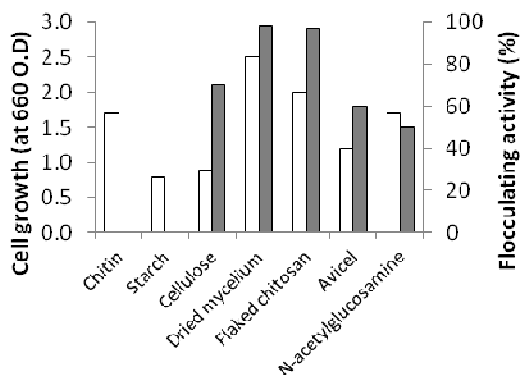


Fig. 1. Effect of carbon source on cell growth (□) and flocculating activity (■). The culture time was 48 h.

IR-spectra of the bioflocculant

The viscous product was analyzed by infrared using a FT-IR-FT Raman (Nexus 670, Nicolet-Madison-WI-USA). The spectrum of the sample was recorded on the spectrophotometer over a wave number range 4000-400 cm^{-1} .

Shelf-life of the bioflocculant

The shelf-life stability of the BPF was studied at room temperature, at 4°C, and under refrigerator conditions. Samples were tested for the FA at different time intervals for up to 12 months.

3. Results

Effect of carbon and nitrogen sources

Strain *B.alvei* NRC-14 grew well with all the carbon sources tested, however, production of the BPF was efficiently produced with FM of *M.rouxii* or flaked chitosan; the FA reached 98% and 97%, respectively (Fig.1). To study the effect of different nitrogen sources on growth and production of the BPF, 0.15% (w/v) each of NaNO_3 , NH_4Cl , NH_4NO_3 , $(\text{NH}_4)_2\text{SO}_4$, as well as yeast extract and peptone were used.

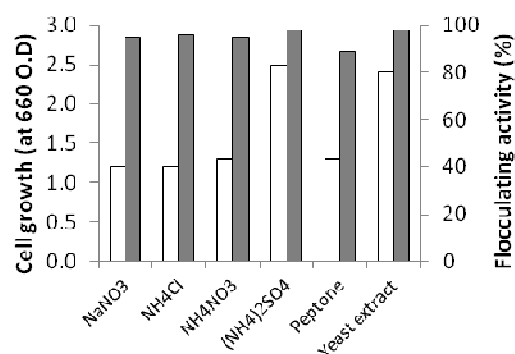


Fig. 2. Effect of nitrogen sources on cell growth (□) and flocculating activity (■). The culture time was 48 h.

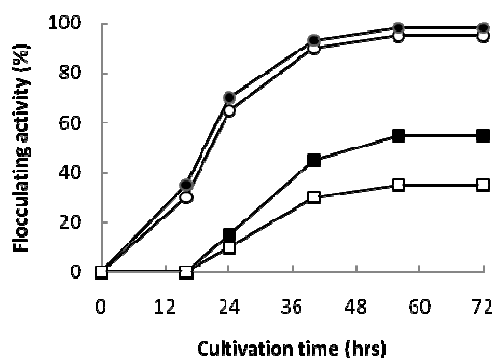


Fig. 3. Effect of initial pH of medium on the bioflocculant production by strain NRC-14. pH values, 4.5 (●), 5.5 (○), 6.5 (■), and 7.5 (□).

As shown in Fig. 2, yeast extract or $(\text{NH}_4)_2\text{SO}_4$ were the most favorable nitrogen source for both the growth and production of the BPF, using FM as carbon source.

Effect of pH

The pH of growth medium greatly affected production of the BPF by strain NRC-14. Highest production was occurred at pH values ranged from 4.5-5.5. At these pH values, a rapid increase in production was observed after less than 48h of

growth (Fig. 3), whereas, higher pH values (6.5-7.5) does not favored the BPF production.

Effect of medium components.

Effect of medium component on maximum production of the BPF was also studied using minimal medium (MM) and enriched medium (EM). Despite of the differences in composition between the two media, the organism had nearly similar growth curve and maximum production throughout the growth period (Fig. 4, A and B). During the cultivation period, the FA increased with culture time and reached its maximum (98%) in early stationary phase. Production of the BPF was in parallel with cell growth curve up to 40 hr, after which the cells aggregated to the fungal mycelium particles and the medium seemed clear (Fig. 5). The FA increased with time, indicating that the BPF is produced during the growth of the strain, not by cell autolysis (Shih et al. 2001; Xia et al. 2007). The pH increased by time probably, due to the liberation and release of alkaline metabolites such as $-NH_2$ from chitosan degradation. Growth of the strain in a minimal medium with maximum production of the BPF elucidate that this strain is not exigent, i.e. the growth of the strain for efficient production of the BPF recommended no growth factors, no stimulants, and no metals cation.

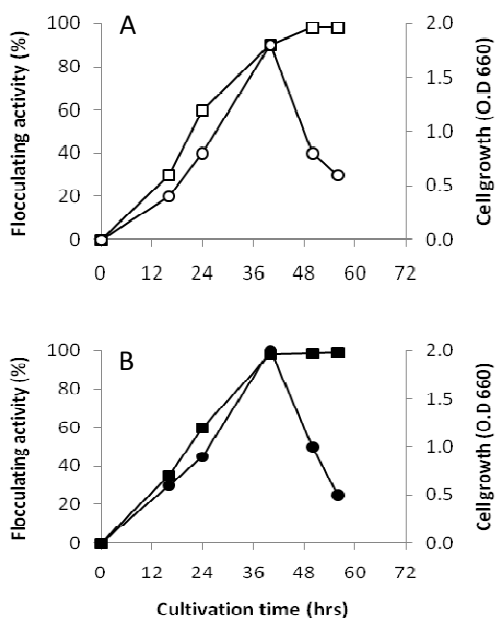


Fig. 4. Effect of medium components on production of the bioflocculant by strain NRC-14. Growth curve (○,●), and flocculating activity (□,■) determined for (A) the minimal (MM), and (B) the enriched (EM) growth media

Recovery of the bioflocculant

From 400 ml of culture supernatant under optimize culture conditions (MM medium, pH 5.5, 30°C, 48 hrs growth), 100 ml of the BPF were recovered by ethanol precipitation as a white, mucoid, ropy bioflocculant. After recovery of the BPF by ethanol, the resultant precipitate was found to be soluble in water, but not in solvents.

Characterization of the bioflocculant

Effect of dosage on the flocculating activity

Optimum dosage of the purified and crude bioflocculant was 3 and 15 ml/L for maximum flocculating activity (Fig. 6). Excess dosage of a bioflocculant may cause re-suspension of charcoal particles and leading to a reduction in the FA.

Effect of pH

Flocculating activity of the BPF of strain NRC-14 varied widely with the pH values. Using citrate buffer, the FA of the crude flocculant increased at pH values of 4-7, whereas FA of the purified flocculant increased at pH range of 8.0-9.5 (Fig. 7). The purified flocculant remained 92% of its FA at pH 9.5.

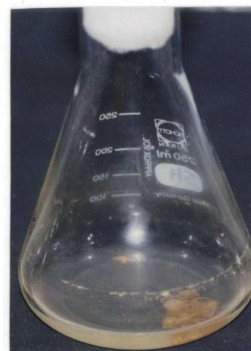


Fig. 5. Aggregation of dried mycelium of the fungus *M. rouxii* and other sediments by the bioflocculant produced by strain NRC-14 after 48 hrs of growth in a minimal medium.

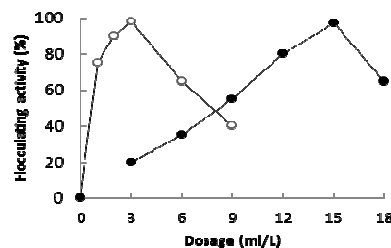


Fig. 6. Relationship between dosage of the crude (●), and purified (○) bioflocculant and its flocculating activity.

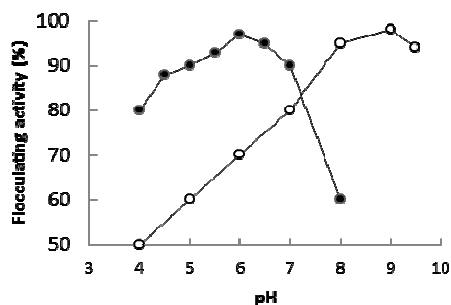


Fig. 7. Effect of pH values on the flocculating activity of the crude (●), and purified (○) biofloculants.

Effect of temperature.

The temperature dependence of the BPF revealed that, the FA of both biofloculants could effectively occur at temperatures ranging from 30-90°C. Below temperatures less than 20°C, the purified biofloculant acquired a mucoid and ropy property; therefore, recovery steps of the BPF were performed with cold distilled water and ethanol. The BPF was stable after heating at 100°C; the residual activity of the crude and purified flocculant reached about 97 and 98%, respectively, after heating at 100°C for 40 min. The main backbone of the BPF

from strain NRC-14 is a polysaccharide. In this respect, complete hydrolysis of the viscous biofloculant was carried out with 2N HCl at 100°C, and it was found that the majority of sugar constituents in the HCl hydrolysate were found to be aminosugars.

IR-spectra of the flocculant

Fig. 8, showed a transmission pattern of the BPF; surprisingly, it is similar to that of authentic chitosan, in which a hydroxyl band at 3420-3450 cm^{-1} , and an amide band at 1550-1655 cm^{-1} , and an amine band at 1550-1630 cm^{-1} were measured as characteristic bands for chitosan (Yokoi et al 1995, Muzzarelli et al 2004). The absorption band at 3428 cm^{-1} suggested the presence of -OH, and the bands at 1587 cm^{-1} and 1414 cm^{-1} may be assigned to the C=O asymmetrical and symmetrical stretching in carboxylate, respectively (Dermlim et al 1999). The absorption peaks observed at 989 cm^{-1} and 1273 cm^{-1} are generally known to be typical characteristics of aminosugar derivatives (Suh et al 1997). The infrared spectrum of this biofloculant, thus, shows the presence of carboxyl, hydroxyl, and amino groups which are known to contribute to the flocculation property of a biofloculant (Zajic and Knetting 1970).

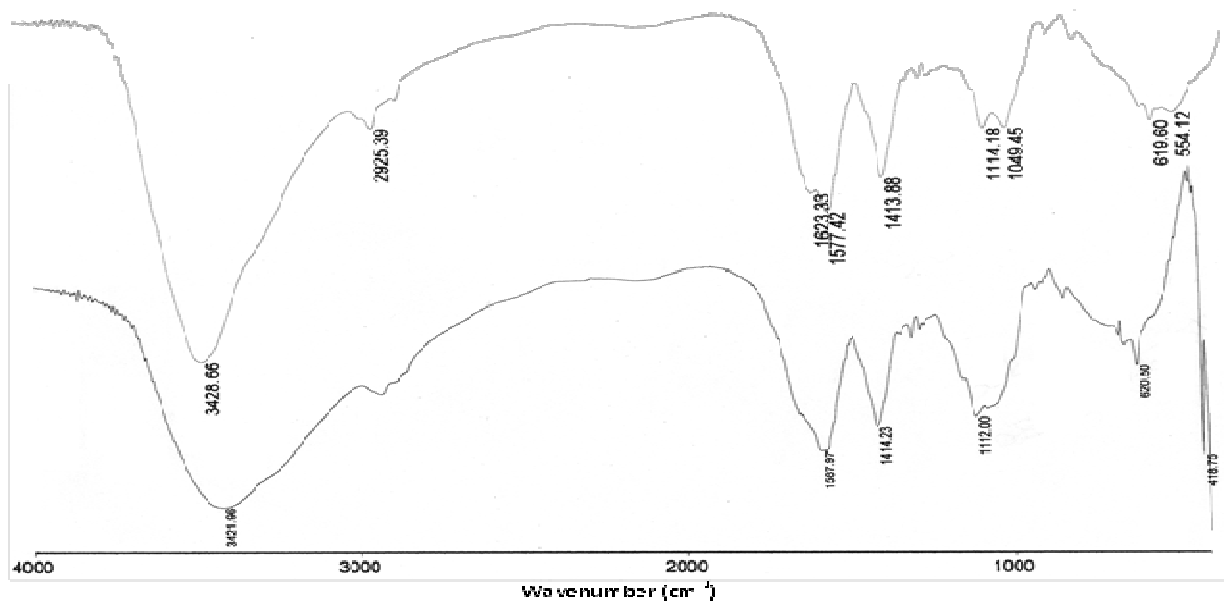


Fig. 8. IR-spectra of the original chitosan (upper curve) and the produced biofloculant (lower curve) by *B. alvei* NRC-14.

Shelf- life stability

The shelf-life stability of the purified BPF from strain NRC-14 was studied at refrigerator conditions (0°C), 4°C, and at room temperature (20-38°C) up to 12 months. The stability of the purified BPF is wonderful; it kept all of its activity at refrigerator and at 4°C for up to 12 months, and retained 94% of its FA for up to 6 months at room temperature (Fig. 9). Worthy mention is that, the FA of the crude BPF showed similarities to the flocculating efficacy of the purified one; the efficacy of precipitating charcoal particles by the crude BPF reached 90% after 6 months of keeping at room temperature (data not shown). The bioflocculant produced by strain NRC-14 did not require any metals to show maximum FA, some other flocculants need addition of metals to achieve high flocculating rates.

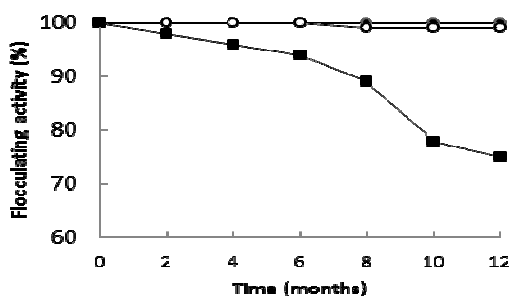


Fig. 9. Shelf-life stability of the purified bioflocculant produced by strain NRC-14. The flocculating activity was determined during 12-month period kept at refrigerator (●), 4 °C (○), and room temperature (■).

4. Discussion

Most bioflocculants are produced by microorganisms during their growth periods. Bacteria can utilize the nutrients in the culture medium to synthesize high molecular-weight polymers internally within the cells under the action of specific enzymes, and these polymers can be exerted and exist in the medium or on the surface of the bacterium as capsules. Therefore, by the action of such bacteria, the simple substances in their environment can be converted into complex polymers (Tenny and Verhoff, 1973). In the present study, it could be concluded that chitosan or chitosan-containing substrate are essential for the formation of the flocculant by the strain. Biosynthesis of this BPF, in fact, suggests a relationship between the presence of chitosan and the production of the flocculant. In previous studies (Abdel-Aziz, 1999; Abdel-Aziz et al. 2008) for production of chitosanase by strain NRC-14 using flaked chitosan, a bioflocculant was frequently produced by the strain. We concluded that,

degradation of chitosan by enzyme(s) secreted by the strain may probably result in accumulation of aminosugars. e.g. glucosamine which may polymerize to form the bioflocculant. The structure of the BPF which is extremely similar to that of chitosan would provide evidence that a monomer such as glucosamine may be an important precursor for the synthesis of the bioflocculant by the strain. Of interest is that, during the twenty-year history usage of strain NRC-14 under laboratory conditions, no variability or cell lyses was observed. Moreover, the BPF is a fairly stable polymer and it may have a protective function for the cells of the strain. The genetic stability of the strain is probably due to the presence of the BPF, which is highly stable (Pirog et al. 1997).

Optimization of medium composition in the present study revealed the significant effect of medium components. Low nutritional requirements have shown that strain NRC-14 is not an exigent organism, i.e. high BPF is produced under low nutritional medium, using low-cost substrate. Production of the bioflocculant is induced only in presence of chitosan as a determinant carbon source, while the best nitrogen sources were yeast extract or $(\text{NH}_4)_2\text{SO}_4$. Many reported strains can use organic nitrogen sources or organic combined with inorganic nitrogen sources to produce bioflocculants. For example, peptone (organic nitrogen source) and sodium nitrate (inorganic nitrogen source) provided the best nitrogen source for *Aspergillus parasiticus* for production of the bioflocculant, whereas with $(\text{NH}_4)_2\text{SO}_4$ no flocculant was produced (Deng et al. 2005). Compared with inorganic sources, beef or yeast extract were also more favorable for bioflocculant production by strain X-14 (Li et al. 2009). However, a complex of nitrogen source consisting of beef extract and urea was better than solely inorganic or organic nitrogen source (Gong et al. 2008). Strain TJ-1 was able to use beef extract, yeast extract, or peptone as an organic nitrogen source for production of a bioflocculant (Xia et al. 2008). In our study, strain NRC-14 can effectively use both inorganic or organic nitrogen sources to produce a bioflocculant. This result is in accordance with that reported for strain, *B. licheniformis* X-14.

During the logarithmic phase, the production of the BPF by strain NRC-14 almost paralleled the cell growth up to 40 hrs of growth, while maximum production of the BPF reached about 98% after 48 hrs of growth. Many reported bioflocculants are collected in the late logarithmic growth phase and the early stationary phase because the FA began to decrease due to the activity of deflocculating enzymes (Kurane et al. 1986). However, the FA of the bioflocculant from strain NRC-14 did not

decrease when the strain entered the decline phase (at 60 hrs), suggesting that this strain did not secrete deflocculating enzymes.

The purified bioflocculant was found to be dissolved in aqueous solutions but not in organic solvents. Since the bioflocculant contained hydroxyl groups, it had the possibility of hydrogen bonding to one or more water molecules. The abundance of hydroxyl groups build up strong forces of attraction between the bioflocculant molecules, resulting in relatively hard crystalline form. These forces are too great to be broken by organic solvents, so the purified bioflocculant is insoluble in organic solvents (James et al., 1986).

The relationship between the bioflocculant dosage and the FA revealed that, the activity initially increased with increasing the flocculant dosage, but then decreased. This is because, the adsorption of excess bioflocculant restabilize the charcoal particles; only the particles around bioflocculant precipitated in the flocculating reaction in a moment, and other particles did not precipitate, subsequently the FA decreased (Suh et al. 1997).

The MW of the BPF was found to be 6.9×10^4 Da. The MW and functional groups at the molecular chains are the most important factors in the FA of a bioflocculant. Currently, the components and structures of bioflocculants are complex, and different flocculants produced by microbes can have different properties. However, a large molecular-weight bioflocculant is usually long enough and has a sufficient number of free functional groups by which strong and large flocs are formed. Free functional groups can act as bridges to bring many suspended particles together (Michaels, 1954). The mechanism of flocculation in biological system is not entirely clear, highly complex, and depends on many interacting variables such as temperature, pH, microbial species and medium components (Deng et al. 2003, Todd et al. 2010). Flocculation occurs when a chemical or biological additive is mixed with solid-containing slurry causing agglomeration of the solid particles, formation of flocs, and rapid settling of the flocs out of the solution. One mechanism that flocculation can occur, when the flocculant forms molecular "bridges" between the suspended solid particles creating larger solid aggregates. A second mechanism for flocculation, charge neutralization, occurs when the chemical additive interacts with only one (or a few) particles electrostatically. The resulting particle becomes charge neutral and losses much of its surface salvation water (Todd et al. 2010). In our study, the bioflocculant was a cation-independent, whose flocculating capability need no cation addition. This may, probably, be due to its flocculation which may depends primarily on

bridging rather than on the mechanism of charge neutralization (Zheng et al.2008).

The IR-spectrum of the bioflocculant is extremely similar to that of chitosan. Spaink et al. (1994) have reported that, low molecular-weight chitin oligosaccharide has produced by *Rhizobium leguminosarum*. Fujita et al. (2000) have reported for the first time the bacterial production of a biopolymer flocculant by *Citrobacter* sp., which has a structure similar to that of chitin. Within the range of our research, this is the first report on a bioflocculant has chitosan-like structure, produced by the novel strain *Bacillus alvei* NRC-14.

Conclusion

Industrial production of bioflocculants is limited by their high costs and poor yields. The bioflocculant, produced by the newly isolated *Bacillus alvei* NRC-14, is induced by chitosan or chitosan-containing substrate, using low-cost nutritional medium. Studies on the effect of carbon and nitrogen sources revealed that the production of the BPF is affected mainly by the carbon source used and the pH value, but not by the nitrogen source used. The BPF is an exopolysaccharide, heat stable, with relatively low dosage requirement. Addition of metal ions had no positive effects on the flocculating activity, indicating that the bioflocculant is cation-independent, which means that it could avoid second pollution and reduce costs. The IR-spectra of the flocculant is extremely similar to that of chitosan. The shelf-life stability of the crude and purified bioflocculants is wonderful; both flocculants remained most of its activity after 6 months period of keeping at room temperature. The practical application of the bioflocculant in industry would be studied in further progress.

Corresponding author

Shadia M. Abdel-Aziz
Microbial Chemistry Dept.,
National Research Centre, Dokki, Cairo, Egypt.
abdelaziz.sm@gmail.com

References

- Abdel-Aziz, SH. M. (1999). Production and some properties of two chitosanases from *Bacillus alvei*. J. Basic Microbiol.,39, 79-87.
- Abdel-Aziz, SH., Moustafa, Y., and Mouafi, F. (2008). Partial purification and some properties of the chitosanases produced by *Bacillus alvei* NRC-14. J. Appl. Sci. Res.,4,1285-1290.
- Arezoo,C. (2002).The potential role of aluminium in Alzheimer's disease. Nephrol.Dial.Transplant,17, 17-20.
- Cartier, S., Tatoud, L., Theoleyre, M., and Decloux, M. (1997). Sugar refining process by coupling flocculation and crossflow filtration. J. Food Eng., 32, 155-166.
- Chaplin,M. and Kennedy, J. (1986). *Carbohydrate analysis*. IRL Press, Washington, DC, pp. 2-5.
- Deng,S., Bai,R.,Hu,x. and Luo,Q. (2003). Characteristics of a bioflocculant produced by *Bacillus mucilaginosus* and its use

- in starch wastewater treatment. *Appl. Microbiol. Biotechnol.*, 60, 588-593.
- Deng, S., Yu, G. and Ting, Y. (2005). Production of a bioflocculant by *Aspergillus parasiticus* and its application in dye removal. *Colloids and surfactant. Biointerf.* 44,179-186.
- Dermlin,W., Prasertsan,P. and Doelle,H. (1999). Screening and characterization of bioflocculant produced by isolated *Klebsiella* sp. *Appl. Microbiol. Biotechnol.*, 52, 698-703.
- Fujita, M., Ike, M., Tachibana, S., Kitada,G., Kim, S., and Inoue, Z. (2000). Characterization of a bioflocculant produced by *Citrobacter* sp.TKF04 from acetic and propionic acids . *J. Biosci. Bioeng.*, 89, 40-46.
- Gao,J., Bao, H.,Xin,M., Liu,Y., Li,Q. and Zhang,Y. (2006). Characterization of a bioflocculant from a newly isolated *Vagococcus* sp.W31. *J. zhejiang Univ. Sci.*,3, 186-192.
- Gong, W., Wang,S., Sun, X., Liu, X., Yue, Q., and Gao, B. (2008). Bioflocculant production by culture of *Serratia ficaria* and its application in wastewater treatment. *Biores. Technol.*, 99,4668-4674.
- Ho,Y., Norli,i.I., Alkarkhi,A., and Morad,N. (2010). Characterization of biopolymeric flocculant (pectin) and organic synthetic flocculant (PAM): a comparative study on treatment and optimization in kaolin suspension. *Bior. Technol.*, 101,1166-1174.
- Il'ina,A.,Varlamov,V., Melent,A. and Aktuganov, G. (2001). Depolymerization of chitosan with the chitinolytic complex from bacteria of the genus *Bacillus* sp.739. *Prikl. Biokhim. Microbiol.*, 37, 160-163.
- James, K. (1986). *Drugs and the Pharmaceutical Science*. In: Solubility and Related Properties, Vol., 28, Marcel Dekker New York.
- Juni, E. (1986). *Bergey's Manual of Systematic Bacteriology*. In: Genus *Bacillus*, p. 1115-1139, J. G. Holt, (ed.), Williams and Wilkins, London.
- Kurane,R., Takeda,K., and Suzuki,T.,(1986). Screening for and characteristics of microbial flocculants. *Agr. Biol. Chem.*, 50, 2301-2307.
- Kwon,G., Moon,S.,Hong,S.,Lee,H., Kim,H., Oh,H. and Yoon,B.(1996). A novel flocculant biopolymer produced by *Pestalotiopsis* sp. KCTC-8637.*Biotechnol. Letters*, 18, 1459-1464.
- Lazarova,V. and Manem,J. (1995). Biofilm characterization and activity analysis in water and wastewater treatment. *Water Res.*, 29, 2227-2245.
- Leonard, V., Cosa, S., Noxolo, M. and Okoh, A. (2011). *Halomonas* sp. OKOH-A marine bacterium isolated from the bottom sediment of Algoa Bay—produces a polysaccharide bioflocculant: partial characterization and biochemical analysis of its properties. *Molecules*, 16, 4358-4370.
- Li, Z., Zhong, S., Lei, H.,Chen, R., Yu, Q., and Li, H. (2009). Production of a novel bioflocculant by *Bacillus licheniformis* X14 and its application to low temperature drinking water treatment. *Biores. Technol.*, 100, 3650-3656.
- Lijun,Y., Lu,F., Li,D., Qiao,Z., and Yin,Y. (2009). Preparation and flocculation properties of cationic starch/chitosan crosslinking-copolymer. *J. Hazard. Materials*, 172,38-45.
- Lowry, O., rosebrough, N., Farr, A., and Randall, R. (1951). Protein measurement with the folin phenol reagent. *J. Biological Chem.*, 193, 265-275.
- Mao, Y., Tian,C., Zhu, J.,Zhang, T. and Tong, L. (2011). Production of a novel biopolymer by culture of *Bacillus cereus* B-11 using molasses wastewater and its use for dye removal. *Adv. Materials Res.*, 230, 1119-1122.
- Michaels, A. (1954). Aggregation of suspensions by polyelectrolytes. *Industrial Eng. Chem.*, 46, 1485.
- Muzzarelli, G., Tosi, G., Oriano, F., and Muzzarelli, R. (2004). Alkaline chitosan solutions. *Carbohydr. Res.*, 338, 2247-2255.
- Pirog, T., Grenbirg, T., and Malashinko, Y. (1997). Isolation of microorganisms-producing enzymes that degrade *Acinetobacter* sp. exopolysaccharides. *Prikl. Biokhim. Microbiol.*, 33, 491-495.
- Salehizadeh, and shojaosadati,S. (2001). Extracellular biopolymeric flocculants. Resent trends and biotechnological importance. *Biotechnol. Adv.*, 19, 371-385.
- Shih,L.,Van,Y.,Ych,L.,Lin,H. and Chang,Y. (2001). Production of biopolymer flocculant from *Bacillus licheniformis* and its flocculation properties *Biores. Technol.*, 78, 267-272.
- Spaink, H., Wijffjes, A., Drift, V., Haverkamp, J. et al. (1994). Structure identification of metabolites produced by the NodB and NodC proteins of *Rhizobium leguminisarum*. *Mol. Microbiol.*, 13, 821-831.
- Suh,H., Kwon,G., Lee,C., Kim,H., and Oh,H. (1997). Characterization of bioflocculant produced by *Bacillus* sp. SDp-152. *Ferm. Bioeng.*,84,108-112.
- Tabata,S. and Terui,G. (1962). Studies on microbial enzymes active in hydrolyzing yeast cell walls:Isolation of a strain and culture conditions for enzyme formation. *J. Ferm. Technol.*, 40, 366-373.
- Tenny, M. and Verhoff, F. (1973). Chemical and auto flocculation of microorganisms in biological waste treatment. *Biotechnol. Bioeng.*,15, 1045-1053.
- Todd, M. (2010). Polyelectrolyte flocculation of grain stillage for improved clarification and water recovery within bioethanol production facilities. *Biores. Technol.*, 101, 2280-2286.
- Wang, J., Wei, J. and Ma, H. (2011). Screening of a flocculant-producing strain and optimal conditions for production of bioflocculant. *Adv. Materials Res.*,183,829-833.
- Xia, S., Zhang, Z., Wang, S., Yang, A., Chen,L., Zhao,J., Leonard,D. and Jaffrezic-Renault,N. (2007). Production and characterization of a bioflocculant by *Proteus mirabilis* TJ-1. *Biores. Technol.*, 99, 6520-6527.
- Yokoi, H.,Osamu, N., Jun, H., Sachio, H., and Takasaki,Y. (1995). haracteristics of a biopolymer flocculant produced by *Bacillus* sp.PY-90. *J. Ferm. Bioeng.*, 79, 378-380.
- Zajic,J. and Knettig,E. (1970). Flocculants from para-finic hydrocarbons: *Development in industrial microbiology*, p.87-98.American Institute of biological science,Washington DC.
- Zheng, Y., Ye, Z., Fang, X., Li,Y. and Cai, W. (2008). Production and characteristics of a bioflocculant produced by *Bacillus* sp. F19. *Biores. Technol.*, 99, 7686-7691.

11/12/2011

Resveratrol Mediated Protection of Dacarbazine-Induced Mutagenicity in Mice

Ramadan, A.M. Ali

Zoology Dept., College for Girls for Science, Arts and Education, Ain-Shams Univ., Heliopolis, Cairo, Egypt
ramadanali27@gmail.com

Abstract: Dacarbazine (DTIC) is one of the most effective chemotherapeutic drugs that have been successfully applied to treat malignancy. *In vivo* studies revealed that DTIC induced oxidative DNA damage and cell cycle arrest. Resveratrol (RES) is a natural polyphenol (*trans*-3,5,4-trihydroxy stilbene) found in grapes and attracts public attention because it possesses diverse biochemical, anticancer and antigenotoxic actions. The present work was aimed to investigate the antigenotoxic activity of RES against DTIC-induced chromosomal aberrations (CA) and micronucleated polychromatic erythrocytes (Mn-PCEs) formation, micronucleated peripheral blood reticulocytes (Mn-Ret) development and DNA fragmentation in bone marrow cells of mice. The animals divided into 10 groups each with 6 animals. Each animal group received either a single dose of 0, 2.5, 5, 10 and 20 mg/kg b.w. DTIC or pretreated daily with 0, 50 mg/kg b.w. for 15 days with RES. Animals were sacrificed 24 h post treatment with DTIC. RES treatment for 15 days decreased the control base line of CA, Mn-PCEs, Mn-Ret incidences and DNA fragmentation and elevated the averages of mitotic indices and PCEs/NCEs. RES treatment significantly reduced the increased averages of CA, percentages of Mn-Ret and DNA fragmentation induced by DTIC. Moreover, RES significantly ($P < 0.001$) elevated the averages of PCEs/NCEs and percentages of mitotic index induced by DTIC. It is concluded that, administration of resveratrol improved the genotoxic effects of dacarbazine and the results of this work draw attention for application of a safer chemotherapeutic protocol for cancer treatment by using strong antioxidants concurrently with chemotherapeutic agents.

[Ramadan, A.M. Ali **Resveratrol Mediated Protection of Dacarbazine-induced Mutagenicity in Mice**. Life Science Journal, 2011; 8(4):891-899] (ISSN: 1097-8135). <http://www.lifesciencesite.com>.

Key words: Dacarbazine; Resveratrol; Micronucleus; Chromosomal aberrations; DNA fragmentation; Mouse; Bone marrow cells

1. Introduction

Resveratrol (RES) is a natural polyphenol phytoalexin (*trans*-3,5,4-trihydroxy stilbene) found in grapes, peanuts and cranberries and possesses diverse biochemical and physiological actions (Wang *et al.*, 2002). RES ameliorates experimental autoimmune myocarditis (Yoshida *et al.*, 2007), prevents estrogen-DNA adduct formation and neoplastic transformation in MCF-10F cells (Lu *et al.*, 2008), attenuates the experimental neuroinflammation-mediated cognitive deficits in rats (Gong *et al.*, 2010), inhibits the transcription of lytic genes and the lytic cycle of Epstein-Barr Virus to reduce the production of viral particles (Yiu *et al.*, 2010) and reduced lipid peroxidation induced by tert-butyl hydroperoxide in human sperm and in rat spermatocytes and spermatids (Collodel *et al.*, 2011). RES reduces the incidences of comets in lymphocytes induced by platinum compounds (Olas *et al.*, 2005), protects the arsenite induced DNA damage in normal mammalian V79 cells (Roy *et al.*, 2008), inhibites the frequencies of micronuclei induced by hydrogen peroxide in astroglial cells (Quincozes-Santos *et al.*, 2010) and protected against ethanol-induced oxidative DNA damage in human peripheral lymphocytes (Yan *et al.*, 2011).

Dacarbazine (DTIC) [5-(3,3-dimethyl-1-triazeno)imidazole-4-carboxamide] is a synthetic

analogue of the naturally occurring purine precursor, 5-amino-1H-imidazole-4-carboxamide (Rooseboom *et al.*, 2004). DTIC is alkylating cytostatic drug extensively used as a single agent or in combination with other drugs for treatment of malignant melanoma, soft tissue sarcoma, renal adenocarcinoma, solid tumors, osteogenic sarcoma, neuroblastomas and malignant lymphomas (Yi *et al.*, 2011). A combination of mesan, adriamycin, ifosfamide and dacarbazine (MAID combination) is used against advanced soft tissue sarcomas which has been transform many incurable tumors to highly curable ones (Verma *et al.*, 2008). Chronic oral and intraperitoneal administration of DTIC to mice induced mammary adenocarcinomas, thymic and splenic lymphomas, breast, brain and lung cancers (Kakumanu *et al.*, 2011).

In mice, DTIC induced reduction in the mitotic index and increases the chromosomal aberrations in bone marrow cells (Al-Saleh, 2001), increased the micronuclei in peripheral blood cells (Adler *et al.*, 2002) and induced defects in the spermatogenesis (Adler *et al.*, 2002). IARC (1981) reported that, DTIC is mutagenic in mouse lymphoma cells *in vitro*. Moreover, DTIC induces teratogenicity in humans (Aviles *et al.*, 1991), induced micronuclei in peripheral blood lymphocytes of patients treated against metastatic melanoma

(Miele *et al.*, 1998), induced DNA damaged peripheral blood lymphocytes (Yoshida *et al.*, 2006) and in human A375 melanoma cells (Samulitis *et al.*, 2011).

The extensive use of DTIC in malignancy treatment and the associated harmful genotoxic side effects attracts attention to do a trial to reduce the genotoxicity of DTIC by resveratrol antioxidant for the application of a new and safer chemotherapeutic protocols.

2. Materials and Methods:

1- Chemicals:

Dacarbazine (DTIC) purchased from local pharmacies under the trade name DETICENE 200 mg vial provided with a vial containing 19.7 ml of sterile water for injection and produced by SANOFI AVENTIS-EGYPT. Resveratrol (purity 99%), purchased from Sigma (St. Louis, MO, U.S.A. CAS number 501-36-0). Fetal bovine serum was provided from Gibco BRL (Grand Island, NY, U.S.A.). Chemicals were dissolved in appropriate concentrations for animals to receive the injected volumes equivalent to 1.0 ml solution /100 g animal b.w.

2- Animals and treatments:

Total of 60 BALB/C adult male albino mice, aged 9-10 weeks and weighing 24-26 g purchased from The Holding Company for Biological Products and Vaccines (VACSERA), Giza, Egypt were utilized in this work. Animals were acclimatized for one week prior to experimentation and housed in plastic cages (40 × 30 × 16 cm) at 22 ± 2°C and 30–70% relative humidity. The mice were accommodated 6 per cage with wooden chip bedding and given commercial food pellets and water *ad libitum*. All experimental procedures were performed according to the Institutional Animal Care and Experiment Committee of Ain-Shams University. The doses were proportional to the dose rate used for human treatment. Animals were arranged in groups of 6 animals / experimental point. Animals divided into two main groups. Group one included 30 mice and subdivided into 5 subgroups; 6 mice each. One subgroup includes animals of the control group and received 0.2 ml dis H2O. The 4 subgroups received either single dose of 0, 2.5, 5, 10 and 20 mg/kg b.w. DTIC for 24 h. Group two included 30 mice and subdivided into 5 subgroups; 6 mice each. One subgroup includes animals received oral dose of 50 mg/kg b.w. RES daily for 15 days. The 4 subgroups received oral daily doses of 50 mg/kg b.w. RES for 15 days. At day 14 of RES treatment, the animal subgroups are injected intraperitoneally with single doses of 2.5, 5, 10 and 20 mg/kg b.w DTIC. The animals were sacrificed 24 h post last treatment(s).

3- Bone marrow chromosomal aberration assay:

Chromosomes were prepared from bone marrow cells of mice according to the method previously postulated by Preston *et al.* (1987). 200 well spread metaphases were examined per animal with oil immersion of Meiji microscope. The chromosomal aberrations were classified according to Savage (1976). Mitotic indices were determined from scoring 1000 cells for each animal. The counts were carried out with the hand tally counter.

4- Bone marrow micronucleus (Mn) assay:

Animals were sacrificed by cervical dislocation and bone marrow cells smeared on glass slides, fixed with methanol. The slides were stained just before examination with 20.0 µL of the fluorescence dye acridine orange (1.0 mg/mL) and coverslipped (Hayashi *et al.*, 1983). The slides examined by fluorescence microscopy, using blue light (488 nm) and an orange filter, with a 40 times objective. For each animal, 2000 PCEs scored for the presence of Mn. In addition to that, the frequencies of PCEs among 2000 bone marrow erythrocytes (NCEs + PCEs) calculated to determine the frequencies of bone marrow depression, and the values were expressed as PCE/NCE.

5- Micronucleus assay in peripheral blood:

The peripheral blood micronucleus assay carried out according to Hayashi *et al.* (1990). A total of 2000 reticulocyte /animal were examined for statistical analysis. The reticulocytes (Ret) are characterized by their red fluoresces due to the presence of remnants of variable amounts of RNA, that related to the maturity of reticulocyte. The micronucleus appears as a small rounded body that has yellowish green fluoresces inside the Ret.

6- DNA fragmentation assay

The DNA fragmentation was assessed by agarose gel electrophoresis according to Enari *et al.* (1998) with some modifications. Bone marrow cells were suspended in 1 ml of hypotonic solution (5.6 g/L KCl) and incubated for 10 min at 37°C. The clear supernatant is discarded and the cell pellet is suspended in 500 µL of lysing buffer (50 mM NaCl, 1 mM Na EDTA, 0.5 % SDS, pH 8.3) and incubated at 37°C overnight with 1 mg/ml proteinase K. Cellular DNA was isolated by phenol extraction and the DNA samples were carefully loaded into the wells of a 2.0% agarose gel. Electrophoresis was carried out in TBE buffer at 50 V for 1 h and the DNA was visualized by ethidium bromide staining.

7-Statistics

All values are reported in the form of averages ± SD of the mean, except where indicated. The results of the different treatment groups were compared using Students't-test (Fowler *et al.*, 1998). Significance was indicated by P values <0.05. A set

of statistical calculations were carried out to compare between the results obtained from animals treated with DTIC with control untreated animals. Another set of comparisons was carried out between results of animals treated with DTIC alone and those treated with the same doses of DTIC and 50 mg/kg b.w. RES.

3. Results

As shown in table 1 and figure 1; DTIC (5, 10 and 20 mg/kg b.w.) induced significant ($P < 0.001$) increases in both the averages of structural chromosomal aberrations and the percentages of aberrant cells. In addition, DTIC induced a significant inhibition in percentages of mitotic indices in a dose dependent and linear manner. Structural chromosomal aberrations appeared in the form of chromatid gap, chromatid break, acentric fragments, deletions, dicentric chromosomes and centric fusions. RES treatment induced significant inhibitions in the percentages of chromosomal aberrations and increases in mitotic indices. The aberrant metaphases showed a statistically significant decrease ($P < 0.05$) after treatment with RES and DTIC in comparison with those induced by DTIC treatment alone. While, animals treated with RES showed a non-significant decrease in percentages of chromosomal aberrations or elevations in the mitotic indices in comparison to the control level.

As shown in table 2, figure 2 and figure 3; Bone marrow cells of mice treated with DTIC at dose levels of 0, 2.5, 5, 10 and 20 mg/kg showed high significant ($P < 0.001$) increases in incidences of Mn-PCEs in comparison to the control level. The increases in Mn-PCEs was dose dependent and highly significant ($P < 0.001$). The PCEs were appeared as a progenitor of RBCs that have a reddish cytoplasm because of some RNA presence, that make them easily differentiated from mature normochromatic erythrocytes (NCEs) which has not stained. The Mn-PCEs appeared as PCEs that having small rounded bodies called the micronucleus which stained greenish yellow. Moreover, signs of bone marrow depression were detected in the form of a dose-related significant reduction in the percentages of PCEs. Animals treated daily with 50 mg/kg resveratrol for 15 consecutive days did not induce a significant elevation in Mn-PCEs than the control level. However, resveratrol could protect against DTIC induced Mn-PCEs. Treatment with 0, 2.5, 5, 10 and 20 mg/kg DTIC without and with 50 mg/kg resveratrol induced 1.83 ± 0.75 , 6.83 ± 13.67 , 23.67 ± 1.63 , 43.83 ± 3.97 and 1.50 ± 0.84 , 2.0 ± 0.89 , 8.67 ± 1.63 , 18.17 ± 1.94 , 33.17 ± 3.31 Mn-PCEs per 2000 PCEs, respectively. RES significantly ($P < 0.001$) elevated the averages of PCEs/NCEs.

As shown in in table 2 and figure 4; peripheral blood Mn-Ret showed significant increases in micronuclei formation due to treatment with DTIC. In peripheral blood samples, Ret appears to have variable amounts of RNA that makes them easily observable from the mature RBCs presented in Fig. 5. While, Mn-Rets are having a small rounded body that fluoresces yellowish green this considered as an indicator for the presence of DNA.

The graded doses of 0, 2.5, 5, 10 and 20 mg/kg b.w. DTIC showed a fragmentation of DNA in the form of low molecular weight DNA fragments in comparison to the intact DNA of bone marrow cells derived from control untreated animals (Fig. 6). RES treatment could induce a reduction in DNA fragmentation induced by DTIC. Unfortunately, RES did not retain the DTIC-induced DNA fragmentation to the base line of the control level of damage.

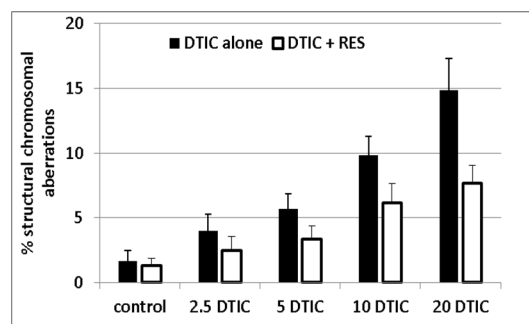


Fig.1. Percentages of chromosomal aberrations in mice treated with 0, 2.5, 5, 10 and 20 mg/kg b.w DTIC alone (black columns) or in combination with 0 and 50 mg/kg RES (white columns). DTIC induced significant elevations with all dose levels. RES could induce a statistically significant inhibition in DTIC-induced % chromosomal aberrations ($P < 0.05$).

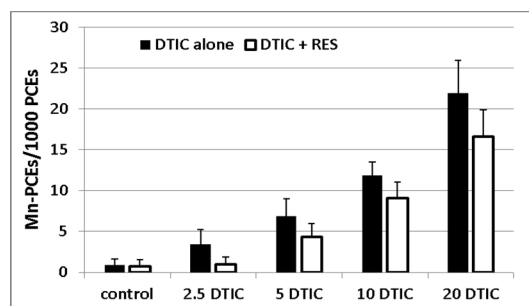


Fig. 2. Averages of Mn-PCEs in bone marrow samples of animals treated with 0, 2.5, 5, 10 and 20 mg/kg b.w. DTIC alone (Black columns) or in combination with 0 and 50 mg/kg b.w. RES (white columns). Note that, RES reduced the averages of Mn-PCEs induced by 2.5 mg/kg b.w DTIC to the control level and significantly induced an inhibition in the averages of Mn-PCEs in comparison to those induced by 5, 10 and 20 mg/kg b.w. alone.

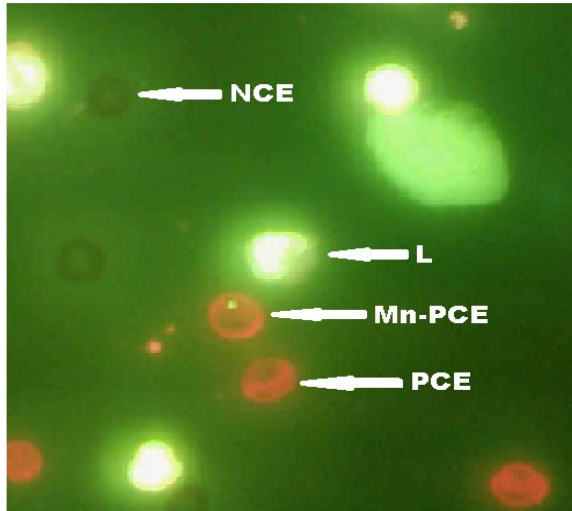


Fig. 3. Bone marrow smear showing Mn-PCE from femoral bone marrow of mouse. The arrows point out to Mn-PCE, the micronucleus is visualized as a small rounded body that has a yellowish green fluoresces due to the presence of DNA that stained green. The polychromatic erythrocyte (PCE) are characterized by their red fluoresces due to the presence of remnants of RNA, as shown in the figure the reticulocytes have variable amounts of RNA. The mature normochromatic erythrocyte (NCE) appears as an opaque unstained rounded bodies. Leucocytes (L) appear as brightly fluoresces green bodies.

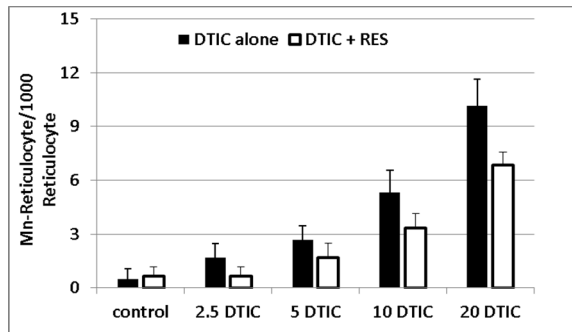


Fig. 4. Averages of Mn-Ret/1000 Ret in peripheral blood of animals treated with 0, 2.5, 5, 10 and 20 mg/kg b.w. DTIC alone (Black columns) or in combination with 0 and 50 mg/kg b.w. RES (white columns). Note that, RES reduced the averages of Mn-Ret induced by 2.5 mg/kg b.w DTIC to the control level.

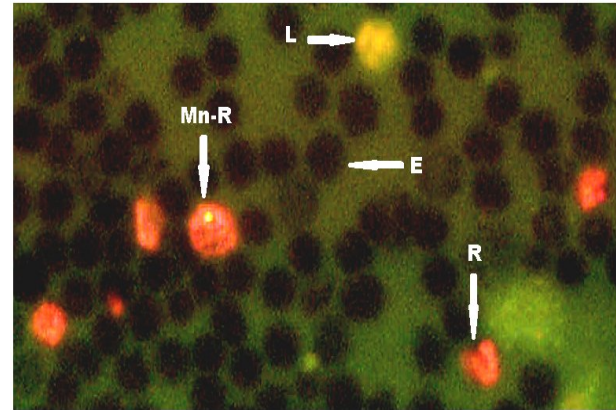


Fig. 5 : Peripheral blood Micronucleated-Reticulocyte (Mn-R) from caudal vein of mouse treated with 20 mg/Kg b.w. DTIC. The arrow point out to Mn-Reticulocyte (MN-R), the micronucleus is visualized as a small rounded body that has a yellowish green fluoresces. The reticulocytes (R) are characterized by their red fluoresces due to the presence of remnants of RNA, as shown in the figure the reticulocytes have variable amounts of RNA related to the maturity of reticulocyte. The mature erythrocyte (E) appear as an opaque unstained rounded bodies. Leucocytes (L) appear as brightly fluoresces green bodies.

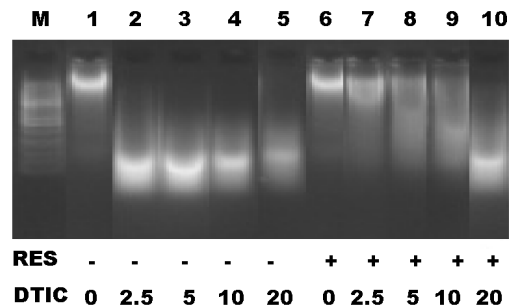


Fig. 6 : Resveratrol (RES) mediated protection of dacarbazine (DTIC) induced mutagenicity in mice bone marrow cells. Bone marrow cells were derived from animals treated for 24 h with 0, 2.5, 5, 10 and 20 mg/kg b.w. DTIC represented in lanes 1-5, respectively. The graded doses of DTIC (Lanes 2-5) showed a fragmentation of DNA in the form of low molecular weight DNA fragments in comparison to the intact DNA of bone marrow cells derived from control untreated animals (Lane 1). The lanes 6-10 represent the DNA fragmentation pattern in bone marrow cells derived from animals treated daily with 50 mg/kg b.w. resveratrol (RES) for 15 days, animals received 0, 2.5, 5, 10 and 20 mg/kg. b.w. dacarbazine (DTIC) concurrently with the last dose of RES. As shown in lanes 7-10 the effect of RES is reversibly with the increased doses of DTIC.

Table (1). Effect of resveratrol (0, 50 mg/kg b.w. daily doses for 15 days) on the induction of mouse bone marrow chromosomal aberrations by dacrabazine (0, 2.5, 5, 10 and 20 mg/kg b.w. single dose concurrently administered with the last dose of resveratrol).

Treatment (mg/kg b.w.)	Structural Chromosomal aberrations						Aberrations/600 metaphases (Average ± S.D.)	Aberrant cells (%)	Mitotic Index (%)	
	Chromatid Gap	Break	Deletion	Acentric Fragment	Dicentric	Centric Fusion				
DTIC	RES									
0	0	1	0	2	2	2	3	10 (1.67 ± 0.82) ^a	1.50 ± 0.55 ^a	5.17 ± 1.17 ^a
2.5	0	4	4	5	3	4	4	24 (4.00 ± 1.26) ^{b*}	3.17 ± 0.75 ^{b*}	4.67 ± 1.03 ^b
5	0	4	5	5	7	9	4	34 (5.67 ± 1.21) ^{c***}	4.50 ± 0.55 ^{c**}	3.67 ± 0.82 ^{c*}
10	0	12	10	9	10	9	9	59 (9.83 ± 1.47) ^{d***}	6.83 ± 0.98 ^{d***}	3.00 ± 0.63 ^{d**}
20	0	14	12	13	14	17	19	89 (14.83 ± 2.48) ^{e***}	9.00 ± 1.41 ^{e***}	2.17 ± 0.75 ^{e***}
0	50	0	0	2	3	2	1	8 (1.33 ± 0.52) ^f	1.30 ± 0.52 ^f	5.50 ± 1.05 ^f
2.5	50	2	2	1	2	4	4	15 (2.50 ± 1.05) ^{g**}	2.30 ± 1.03 ^g	5.17 ± 1.17 ^{g*}
5	50	2	5	5	3	4	1	20 (3.33 ± 1.03) ^{h**}	3.00 ± 0.89 ^{h*}	4.83 ± 0.75 ^{h*}
10	50	5	5	6	6	6	9	37 (6.17 ± 1.47) ^{i***}	5.50 ± 1.05 ^{i*}	4.50 ± 0.66 ^{i*}
20	50	8	4	7	9	7	11	46 (7.67 ± 1.37) ^{j***}	7.67 ± 0.89 ^{j*}	2.67 ± 0.82 ^j

^{b, c, d, e} compared to ^a

^f compared to ^a

^g compared to ^b

^h compared to ^c

ⁱ compared to ^d

^j compared to ^e

p*<0.05, *p*<0.01, ****p*<0.001

Table (2). Effect of resveratrol (0, 50 mg/kg b.w. daily doses for 15 days) on the induction of mouse bone marrow and peripheral blood micronuclei by dacrabazine (0, 2.5, 5, 10 and 20 mg/kg b.w. single dose concurrently administered with the last dose of resveratrol).

Treatment (mg/kg b.w.)	Bone marrow Mn-PCEs/2000 PCEs/ animal (Total, Average ± S.D.)	Bone marrow PCE/NCEs (Average ± S.D.)	Peripheral blood Mn-Ret/1000 Ret (Average ± S.D.)	
DTIC	RES			
0	0	1, 2, 2, 3, 1, 2 (11, 1.83 ± 0.75) ^a	0.83 ± 0.09 ^a	0.50 ± 0.55 ^a
2.5	0	6, 9, 5, 5, 9, 7 (41, 6.83 ± 1.83) ^{b**}	0.73 ± 0.05 ^b	1.67 ± 0.82 ^b
5	0	14, 13, 11, 17, 15, 12 (82, 13.67 ± 2.16) ^{c***}	0.64 ± 0.06 ^{c*}	2.67 ± 0.82 ^{c*}
10	0	22, 23, 22, 26, 25, 24 (142, 23.67 ± 1.63) ^{d***}	0.51 ± 0.04 ^{d**}	5.33 ± 1.21 ^{d**}
20	0	46, 41, 42, 39, 45, 50 (263, 43.83 ± 3.97) ^{e***}	0.36 ± 0.07 ^{e***}	10.17 ± 1.47 ^{e***}
0	50	2, 1, 1, 1, 3, 1 (9, 1.50 ± 0.84) ^f	1.11 ± 0.13 ^{f*}	0.67 ± 0.52 ^f
2.5	50	3, 2, 3, 1, 2, 1 (12, 2.00 ± 0.89) ^{g**}	0.87 ± 0.08 ^g	0.67 ± 0.52 ^{g*}
5	50	9, 7, 7, 8, 10, 11 (52, 8.67 ± 1.63) ^{h**}	0.79 ± 0.08 ^{h*}	1.67 ± 0.82 ^{h*}
10	50	17, 19, 15, 20, 18, 20 (109, 18.17 ± 1.94) ^{i***}	0.71 ± 0.08 ^{i*}	3.33 ± 0.82 ^{i*}
20	50	35, 29, 32, 36, 37, 30 (199, 33.17 ± 3.31) ^{j***}	0.62 ± 0.06 ^{j**}	6.83 ± 0.75 ^{j**}

^{b, c, d, e} compared to ^a

^f compared to ^a

^g compared to ^b

^h compared to ^c

ⁱ compared to ^d

^j compared to ^e

p*<0.05, *p*<0.01, ****p*<0.001

Discussion

To establish the antigenotoxic action of resveratrol on DTIC-induced chromosomal damage and micronuclei formation in bone marrow cells of mice; animals treated daily with 0 and 50 mg/kg b.w. RES for 15 days followed by a single dose of 0, 2.5, 5, 10 and 20 mg/kg b.w.

Induction of bone marrow chromosomal aberrations (CA) and micronucleated polychromatic erythrocytes (MN-PCEs) has been commonly used as sensitive biological indicator with high veracity in the mutagenic bioassays of the drugs (Adekunle *et al.*, 2009).

In the present work, DTIC induced significant ($P < 0.001$) increases in averages of chromosomal aberrations. In addition to that, DTIC induced a significant ($P < 0.001$) elevations in the incidences of Mn-PCEs and Mn-Rets that having one or more micronuclei of the small type. Small type micronucleus has a diameter less than 1/5 the diameter of the containing cell. These Mn-PCEs and Mn-Rets are having small type micronucleus that most probably containing chromosomal fragments (Norppa and Falck, 2003). The production of small micronuclei in bone marrow cells induced by DTIC was previously reported (Al-Hawary and Al-Saleh, 1989; Jeremice *et al.*, 1996; Adler *et al.*, 2002; Khan *et al.*, 2010). Moreover, DTIC induced cytotoxicity in the form of reduction of percentages of PCEs and in the mitotic indices (MI) which pointed out that there is an inhibition in mitotic processes (Al-Hawary and Al-Saleh, 1989; Adler, *et al.*, 2002). Literatures showed that, DTIC induced sister-chromatid exchanges in bone marrow cells of CBA/Ca mice (Varga *et al.*, 1991), cytokinesis-blocked micronuclei in murine SCCVII cell line (Jeremic *et al.*, 1996), micronuclei containing whole chromosomes from peripheral blood derived from melanoma patients (Miele *et al.*, 1998), bone marrow micronuclei of mice (Adler *et al.*, 2002) and micronuclei in Chinese hamster V79 cells (Kersten *et al.*, 2002).

The mechanism by which DTIC produces its genotoxic action is still unclear. However, the possible mechanism of genotoxicity exerts by DTIC is summarized as follows; DTIC is P450-activated prodrug. DTIC is activated by hydroxylation to produce 5-(3-hydroxymethyl-3-methyl-triazen-1-yl)imidazole-4-carboxamide (HMMTIC). Formaldehyde is subsequently eliminated from HMMTIC nonenzymatically, resulting in 5-(3-methyltriazen-1-yl)imidazole-4-carboxamide (MTIC), which rapidly decomposes to the genotoxic agents aminoimidazole carboxamide, N_2 , and CH_3^+ (Rooseboom *et al.*, 2004; Basaran *et al.*, 2010). P450-mediated DTIC

bioactivation induces apoptosis and mutagenicity via the formation of O^6 -methylguanine-DNA adducts (Kaina *et al.*, 2007; Pourahmad *et al.*, 2009). The O^6 -methylguanine preferentially pairs with thymine and leads to GC to AT base pair transitions (Gerson, 2002). Moreover, DTIC produces its cytotoxicity via another possible mechanism. DTIC induced interstrand DNA cross-links which are particularly cytotoxic because they block DNA replication and lysosomal breakdown with the release of DNase and alterations in the level of enzymes and co-enzymes (Fulda and Debatin, 2006; Apraiz *et al.*, 2011).

Diet represents a major influence on the reduction of cancer and chemotherapeutic side effects (Riso *et al.*, 2009). A micronutrient- equilibrated diet can contribute to genomic stability and hence cancers cure (Prado *et al.*, 2010). In the present work, RES significantly attenuates the frequencies of CA, Mn-PCEs, Mn-Ret and DNA fragmentation induced by DTIC. As well as, RES significantly improved the averages of mitotic index and PCEs/NCEs induced by DTIC. Previous work of Fusser *et al.* (2011) showed that, application of RES either for 7 days per gavage (100 mg/kg body w.t.) or for 3–9 months in the diet (0.04% ad libitum), reduces the endogenous oxidative DNA base damage in the livers of the *Csb^{m/m}Ogg1^{-/-}* mice by 20–30% ($P < 0.01$). Moreover, RES and its analogues protects against ethanol-induced oxidative DNA damage in human peripheral lymphocytes (Yan *et al.*, 2011) and protects mouse embryonic stem cells from ionizing radiation by accelerating recovery from DNA strand breakage (Denissova *et al.*, 2011).

Previous observations showed that, deficiencies in dietary microelements like vitamins and minerals in human diet are thought to generate DNA damage by enhancing the occurrence of breaks and oxidative lesions (Brevik *et al.*, 2011). Since mutations are the key elements in neoplastic processes, there is a considerable amount of epidemiological evidence relating diets rich in fresh fruit and vegetables and a decrease in cancer incidence (Chang *et al.*, 2010; Brevik *et al.*, 2011).

Resveratrol protects DNA through redox state of cells so, it is indirectly enhances the integrity of genomic DNA and acts as inhibitor of tumor initiation (Jang *et al.*, 1997; Gatz and Wiesmuller, 2008). The antioxidant activity of resveratrol was realized by *in vitro* experiments of Leonard *et al.* (2003) where, resveratrol at high doses can act as radical scavenger in hydroxyl and superoxide radical generating systems.

In conclusion dacarbazine is clastogenic to mice bone marrow cells causing severe damage at the level of DNA. The administration of resveratrol improved the genotoxic effects of dacarbazine. The

results of this work draw attention for application of a safer chemotherapeutic protocol for cancer treatment by using strong antioxidants with chemotherapeutic agents.

Corresponding author

Ramadan, A.M. Ali

Zoology Dept., College for Girls for Science, Arts and Education, Ain-Shams Univ., Heliopolis, Cairo, Egypt.

ramadanali27@gmail.com

References

- Adekunle, B.; Alabi, O.; Olusanmi, A. and Hafeez, J. (2009):** Genotoxicity assessment of a pharmaceutical effluent using four bioassays. *Genet. Mol. Biol.*, 32 (2): 373-381.
- Adler, D.; Kliesch, U.; Jentsch, I. and Speicher, R. (2002):** Induction of chromosomal aberrations by dacarbazine in somatic and germinal cells of mice. *Mutagenesis*, 17: 383-389.
- Al-Saleh, A. (2001):** Human lymphocyte chromosomes exposed to Dacarbazine. *J. Egypt. Ger. Soc. Zool.*, 36C:173-178.
- Al-Hawary, A. and Al-Saleh, A. (1989):** Cytogenetic effects of dacarbazine on mouse bone marrow cells in vivo. *Mutat. Res.*, 223: 259-266.
- Apraiz, A.; Boyano, M.; Asumendi, A. (2011):** Cell-centric view of apoptosis and apoptotic cell death-inducing antitumoral strategies. *Cancers*, 3: 1042-1080.
- Avilés, A.; Díaz-Maqueo, C.; Talavera, A.; Guzmán, R. and García, L. (1991):** Growth and development of children of mothers treated with chemotherapy during pregnancy: current status of 43 children. *Am. J. Hematol.* 36(4):243-8.
- Basaran, G.; Agaoglu, F. and Basaran, M. (2010):** Doxorubicin, bleomycin, vinblastine, and dacarbazine alone in treatment of favorable, limited-stage Hodgkin's lymphoma: do we really have robust data? *J. Clin. Oncol.* 28(27): 485-486.
- Brevik, A.; Gaivão, I.; Medin, T.; Jørgensen, A.; Piasek, A.; Elilasson, J.; Karlsen, A.; Blomhoff, R.; Veggan, T.; Duttaroy, K. and Collins, R. (2011):** Supplementation of a western diet with golden kiwifruits (*Actinidia chinensis* var. 'Hort 16A') effects on biomarkers of oxidation damage and antioxidant protection. *Nutr. J.*, 10: 54-61.
- Chang, L.; Chen, G.; Ulrich, M.; Bigler, J.; King, B.; Schwarz, Y.; Li, S.; Li, L.; Potter, D. and Lampe, W. (2010):** DNA damage and repair: fruit and vegetable effects in a feeding trial. *Nutr. Cancer*, 62(3): 329-335.
- Collodel, G.; Federico, G.; Geminiani, M.; Martini, S.; Bonechi, C.; Rossi, C.; Figura, N. and Moretti, E. (2011):** Effect of trans-resveratrol on induced oxidative stress in human sperm and in rat germinal cells. *Reprod. Toxicol.*, 31(2): 239-246.
- Denissova, N.; Nasello, C.; Yeung, P.; Tischfield, J. and Breneman, M. (2011):** Resveratrol protects mouse embryonic stem cells from ionizing radiation by accelerating recovery from DNA strand breakage. *Carcinogenesis*, 32: 125-131.
- Enari, M.; Sakahira, H.; Yokoyama, H.; Okawa, K.; Iwamatsu, A. and Nagata, S. (1998):** A caspase-activated DNase that degrades DNA during apoptosis, and its inhibitor ICAD. *Nature*, 391: 43-50.
- Fowler, J.; Cohen, L. and Jarvis, P. (1998):** Practical statistics for field biology. 2nd ed. John Wiley & Sons, Chichester, New York.
- Fulda, S. and Debatin, K. (2006):** Extrinsic versus intrinsic apoptosis pathways in anticancer chemotherapy. *Oncogene*, 25: 4798-4811.
- Fusser, M.; Nesse, G.; Khobta, A.; Xia, N.; Li, H.; Klungland, A. and Epe, B. (2011):** Spontaneous mutagenesis in *Csb^{mm}Ogg1^{-/-}* mice is attenuated by dietary resveratrol. *Carcinogenesis*, 32: 80-85.
- Gatz, S. and Wiesmuller, L. (2008):** Take a break—resveratrol in action on DNA. *Carcinogenesis*, 29(2): 321-332.
- Gerson, L. (2002):** Clinical relevance of MGMT in the treatment of cancer. *J. Clin. Oncol.*, 20: 2388-2399.
- Gong, Q.; Li, F.; Jin, F. and Shi, J. (2010):** Resveratrol attenuates neuroinflammation-mediated cognitive deficits in rats. *J. Health Sci.*, 56(6): 655-663.
- Hayashi, M.; Sofuni, T. and Ishidate, M.J. (1983):** An application of Acridine Orange fluorescent staining to the micronucleus test. *Mutat. Res.*, 120: 241-247.
- Hayashi, M.; Morita, T.; Kodama, Y.; Sofuni, T. and Ishidate, M. (1990):** The micronucleus assay with mouse peripheral blood reticulocytes using acridine-orange coated slides. *Mutat. Res.*, 245: 245-249.
- IARC (1982):** On the evaluation of the carcinogenic risk of chemicals to humans, Vol.29, pp. 1-292.
- Jang, M.; Cai, L.; Udeani, G.; Slowing, K.; Thomas, C.; Beecher, C.; Fong, H.; Farnsworth, N.; Kinghorn, A.; Mehta, R.; Moon, R. and Pezzuto, J. (1997):** Cancer chemopreventive activity of resveratrol, a natural product derived from grapes. *Science*, 275: 218-220.
- Jeremic, B.; Shibamoto, Y. and Abe, M. (1996):** Assessment of micronucleus induction in murine SCCVII cells treated with various anticancer agents. *Chemotherapy*, 42: 266-272.
- Kaina, B.; Christmann, M.; Naumann, S. and Roos, W. (2007):** MGMT: Key node in the battle against genotoxicity, carcinogenicity and apoptosis

- induced by alkylating agents. *DNA Repair*, 6 (8): 1079-1099.
- Kakumanu, S.; Tagne, B.; Wilson, A. and Nicolosi, J. (2011):** A nanoemulsion formulation of dacarbazine reduces tumor size in a xenograft mouse epidermoid carcinoma model compared to dacarbazine suspension. *Nanomedicine*, 7(3): 277-283.
- Kersten, B.; Kasper, P.; Brendler-Schwaab, S. and Müller, L. (2002):** Use of the photo-micronucleus assay in Chinese hamster V79 cells to study photochemical genotoxicity. *Mutat. Res.*, 519:49-66.
- Khan, F.; Sherwani, A. and Afzal, M. (2010):** Analysis of genotoxic damage induced by dacarbazine: an in vitro study. *Toxin Reviews*, 29: 130-136.
- Leonard, S. Xia, C. Jiang, B. Stinefelt, B. Klandorf, H. Harris, G. and Shi, X. (2003):** Resveratrol scavenges reactive oxygen species and effects radical-induced cellular responses. *Biochem. Biophys. Res. Commun.*, 309: 1017-1026.
- Lu, F.; Zahid, M.; Wang, C.; Saeed, M.; Cavalieri, L. and Rogan, G. (2008):** Resveratrol prevents estrogen-DNA adduct formation and neoplastic transformation in MCF-10F cells. *Cancer Prev. Res. (Phila.)*, 1(2): 135-145.
- Miele, M.; Bonassi, S.; Boatti, S.; Martini, E.; Miglio, L.; Ottaggio, I.; Queirolo P.; Sertoli, M. and Abbondandolo, A. (1998):** Micronucleus analysis in peripheral blood lymphocytes from melanoma patients treated with dacarbazine. *Anticancer Res.*, 18: 1967-1971.
- Norppa, H. and Falck, G. (2003):** What do human micronuclei contain?. *Mutagenesis*, 18(3): 221-233.
- Olas, B.; Wachowicz, B.; Majsterek, I. and Blasiak, J. (2005):** Resveratrol may reduce oxidative stress induced by platinum compounds in human plasma, blood platelets and lymphocytes. *Anticancer Drugs*, 16(6): 659-665.
- Pourahmad, J.; Amirmostofian, M.; Kobarfard, F. and Shahraki, J. (2009):** Biological reactive intermediates that mediate dacarbazine cytotoxicity. *Cancer Chemother. Pharmacol.*, 65: 89-96.
- Prado, R.; Santos, B.; Pinto, C.; Assis, K.; Salvadori, D. and Ladeira, M. (2010):** Influence of diet on oxidative DNA damage, uracil misincorporation and DNA repair capability. *Mutagenesis*, 25(5): 483-487.
- Preston, R. J.; Dean, B. J.; Galloway, S.; Holden, H.; McFee, F. and Shelby, M. (1987):** Mammalian *in vivo* cytogenetic assays. Analysis of chromosome aberrations in bone marrow cells. *Mutat. Res.*, 189: 157-165.
- Quincozes-Santos, A.; Andrezza, C.; Gonçalves, A. and Gottfried, C. (2010):** Actions of redox-active compound resveratrol under hydrogen peroxide insult in C6 astroglial cells. *Toxicol. In Vitro*, 24(3): 916-920.
- Riso, P.; Martini, D.; Visioli, F.; Martinetti, A. and Porrini, M. (2009):** Effect of broccoli intake on markers related to oxidative stress and cancer risk in healthy smokers and nonsmokers. *Nutr. Cancer*, 61(2): 232-237.
- Rooseboom, M.; Commandeur, N. and Vermeulen, P. (2004):** Enzyme-catalyzed activation of anticancer prodrugs. *Pharmacol. Rev.*, 56(1): 53-102.
- Roy, M.; Sinha, D.; Mukherjee, S.; Paul, S. and Bhattacharya, K. (2008):** Protective effect of dietary phytochemicals against arsenite induced genotoxicity in mammalian V79 cells. *Indian J. Exp. Biol.*, 46(10): 690-697.
- Samulitis, K.; Dorr, T. and Chow, H. (2011):** Interaction of dacarbazine and imexon, in vitro and in vivo, in human A375 melanoma cells. *Anticancer Res.*, 31(9): 2781-2785.
- Savage, K. (1976):** Classification and relationships of induced chromosomal structural changes. *J. Med. Genetics*, 13: 103-122.
- Varga, C.; Ember, I. and Raposa, L. (1991):** Comparative studies on genotoxic and carcinogenic effects of different cytogenetic analyses in CB mice. *Cancer Let.*, 60: 199-203.
- Verma, S.; Younus, J.; Stys-Norman, D.; Haynes, E. and Blackstein, M. (2008):** Meta-analysis of ifosfamide-based combination chemotherapy in advanced soft tissue sarcoma. *Cancer Treat. Rev.*, 34(4):339-347.
- Walter, T.; Bruneton, D.; Cassier, A.; Hervieu, V.; Pilleul, F.; Scoazec, Y.; Chayvialle, A. and Lombard-Bohas, C. (2010):** Evaluation of the combination 5-fluorouracil, dacarbazine, and epirubicin in patients with advanced well-differentiated neuroendocrine tumors. *Clin. Colorectal. Cancer*, 9(4):248-254.
- Wang, Y.; Catana, F.; Yang, Y. Roderick, R. and van Breemen, B. (2002):** An LC-MS method for analyzing total resveratrol in grape juice, cranberry juice, and in wine. *J. Agric. Food Chem.*, 50: 431-435.
- Yan, Y.; Yang, J.; Chen, G.; Mou, Y.; Zhao, Y.; Pan, L.; Ma, C.; Liu, X. and Wu, C. (2011):** Protection of resveratrol and its analogues against ethanol-induced oxidative DNA damage in human peripheral lymphocytes. *Mutat. Res.*, 721(2): 171-177.
- Yi, H.; Yi, Y.; Lee, R.; Lee, I.; Lim do.; H.; Kim, H.; Park, W. and Lee, J. (2011):** Dacarbazine-based chemotherapy as first-line treatment in noncutaneous metastatic melanoma: multicenter,

retrospective analysis in Asia. *Melanoma Res.*, 21(3): 223-227.

Yiu, C.; Chen, S.; Chang, L.; Chiu, Y. and Lin, T. (2010): Inhibitory effects of resveratrol on the Epstein-Barr virus lytic cycle. *Molecules*, 15: 7115-7124.

Yoshida, J.; Kosaka, H.; Tomioka, K. and Kumagai, S. (2006): Genotoxic risks of nurses

from contamination of the work environment with antineoplastic drugs in Japan. *J. Occup. Health*, 48: 517-522.

Yoshida, Y.; Shioi, T. and Izumi, T. (2007): Resveratrol ameliorates experimental autoimmune myocarditis. *Circ. J.*, 71: 397-404.

12/12/2011

Nervi Terminalis, Vomeronasalis and Olfactorius of *Uromastyx aegyptius* (Squamata – Lacertilia - Agamidae)Dakrory, A.I.^{*1}; Issa, A.Z.¹ and Ali, R.S²¹Department of Zoology, Faculty of Science, Cairo University, Cairo, Egypt²Department of Zoology, Faculty of Science, Helwan University, Cairo, Egyptdakrory2001@yahoo.com

Abstract: The present work was aimed to study the anterior cranial nerves which innervate the olfactory apparatus of *Uromastyx aegyptius*. The olfactory apparatus of *Uromastyx aegyptius* includes the main olfactory organ and the vomeronasal organ or organ of Jacobson. The main olfactory organ is innervated by the olfactory nerve which arises from the sensory olfactory epithelium and leaves the capsular cavity through a separate foramen, i.e., there is no foramen olfactorium advehens. The vomeronasal organ is innervated by two nerves: the terminal and the vomeronasal nerves. They arise from the sensory epithelium in combination. The terminal nerve carries a terminal ganglion. The nervi terminalis and vomeronasalis combined together as one separate nerve which leaves the cavity of the nasal capsule together with few bundles of the olfactory nerves through a special foramen. The nervi terminalis, vomeronasalis and olfactorius enter the cranial cavity through a large foramen olfactorium evehens and they connect separately the anterior part of the brain. The vomeronasal nerve enters the accessory olfactory bulb (vomeronasal formation) of the fore brain. The nervus olfactorius enters the main olfactory bulb whereas the terminal nerve connects the anterior end of the olfactory lobe. The olfactory bulb has a long olfactory peduncle. The three nerves carry pure special somatic sensory fibres.

[Dakrory, A.I.; Issa, A.Z. and Ali, R.S **Nervi Terminalis, Vomeronasalis and Olfactorius of *Uromastyx aegyptius* (Squamata – Lacertilia - Agamidae)** Life Science Journal, 2011; 8(4):900-907] (ISSN: 1097-8135).
<http://www.lifesciencesite.com>.

Keywords: *Uromastyx aegyptius* – Nervus terminalis – Nervus olfactorius.

1. Introduction

Agamid lizards constitute a relatively large family of suborder Lacertilia of the order Squamata.

Many studies were carried out on the skeletal system of the agamid lizards (Ramaswami, 1946; Malan, 1946; Barry, 1953; Eyal-Giladi, 1964). However, little works were obtained on their cranial nerves such as Soliman *et al.* (1984 & 1990) on *Agama pallid* and Shamakh (2009) on *Laudakia stellio*. Concerning the cranial nerves in reptiles, in general, many studies were reported in Lacertilia and Ophidia such as Soliman and Hegazy (1969) on *Chalcidid ocellatus*, Soliman and Mostafa (1984) on *Tarentola mauritanica*, Dakrory (1994) on the amphisbaenian *Diplometopon zarudnyi*, Abdel-Kader (2006) on the cat snake *Telescopus dhara* and Abdel-Kader *et al.* (2007) on *Mabuya quinquetaeniata*.

Uromastyx aegyptius is chosen for this study. It is known as spiny-tailed lizard or dabb lizard. This species is adapted to the arid habitat. The anatomy and morphology of the cranial nerves of member of the family Agamidae is poor and scarce. Hence, it was convenient to study the anterior cranial nerves which innervate the olfactory apparatus of the animal to elucidate their neural characters and to analyze the fibre components of these nerves. This may help in understanding the phylogeny, taxonomy and behavior of this primitive lacertilian family.

2. Materials and Methods

The fertilized eggs of *Uromastyx aegyptius* are collected from Gabal Al-Maghara, South of El-Arish City, Northern Sinai, Egypt, during August 2004, at the last days of the incubation period. After careful removing of the embryos from the shells, they were fixed immediately in an aqueous Bouin's fluid for 24 hours, and then washed with 70% ethyl alcohol for several days to remove the excess of fixative. Thereafter, the heads were decalcified using EDTA solution for about 3-4 weeks, changing the solution every 4 days. The heads were then dehydrated, cleared, mounted and embedded in paraffin wax and serially sectioned transversely at 10 µm thick. The serial sections were stained with Mallory's Triple Stain.

The transverse sections were drawn with the help of a projector microscope. In order to show the relations of the nerves to the different parts of the head, several sections were also photomicrographed.

3. Results**Nervus Terminalis (N. 0)**

In the agamid lizard *Uromastyx aegyptius*, the fibres of the nervus terminalis arise from the sensory epithelium of the vomeronasal organ along its entire length in combination with the fibres of the vomeronasal nerve. The nerve fibres are originated from the medial, dorsal and lateral aspects of the

sensory epithelium at the anterior blind end of the organ, and collect into three branches. These branches are located, dorsomedial, dorsal and dorso lateral to the organ epithelium (Fig. 1, N.O). Shortly posterior, and opposite to the anterior end of the organ cavity, the nerve fibres originating from the sensory epithelium collect into four small nerve branches (Fig. 2, N.O). Thereafter, fine branches are formed from the nerve fibres arising from the medial, dorsal and dorso lateral sides of the organ epithelium lining the anterior half of the organ. These branches extend posteriorly passing dorsomedial, dorsal and dorsolateral to the organ epithelium, where they gradually approach each other and fuse forming four small nerve bundles (Fig. 3, N.O). These nerve bundles gradually fuse together near the posterior aspect of the organ forming one large bundle that run posteriorly. It runs posteriorly passing dorsomedial to the organ epithelium and lateral to the internasal septum.

The nerve fibres originating from the epithelium of the middle part of the organ aggregate together into three small nerve branches. These branches run posteromedially passing dorsal to the organ epithelium and ventral to both the organ cartilaginous roof and the septomaxillary bone (Fig. 4). Shortly backwards, another five branches are formed; one from the medial epithelium and four from the lateral and dorsolateral epithelium of the organ, opposite to the organ duct (Fig.3, N.O). These branches extend posteromedially passing dorsal to the organ epithelium and ventral to the septomaxillary bone. They gradually fuse together forming a second large bundle. The two bundles extend posterodorsally passing lateral to the internasal septum and medial to the septomaxillary bone till they leave the organ capsule and enter the nasal capsule.

The sensory nerve fibres arising from the caudal end of the organ collect together forming numerous branches. These branches extend posterodorsally to leave the organ capsule and enter the olfactory capsule (Fig. 4, N.O). At this point, some of these branches are added to the previously formed bundles and the remainder fuse together forming third nerve bundle (Fig. 6, N.O).

Shortly posterior, within the olfactory capsule, the first large bundle carries few scattered ganglionic cells. These cells represent the ganglion terminale (Fig. 5, GT). The three large nerve bundles continue running posterodorsally within the olfactory capsule passing medial to the olfactory epithelium, dorsal to both the paraseptal cartilage

and the prevomer bone and lateral to the internasal septum, where the second bundle receives fine branches from the olfactory nerve. More backwards, the three

bundles gradually approach and fuse together forming the nervus terminalis carrying the vomeronasal fibres. In the posterior part of the olfactory capsule, the internasal septum degenerates and the two nervi terminale extend side by side till they leave the cavity of the nasal capsule through their own common foramen; terminal foramen (Figs. 10&11, F.NT).

The terminal foramen is located at the most medial aspect of the posterodorsal edge of the olfactory capsule. Extracapsullary, this nerve enters directly the cranial cavity through the foramen olfactorium evehens (Figs. 7, 10&11, F.OE). Within the cranial cavity, the nervus terminalis carrying the vomeronasal fibres extends posteriorly passing ventromedial to the main olfactory bulb. After a posterior distance, it separates from the vomeronasal nerve fibres. The later nerve enters the accessory olfactory bulb (Fig. 12, AOLB); whereas the terminale nerve connects the anterior end of the fore brain.

Nervus Olfactorius (N.I)

In *Uromastix aegyptius*, the fibres of the nervus olfactorius arising from the sensory olfactory epithelium aggregate forming several branches. These branches run posterodorsally around the walls of the olfactory chamber at the middle and the posterior regions of the nasal cavity. They extend in a place bounded dorsally and laterally by the parietotectal cartilage and medially by the internasal septum.

During their backward course these branches gradually approach and unite together into separate bundles, constituting the ordinary nervus olfactorius (Figs. 7, 8 &11, N.I). The nerve branches formed from the most ventral and middle parts of the medial olfactory epithelium extend posterodorsally passing lateral to the paraseptal cartilage and medial to the the olfactory epithelium and ventrolateral to the nervus terminalis. After a short distance, these reach and fuse with latter nerve (Figs. 6&8, N.I).

The olfactory nerve branches formed from the sensory epithelium of the dorsal part of the medial epithelium, at its anterior end extend posterodorsally to leave the nasal capsule through the posteromedial corner of the largest olfactory foramen (Fig. 8, N.I). An olfactory nerve branch is formed from the aggregation of the sensory nerve fibres arising from the most posterior part of the medial olfactory epithelium. This branch extends posterodorsally to leave the nasal capsule together with the nervus terminalis through the terminal foramen (Figs. 10&11).

The olfactory nerve branches formed from the dorsal sensory epithelium run posterodorsally passing medial and ventral to the parietotectal

cartilage. These branches leave the capsular cavity through a somewhat large foramen as two or three large bundles (Fig. 7, F.OL). This foramen is bundled anteriorly by parietotectal cartilage medially by the internasal septum, anteriolaterally the sphenoidal commissure and posteriorly by the lamina orbitonasalis (Planum antorbitale). From the posterior region of the sensory olfactory epithelium several fine olfactory nerve branches (about seven branches) are formed and leave the capsular cavity separately, each through its own foramen in the lamina orbitonasalis (Figs. 7,8,10&11, F.OL).

Extracapsular, the olfactory nerve branches run posterodorsally to enter the cranial cavity through a large foramen olfactorium evehns (Figs. 9,10&11, F.OE). Within the latter cavity, these branches join the main olfactory bulb from its ventral, ventromedial and ventrolateral sides (Figs. 8&11, N.I). This bulb has a posteromedial part which is termed accessory olfactory bulb (Fig. 12, AOLB) or vomeronasal formation that receives the

vomeronasal nerve.

Both the main and the accessory olfactory bulbs are connected with the anterior part of the fore brain (olfactory lobe) by a somewhat elongated olfactory peduncle or tract (stalk).

It is obvious from the above description that, the olfactory apparatus of *Uromastix aegyptius* is innervated by three nerves: terminale, vomeronasal and the main olfactory. Both the nervi terminalis and vomeronasalis originate from the sensory epithelium of Jacobson's organ (an accessory olfactory organ), whereas, the nervus olfactorius arises from the epithelium of the main olfactory organ. These nerves carries special somatic sensory fibres. There is no foramen olfactorium advehens, but instead, there are many olfactory foramina and one foramen for the combined nervi terminalis, vomeronasalis and few branches of the olfactory nerve.

The olfactory bulb is pedunculated, i.e., there is an olfactory peduncle "tract or stalk" connecting it with the olfactory lobe.

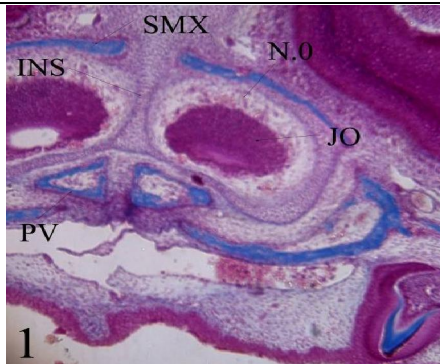


Fig. (1): Photomicrograph of a part of transverse section of the olfactory region of *Uromastix aegyptius* showing the issue of the nerve fibres from the anterior wall of the sensory epithelium of Jacobson's organ(x 40).

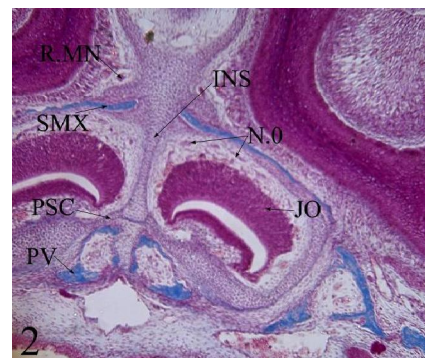


Fig. (2):Photomicrograph of a part of transverse section of the olfactory region of *Uromastix aegyptius* showing the issue of the nerve fibres from the dorsal side of the sensory epithelium of Jacobson's organ. (x 40).

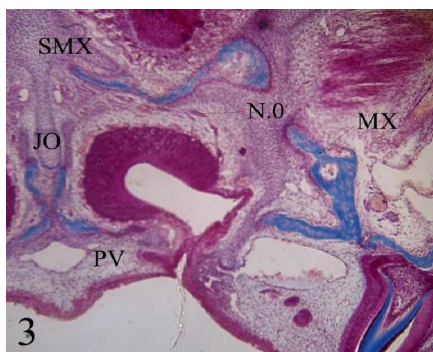


Fig. (3): Photomicrograph of a part of transverse section of the olfactory region of *Uromastix aegyptius* showing the issue of the nerve fibres from the sensory epithelium of Jacobson's organ opposite to the organ duct(x 40).

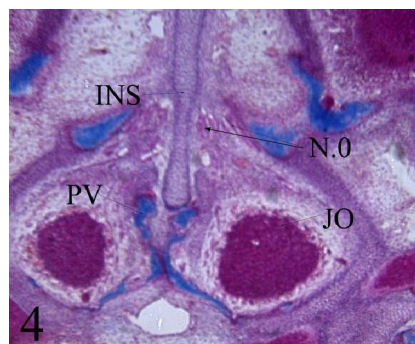


Fig. (4): Photomicrograph of a part of transverse section of the olfactory region of *Uromastix aegyptius* showing the issue of the nerve fibres from the posterior wall of the sensory epithelium of Jacobson's organ (x 40).

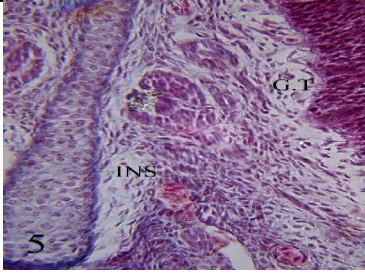


Fig. (5): Photomicrograph of a part of transverse section of the olfactory region of *Uromastix aegyptius* illustrating the terminal ganglion (x 100).

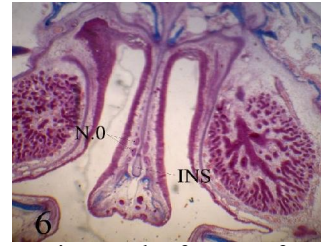


Fig. (6): Photomicrograph of a part of transverse section of the olfactory region of *Uromastix aegyptius* showing the bundles of the terminal nerve passing within the olfactory capsule (x 40).

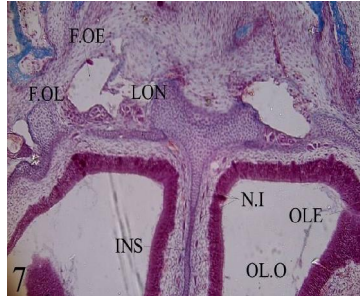


Fig. (7): Photomicrograph of a part of transverse section of the olfactory region of *Uromastix aegyptius* demonstrating the origin of the olfactory nerve, the olfactory foramen and the foramen olfactorium evehens (x 40).

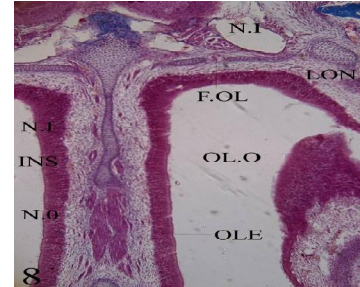


Fig. (8): Photomicrograph of a part of transverse section of the olfactory region of *Uromastix aegyptius* showing the bundles of the terminal nerve passing within the olfactory capsule, the origin of the olfactory nerve and the foramen olfactorium evehens (x 40).



Fig. (9): Photomicrograph of a part of transverse section of the olfactory region of *Uromastix aegyptius* illustrating the foramen olfactorium evehens, olfactory bulb and the passage of the terminal nerve within the olfactory capsule (x 40).

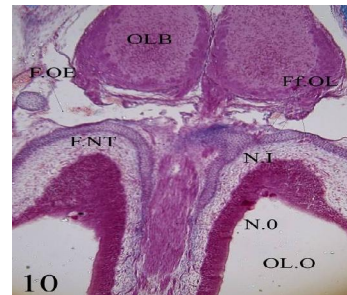


Fig. (10): Photomicrograph of a part of the transverse section of the olfactory region of *Uromastix aegyptius* showing the foramina of the olfactory nerve, the foramen olfactorium evehens and the foramen of the terminal nerve (x 60).

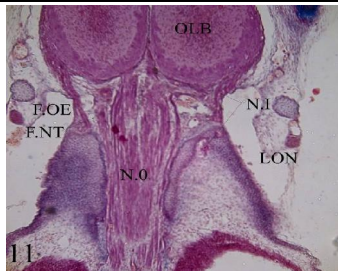


Fig. (11): Photomicrograph of a part of transverse section of the olfactory region of *Uromastix aegyptius* illustrating the passage of the terminal nerve through its own foramen and the olfactory foramina in the lamina orbitonasalis (x 60).

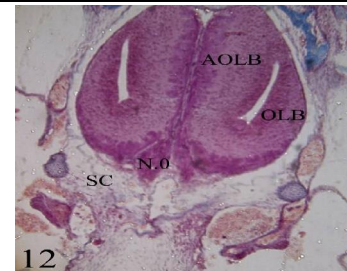


Fig. (12): Photomicrograph of a part of transverse section of the olfactory region of *Uromastix aegyptius* illustrating the main olfactory bulb, the accessory olfactory bulb and terminal nerve (x 60).

4. Discussion

The microscopic examination of the innervation of the olfactory apparatus in *Uromastix aegyptius* succeeds in demonstrating three groups of nerve fibres which arise from the sensory cells of this apparatus and connect separately to the anterior portion of the forebrain. These fibres constitute the nervus terminalis, the ordinary olfactory nerve and the vomeronasal nerve. The fibres of the nervus terminalis differ essentially from those of the latter two nerves.

The nervus terminalis was identified nearly in all the vertebrate classes except cyclostomes and birds, as has been reported by Watanabe and Yasuda (1968), Romer and Parsons (1985), Soliman *et al.* (1986) and Shamakh (2009). On the other hand, Von Bartheld *et al.* (1987) and Northcutt and Puzdrowski (1988) stated that a terminal nerve is found in lampreys, follows the application of horseradish peroxidase to the olfactory mucosa.

Some anatomists suggested that this nerve is possibly a ganglionated remnant of an anterior branchial nerve which primitively innervated the mouth region (Weichert, 1958; Kent, 1978; Goodrich, 1986).

Concerning the structural components of the nervus terminalis, it was reported that this nerve contains elements of a sympathetic nature. According to Haller von Hallerstein (1934) the nervus terminalis carries somatic sensory fibres in addition to some sympathetic ones. Jollie (1968), however, mentioned that this nerve is presumed a sensory nerve (general cutaneous), but it may be a part of the autonomic system.

Eventually, there is a conflict of opinion about the exact function of the nervus terminalis. Haller von Hallerstein (1934) suggested that this nerve acts as a Jacobson's organ nerve in terrestrial vertebrates, while in aquatic forms it performs a special function. However, Weichert (1958), Kent (1978), Romer and Parsons (1985) and Goodrich (1986) are of the opinion that the function of the nervus terminalis is not clear. It has been reported that although this nerve is apparently sensory, yet it is unrelated to olfaction.

In the present study, the nervus terminalis arise from Jacobson's organ in combination with the vomeronasal nerve. The fibres of the two nerves are also closely associated throughout their nasal course as well as their intracranial distribution. A similar condition was described in lizards *Diplometopon zarudayi* (Dakrory, 1994), *Acanthodactylus boskianus* (El-Ghareeb, 1997) and in the serpents *Naja haje haje* (Abdel-Kader *et al.*, 2000) and in *Natrix tessellate* (El-Ghareeb *et al.*, 2004). On the

other hand, the result of the present study is totally different from what was described by Hegazy (1976) in serpents *Psammophis sibilans*, *Eryx jaculus* and *Cerastes vipera* and by Mostafa (1990a) in *Psammophis schokari*, *Coluber elegantissimus* and *Spalerosophis diadema*. In such snakes the nervus terminalis was found to arise from Jacobson's organ in a separate manner that is apart from the vomeronasal nerve.

In *Uromastix aegyptius*, a number of ganglion cells are found associated with some of the nerve bundles forming the terminal and vomeronasal nerve. These ganglionic cells evidently represent the ganglion terminale as mentioned by Arey (1966), Bhatnagar and Kallen (1974), Hegazy (1990), Dakrory (1994), El-Ghareeb (1997), Abdel-Kader *et al.* (2000), El-Ghareeb *et al.* (2004) and Shamakh (2009).

The configuration of the terminal ganglion, met with in the present study, differs entirely from what was described by Hegazy (1976) and Mostafa (1990a) in Ophidia. These authors recorded that the terminal nerve arises apart from the vomeronasal nerve of Jacobson's organ and it carries the ganglion intracranially near its termination in the forebrain.

According to Haller von Hallerstein (1934), Weichert (1958), Grüneberg (1973), Goodrich (1986) and Dakrory (1994) the nervus terminalis of fishes, amphibians, reptiles and mammals bears during its course one or two ganglia terminale.

In the present study, the olfactory bulb lies at a considerable distance anterior to the cerebral hemisphere of the brain, to which it is joined by an olfactory peduncle. This was generally found in Lacertilia and Ophidia by Haller von Hallerstein (1934). The presence of an olfactory peduncle has been described by many authors in the majority of Lacertilia and Ophidia, and consequently it seems a common character in Squamata. It was described by in the lizards *Lacerta viridis* (Goldby, 1934), *Anguis fragilis* (Pratt, 1948), *Chalcides ocellatus* (Hegazy, 1969), *Tarentola mauritanica* (Mostafa, 1970), *Agama pallida* and *Ptyodactylus hasselquistii* (Abdel-Kader, 1990), *Uromastix aegyptius* (Mostafa, 1990b). An olfactory peduncle was also described by Hegazy (1976) in *Psammophis sibilans*, *Eryx jaculus* and *Cerastes vipera* by Mostafa (1990a) in *Psammophis schokari*, *Coluber elegantissimus* and *Spalerosophis diadema* by Abdel-Kader *et al.* (2000) in *Naja haje haje* and by El-Ghareeb *et al.* (2004) in *Natrix tessellate*. In Chelonia, on the other hand, Soliman (1964) found that the olfactory peduncles are absent and the olfactory bulbs join the cerebral hemispheres directly.

The connection of the vomeronasal nerve with

the organ of Jacobson from one side and the vomeronasal formation (accessory olfactory bulb) from the other side, met with in the present study, is the case found in the lizards by Pratt (1948), Dakrory (1994 & 2011), El-Ghareeb (1997) and by Shamakh (2009) and also in the snakes described by Abdel-Kader *et al.* (2000) and Mahgoub (2004). According to Bellairs (1950) and Jollie (1968), this condition seems to be a common character in *Sphenodon* and squamates.

The vomeronasal nerve, Jacobson's organ, and consequently the accessory olfactory bulbs, are not represented in chelonians and crocodylians among reptiles, and in all birds (Jollie, 1968; Romer and Parsons, 1985; Soliman *et al.*, 1986). Among mammals, the structures in question, are lacking in many bats, various aquatic forms as whales, in some carnivorous and in man and the other higher primates as maquque (Jawlowski, 1955; Mann, 1961; Bhatnagar and Kallen, 1974; Romer and Parsons, 1985). Evidently, these findings affirm satisfactorily the concept which has been accepted among morphologists that the accessory olfactory bulb is apparently restricted to animals having a vomeronasal organ.

In *Uromastix aegyptius* studied, the nervus terminalis, being associated with the vomeronasal nerve carrying few olfactory bundles, exits from the cavity of the nasal capsule through special foramen. Also, the nervus olfactorius leaves the capsular cavity as separate bundles through separate foramina (found in the olfactory capsule; one for each bundle). Among agamids, a typical condition was found in *Agama stellio* (Eyal-Giladi, 1964) and in *Laudakia stellio* (Shamakh, 2009). Also, Malan (1946) recorded a number of foramina for the emersion of these nerves from the capsular cavity in *Sceloporus undulates* and *Iguana iguana*. It appears that the exit of these nerves from the olfactory capsule in agamides is modified completely from that found in other lacertilians, where there is a single foramen olfactorium advehens for their exit. Such modifications are due to the backward movement of the dorsal part of the nasal capsule relative to its ventral part. Malan (1946) reported that the nervus vomeronasalis leaves the capsular cavity through a separate foramen which is situated so low down on the posterior face of the capsule as to be located almost ventral in position. This condition is very similar to that found in *Laudakia stellio* (Shamakh, 2009).

On the other hand, a closed foramen olfactorium advehens is found in most of the lizards so far described. It is mentioned by Rice (1920) in *Eumeces* and by Ramaswami (1946) in *Calotes*. This appears to be due to the fusion between the planum

antorbitale and the nasal septum. However, the foramen olfactorium advehens of amphisbaenian *Diplometopon zarudnyi* (Dakrory, 1994) is in the form of a wide incisura and not a closed foramen. This is due to the lack of connection between the planum antorbitale and the nasal septum.

Among Ophidia, a closed foramen olfactorium advehens was recorded in *Vipera resselii* (Srinivasachar, 1955), *Cerastes vipera* (Hegazy, 1976), *Spalerosophis diadema* (Mostafa, 1990a) and in *Naja haje haje* (Abdel-Kader *et al.*, 2000). On the other hand, such foramen is in the form of a wide incisura and not a complete foramen in the snakes *Typhlops delalandii* (Smit, 1949), *Malpolon monospessulana* (El-Toubi *et al.*, 1973), *Psammophis sibilans* and *Eryx jaculus* (Hegazy, 1976) and in both *Psammophis schokari* and *Coluber elegantissinus* (Mostafa, 1990a).

Among birds, the presence of a defined fenestra olfactorium advehens appears to be common (Soliman *et al.*, 1986). However, the nervus olfactorius leaves the capsular cavity through fissura orbitonasalis in *Sternus vulgaris* (De Kock, 1955) and by means of a bony canal in *Colius indicus* (Schoonees, 1963).

In Mammalia, the fenestra olfactoria advehens, or fenestra cribrosa, is subdivided into numerous pores of the cribriform plate. The subdivision of the fenestra olfactoria advehens was described in *Galago senegalensis* (Kanagasuntheram and Kanan, 1964) and *Manis javanica* (Jollie, 1968). The subdivision of the fenestra olfactoria advehens seems to be a typical mammalian character, except in monotremes. In such case, nervus terminalis, being combined with the vomeronasal nerve, and the ordinary nervus olfactorius leaves the nasal cavity through two separate foramina of the cribriform plate (Hegazy, 1990) in the hedgehog. Earlier, Huber and Guild (1913) and McCotter (1915) dealing with the rabbit and man, respectively, mentioned that the nervus terminalis passes through the cribriform plate anterior to the exit of the vomeronasal nerve.

In the present study, the nervi terminalis, vomeronasalis and olfactorius enter the cranial cavity through the foramen olfactorium advehens. This result agrees with the result of Ramaswami (1946) in *Calotes versicolor*, Hegazy (1969) in *Chalcides ocellatus*, Mostafa (1970) in *Tarentola mauritanica* and Shamakh (2009) in *Laudakia stellio*. On the other hand, due to the absence of a foramen olfactorium advehens, the nervi terminalis, vomeronasalis and olfactorius enter the cranial cavity through the membranous cranial wall as recorded in the amphisbaenian *Diplometopon zarudnyi* (Dakrory, 1994).

In Ophidia, the lack of the foramen olfactorium

evehens seems to be a common pattern (Pringle, 1954; Hammouda, 1963; El-Toubi *et al.*, 1973; Mostafa, 1990a; Abdel-Kader *et al.*, 2000). These authors concluded that the lacking of the foramen olfactorium evehens is due to the complete lack of the sphenethmoid commissure.

Corresponding author:

Dakrory, A.I
Department of Zoology, Faculty of Science, Cairo University, Cairo, Egypt
dakrory2001@yahoo.com

References

- Abdel-Kader, I.Y.** (1990): Anatomical studies on the cranial nerves of the lizards *Agama pallida* and **Abdel-Kader, I.Y.** (2006): The cranial nerves of the cat snake *Telescopus dhara* (Colubridae, Ophidia): I. The eye muscle nerves and the ciliary ganglion. J. Egypt. Ger. Soc. Zool., **50(B)**: 1-16.
- Ptyodactylus hasselquistii*. Ph.D. Thesis, Fac. Sci. Cairo Univ. Egypt.
- Abdel-Kader, I.Y.; Soliman, M.A. and Hegazy, R.M.** (2000): Innervation of the nasal region of the Egyptian cobra *Naja haja haja*. J. Egypt. Ger. Soc. Zool., **33**: 57-76.
- Abdel-Kader, T.G.; Shamakh, A.A. and Dakrory, A.I.** (2007): The cranial nerves of *Mabuya quinquetaeniata*. I. The eye muscle nerves and the ciliary ganglion. Egypt. J. Zool., **49**: 193-209.
- Arey, L.B.** (1966): Developmental Anatomy. Seventh Ed. Saunders, Philadelphia, USA.
- Barry, T.H.** (1953): Contributions to the cranial morphology of *Agama hispida* (Linn.). Ann. Univ. Stellenbosch, **29(A)2**: 55-57.
- Bellairs, A. d'A.** (1950): Observation on the cranial anatomy of *Anniella*, and a comparison with that of other burrowing lizards. Proc. Zool. Soc. Lond., **119(4)**: 887-904.
- Bhatnagar, K.P. and Kallen, F.C.** (1974): Morphology of the nasal cavities and associated structures in *Artibeus jamaicensis* and *Myotis lucifugus*. Amer. J. Anat., **139**: 167-190.
- Dakrory, A.I.** (1994): Anatomical studies on the cranial nerves of the Amphisbaenian (*Diplometopon zarudnyi*). M.Sc. Thesis, Fac. Sci. Cairo Univ. Egypt.
- Dakrory, A.I.** (2011): Innervation of the olfactory apparatus of *Varanus niloticus* (Squamata-Lacertilia-Varanidae). J. Amer. Sci., **7(9)**: 118-125.
- De Kock, J.M.** (1955): The cranial morphology of *Sturnus vulgaris vulgaris* Linnaeus. Ann. Univ. Stellenbosch, **31 (A) 3**: 153-177.
- El-Ghareeb, A.A.** (1997): Anatomical studies on the cranial nerves of the lizard *Acanthodactylus boskianus* (Daud). Ph.D. Thesis, Fac. Sci., Cairo Univ., Egypt.
- El-Ghareeb, A.A.; Abdel-Kader and Mahgoub, A.F.** (2004): The cranial nerves of the snake *Natrix tessellata* (Ophidia, Colubridae). The eye muscle nerves, and the ciliary ganglion. J. Union Arab Biol. Cairo, **22(A)**: 305-330.
- El-Toubi, M.R.; Kamal, A.M. and Zaher, M.M.** (1973): The development of the chondrocranium of the snake, *Malpolon monospessulana*. II. The fully formed stage. Acta Anat., **85**: 593-619.
- Eyal-Giladi, H.** (1964): The development of the chondrocranium of *Agama stellio*. Acta Zool., **45**: 139-165.
- Goldby, F.** (1934): The cerebral hemispheres of *Lacerta viridis*. J. Anat., **68**: 157-215.
- Goodrich, E.S.** (1986): The Structure and Development of Vertebrates. Maxmillan and Co. London, UK.
- Grüneberg, H.** (1973): A ganglion probably belonging to the N. Terminalis System in the nasal mucosa of mouse. Z. Anat. Entwickl. Gesch., **140**: 39-52.
- Haller von Hallerstein, V.** (1934): Anatomie der Wirbeltiere 2/1, herausgegeben von Bolk, Göppert, Kallius, Lubosch. Berlin und Wien.
- Hammouda, H.G.** (1963): Studies on the development of the ophidian skull. Ph.D. Thesis, Fac. Sci., Cairo Univ.
- Hegazy, M.A.** (1969): The cranial nerves of *Chalcides ocellatus*. M.Sc. Thesis, Fac. Sci., Cairo Univ., Egypt.
- Hegazy, M.A.** (1976): Comparative Anatomical studies on the cranial nerves of Ophidia. Ph.D. Thesis, Fac. Sci., Cairo Univ. Egypt.
- Hegazy, M.A.** (1990): A contribution to the Anatomy of the vomeronasal organ of Jacobson of Mammals with special reference to the Insectivore *Hemiechinus auritus* (Gmelin). Proc. Zool. Soc. A.R. E., **19**: 33-50.
- Huber, G.C. and Guild, S.R.** (1913): Observations on the peripheral distribution of the nervus terminalis in Mammalia. Acta Rec., **7**: 253-272.
- Jawlowski, H.** (1955): On the bulbus olfactorius and bulbus olfactorius accessories of some mammals. Ann. Univ. Mariae Curie-Sklodowska, Sect. C. Biol., **10(3)**: 67-86.
- Jollie, M.T.** (1968): The head skeleton of a new-born *Manis javanica* with comments on the ontogony and phylogeny of the mammal head skeleton. Acta Zool., **49**: 227-305.
- Kanagasuntheram, R. and Kanan C.V.** (1964): The chondrocranium of a 19 mm C.R. length embryo of *Galago senegalensis senegalensis*. Acta Zool., **45**: 107-121.
- Kent, G.C.** (1978): Comparative Anatomy of the

- Vertebrates. The C.V. MOSBY Co., Saint Louis, USA.
- Mahgoub, A.F.** (2004): Anatomical studies on the cranial nerves of the snake *Natrix tessellate*. Ph.D. Thesis, Fac. Sci., Cairo Univ.
- Malan, M.E.** (1946): Contributions to a comparative anatomy of the nasal capsule and organ of Jacobson of Lacertilia. Ann. Univ. Stellenbosch, **24(A)**: 69-137.
- Mann, G.** (1961): Bulbus olfactorius accessories in Chiroptera. J. Comp. Neurol., **116**: 135-141.
- McCotter, R.E.** (1915): A note on the course and distribution of the nervus terminalis in man. Anat. Rec., **9(3)**: 243-246.
- McKibben, P.S.** (1914): Ganglion cells of the nervus terminalis in the dog-fish (*Mustelus canis*). J. Comp. Neurol., **24**: 159-175.
- Mostafa, R.H.** (1970): A detailed study on the cranial nerves of the gecko *Tarentola mauritanica* Linn. M.Sc. Thesis, Fac. Sci., Cairo Univ., Egypt.
- Mostafa, R.H.** (1990a): The nervi terminalis, vomeronasalis and olfactorius in Ophidia. Egypt. J. Anat., **13 (2)**: 259-269.
- Mostafa, R.H.** (1990b): On the main special sensory nerves Olfactorius, Opticus and Acusticus in *Uromastix aegypticus microlepis* (Blanford). Egypt. J. Anat., **13 (2)**: 247-258.
- Northcutt, R.G. and Puzdrowski, R.L.** (1988): Projections of the olfactory bulb and nervus terminalis in the silver lamprey. Brain Behav. Evol., **32**: 96-107.
- Pratt, C.W.M.** (1948): The morphology of the ethmoidal region of *Sphenodon* and lizards. Proc. Zool. Soc. Lond., **118**: 171-201.
- Pringle, J.A.** (1954): The cranial development of certain South African snakes and the relationship of this group. Proc. Zool. Soc. London, **123**: 813-865.
- Ramaswami, L.S.** (1946): The chondrocranium of *Calotes versicolor* (Daud.) with a description of the osteocranium of a just-hatched young. Quart. J. Micr. Sci., **87**: 237-297.
- Rice, E.L.** (1920): The development of the skull in the skink, *Eumeces quinelineatus*. J. Morph., **34**: 119-220.
- Romer, A.S. and Parsons, T.S.** (1985): The Vertebrate Body, 6th edit. W.B. Saunders Co. Philadelphia and London.
- Schoonees** (1963): Some aspects of the cranial morphology of *Colius indicus*. Ann. Univ. Stellenbosch, **38**: 215-246.
- Shamakh, A.A.** (2009): Innervation of the olfactory apparatus of *Laudakia stellio* (Reptilia – Squamata – Agamidae). Egypt. J. Zool., **52**: 453-469.
- Smit, A.L.** (1949): Skädelmorfologie en-kinese von *Typhlops delalandii* (Schlegel). S. Afr. J. Sci., **45**: 117-140.
- Soliman, M.A.** (1964): Die Kopfnerven der Schildkröten. Z. F. W. Zool., **169**: 215-312.
- Soliman, M.A. and Hegazy, M.A.** (1969): The cranial nerves of *Chalcides ocellatus*. I. The eye-muscle nerves. Bull. Fac. Sci., Cairo Univ., **43**: 49-62.
- Soliman, M.A. and Mostafa, R.H.** (1984): A detailed study on the cranial nerves of the gecko *Tarentola mauritanica*. I. The ciliary ganglion and eye-muscle nerves. Proc. Zool. Soc., A.R.E., **VII**: 289-309.
- Soliman, M.A.; Mostafa, R.H. and Abdel-Kader, I.Y.** (1984): Anatomical studies on the cranial nerves of *Agama pallida* (Reuss). I. The eye-muscle nerves and ciliary ganglion. Egypt. J. Anat., **8**: 135-158.
- Soliman, M.A.; Hegazy, M.A. and Mostafa, R.H.** (1986): The cranial nerves of birds. II. The main special sensory nerves, nervus olfactorius, nervus opticus and nervus octavus. Proc. Zool. Soc. A.R.E., **10**: 211-232.
- Soliman, M.A.; Mostafa, R.H.; Hegazy, M.A. and Abdel-Kader, I.Y.** (1990): A comparative detailed study on the cranial nerves of *Agama pallida* (Reuss) and *Ptyodactylus hasselquistii* (Anderson). 1. The nervus facialis. Proc. Zool. Soc., A.R.E., **19**: 71-86.
- Srinivasachar, H.R.** (1955): Observations on the development of the chondrocranium in *Vipera*. Anat. Anz., **101**: 219-225.
- Von Bartheld, C.S.; Lindorfer, H.W. and Meyer, D.L.** (1987): The nervus terminalis also exists in cyclostomes and birds. Cell Tissue Res., **244**: 181-186.
- Watanabe, T. and Yasuda, M.** (1968): Comparative and Topographical anatomy of the fowl: II. Peripheral course of the olfactory nerve in the fowl. Jap. J. Vetr. Sci., **30**: 275-279.
- Weichert, C.K.** (1958): Anatomy of the chordates. Mc Graw-Hill, New York, Toronto and London.

12/12/2011

Role of IL28B Gene Polymorphisms in Response to the Standard of Care Treatment in Egyptian Patients with Chronic HCV Genotype Four

Olfat M Hendy¹, Elhamy Abd El Moneam¹, Mona A Al shafie², Maha El-Sabawy³, Mohammed A Rady³ and Sherif A El Baz⁴

Departments of Clinical Pathology¹& Hepatology³ - National Liver Institute- Menoufiya University, Clinical Pathology² – Menoufiya Faculty of Medicine and Tropical Medicine⁴ –NMC
aklrady@yahoo.com

Abstract: Egypt has the highest prevalence of HCV (predominantly genotype 4) all over the world with 9% countrywide and up to 50% in certain rural areas. Combined PEG-IFN and ribavirin is still the only standard of care treatment in spite of its side effects, high costs and low sustained virological response rates. Hence, this provides a compelling reason for the identification of biomarker predictors of disease response to treatment. Genetic variation in the interleukin 28B (IL28B) genes has been associated with the response to interferon-alfa/ribavirin therapy in hepatitis C virus (HCV) genotype 1-infected patients, however its importance for HCV genotype 4-infected patients is still unevident. This study aimed at assessing whether specific IL28B gene polymorphisms (SNPs), known as rs8099917 and rs12979860 could predict treatment outcomes among chronic HCV genotype4 patients treated with the standard of care treatment. Methods: One hundred of naïve chronic HCV patients were selected and submitted to combined interferon/ ribavirin therapy, 48% of them have sustained viral response and (SVR) while the remaining 52% failed to respond (non responders). SNPs for rs12979860 and rs8099917 were done by PCR-RFLP technique for all patients before therapy. The CC genotype of rs12979860 was identified in 39 patients, 34 of them (87.2%) achieved SVR, while the CT heterozygous was detected in 51 (51%) patients, 13 of them achieved SVR (25.5%) and the TT was found in 10 patients and only one of them (10%) was responder. The SVR was significantly associated with CC genotypes as compared to other two genotypes ($p < 0.001$), but TT genotype was associated with failed response to therapy. The TT homozygous of rs8099917 genotype was detected in 46 (46%) of overall HCV patients, 37 of them (80.4%) achieved SVR. The GT heterozygous was detected in 42 (42%) of HCV patients, SVR was achieved in 9 (21.4%) of them. While, the GG genotype was found in 12 patients and two of them only (16.7%) were responders. Conclusion: These data suggest that host genetics may be useful for the prediction of treatment outcomes and that IL28B SNP genotype is an important predictive biomarker for SVR in patients with HCV genotypes 4. Further studies based on a larger number of patients are necessary to investigate the present results. [Olfat M Hendy, Elhamy Abd El Moneam, Mona A Al shafie, Maha El-Sabawy, Mohammed A Rady and Sherif A El Baz **Role of IL28B Gene Polymorphisms in Response to the Standard of Care Treatment in Egyptian Patients with Chronic HCV Genotype Four.** Life Science Journal, 2011; 8(4):908-915] (ISSN: 1097-8135). <http://www.lifesciencesite.com>.

Key words: IL28 gene polymorphism, SOC therapy in CHC, HCV genotype 4 in Egyptian patients.

Introduction

Egypt has the highest prevalence of HCV worldwide with 9% countrywide and up to 50% in certain rural areas (**Kamal and Nasser, 2008**) and the highest prevalence of HCV-4, (previously called the Egyptian genotype) which is responsible for almost 90% of infections and is considered a major cause of chronic hepatitis, liver cirrhosis, hepatocellular carcinoma, and liver transplantation in the country (**Abdel-Hamid et al., 2007**).

The published studies estimate the overall rates of spontaneous resolution in acute HCV-4 infections to range between 20% and 50%, which is not historically different than other genotypes (**Kamal et al., 2006**). The fibrosis progression rate in patients with chronic HCV-4 was 0.1_0.06 fibrosis units per year, with significantly higher grading and staging

scores in Egyptian patients infected with HCV-4a (**Roulot et al., 2007**).

Up to now, the standard of care (SOC) treatment consists of (pegylated) interferon-Alfa and ribavirin. However, depending on the viral genotype, treatment response rates differ significantly among infected patients. While up to 80% of the genotype 2 and 3 infected and 40–50% in genotype 1 patients can be cured, the response rate of genotype 4 in many clinical reports is showing SVR rates exceeding 60% (**Kamal and Nasser, 2008**). There is no doubt that the high treatment cost presents a high economic burden in developing country like Egypt, necessitating a more meticulous research on predictors of (SOC) treatment response. Such as viral factors as viral load, genotype and host factors as steatosis, gender, liver cirrhosis and genetics as IL28 polymorphisms.

Viral Characteristics (viral load, genotype, viral variants for example within the interferon sensitivity determining region, ISDR) may be responsible for these differences but also clinical parameters (age, gender, BMI, fibrosis stage, liver enzymes) have been shown to be associated with virological response (Kau *et al.*, 2008).

Cytokines are among the predominant mechanisms of host defence against infection; they induce inflammatory response that often leads to tissue injury, but also act as antiviral effectors as well. Cytokine synthesis capacity has a significant genetic component, which explains why there are differences between individuals in their ability to produce cytokines; it may also be due to single-nucleotide polymorphisms (SNPs) within the coding regions of cytokine genes. Cytokine genes are polymorphic and some of these variants modify the production of the specific cytokines and affect the host immune response. In HCV infection, secretion of inappropriate amounts of cytokines may be associated with chronicity or resistance to interferon (IFN) treatment (Thio, 2008).

Recently, three independent research groups have reported the results of separate genome-wide association studies (GWAS), supporting a strong association of two single nucleotide polymorphisms (change at a particular position in the gene sequence) of the IL28B gene on chromosome 9, which encodes type III interferon lambda (IFN- λ -3), rs8099917 and rs12979860, with treatment outcomes of Peg-IFN α -2a plus RBV therapy (Ge *et al.*, 2009; Suppiah *et al.*, 2009; Tanaka *et al.*, 2009). These variations in the IL28B gene correlated well with natural clearance of HCV and with SVR. In the first study, performed with European-American, African-American, and Hispanic individuals, the rs12979860 SNP was most strongly associated with SVR, which is located 3 kilo bases upstream of the *IL28B* gene. The minor allele (T) was associated with a lower rate of SVR (26% in those with genotype TT and 79% in those with genotype CC) (Ge *et al.*, 2009). In the second study, carried out with 293 Australian patients, a significant association between the SNP rs8099917 and SVR was found. This was further validated by an independent cohort of 555 European individuals. From 392 patients who achieved SVR, 247 (63%) were homozygotes for the allele T, which was significantly higher than genotype GG (SVR of 3.8%) (Suppiah *et al.*, 2009). Similar findings were also reported in a Japanese study. Results of a GWAS showed a significant association between treatment response with two SNPs (rs12980275 and rs8099917), both located in the IL28B gene region, with the latter being the same SNP found by Australian researchers. In this case, for the SNP

rs8099917, the G allele was associated with a significantly lower SVR (0% for genotype GG and 78% for genotype TT) (Tanaka *et al.*, 2009).

Although, several groups have reported an association between several SNPs in the IL28 locus and the effect of PEG-RBV combination therapy for genotype 1 (Thomas *et al.*, 2009; Rauch *et al.*, 2010), but only a few studies have examined the role of these SNPs in the treatment of other genotypes especially genotype 4.

Aim:

In this study, we investigated whether the IL28B polymorphisms are associated with response to the therapy of PEG-IFN and ribavirin in Egyptian chronic HCV infection patients mostly with genotype four.

2. Patients and Methods:

The current study was conducted on 100 naïve (not treated before, first time to receive treatment) chronic HCV patients from interferon clinic of National Liver Institute-Menoufiya University in the period from February 2010 to July 2011. Selected patients were planned to receive combined interferon and ribavirin therapy. They had persistent (>6 months) elevation of alanine aminotransferase 1.5 times above the upper normal limit, with detectable HCV antibodies and HCV RNA with negative both HBs and HBe antigens with histological evidence of HCV. The stage of fibrosis was determined according to Ishak scoring system (Ishak *et al.*, 1995), fibrosis score from 0-6, 0=no fibrosis, 1-2=portal fibrosis (mild fibrosis), 3-4=bridging fibrosis (moderate fibrosis) and 5-6=cirrhosis (advanced fibrosis). All patients gave their written informed consent before the study and this study was approved by the ethical committee of National Liver Institute-Menoufiya University.

All chronic HCV patients were genotype 4, and were all submitted to the (SOC) therapy. of pegylated interferon-alfa 2a 180 mcg per week or pegylated interferon-alfa 2b 1.5 mcg per kg body weight in combination with ribavirin 600–1400 mg per day according to body weight for 24–48 weeks. Patients will be stratified according to response to (SOC) therapy into two groups: The first group is responders to treatment, the chronic HCV patients who had received the (SOC) therapy and have shown negative HCV RNA 6 months (24 weeks) following completion of a 48 weeks treatment course. The second group is non responders to the (SOC) therapy (no disappearance of HCV RNA at the end of the 12 week). Epidemiological, biochemical, and virological characteristics of these patients are shown in Table 1.

The following investigations were done for the patients:

- Liver function tests were done on Integra-400 (Roche-Germany), Complete blood counts were done on Sysmex KX-21 automatic cell counter (Japan). HCV antibodies were done by EIA (COBAS-Amplicore, Germany). HCV-RNA levels were analyzed by reverse transcriptase polymerase chain reaction (RT-PCR) at 0, 4, 12, 24, 48, 72 weeks of starting treatment, using a commercial kit (Roche Diagnostic, Branchburg, NJ) according to the manufacturer's instructions.
- HCV genotyping was done using INNO-LiPA III (line immunoprobe assay) provided by Innogenetics, Ghent, Belgium.
- Liver biopsies were done for all patients included before therapy to assess fibrosis stage.

Single nucleotide polymorphisms (SNPs) of the IL28B genotype:

Blood was collected into EDTA tubes following standard procedures. Genomic DNA was prepared from peripheral blood lymphocytes by QIAGEN EZ1 DSP DNA Blood System. In brief, 2 ml of whole blood was mixed with 8 ml of triton lysis buffer 1 (0.32M Sucrose, 5mM MgCl₂.6H₂O, 12mM Tris-HCl, pH 7.5, 1%V/V Triton X-100). Leukocytes and nuclei were spun down (3500g, 5min), the pellet was washed with dH₂O and then resuspended in 0.9 ml of lysis buffer 2 (0.375M NaCl, 0.12M EDTA, pH 8.0), 25 µl SDS 10%, and 0.22 ml NaClO₄ (4M) and was shaken vigorously, spun down (13000g, 5 min) and subsequently salted out using a saturated NaCl solution. DNA in the supernatant was precipitated with 99.5% ethanol. Finally, DNA pellet was dissolved in 100 µl of ddH₂O. After quantification of DNA by UV spectrophotometer, 100ng of genomic DNA was used for each 20 µl PCR reaction (Newton *et al.*, 1989).

The rs12979860 and rs8099917 SNPs genotyping was carried out by polymerase chain reaction (PCR), and restriction fragment length polymorphism (RFLP). For rs12979860, oligonucleotide primers were: 5'- AGG GCC CCT AAC CTC TGC ACA GTC T -3' (sense), and 5'- GCT GAG GGA CCG CTA CGT AAG TCA CC -3' (antisense). For rs8099917, oligonucleotide primers were: 5'- TTC ACC ATC CTC CTC TCA TCC CTC AT -3' (sense) and 5'- TCC TAA ATT GAC GGG CCA TCT GTT TC -3' (antisense).

PCR reaction conditions (30 µL) were: initial denaturation at 94 °C for 10 min, followed by 40 cycles of: denaturation at 94 °C for 1 min, annealing at 58 °C for 40 s, and extension at 72 °C for 1 min.

The PCR product for rs12979860 and rs8099917 was of 403 and 401 base pairs, respectively.

Restriction fragment length polymorphism (RFLP) analyses for IL28B alleles:

In order to perform RFLP assay for the rs12979860 genotype, 20 µL of amplicons were digested with 5U of *Bst*U I restriction endonuclease (New England Biolabs, MA, United States) at 60 °C for 2 h. *Bst*U I digestion of allele CC yields fragments of 184, 105, 89 and 25 base pairs, whereas DNA containing the allele TT polymorphism yields fragments of 184, 130 and 89 base pairs. For the RFLP assay for the rs8099917 genotype, 20 µL of amplicons were digested with 1U of *Mae* III restriction endonuclease (Roche Molecular Systems, Branchburg, NJ, United States) at 55 °C for 2 h. *Mae* III digestion of allele TT yields fragments of 105, 110 and 186 base pairs, whereas DNA containing the allele GG polymorphism yields fragments of 105, 110, 39 and 147 base pairs. Restriction digestion products for each were separated on agarose gels stained with ethidium bromide for visualization on a UV trans-illuminator (Venegas *et al.*, 2011).

Statistical analysis:

Statistical package for SPSS (statistical package for social science) program version 13 for windows and Epi info computer program was used for data analysis. Quantitative variables were summarized using Mean±SD. Student's t-test was done to compare two normally distributed variables Mann Whitney non parametric variables. Fisher's exact test and the Chi square (X²) test for categorical variables. Correlation coefficients (r) were calculated using the Pearson's correlation analysis. *p* value was significant at <0.05 level.

3. Results

The characteristics of the total 100 patients with chronic HCV infection (before therapy) are shown in Table (1). The study includes, 27% of stage 1 fibrosis, 38% of stage 2, 20% of stage 3 and 15% of stage 4, all HCV patients were genotype 4. The frequency of SNPs of IL28B showed that: for genotype rs12979860, CC was detected in 39%, CT in 51% and TT in 10% of overall HCV patients, but for rs8099917, the frequency was 46%, 42% and 12% for TT, GT, and GG respectively.

About 48(48%) among overall 100 HCV patients achieved SVR (responders), and the remaining 52(52%) of patients failed to respond (non responders). The CC genotype of rs12979860 was identified in 39 patients, 34 of them (87.2%) were achieved SVR. The unfavourable SNP genotype (TT)

was found in 10 patients and only one of them (10%) was responder. The CT heterozygous was detected in 51 (51%) patients, SVR was achieved in 13 (25.5%) of them, the frequency of CC genotypes was associated with SVR as compared to other genotypes ($p<0.001$). In contrast, the frequency of TT genotypes was associated with non responder patients ($p<0.01$) (Table 2).

As regard the TT homozygous of rs8099917 genotype, it was detected in 46 (46%) of overall HCV patients, and 37 of them (80.4%) were achieved SVR. The GT heterozygous was detected in 42 (42%) of HCV patients, SVR was achieved in 9 (21.4%) of

them. While, the GG genotype was found in 12 patients and two of them only (16.7%) were responders ($p<0.001$; <0.05 for SVR and non responders) respectively (Table 3).

The comparison between rs12979860 genotypes revealed a significant increase in ALT, AST ($p<0.05$) and viral load ($p<0.01$) in CC genotype as compared to CT+TT genotypes. As regard rs8099917 genotypes, the ALT, AST levels were significantly higher in TT genotype as compared to GT+GG ($p<0.05$). But no significant difference was detected as regard other parameters (Table 4).

Table (1) Epidemiological, biochemical, and virological characteristics of patients:

	Chronic HCV patients (n=100)
Age (Years)	38.5 ± 10.4 (29-52)
Gender (Male/female)	68/32
BMI (kg/m ²)	23.2±4.6 (18-29)
ALT (U/L)	104.6±21.3 (78-122)
AST (U/L)	83.9 ± 25.7 (61-103)
GGT (U/L)	39.4±10.3 (27-41)
S. albumin (gm/dl)	3.9 ± 0.33 (3.5-4.2)
Prothrombin conc. %	77.2±3.6 (74-82)
Total leukocytic count (x10 ³ /μl)	5.7±1.5 (4.3-7.6)
Hemoglobin (gm/dl)	12.6 ±1.4 (11-13.9)
Platelet count (x10 ³ /μl)	230±90 (129-310)
AFP (mg/ml)	22.7±16.2 (6-39)
Viral load (log IU/mL)	7.5± 2.4 (5.1-9.7)
Fibrosis stage:	
Stage 1	27%
Stage 2	38%
Stage 3	20%
Stage4	15%
IL28B genotypes frequency:	
rs12979860	CC=39%, CT=51%, TT=10%
rs8099917	TT=46%, GT=42%, GG=12%

Table (2) rate of IL28B (rs12979860) genotypes among HCV patient groups

Variables	rs12979860 genotypes			p-value
	CC (n=39)	CT (n=51)	TT (n=10)	
Responders (SVR) (n=48)	34/39 (87.2%)	13/51(25.5%)	1/10 (10%)	<0.001
Non responders (n=52)	5/39 (12.8%)	38/51(74.5%)	9/10 (90%)	<0.01

Table (3) rate of IL28B (rs8099917) genotypes among HCV patient groups

Variables	rs8099917 genotypes			p-value
	TT (n=46)	GT (n=42)	GG (n=12)	
Responders (SVR) (n=48)	37/46 (80.4%)	9/42 (21.4%)	2/12 (16.7%)	<0.001
Non responders (n=52)	9/46 (19.6%)	33/42 (78.6%)	10/12(83.3%)	<0.05

Table (4) Comparison between IL28B genotypes

Variables	rs12979860 genotypes			rs8099917 genotypes		
	CC	CT+ TT	p-value	TT	GT+GG	p-value
Age	43.8 ± 7.3	37.4 ± 4.9	>0.05	48.1 ± 6.5	43.2 ± 4.3	>0.05
Gender	28/11	40/21	>0.05	26/20	42/12	>0.05
ALT	121.6± 32.4	81.2±10.6	<0.05	134.1± 28.5	98.1±16.2	<0.05
AST	113.2 ± 17.4	73.2±12.5	<0.05	102.4 ± 15.2	82.1±9.8	<0.05
Albumin	3.5 ± 0.23	4.0 ± 0.51	>0.05	3.8 ± 0.41	4.1 ± 0.45	>0.05
P. C	75.4±2.3	72.8±4.2	<0.05	77.2±6.2	70.6±2.2	>0.05
Hb	11.9 ± 1.6	12.5 ± 2.1	>0.05	12.1 ± 1.4	11.5 ± 1.1	>0.05
TLC	5.9 ±2.3	4.9±1.8	>0.05	6.2 ±1.9	5.4±1.2	>0.05
Platelets	189±50	210±90	>0.05	197±23	176±65	>0.05
Viral load	7.3±1.9	5.8± 1.2	<0.01	4.9±1.3	5.6±1.8	>0.05

4. Discussion:

IL-28B is a Th1 type cytokine, a class II cytokine receptor ligand, a 200 amino acid long protein, a member of type III IFN-s, that distantly structurally relates to the members of IL-10 superfamily of cytokines, but shares also limited sequence similarity and functional characteristics with the type I IFN-s (α , β). IL-28B has a role in the regulation of intracellular IFN stimulated gene (ISG) expression (Sheppard *et al.*, 2003). It is expressed by peripheral blood mononuclear cells; dendritic cells upon infection with viruses. IL-28B exhibits antiviral activity, having an impact on natural clearance of HCV (Par *et al.*, 2011). The current study was designed to clarify, the effect of rs12979860 and rs8099917, SNP located nearest to interleukin 28B (*IL28B*), the gene that encodes for IFN lambda-3 on HCV-4 outcome after combined IFN/RVN therapy.

In the current study, CC genotype of rs12979860 was identified in 39 % of overall HCV patients; the CT heterozygous was detected in 51% and the TT 10%. Mangia *et al.* (2010) recorded that, the frequencies of the IL-28B genotypes were as follows: CC, 37%; CT, 48%; and TT, 15%

After therapy, 48 (48%) among overall 100 HCV patients were achieved SVR (responders), and the remaining 52 (52%) of patients failed to respond (non responders). The CC genotype of rs12979860 who achieved SVR was 87.2%, which is significantly higher compared to CT (25.5%) and TT (10%) genotypes. This finding was supported by previous studies (Suppiah *et al.*, 2009; Tanaka *et al.*, 2009).

Mangia *et al.*(2010) reported that, 82% of patients with the CC genotype achieved a SVR, compared with 75% with the CT and 58% with the TT genotypes ($P=0.0046$). De Nicola *et al.* (2011), found that, of 112 treated patients (98 males, 75 of Egyptian descent, 26 with cirrhosis), 23% were genotype CC, 63% CT and 14% TT. An SVR was achieved in 49%, and 88% of them were CC patients vs 37% of CT/TT ($p<0.0001$). Kurbanov *et al.*

(2011) showed that the protective C allele was more common in those with spontaneous viral clearance (76.3% vs 57.9%; $P=0.0006$). Individuals with clearance were 3.4 times more likely to have C/C genotype. Thus, *IL28B* plays a role in spontaneous clearance of HCV genotype 4 in North Africa. Asselah *et al.* (2011) showed a better treatment response rate of the C Allele of the IL28B Gene SNP rs12979860. The response rates were 81.8%, 46.5% and 29.4% for genotype CC, CT and TT respectively. Lin *et al.* (2011) reported that in patients with genotype 1, SVR was achieved in 68.6% of the patients and it was higher in CC genotype of rs12979860 ($p<0.001$) but no other SNPs were independent predictors for SVR.

Par *et al.*(2011) reported that, the high IL-28B cytokine producing C/C genotype of this polymorphism was associated with a two- to threefold greater rate of SVR to anti-HCV therapy compared with the low cytokine producing T/T genotype. They added that the frequency of IL-28B C/C genotype was lower in HCV patients than in controls, it may be regarded as being protective against the chronic HCV infection, and that is, it may confer protection against the disease. Thomas *et al.* (2009), reported that the IL-28B C/C genotype enhanced the spontaneous resolution of HCV infection and patients who harbour the C allele at *rs12979860* are more prone to respond to treatment and clear HCV than patients who do not possess this genetic polymorphism, which suggests a primary role for IL-28B in the resolution of HCV infection.

Ge *et al.* (2009) suggested that their IL-28B polymorphism was associated with decreased IL-28B (and IL-28A) expression-- a biologically plausible suggestion because IL-28B encodes interferon-lambda3, which may be involved in interfering with viral replication. Chevaliez *et al.* (2010), added that, most patients who fail to respond to pegylated IFN and ribavirin carry either TT or CT rs12979860 genotypes. CT patients are significantly more likely

to respond to higher doses of IFN. This indicates that the IL28B genotype is a marker of host cell responsiveness to IFN.

Furthermore, our results revealed that, SVR was detected in 80.4% of patients who harbour homozygous TT of rs8099917, in 21.4% of heterozygous GT and in 16.7% of the GG genotype. Similarly, **Rauch and colleagues (2010)** suggested that, the strongest association with spontaneous recovery was detected for rs8099917, a SNP located nearest to interleukin 28B (*IL28B*), the gene that encodes for IFN lambda-3. Patients who are homozygous for C at rs12979860 (C/C) have a >2.5-fold increased likelihood of spontaneous resolution of HCV compared with patients who have persistent HCV infection. The association of the *IL28B* locus with natural and treatment-associated control of HCV suggests the importance of innate immunity and IFN lambda-3 in the pathogenesis of HCV infection.

Suppiah et al. (2009) reported an association to SVR within the gene region encoding interleukin 28B (rs8099917. *IL28B* contributes to viral resistance and is known to be upregulated by interferons and by RNA virus infection. These data suggest that host genetics may be useful for the prediction of drug response, and they also support the investigation of the role of *IL28B* in the treatment of HCV and in other diseases treated with IFN- α .

In a study by **Aparicio et al. (2010)**, the rs12979860 SNP genotype was also highly associated with treatment success in HCV genotype 4-infected patients ($P < 0.0001$), and patients carrying rs8099917 G alleles had high rates of treatment failure. The rate of treatment failure in patients infected with HCV genotype 3 was not affected by rs8099917 genotype. Similar results reported by **Pineda et al. (2010)** and **Rallon et al. (2010)**, which have demonstrated a significant influence of the rs12979860 SNP, that is in linkage disequilibrium with rs8099917 (**Rauch et al., 2010**), on the treatment response of HIV-1 patients coinfecting with HCV genotypes 1 and genotype 4. **Akuta et al. (2010)**, showed that genetic variation near the *IL28B* gene (rs8099917, rs12979860) are pre-treatment predictors of virological response to PEG-IFN plus ribavirin combination therapy in individuals infected with HCV.

The high prevalence of the rs8099917 G allele in HCV genotype 1- or 4-infected patients shows that the rs8099917 TT genotype may have a protective effect in terms of preventing the persistence of these two HCV genotypes. Since the rs8099917 G allele has been correlated with lower expression levels of *IL28* genes (**Tanaka et al., 2009**), the different frequencies of the rs8099917 G allele in patients infected with different HCV genotypes may indicate

that the innate immune system interacts differently with the different HCV genotypes. However, the viral factors involved in this interaction remain unknown. The *IL28B*, *IL28A*, and *IL29* genes are closely related cytokine genes in chromosomal region 19q13 that encode proteins known as type III IFNs (IFN-Is) (**Kotenko et al., 2003**). IFN-I has been proposed as a possible treatment for hepatitis C (**Dodds et al., 2009**; **Muir et al., 2009**).

An interesting finding in our study was the significant higher levels of ALT, AST and viral load were detected in CC genotype. **Pablo et al. (2011)** reported that, HIV/HCV-co-infected patients with the C allele at rs12979860 show significantly higher plasma HCV-RNA load than TT carriers. Notably, plasma HCV-RNA levels associated with poorer response to IFN- α based therapy are significantly more frequent in CC/CT than TT carriers. Hypothetically, patients harbouring the rs12979860 allele C could display a lower activity of endogenous IFN- α , allowing higher HCV replication while keeping an enhanced susceptibility to exogenous IFN- α therapy.

Kawaoka et al. (2011) reported that, HCV RNA viral load, treatment regimen, and rs8099917 genotypes independently contributed to the effect of the therapy. For patients treated with PEG-RBV, rs8099917 and viral load were independent predictive factors for SVR in genotype 2b but not in genotype 2a. Conversely, in patients treated with interferon monotherapy, viral load and rs8099917 were independent predictive factors for SVR in genotype 2a but not in genotype 2b. The favourable rs8099917 genotype is also associated with a steep decline in viral load by the second week of treatment. On the contrary, **Lin et al. (2011)**, suggested that, none of the ten SNPs examined were associated with baseline viral load and stages of liver fibrosis, but CC genotype of rs12979860 was the only treatment predictor.

What functional mechanism underlies the *IL28B* response? HCV RNA triggers production of type I interferons by hepatocytes; these molecules stimulate transcription of interferon-stimulated genes (ISGs). Exogenous (therapeutic) interferon alpha signals similarly. Given that the polymorphism 3-kb upstream of *IL28B* appears to be associated with natural clearance as well as treatment response, it seems likely that the gene product is involved in the innate control of HCV. The specific *IL28B* polymorphism (C/C) is strongly associated with reduced expression of intrahepatic ISGs and the response rate to PEG-IFN and ribavirin (**Tanaka et al., 2009**). Genetic variation in *IL28B* regulates the innate immune response to HCV in the liver, priming

patients for a stronger response to exogenous IFN alpha therapy.

The question may arise whether HCV patients homozygous for the *IL-28 T/T* genotype (and low *IFNλ-3 production*) will need more intensive PEG-IFN/RBV treatment or more complex (e.g. triple) anti-HCV therapy in the future? Alternatively, for patients with *IL-28B C* homozygosity would a shorter treatment be appropriate? According to the *IL-28 deficiency hypothesis*, it would also be of importance to find compounds which can increase the expression of *IL-28B* on leukocytes, or to identify compounds which upregulate *IL-28B* transcription.

In conclusion: This study identified a polymorphism 3 kb upstream of *IL28B* (namely; rs12979860 and rs8099917) that is significantly associated with response to PEG-IFN and RBV for patients with chronic genotype 4 HCV infection. The polymorphism explains much of the difference in response between other HCV genotypes. Given that the polymorphism appears to associate with natural clearance as well as treatment response, it seems likely that the gene product is involved in the innate control of HCV. These findings, and further study of the functional mechanism underlying the *IL28B* response association, may help to identify patients for whom therapy is likely to be successful.

Corresponding author

Mohammed A Rady

Hepatology Department, National Liver Institute-Menoufiya University, Menoufiya, Egypt
aklrady@yahoo.com

References

Abdel-Hamid M, El-Daly M, Molnegen V, El-Kafrawy S, Abdel-Latif S, Esmat G, Strickland GT, Loffredo C, Albert J and Widell A(2007). Genetic diversity in hepatitis C virus in Egypt and possible association with hepatocellular carcinoma. *Virology*, 88:1526–1531.

Akuta N, Suzuki F, Hirakawa M, Kumada H *et al.* (2010). Amino Acid Substitution in Hepatitis C Virus Core Region and Genetic Variation Near the Interleukin 28B Gene Predict Viral Response to Telaprevir with Peginterferon and Ribavirin. *Hepatology*;52:421-429

Aparicio E, Parera M, Franco S, Angel M *et al.* (2010). *IL28B* SNP rs8099917 Is Strongly Associated with Pegylated Interferon-a and Ribavirin Therapy Treatment Failure in HCV/HIV-1 Coinfected Patients PLoS ONE, October, Volume 5, Issue (10): e13771

Asselah T, De Muynck S, Broët P, Marcellin P. *et al.* (2011). *IL28B* polymorphism is associated with treatment response in patients with genotype 4 chronic hepatitis C. *J Hepatol.* 24. [Epub ahead of print].

Berg T, Sarrazin C, Herrmann E, Hinrichsen H, Gerlach T, Zachoval R, Wiedenmann B, Hopf U, and Zeuzem S(2003). Prediction of treatment outcome in patients with chronic hepatitis C: Significance of baseline parameters

and viral dynamics during therapy. *Hepatology*, 37:600–609.

Chevaliez S; Soulier A; Hezode C; Pawlotsky J *et al.* (2010). The *IL28B* genotype is a major determinant in the induction of a virological response by high-dose peginterferon and ribavirin in null-responders to standard-of-care therapy.(AASLD),*Hepatology*;52:383A.(abstract for reference8)

De Nicola S, Aghemo A, Rumi MG, Colombo M. *et al.* (2011). An *IL28B* polymorphism predicts pegylated interferon plus ribavirin treatment outcome in chronic hepatitis C genotype 4. *Hepatology*, 19. doi: 10.1002/hep.24683. [Epub ahead of print] it is exactly written like this in *Hepatology Journal* 2011, Sept,21

Dodds MG, Hausman DF, Miller DM(2009). Viral kinetic modelling during treatment with interferon lambda-1A in genotype 1 chronic hepatitis C patients. *J. Hepatology* , 50: 942.

European Association for the study of the Liver. EASL Clinical practice guidelines: management of hepatitis C virus infection. *Journal of Hepatology* 2011 vol.55:245-264.

Fried MW, Shiffman ML, Reddy KR, Smith C, Marinos G, *et al.* (2002).

Peginterferon alfa-2a plus ribavirin for chronic hepatitis C virus infection. *N Engl J Med.*, 347: 975–982.

Gao B, Hong F, Radaeva S (2004). Host factors and failure of interferon-alpha treatment in hepatitis C virus. *Hepatology*, 39: 880–890.

Ge D, Fellay J, Thompson AJ, *et al.* (2009). Genetic variation in *IL28B* predicts hepatitis C treatment-induced viral clearance. *Nature*; 461:399–401.

Hadziyannis SJ, Sette H, Jr., Morgan TR, Balan V, Diago M, *et al.* (2004)

Peginterferon-alpha2a and ribavirin combination therapy in chronic hepatitis C: a randomized study of treatment duration and ribavirin dose. *Ann Intern Med.*;140: 346–355.

Hoofnagle, J.H. (2002). Course and outcome of hepatitis C. *Hepatology*. 36:S21–S29.

Hsua SC, Hsueh SJ, Chene SC, Chenc DS *et al.* (2010). Association of *IL28B* gene variations with mathematical modeling of viral kinetics in chronic hepatitis C patients with IFN plus ribavirin therapy., www.pnas.org/cgi/doi/10.1073/pnas.1100349108.

Ishak K., Baptista A., Bianchi L., Callea F., De Groote J. *et al.* (1995). Histological grading and staging of chronic hepatitis. *J Hepatol.*; 22:696—699.

Kamal SM, Moustafa KN, Chen J, Fehr J, Abdel Moneim A, Khalifa KE, *et al.* (2006). Duration of peginterferon therapy in acute hepatitis C: a randomized trial. *HEPATOLOGY*;;43:923-931.

Kamal SI and Nasser. *et al.* (2008). Hepatitis C Genotype 4: What We Know and What We Don't Yet Know. *Hepatology*;47:1371-1383.

Kao JH, Chen DS. Transmission of hepatitis C virus in Asia: Past and present perspectives. *J Gastroenterol Hepatol*, 2000, 15 (Suppl):E91–E96.

Kau A, Vermehren J, Sarrazin C. Treatment predictors of a sustained virologic436 response in hepatitis B and C. *J Hepatol* 2008;49:634–651.

- Kawaoka T, Hayes CN, Chayama K. et al. Predictive value of the IL28B polymorphism on the effect of interferon therapy in chronic hepatitis C patients with genotypes 2a and 2b. *J Hepatol.* 2011 Mar;54(3):408-14.
- Kotenko SV, Gallagher G, Baurin VV, Lewis-Antes A, Shen M, et al. (2003) IFN-lambdas mediate antiviral protection through a distinct class II cytokine receptor complex. *Nat Immunol* 4: 69–77.
- Kronenberger B, Zeuzem S. Current and future treatment options for HCV. *Ann Hepatol* 8, 2009: 103–112.
- Kurbanov F, Abdel-Hamid M, Latanich R, Thio CL et al Genetic Polymorphism in *IL28B* Is Associated With Spontaneous Clearance of Hepatitis C Virus Genotype 4 Infection in an Egyptian Cohort. *J Infect Dis.* (2011) 204 (9): 1391-1394.
- Lin CY, Chen JY, Huang CW, Sheen S. IL28B SNPs rs12979860 Is a Critical Predictor for On-Treatment and Sustained Virologic Response in Patients with Hepatitis C Virus Genotype-1 Infection. *PLoS ONE*, 2011, 6, 3, Publisher: Public Library of Science, Pages: 9
- Lotrich FE, Loftis JM, Ferrell RE, Rabinovitz M, Hauser P IL28B Polymorphism Is Associated with Both Side Effects and Clearance of Hepatitis C During Interferon-Alpha Therapy. *J Interferon Cytokine Res.* 2010 Dec 6;
- Magna A, Thompson AJ, Santoro R, Goldstein DB et al., An *IL28B* Polymorphism Determines Treatment Response of Hepatitis C Virus Genotype 2 or 3 Patients Who Do Not Achieve a Rapid Virologic Response *Gastroenterology*, 2010 139, 3, 821-827.
- Manns MP, McHutchison JG, Gordon SC, Rustgi VK, Shiffman M, et al. (2001) Peginterferon alfa-2b plus ribavirin compared with interferon alfa-2b plus ribavirin for initial treatment of chronic hepatitis C: a randomised trial. *Lancet* 358: 958–965.
- McHutchison JG, Lawitz EJ, Shiffman ML, Sulkowski MS. et al. Peginterferon alfa-2b or alfa-2a with ribavirin for treatment of hepatitis C infection. *N Engl J Med* 2009; 361: 580-593
- Muir A, Shiffman ML, Zaman A, Yoffe B, Lopez-Talavera JC, et al. A Phase 1B dose-ranging study of 4 weeks of peg-interferon (IFN) lambda in combination with ribavirin (RBV) in patients with genotype 1 chronic hepatitis C infection. *Hepatology*, 2009, 50: 1591.
- Newton CR, Graham A, Heptinstall LE, Markham AF. Et al. Analysis of any point mutation in DNA. The amplification refractory mutation system (ARMS). *Nucleic Acids Res* 1989 Apr 11;17(7):2503-16.
- Pablo L; Vincent S; José M; Juan AB. on behalf of CoRIS. Association between IL28B gene polymorphisms and plasma HCV-RNA levels in HIV/HCV-co-infected patients. *Clinical Science*, 27 March 2011 - Volume 25 - Issue 6 - p 761–766
- Par A, Kisfali P, Melegh B, Vincze A et al. Cytokine (IL-10, IL-28B and LT-A) Gene Polymorphisms in Chronic Hepatitis C Virus Infection. *CEMED*, 2011, *Volume 5*, :9–19.
- Pineda JA, Caruz A, Rivero A, Neukam K, Salas I, et al. (2010) Prediction of Response to Pegylated Interferon plus Ribavirin by IL28B Gene Variation in Patients Coinfected With HIV and Hepatitis C Virus. *Clin Infect Dis* 51: 788–795.
- Rallon NI, Naggie S, Benito JM, Medrano J, Restrepo C, et al. (2010) Association of a single nucleotide polymorphism near the interleukin-28B gene with response to hepatitis C therapy in HIV/hepatitis C virus-coinfected patients. *AIDS* 24: F23–29.
- Rauch A, Kutalik Z, Descombes P, Cai T, Di Iulio J, Mueller T, et al. Genetic variation in IL28B is associated with chronic hepatitis C and treatment failure: a genome-wide association study. *Gastroenterology* 2010;138:1338–1345.
- Roulot D, Bourcier V, Grando V, Deny P, Baazia Y, Fontaine H, et al.; Observational VHC4 Study Group. Epidemiological characteristics and response to peginterferon plus ribavirin treatment of hepatitis C virus genotype 4 infection. *J Viral Hepat* 2007;14:460-467.
- Sheppard, P., Kindsvogel, W., Xu, W. et al.: *IL-28, IL-29 and their class II cytokine receptor IL-28B*. *Nat. Immunol.*, 2003, 4, 63–68.
- Shire NJ, et al.; Multicenter Hemophilia Cohort HCV Study Group (2006) HCV kinetics quasispecies, and clearance in treated HCV-infected and HCV/HIV-1-coinfected patients with hemophilia. *Hepatology* 44:1146–1157.
- Suppiah V, Moldovan M, Ahlenstiel G, et al. IL28B is associated with response to chronic hepatitis C interferon-alpha and ribavirin therapy. *Nat Genet* 2009; 41: 1100–1104.
- Tanaka, Y., Nishida, N., Sugiyama, M.: Genome-wide association of IL28B with response to pegylated interferon and ribavirin therapy for hepatitis C. *Nat. Genet.*, 2009, 41, 1105–1109.
- Thio, C. L.: Host genetic factors and antiviral immune responses to hepatitis C virus. *Clin. Liver Dis.*, 2008, 12, 713–725.
- Thomas DL, Thio CL, Martin MP, Qi Y, Ge D, O’Huigin C, et al. Genetic variation in IL28B and spontaneous clearance of hepatitis C virus. *Nature* 2009;461:798–801.
- Venegas M, Villanueva RA, González K, Brahm J IL28B polymorphisms associated with therapy response in Chilean chronic hepatitis C patients. *World J Gastroenterol* 2011 August 21; 17(31): 3636-3639.
- Walsh MJ, Jonsson JR, Richardson MM, Lipka GM, Purdie DM, et al. (2006) Non-response to antiviral therapy is associated with obesity and increased hepatic expression of suppressor of cytokine signalling 3 (SOCS-3) in patients with chronic hepatitis C, viral genotype 1. *Gut* 55: 529–535.